

Expression and functional domains of Arabidopsis and tobacco *NIM1-INTERACTING* (*NIMIN*) genes

Dissertation to obtain the doctoral degree of Natural Sciences (Dr. rer. nat.)

Faculty of Natural Sciences

University of Hohenheim

Institute of Biology

submitted by

Mathias Saur

from Göppingen

2021

Dean:	Prof. Dr. Uwe Beifuss
1 st reviewer/examiner:	Prof. Dr. Artur J. P. Pfitzner
2 nd reviewer/examiner:	Prof. Dr. Andreas Schaller
3 rd examiner	Prof. Dr. Anke Steppuhn

Submitted: 22.07.2021

Oral exam: 17.12.2021

The present thesis was accepted on the 15.10.2021 by the Faculty of Natural Sciences of the University of Hohenheim as “Dissertation to obtain the doctoral degree of Natural Sciences (Dr. rer. nat.)”.

Table of contents

Summary	vii
Zusammenfassung	ix
Abbreviations	xii
Table of Figures	xix
1. Introduction	1
1.1. Innate immunity.....	2
1.1.1. Pattern-triggered immunity (PTI).....	2
1.1.2. Effector-triggered immunity (ETI).....	4
1.2. Systemic acquired resistance (SAR).....	7
1.2.1. Components of SAR.....	8
1.2.2. Regulators of SAR.....	10
1.3. NONEXPRESSOR OF PATHOGENESIS RELATED GENES 1.....	11
1.4. NPR1 as transcriptional co-activator of bZIP TGA transcription factors.....	13
1.5. NIMIN proteins.....	16
1.5.1. Differential interaction with NPR proteins.....	17
1.5.2. Transcriptional repression of <i>PR1</i> promoters.....	19
1.5.3. Role of NIMIN proteins in perception of salicylic acid.....	20
1.6. Aims and objectives.....	23
2. Materials	24
2.1. Enzymes & chemicals.....	24
2.2. Biological Materials / Organisms.....	24
2.2.1. Bacteria.....	24
2.2.2. Plants.....	24
2.2.3. Yeast.....	24
2.2.4. Viruses.....	25
2.2.5. DNA standard.....	25
2.2.6. Protein standard.....	25
2.3. Kits.....	25
2.3.1. Plasmid preparation.....	25
2.3.2. DNA elution from agarose gels.....	25
2.4. Plasmids.....	26
2.4.1. pBluescriptII (pBSKS(+)) / T-vector.....	26
2.4.2. pGBT9.....	26
2.4.3. pGAD424.....	26
2.4.4. pUC19.....	26
2.4.5. pBin19/35S.....	27
2.4.6. pRK2013.....	27
2.5. Synthetic oligonucleotides.....	27
2.6. Antisera.....	29

2.6.1.	GFP (FL) antiserum	29
2.6.2.	GFP (MC) antiserum	29
2.6.3.	GST-N1 antiserum.....	29
2.6.4.	PR1 antiserum.....	29
2.6.5.	GAL4BD antiserum.....	29
2.6.6.	Anti rabbit IgG-HRP conjugate	29
3.	Methods.....	30
3.1.	Standard molecular biological methods	30
3.1.1.	Growth of <i>E. coli</i>	30
3.1.2.	Preparation of chemically competent <i>E. coli</i> DH5a cells.....	30
3.1.3.	Transformation of chemically competent <i>E. coli</i> DH5a cells	31
3.1.4.	Blue-white screening of <i>E. coli</i> DH5a	31
3.1.5.	Preparation of stock cultures.....	31
3.1.6.	Growth of <i>A. tumefaciens</i>	32
3.1.7.	Triparental mating.....	32
3.1.8.	Plasmid preparation from bacterial cells.....	33
3.1.9.	Sequence specific restriction of DNA.....	33
3.1.10.	Dephosphorylation of DNA fragments.....	34
3.1.11.	Separation of DNA fragments (Gel electrophoresis).....	34
3.1.12.	Elution of DNA Fragments from agarose gels.....	34
3.1.13.	Ligation of DNA Fragments	34
3.1.14.	PCR amplification	35
3.1.15.	PCR site directed mutagenesis.....	35
3.1.16.	Screening bacterial colonies using PCR	36
3.1.17.	Cloning of PCR products	36
3.1.18.	Estimation of nucleic acids concentration	36
3.1.19.	DNA sequencing.....	37
3.2.	Experimental methods using <i>Saccharomyces cerevisiae</i>	37
3.2.1.	Yeast media	37
3.2.2.	Cultivation of yeast cells.....	38
3.2.3.	Preparation of competent yeast cells (HF7c)	38
3.2.4.	Transformation of yeast cells.....	38
3.2.5.	The yeast two-hybrid system for characterization of protein-protein interactions.....	39
3.2.6.	Quantitative Test of protein-protein interaction in yeast	39
3.2.7.	Protein extraction from yeast cells.....	40
3.3.	Experimental methods using plants.....	41
3.3.1.	Cultivation of plant seeds on MS Medium	41
3.3.2.	Plant cultivation and growth in the greenhouse	41
3.3.3.	Isolation of genomic DNA from plants.....	41
3.3.4.	Virus inoculation of <i>N. tabacum</i>	42
3.3.5.	Agroinfiltration-based transient gene expression in <i>Nicotiana benthamiana</i>	42
3.3.6.	Induction of the <i>GUS</i> reporter gene activity in transgenic plants	43

3.3.7.	Protein extraction from plant cells.....	43
3.3.8.	GUS Reporter gene assay	44
3.3.9.	Protease assay on protein extracts from <i>N. benthamiana</i>	45
3.3.10.	Subcellular localization studies using fluorescence microscopy	46
3.4.	Standard protein biochemical methods	46
3.4.1.	Protein concentration determination after Bradford	46
3.4.2.	SDS-polyacrylamide gel electrophoresis (SDS-PAGE)	47
3.4.3.	Western Transfer	48
3.4.4.	Immunodetection of Proteins with specific antibodies.....	48
3.4.5.	Ponceau S staining of nitrocellulose membranes.	49
4.	Results	50
4.1.	Expression of Arabidopsis <i>NIMIN</i> genes	50
4.1.1.	Subcellular localization of NIMIN1 and NPR fusion proteins	50
4.1.2.	Chemical induction of <i>NIMIN1</i> and <i>NIMIN2</i> promoters	53
4.1.3.	Expression from the <i>NIMIN1b</i> promoter.....	58
4.1.3.1.	Transient expression of <i>ProNIMIN1b:Bax</i> in <i>N. benthamiana</i>	58
4.1.3.2.	Germination of tobacco seeds harboring <i>ProNIMIN1b:Bax</i>	60
4.1.3.3.	Phenotype of tobacco plants harboring <i>ProN1b:Bax</i>	63
4.2.	Phenotypic effects of overexpression of Arabidopsis and tobacco <i>NIMIN</i> genes in <i>N. benthamiana</i> and <i>N. tabacum</i>	65
4.2.1.	Phenotypic effects of overexpression of Arabidopsis <i>NIMIN</i> genes in <i>N. benthamiana</i>	65
4.2.1.1.	Comparison of <i>NIMIN1</i> and <i>NIMIN1-Venus</i> overexpression.....	66
4.2.1.2.	Phenotypic effects of overexpression of <i>NIMIN1b</i> , <i>N2</i> , and <i>N3-Venus</i> fusion genes.....	70
4.2.1.3.	Effects of <i>N1-</i> and <i>N2-Venus</i> overexpression on N1 and N2 promoter activity	74
4.2.2.	Phenotypic effects of overexpression of tobacco <i>NIMIN-Venus</i> fusion genes in <i>N. benthamiana</i>	76
4.2.3.	Phenotypic effects of overexpression of <i>NIMIN</i> genes in <i>N. tabacum</i>	81
4.2.3.1.	Phenotypes of tobacco plants harboring <i>Pro35S:N1-Venus</i> and <i>Pro35S:N1 F49/50S</i>	81
4.2.3.2.	Effects of <i>N1-Venus</i> and <i>N1 F49/50S</i> overexpression on PR1 accumulation in <i>N. tabacum</i>	89
4.2.3.3.	Phenotypes of tobacco plants harboring <i>Pro35S:NtN2c-Venus</i> and <i>Pro35S:FS-Venus</i>	94
4.3.	Phenotypic effects of overexpression of Arabidopsis and tobacco <i>NIMIN</i> mutant genes in <i>N. benthamiana</i>	97
4.3.1.	Analysis of NIMIN1 mutants in the NPR1 binding motifs	97
4.3.2.	Analysis of EAR motif mutants regarding their cell promoting activity	103
4.3.3.	Analysis of tobacco NIMIN2 mutants in the NPR1 binding and EAR motifs	111
4.3.4.	Phenotypic effects of overexpression of TOPLESS in <i>N. benthamiana</i>	115
4.3.5.	Phenotypic effects of overexpression of Bax	118
4.4.	Identification of a novel domain in NIMIN1 important for protein accumulation.....	120
4.4.1.	Domain architecture of NIMIN1	120
4.4.2.	Analysis of NIMIN hybrid proteins comprising the N1 N-terminal domain.....	124
4.4.2.1.	Analysis of hybrid N1nT-N1b proteins	124
4.4.2.2.	Analysis of hybrid N1nT-NIMIN2-Venus	129
4.4.2.3.	Analysis of Venus proteins comprising the N1 N-terminal domain.....	131
4.4.2.4.	Analysis of mutants in the N1 N-terminal domain	136

5.	Discussion.....	143
5.1.	The <i>NIMIN1</i> and <i>NIMIN2</i> promoters are regulated similarly to <i>PR1a</i>	144
5.2.	The activity of the <i>NIMIN1b</i> promoter remains ambiguous.....	146
5.3.	Some NIMIN proteins promote cell death during transient overexpression in <i>N. benthamiana</i> and in transgenic tobacco plants.....	147
5.4.	Cell death promoting activity is strongly connected to the EAR motif.....	149
5.5.	Repression of PR1a promoter activity is often interlinked with cell death	152
5.6.	Accumulation of N1 is mediated by its N-terminal domain.....	153
	Literature	158
	Appendix	180
	Affidavit.....	196
	Curriculum vitae.....	197
	Scientific contributions	198
	Acknowledgements	199

Summary

Systemic acquired resistance (SAR) is an important defense mechanism in plants initiated after exposure to biotrophic pathogens. Characterized by accumulation of pathogenesis-related (PR) proteins in non-infected tissues, SAR is also associated with increased concentrations of the phytohormone salicylic acid (SA), acting as the SAR signal. SA is directly perceived by NPR1, the key regulator of SAR. Through interaction with TGA transcription factors, which facilitate binding to SA-responsive *as-1* like elements within the promoter of *PR1*, and NIM1-INTERACTING (NIMIN) proteins, NPR1 mediates the SA-dependent induction of *PR1* gene expression. The Arabidopsis genome contains four *NIMIN* genes – *NIMIN1*, *NIMIN1b*, *NIMIN2*, and *NIMIN3* – but members of the *NIMIN* family can also be found in many other higher plants like tobacco and rice. While NIMIN proteins are clearly structurally related and share their general domain architecture and ethylene-responsive element binding factor (ERF)-associated amphipathic repression (EAR) motif, they differ in other aspects. *NIMIN* genes are expressed differentially during pathogen infection and development. NIMIN proteins can be sorted into groups based on their NPR1-interaction motifs, the DXFFK and the EDF motif. NIMIN1-type proteins harbor both domains, while NIMIN2-type and NIMIN3-type carry only the DXFFK or the EDF motif, respectively. Accordingly, NIMIN proteins interact differentially with NPR1, with NIMIN1, NIMIN1b and NIMIN2 binding to the C-terminal moiety of NPR1, while NIMIN3 binds to the N-terminus instead. Overexpression studies revealed a role for NIMIN1 and NIMIN3 proteins in the transcriptional repression of *PR1* gene induction, increasing susceptibility of affected plants against pathogen infection. Strikingly, infiltrated plants overexpressing Arabidopsis *NIMIN1* and *NIMIN3* or tobacco *NtNIMIN2c* manifest significantly accelerated emergence of cell death. Differences in expression, NPR1 binding, transcriptional repression, and the ability to promote cell death indicate diverse functions of NIMIN proteins during SAR establishment and beyond. The objective of this work was to further characterize differences between NIMIN proteins from Arabidopsis and tobacco regarding biochemical properties and biological functions with special emphasis on their cell death promoting activity. For this purpose, reporter constructs harboring promoter and coding regions from Arabidopsis and tobacco *NIMIN* genes were analyzed in transient gene expression experiments in *Nicotiana benthamiana* and in transgenic tobacco plants. Functional domains were examined using the introduction of targeted mutations to study their significance for NIMIN protein function. The results from this study are set out below.

1. The *NIMIN1b* 1135 bp upstream promoter region is functional and two reporter genes under its control, *GUS* and the proapoptotic *Bax*, are active during transient overexpression. In transgenic tobacco plants the *NIMIN1b* promoter is not responsive to chemical induction by SA or its functional analog BTH and phenotypical studies showed no expression of the *Bax* reporter gene during plant development. To what extent the *NIMIN1b* gene is expressed in plants must therefore remain open.
2. Transient overexpression of Arabidopsis *NIMIN1* and *NIMIN3* and tobacco *NtNIMIN2c* and *NtNIMIN2-like (FS)* in *N. benthamiana* results in accelerated cell death. These proteins belong to

different groups, NIMIN1-type and NIMIN3-type in Arabidopsis and NIMIN2-type in tobacco, and enhanced emergence of cell death is associated with strong protein accumulation. In self-pollinated transgenic tobacco plants overexpression of the *NIMIN1*, *NtNIMIN2c* and *FS* genes is also accompanied by increased emergence of cell death especially near the flower, resulting in low seed production. Furthermore, the affected plants display defects in growth and leaf morphology.

3. The ability to promote cell death is strongly associated with the C-terminal EAR motif, a conserved transcriptional repression domain. Mutation or deletion of the EAR motif in NIMIN1, NtNIMIN2c and FS significantly reduces the emergence of cell death. EAR motifs are known for their interaction with transcriptional co-repressors like TOPLESS (TPL), which is involved in developmental cell death. In yeast, the N-terminal TPL fragment TPL1/333 can interact with the EAR motif of NIMIN1 and NIMIN3. During transient overexpression in *N. benthamiana* TPL1/333 induces comparable levels of cell death but coexpression with NIMIN1 or NIMIN3 reduces cell death emergence, indicating that NIMIN proteins not only affect NPR1 but also modulate the activity of TPL.
4. Transcriptional repression of the *PR1* promoter by transient overexpression of *NIMIN* genes is often associated with subsequent emergence of cell death. Likewise, overexpression of *Bax* strongly decreases induction of the *ProPR1a::GUS* reporter gene in tissues predetermined for cell death. EAR motif mutants with reduced cell death emergence exhibit similar *PR1a* repression compared to wild type proteins while the *NIMIN1 F49/50S E94A D95V ΔEAR* mutant, which is also unable to bind NPR1, shows significantly decreased *PR1a* repression. Therefore, transcriptional repression by cell death promoting NIMIN proteins can be examined in EAR motif mutants. However, in transgenic tobacco plants no correlation between accumulation of PR1 proteins and NIMIN1 was found.
5. NIMIN1 contains a conserved domain at its N-terminus which regulates its accumulation. When placed in N-terminal position, this 15 amino acid domain, named the N1nT domain, functions autonomously with other NIMIN proteins and Venus, increasing their accumulation. Mutational analysis has not yet revealed reliance on certain sequences. N-terminal fusion of N1nT to NIMIN1b confers the ability to interact with TPL1/333 and induce cell death which is prevented by removal of the EAR domain. Presence of the N-terminal methionine is not required for function of the N1nT domain and M1L mutants still show strong accumulation.

NIMIN proteins are multifunctional and could perform different functions through different conserved domains. While their role in SA-signaling by transcriptional repression of *PR* genes is well known, the results indicate that NIMIN proteins, through their interaction with TOPLESS, could also affect other hormone-dependent signal pathways, e.g., auxin, ethylene, and jasmonic acid signaling. It will therefore be important to analyze the connection between different signaling networks and how they are affected by *NIMIN* gene expression during defense responses. While the exact mechanism behind the enhanced protein accumulation bestowed by the N1nT domain of NIMIN1 is not yet fully understood, it could allow for more effective study of otherwise poorly accumulating proteins.

Zusammenfassung

Die systemisch aktivierte Resistenz (SAR) in Pflanzen ist ein wichtiger Abwehrmechanismus, welcher infolge eines Befalls mit biotrophen Pathogenen initiiert wird. Die SAR geht einher mit der Akkumulation von „pathogenesis-related“ (PR) Proteinen in nichtinfiziertem Gewebe, sowie mit erhöhter Konzentration des Phytohormons Salicylat (SA), dem Signalmolekül der SAR. SA wird direkt von NPR1, dem zentralen Regulatorprotein der SAR, wahrgenommen. NPR1 ermöglicht die SA-abhängige Induktion der *PR1* Genexpression durch Interaktion mit TGA Transkriptionsfaktoren, welche die Bindung an SA-sensitive *as-1* ähnliche Elemente im Promotor des *PR1* Gens vermitteln, und NIM1-INTERACTING (NIMIN) Proteinen. Das Genom von Arabidopsis enthält vier *NIMIN* Gene – *NIMIN1*, *NIMIN1b*, *NIMIN2* und *NIMIN3* – aber Mitglieder der *NIMIN*-Familie sind auch in vielen höheren Pflanzen, wie Tabak und Reis, vertreten. Obwohl NIMIN Proteine deutliche strukturelle Verwandtschaft aufweisen und sowohl ihren generellen Aufbau als auch ein EAR-Motiv (ethylene-responsive element binding factor (ERF)-associated amphiphilic repression motif) gemeinsam haben, unterscheiden sie sich dennoch in anderen Aspekten. Die *NIMIN*-Gene werden während der Entwicklung und Pathogenabwehr unterschiedlich exprimiert. NIMIN Proteine können anhand ihrer NPR1-Interaktionsdomänen, dem DXFFK und dem EDF Motiv, in Gruppen eingeteilt werden. Proteine vom NIMIN1-Typ enthalten beide Domänen, während Proteine vom NIMIN2-Typ nur das DXFFK Motiv und jene vom NIMIN3-Typ nur das EDF Motiv enthalten. Dementsprechend interagieren NIMIN Proteine unterschiedlich mit NPR1 und während NIMIN1, NIMIN1b und NIMIN2 an den C-terminalen Teil von NPR1 binden, interagiert NIMIN3 stattdessen mit dem N-Terminus. In Überexpressionsstudien konnte gezeigt werden, dass NIMIN1 und NIMIN3 eine Rolle in der transkriptionellen Repression der *PR1*-Geninduktion spielen und betroffene Pflanzen eine höhere Anfälligkeit gegen Pathogenbefall aufweisen. Interessanterweise führt Überexpression von Arabidopsis *NIMIN1* und *NIMIN3* oder Tabak *NtNIMIN2c* zu beschleunigtem Auftreten von Zelltod. Die Unterschiede in der Genexpression, der Interaktion mit NPR1, der transkriptionellen Repression von *PR*-Genen, sowie der Förderung von Zelltod legen nahe, dass NIMIN Proteine verschiedene Funktionen innerhalb und außerhalb der SAR innehaben. Ziel dieser Arbeit war es, die unterschiedlichen biochemischen Eigenschaften und biologischen Funktionen der verschiedenen NIMIN Proteine aus Arabidopsis und Tabak genauer zu charakterisieren, wobei besonderes Augenmerk auf ihre Zelltod-fördernde Wirkung gelegt wurde. Zu diesem Zweck wurden Reporter-genkonstrukte mit Promotorsequenzen sowie codierenden Sequenzen von Arabidopsis und Tabak *NIMIN*-Genen in transgenen Tabakpflanzen und während transientscher Genexpression in *Nicotiana benthamiana* analysiert. Funktionelle Domänen wurden durch Einbringen zielgerichteter Mutationen auf ihre Bedeutung für die Funktion der NIMIN Proteine untersucht. Die Ergebnisse dieser Arbeit sind im Folgenden aufgeführt:

1. Die 1135 bp 5'-Promotorregion von *NIMIN1b* ist funktionsfähig in transientscher Expression und erlaubt Aktivität des *GUS*-Reportergens, sowie des proapoptotischen *Bax* Reportergens. In transgenen Tabakpflanzen ist der *NIMIN1b* Promotor jedoch nicht durch Behandlung mit SA oder

dessen funktionellem Analogon BTH induzierbar und auch phänotypische Untersuchungen konnten keine Expression des *Bax* Reportergens während der Entwicklung der Pflanze feststellen. Inwieweit das *NIMIN1b* Gen in der Pflanze exprimiert wird muss daher offenbleiben.

2. Transiente Überexpression von Arabidopsis *NIMIN1* und *NIMIN3*, sowie Tabak *NtNIMIN2c* und *NtNIMIN2-like (FS)* in *N. benthamiana* führt zu beschleunigtem Zelltod. In Arabidopsis gehören diese zu den Gruppen der NIMIN1-Typ und NIMIN3-Typ Proteine, während sie in Tabak zur Gruppe der NIMIN2-Typ Proteine gerechnet werden. Das verstärkte Auftreten von Zelltod steht dabei oft in Verbindung mit starker Proteinakkumulation. In selbstbestäubten transgenen Tabakpflanzen geht Überexpression von *NIMIN1*, *NtNIMIN2c* und *FS* mit vermehrtem Auftreten von Zelltod im Blütenbereich einher, was unter anderem in einer geringen Samenproduktion resultiert. Dazu weisen betroffene Pflanzen oft Defekte in Wachstum und Blattmorphologie auf.
3. Die Zelltod-fördernde Wirkung von NIMIN Proteinen steht in direkter Verbindung mit dem C-terminalen EAR Motiv, einer konservierten, transkriptionellen Repressionsdomäne. Mutation oder Deletion des EAR Motivs in *NIMIN1*, *NtNIMIN2c* und *FS* reduziert das Auftreten von Zelltod erheblich. EAR Motive sind für ihre Interaktion mit dem transkriptionellen Co-Repressor TOPLESS (TPL) bekannt, welcher auch in entwicklungsbedingtem Zelltod involviert ist. In Hefe kann das N-terminale TPL Fragment TPL 1/333 mit den EAR Motiven von *NIMIN1* und *NIMIN3* interagieren. In transients Überexpression induziert TPL1/333 vergleichbare Mengen von Zelltod aber Co-Expression mit *NIMIN1* oder *NIMIN3* verringert diese Entwicklung, was darauf hindeutet, dass NIMIN Proteine nicht nur NPR1 beeinflussen, sondern auch die Aktivität von TPL regulieren.
4. Die durch Überexpression von *NIMIN* Genen induzierte Repression des *PRI* Promotors ist häufig mit einer späteren Ausprägung von Zelltod verknüpft. Ebenso reduziert die Überexpression von *Bax* die Induktion des *ProPRIa:GUS* Reportergens in für Zelltod vorbestimmtem Gewebe. EAR-Motiv Mutanten mit reduzierter Entwicklung von Zelltod zeigen vergleichbare *PRIa* Repression wie der Wildtyp, während die *NIMIN1 F49/50S E94A D95V ΔEAR* Mutante, welche NPR1 nicht binden kann, erheblich reduzierte Repression von *PRIa* aufweist. Die durch Zelltod-fördernde NIMIN Proteine ausgelöste transkriptionelle Repression kann also mittels EAR-Motiv Mutanten untersucht werden. In transgenen Tabakpflanzen konnte jedoch keine direkte Korrelation zwischen der Akkumulation von PR1 Proteinen und *NIMIN1* gezeigt werden.
5. *NIMIN1* enthält am N-Terminus eine konservierte, 15 Aminosäuren lange Domäne, genannt die N1nT Domäne, welche die Akkumulation von *NIMIN1* reguliert. Wenn diese Domäne am N-Terminus anderer NIMIN Proteine und Venus platziert wird, wirkt sie autonom und verstärkt die Proteinakkumulation. Analyse von Mutanten konnte bisher noch keine Sequenzabhängigkeit zeigen. Die N-terminale Fusion von N1nT an *NIMIN1b* verleiht diesem die Fähigkeit zur Interaktion mit TPL1/333, welche durch Entfernen des EAR Motivs verhindert werden kann. Die Anwesenheit des N-terminalen Methionins ist jedoch nicht notwendig für die Funktion der N1nT Domäne und MIL Mutanten weisen noch immer starke Akkumulation auf.

NIMIN Proteine sind multifunktionell und können verschiedene Funktionen durch verschiedene konservierte Domänen ausüben. Während ihre Rolle im SA-Signalweg in der transkriptionellen Repression von *PR*-Genen wohlbekannt ist, deuten die Ergebnisse dieser Arbeit darauf hin, dass NIMIN Proteine, durch ihre Interaktion mit TOPLESS, auch andere Phytohormon-abhängige Signalwege beeinflussen könnten, wie zum Beispiel die Auxin-, Ethylen- und Jasmonsäure-Signalwege. Es wird deshalb wichtig sein die Verbindung zwischen verschiedenen Signalnetzwerken genauer zu analysieren und zu beobachten, wie sie durch die Expression von *NIMIN* Genen während der Pathogenabwehr beeinflusst werden. Während der Mechanismus hinter der, durch die N1nT Domäne verliehenen, erhöhten Proteinakkumulation noch nicht vollständig aufgeklärt ist, könnte diese Domäne dennoch zur effizienteren Untersuchung von Proteinen mit ansonsten niedriger Akkumulation beitragen.

Abbreviations

°C	degrees Celsius
Ø	diameter
A	Ampere
aa	amino acid
AA	anthranilic acid
acd	accelerated cell death
AD	activation domain
AIM1	abnormal fluorescence meristem1
Ala	alanine
ALD1	AGD2-like defense response protein1
Amp	ampicillin
Amp ^R	ampicillin resistance
ARF	auxin response factor
Arg	arginine
<i>as-1</i>	<i>as-1</i> element (<i>activation sequence 1</i>)
ASF-1	<i>as-1</i> binding factor
Asp	aspartic acid
At	<i>Arabidopsis thaliana</i>
<i>A. tumefaciens</i>	<i>Agrobacterium tumefaciens</i>
AUX/IAA	auxin/indole-3-acetic acid
Avr	avirulence
AZA	azelaic acid
BA	benzoic acid
BAK1	Brassinosteroid insensitive-1 (BRI1)-associated receptor kinase1
BD	binding domain
BGL2	β-1,3-glucanase
bHLH	basic helix-loop-helix
BOP	blade-on-petiole
bp	base pairs
BP	NIMIN1-like1 (<i>N. tabacum</i>)
BTH	S-methyl-1,2,3-benzothiadiazole-7-carbothioate
BTB/POZ	broad complex, tramtrack and bric-à-brac/pox virus and zinc finger

bZIP	basic leucine zipper
<i>CaMV</i>	Cauliflower mosaic virus
CAP	cysteine-rich secretory protein, antigen 5, and pathogenesis-related-1
CAPE	CAP-derived peptide
CC	coiled-coil
CDK	cyclin-dependent kinase
CDPK	calcium-dependent protein kinase
CIAP	calf intestine alkaline phosphatase
cim	constitutive immunity
CM	chorismate mutase
cpr	constitutive expressor of PR genes
C-terminus	carboxy terminus
Cys	cysteine
DA	dihydroabietinal
DAMP	damage-associated molecular pattern
DCA	dichloro-anthranilic acid
ddTTP	2',3'-dideoxythymidine-5'-triphosphate
dH ₂ O	deionized water
DIR1	defective in induced resistance 1
DMSO	dimethyl sulfoxide
DNA	deoxyribonucleic acid
dNTP	2'-deoxynucleotide-5'-triphosphate (dATP, dCTP, dGTP, dTTP)
dpi	days post inoculation
dsDNA	double stranded DNA
DTT	dithiothreitol
EAR	ERF binding factor-associated amphiphilic repression
ECL	enhanced chemiluminescence
<i>E. coli</i>	<i>Escherichia coli</i>
EDS	enhanced disease susceptibility
EDTA	ethylenediaminetetraacetic acid
EF-Tu	elongation factor Tu
EFR	EF-Tu receptor
e.g.	<i>exempli gratia</i> (for example)
EGF	epidermal growth factor

Abbreviations

ERF	ethylene-responsive element
<i>et al.</i>	<i>et alii</i> (and others)
EtBR	ethidiumbromide
ET	ethylene
ETI	effector triggered immunity
EtOH	ethanol
ETS	effector triggered susceptibility
FG	NIMIN1-like2 (<i>N. tabacum</i>)
Fig.	Figure
FLS2	flagellin sensing2
FMO1	flavin-dependent monooxygenase1
FS	NIMIN2-like1 (<i>N. tabacum</i>)
g	gram
G3P	glycerol-3-phosphate
Gent	gentamycin
GFP	green fluorescent protein
Glu	glutamic acid
GNSO	S-nitrosoglutathione
GUS	β -glucuronidase
HCl	hydrochloric acid
His	histidine
HR	hypersensitive response
HRP	horseradish peroxidase
ICS	isochorismate synthase
IgG	Immunoglobulin G
I κ B	Inhibitor of κ B
INA	2,6-dichloro-isonicotinic acid
IPTG	Isopropyl- β -D-1-thiogalactopyranoside
JA	jasmonic acid
JAZ	jasmonate-ZIM domain
Kan	kanamycin
Kan ^R	kanamycin resistance
kb	kilo base pairs
kDa	kilo Dalton

KNOX	Knotted-like homeox
KOAc	potassium acetate
KOH	potassium hydroxide
l	liter
lacZ	β -galactosidase
LB	Luria Bertani Medium
LBD	ligand-binding domain
Leu	Leucine
LRR	leucine-rich-repeat
lsd	lesion stimulating disease
LS	linker scan
LSU	large subunit
Lys	lysine
LysM	lysine motif
M	molar
MAMP	microbe-associated molecular pattern
MAPK	mitogen-activated protein kinase
MCS	multiple cloning site
MeSA	methylsalicylic acid
min(s)	minute(s)
mRNA	messenger RNA
MS	Murashige und Skoog
MSH	β -mercaptoethanol
MTB	Myc2-targeted bHLH
MU	4-methylumbelliferone
MUG	4-methylumbelliferyl- β -D-glucuronide
N1/N2BD	NIMIN1/NIMIN2 binding domain
N1	AtNIMIN1
N2	AtNIMIN2
N3	AtNIMIN3
N ₂	nitrogen
NaCl	sodium chloride
Na-MOPS	sodium 3-(N-morpholino) propanesulfonic acid
NaOH	sodium hydroxide

Abbreviations

<i>N. benthamiana</i>	<i>Nicotiana benthamiana</i>
NBS	nucleotide-binding site
NF- κ B	nuclear factor binding near the κ light-chain gene in B cells
NH	NPR1 homologue
NHP	N-hydroxy-pipecolic acid
NIM1	non-inducible immunity1
NIMIN	NIM1-interacting protein
NLS	nuclear localization signal
NLR	NBS-LRR, nucleotide-binding site leucine-rich-repeat
NPR1	nonexpressor of pathogenesis related genes1
NRR	negative regulator of resistance
N-terminus	amino terminus
Nt	<i>Nicotiana tabacum</i>
OD _x	optical density at x nm
o/n	over night
oNPG	o-nitrophenyl- β -galactoside
ORF	open reading frame
ori	origin
Os	<i>Oryza sativa</i>
<i>p.a.</i>	<i>pro analysis</i> (analytically pure)
PAL	phenylalanine ammonia-lyase
PAMP	pathogen-associated molecular pattern
PAN	PERIANTHIA
PBS	avrPphB susceptible
PCD	programmed cell death
PCR	polymerase chain reaction
pH	potential of hydrogen, negative base 10 logarithm of the molar concentration of hydrogen ions in solution
Phe	phenylalanine
Pip	pipecolic acid
PR	pathogenesis related
PRR	pattern recognition receptor
<i>ProXX</i>	promoter of gene XX
<i>P. syringae</i>	<i>Pseudomonas syringae</i>
<i>Pst</i>	<i>Pseudomonas syringae</i> pv. <i>tomato</i>

PTI	PAMP-triggered-immunity
<i>pv</i>	pathovar
R	resistance
RBOHD	respiratory burst oxidase homolog D
RH	NRR repressor homologue
Rif	rifampicin
RKS1	resistance related kinase1
RLCK	receptor-like cytoplasmic kinase
RLK	receptor-like kinase
RLP	receptor-like proteins
RNA	ribonucleic acid
RNase	ribonuclease
ROS	reactive oxygen species
rpm	revolutions per minute
RuBisCO	ribulose-1,5-bisphosphate carboxylase/oxygenase
s	second(s)
SA	salicylic acid
SAI1	salicylic acid insensitive1
SAR	systemic acquired resistance
SARD4	SAR deficient4
SBC	SA-binding core
<i>S. cerevisiae</i>	<i>Saccharomyces cerevisiae</i>
SD	synthetic drop-out
SDS-PAGE	sodium dodecyl sulfate polyacrylamide gel electrophoresis
Ser	serine
SINC	SA-induced NPR1 condensate
SNRK2.8	sucrose non-fermenting1 (SNF1)-related kinase 2.8
SUMO	small ubiquitin-like modifier
T3SS	type III secretion system
TAE	Tris-acetate-EDTA buffer
Taq-Polymerase	<i>Thermophilus aquaticus</i> DNA-polymerase
TBS	Tris buffered saline
<i>TBSV</i>	Tomato bushy stunt virus
tCA	trans-cinnamic acid

Abbreviations

TCP	Teosinte branched1, Cycloidea, PCF1
TDT	terminal deoxynucleotidyl transferase
TE	Tris-EDTA buffer
TEMED	N,N,N',N'-tetramethylethane-1,2-diamine
TF	transcription factor
Tfb	transformation buffer
Ti	tumor inducing
TIR	Toll/interleukin1 receptor domain
TPL	topless
TRX	thioredoxin
TTBS	Tris buffered saline with Tween 20
<i>TMV</i>	tobacco mosaic virus
<i>TNV</i>	tobacco necrosis virus
Tris	2-amino-2-(hydroxymethyl)propane-1,3-diol
Tyr	tyrosine
U	enzyme unit
UV	ultraviolet
V	Volt
Val	valine
WT	wild type
X-Gal	5-bromo-4-chloro-3-indolyl- β -D-galactopyranoside
X g	X times gravitational constant
YPAD	yeast extract-peptone-adenine-dextrose
Y2H	yeast two-hybrid
ZAR1	HOPZ activated resistance1
w/v	weight per volume
v/v	volume per volume
λ	wavelength in nm

Table of Figures

Fig. 1	Simplified schematic representation of the plant immune system.	5
Fig. 2	Domain architecture of Arabidopsis NIMIN proteins.	16
Fig. 3	Perception of salicylic acid and regulation of <i>PR1</i> gene induction through consecutive interaction of NIMIN proteins and NPR1 during SAR.	21
Fig. 4	Accumulation of Arabidopsis NPR1, NPR3 and NIMIN1 as Venus fusion proteins in <i>N. benthamiana</i>	51
Fig. 5	Subcellular localization of Arabidopsis NIMIN1, NPR1 and NPR3 as Venus fusion proteins in <i>N. benthamiana</i>	52
Fig. 6	Structural formulas of salicylic acid analogs.....	54
Fig. 7	Chemical induction of <i>PR1a</i> , <i>NIMIN1</i> and <i>NIMIN2</i> promoter constructs in transgenic tobacco plants after chemical induction using salicylic acid (SA), 4-hydroxybenzoic acid (4-OH BA), S-Methyl 1,2,3-benzothiadiazole-7-carbothioate (BTH), Anthranilic Acid (AA), 3,5-Dichloroanthranilic acid (3,5-DCA) and Pípecolic acid (Pip).....	57
Fig. 8	Phenotypic effects of transient overexpression of <i>NIMIN1</i> and <i>Bax</i> constructs in <i>N. benthamiana</i> plants.....	59
Fig. 9	Influence of salicylic acid on the germination of transgenic tobacco seeds.....	60
Fig. 10	Influence of salicylic acid on the germination of transgenic tobacco seeds.....	61
Fig. 11	Influence of salicylic acid on the germination of transgenic tobacco seeds.....	62
Fig. 12	Effects of SA and BTH on tobacco plants containing <i>ProN1:Bax</i> and <i>ProN1b:Bax</i> reporter constructs.....	64
Fig. 13	Phenotypic effects of transient overexpression of <i>NIMIN1</i> in <i>N. benthamiana</i> plants.	66
Fig. 14	Interaction of NIMIN1, NIMIN1-Venus and Venus with AtNPR1 in yeast.....	67
Fig. 15	Phenotypic effects of transient overexpression of <i>NIMIN1-Venus</i> in <i>N. benthamiana</i> plants.	68
Fig. 16	Transient overexpression of <i>NIMIN1</i> and <i>NIMIN1-Venus</i> in <i>N. benthamiana Pro-1533PR-1a:GUS</i> plants.....	69
Fig. 17	Transient overexpression of <i>NIMIN1-Venus</i> and <i>NIMIN1b-Venus</i> in <i>N. benthamiana Pro-1533PR-1a:GUS</i> plants.....	71
Fig. 18	Transient overexpression of <i>NIMIN1-Venus</i> and <i>NIMIN2-Venus</i> in <i>N. benthamiana Pro-1533PR-1a:GUS</i> plants.....	72
Fig. 19	Transient overexpression of <i>NIMIN1-Venus</i> and <i>NIMIN3-Venus</i> in <i>N. benthamiana</i> plants.	73
Fig. 20	GUS reporter gene activity of <i>NIMIN1</i> and <i>NIMIN2</i> promoter constructs and phenotype of <i>Nicotiana benthamiana</i> plants after chemical induction during NIMIN protein overexpression.....	75

Fig. 21 Domain architecture of tobacco NIMIN proteins.	76
Fig. 22 Interaction of tobacco NIMIN and NPR proteins in yeast.....	77
Fig. 23 Transient overexpression of <i>NIMIN1-Venus</i> , <i>BP-Venus</i> , and <i>FG-Venus</i> in <i>N. benthamiana</i> <i>Pro-1533PR-1a:GUS</i> plants.	78
Fig. 24 Transient overexpression of <i>NIMIN1-Venus</i> and <i>NtNIMIN2c-Venus</i> in <i>N. benthamiana</i> <i>Pro-1533PR-1a:GUS</i> plants.	79
Fig. 25 Transient overexpression of <i>NIMIN1-Venus</i> and <i>FS-Venus</i> in <i>N. benthamiana</i> <i>Pro-1533PR-1a:GUS</i> plants.	80
Fig. 26 Accumulation of NIMIN-Venus fusion proteins from tobacco during transient overexpression in <i>N. benthamiana</i> plants.	81
Fig. 27 Interaction of NIMIN1 mutants in the DXFFK and EDF motifs and NPR1 proteins in yeast.	82
Fig. 28 Characterization of primary tobacco transformants (T0 generation) harboring <i>Pro35S:NIMIN1-Venus</i> and <i>Pro35S:N1 F49/50S</i>	83
Fig. 29 Accumulation of NIMIN1-Venus and N1 F49/50S in T1 seedlings harboring <i>Pro35S:NIMIN1-Venus</i> and <i>Pro35S:N1 F49/50S</i>	84
Fig. 30 Phenotype development during flower formation of T1 tobacco plants harboring <i>Pro35S:NIMIN1-Venus</i> and <i>Pro35S:N1 F49/50S</i>	85
Fig. 31 Phenotype development during flower formation of T2 tobacco plants harboring <i>Pro35S:NIMIN1-Venus</i>	87
Fig. 32 Leaf morphology and growth phenotype of T3 tobacco plants harboring <i>Pro35S:NIMIN1-Venus</i>	88
Fig. 33 Accumulation of PR1 proteins after SA mediated induction in T1 tobacco plants harboring <i>Pro35S:NIMIN1-Venus</i> and <i>Pro35S:N1 F49/50S</i>	89
Fig. 34 Phenotype and accumulation of PR1 proteins after chemical induction in transgenic T2 tobacco plants expressing <i>N1-Venus</i>	91
Fig. 35 Accumulation of PR1 proteins after TMV infection in transgenic T2 tobacco plants expressing <i>N1-Venus</i>	92
Fig. 36 Accumulation of PR1 proteins during SAR establishment after TMV infection in transgenic T2 tobacco plants expressing <i>N1-Venus</i>	93
Fig. 37 Accumulation of <i>NtN2c-Venus</i> and <i>FS-Venus</i> fusion proteins in primary tobacco transformants (T0 generation).	94
Fig. 38 Germination of transgenic T1 seedlings harboring <i>Pro35S:NtN2c-Venus</i> and <i>Pro35S:FS-Venus</i>	95
Fig. 39 Phenotype development of transgenic tobacco plants expressing <i>NtN2c-Venus</i> and <i>FS-Venus</i> in the T1 generation.	96
Fig. 40 Conservation of NPR1 binding domains from Arabidopsis and tobacco NIMIN proteins.	97

Fig. 41 Transient overexpression of <i>NIMIN1-Venus</i> and <i>NIMIN1 F49/50S-Venus</i> in <i>N. benthamiana Pro-1533PR-1a:GUS</i> plants.	99
Fig. 42 Transient overexpression of <i>NIMIN1-Venus</i> and <i>NIMIN1 E94A D95V-Venus</i> in <i>N. benthamiana Pro-1533PR-1a:GUS</i> plants.	100
Fig. 43 Interaction of N1 and N1 F49/50S E94A D95V with AtNPR1 and AtTPL 1/333 in yeast. ..	101
Fig. 44 Transient overexpression of <i>NIMIN1-Venus</i> and <i>NIMIN1 F49/50S E94A D95V-Venus</i> in <i>N. benthamiana Pro-1533PR-1a:GUS</i> plants.	102
Fig. 45 EAR motifs domains from Arabidopsis and tobacco NIMIN proteins.	103
Fig. 46 Interaction Arabidopsis NIMIN proteins and AtTPL fragments in yeast.....	104
Fig. 47 Transient overexpression of <i>NIMIN1</i> , <i>NIMIN1 L138/140A</i> and Venus fusions in <i>N. benthamiana Pro-1533PR1a:GUS</i> plants.....	106
Fig. 48 Accumulation and PR1a promoter repression of <i>NIMIN1</i> , <i>NIMIN1 L138/140A</i> and Venus fusions in <i>N. benthamiana Pro-1533PR1a:GUS</i> plants during transient overexpression.	107
Fig. 49 Transient overexpression of <i>N1</i> and <i>N1ΔEAR</i> in <i>N. benthamiana Pro-1533PR-1a:GUS</i> plants.	108
Fig. 50 Interaction of N1 F49/50S E94A D95V ΔEAR with AtNPR1 and AtTPL 1/333 in yeast. ...	109
Fig. 51 Transient overexpression of <i>NIMIN1-Venus</i> and <i>NIMIN1 F49/50S E94A D95V ΔEAR-Venus</i> in <i>N. benthamiana Pro-1533PR-1a:GUS</i> plants.....	110
Fig. 52 Interaction of tobacco NIMIN proteins and mutants in the NPR1 binding and EAR motifs with AtTPL1/333 or NgNPR1 in yeast.	111
Fig. 53 Transient overexpression of <i>FS-Venus</i> , <i>FS F48/49S-Venus</i> and <i>FSΔEAR-Venus</i> in <i>N. benthamiana Pro-1533PR-1a:GUS</i> plants.	113
Fig. 54 Protein accumulation of FS-Venus, FS F48/49S-Venus and FSΔEAR-Venus in <i>N. benthamiana Pro-1533PR-1a:GUS</i> plants during transient overexpression.	114
Fig. 55 Transient overexpression of <i>NtN2c-V</i> and <i>NtN2cΔEAR-V</i> in <i>N. benthamiana WT</i> plants.	115
Fig. 56 Transient overexpression of <i>NIMIN1-Venus</i> and <i>TPL1/333</i> in <i>N. benthamiana</i> plants.	116
Fig. 57 Transient coexpression of <i>TPL1/333</i> with <i>NIMIN1</i> , <i>NIMIN2</i> or <i>NIMIN3</i> in <i>N. benthamiana</i> plants.	117
Fig. 58 Concentration dependent effects of transient overexpression of a <i>ProN1b:Bax</i> reporter constructs in <i>N. benthamiana</i> plants.....	119
Fig. 59 Analysis of the amino acids sequence and hydrophobic properties of NIMIN1 and NIMIN1b.	121
Fig. 60 Conservation of the N-terminus of NIMIN1-like proteins.	122
Fig. 61 Transient overexpression of <i>NIMIN1-Venus</i> and <i>NIMIN1 16/142-Venus</i> in <i>N. benthamiana Pro-1533PR-1a:GUS</i> plants.....	123
Fig. 62 Hydrophobic properties and interaction of N1nT-NIMIN1b with AtNPR1 and AtTPL1/333.....	124

Fig. 63 Transient overexpression of <i>NIMIN1-Venus</i> , <i>NIMIN1b-Venus</i> und <i>N1nT-NIMIN1b-Venus</i> in <i>N. benthamiana</i> plants.	126
Fig. 64 Interaction of NIMIN1b, N1nT-NIMIN1b and N1nT-NIMIN1b Δ EAR with AtNPR1 and AtTPL1/333 in yeast.	127
Fig. 65 Transient overexpression of <i>N1nT-NIMIN1b-V</i> and <i>N1nT-NIMIN1bΔEAR-V</i> in <i>N. benthamiana</i> plants.	128
Fig. 66 Hydrophobic properties of N1nT-NIMIN2.	129
Fig. 67 Transient overexpression of <i>NIMIN2-Venus</i> , <i>N1nT-NIMIN1b-Venus</i> and <i>N1nT-NIMIN2-Venus</i> in <i>N. benthamiana</i> WT plants.	130
Fig. 68 Transient overexpression of <i>NIMIN1-Venus</i> and <i>N1nT-Venus</i> in <i>N. benthamiana</i> plants.	131
Fig. 69 Fluorescence and protein accumulation of N1nT-Venus in <i>N. benthamiana</i> plants.	132
Fig. 70 Proteolytic degradation of the fluorescent proteins GFP, Venus and N1nT-Venus under influence of Proteinase K, Trypsin and Papain.	133
Fig. 71 Transient overexpression of <i>N1nT-NIMIN1b-V</i> and <i>NIMIN1b-N1nT-V</i> in <i>N. benthamiana</i> plants.	135
Fig. 72 Fluorescence and protein accumulation of N1nT-Venus and Venus-N1nT in <i>N. benthamiana</i> plants.	136
Fig. 73 Transient overexpression of <i>N1nT-NIMIN1b-Venus</i> , <i>N1nTΔ2-4-NIMIN1b-Venus</i> and <i>N1nT L8G-NIMIN1b-V</i> in <i>N. benthamiana</i> plants.	137
Fig. 74 Transient overexpression of <i>N1nT-NIMIN1b-V</i> and <i>N1nTΔ2-9-NIMIN1b-V</i> in <i>N. benthamiana</i> plants.	138
Fig. 75 Transient overexpression of <i>N1nT-NIMIN1b-V</i> and <i>N1nT SY-NIMIN1b-V</i> in <i>N. benthamiana</i> plants.	139
Fig. 76 Transient overexpression of <i>N1nT-NIMIN1b-V</i> and <i>N1nT MIL-NIMIN1b-V</i> in <i>N. benthamiana</i> plants.	140
Fig. 77 Fluorescence and protein accumulation of N1nT-Venus, N1nT Δ 2-9-Venus and N1nT MIL-Venus in <i>N. benthamiana</i> WT plants.	141
Fig. 78 Amplification and analytic restriction of chimeric N1nT- and N1nT MIL gene constructs.	142
Fig. 79 Predicted secondary mRNA Structure for hybrid <i>N1nT-NIMIN1b-Venus</i> and <i>N1nT-Venus</i> genes.	156
Fig. A1 Differential detection of the fluorescent proteins GFP, Venus and N1nT-Venus by the α -GFP (FL) and α -GFP (MC) antisera.	181

1. Introduction

The increasing demand of food production by means of agriculture presented by a growing world population [Tripathi *et al.*, 2019] is opposed by an increasing abundance of extreme weather conditions like droughts and flooding caused by climate change [Cheeseman, 2016] and emerging plant pathogens [Savary *et al.*, 2019] which compromise agricultural productivity. This is of growing concern regarding food security, making it necessary to develop new approaches for enhancing the resistance of crop plants. Since plants are sessile organisms, they are unable to actively withdraw from their location, while being exposed to different types of stress, both biotic and abiotic, which have severe negative effects on plant growth, development, and reproduction. Because of this, plants had to adapt and develop new mechanisms to cope with these stresses. To endure abiotic stress factors, like humidity, salinity, radiation, and temperature, and to grow in otherwise harmful environments, plants evolved physiological adaptations like water storage in succulents [Eggle & Nyffeler, 2009], salt excretion in certain mangroves [Gilbert *et al.*, 2002], as well as differential gene expression allowing light-stress induced pigment changes [Kuhlemeyer *et al.*, 1987; Strid *et al.*, 1994]. Biotic stress on the other hand is caused by living organisms. Herbivorous macro-organisms like insects, birds, and mammals directly damage plant tissues, while microbial pathogens like fungi, bacteria, and viruses can cause various kinds of infections or diseases. Emerging plant pathogens are one of the most important factors regarding food security causing average yield losses between 10 and 40 % [Anderson *et al.*, 2004; Gurr *et al.*, 2011; Savary *et al.*, 2019]. These phytopathogens can be further divided into three groups: necrotrophs, biotrophs and hemibiotrophs. Necrotrophic pathogens, like the fungi *Botrytis cinera* and *Sclerotinia sclerotiorum*, kill the host tissue and feed on the released nutrients. Biotrophs and hemibiotrophs require a living host and subvert its metabolism to promote their own growth, with the latter killing their host at later stages of infection [Hammond-Kosack & Jones, 1997; Vleeshouwers & Oliver, 2014]. To protect themselves from the plethora of phytopathogens, plants had to adapt and evolve a wide arsenal of defense mechanisms, preventing pathogen entry and growth.

The vast majority of potential pathogens can be deterred through a phenomenon commonly referred to as non-host resistance. This type of resistance includes both, preformed (passive) and induced (active) defense mechanisms, and protects all genotypes of a plant species by preventing non-adapted microbes from causing an infection, allowing the plant to preserve important resources for growth and reproduction. [Heath, 2000; Mysore & Ryu, 2004]. Passive defense mechanisms involve both physical barriers in form of specific morphological structures, as well as stored chemical compounds with antimicrobial properties. Barriers like the waxy cuticle [Yeats and Rose, 2013], the cell wall [Hamann, 2012] and the actin microfilaments of the plant cytoskeleton [Kobayashi *et al.*, 1992, 1997] not only prevent the intrusion of phytopathogens and other microbes but also mediate structural integrity and protection against other external sources of stress. Secondary metabolites comprise a wide variety of substances including alkaloids, tannins, terpenes, and phenols [Wink, 1988]. When preformed and

stored by the plant, they are called phytoanticipins [Van Etten *et al.*, 1994] and can be released upon pathogen perception or as result of cell damage. These substances act as chemical barriers by affecting or harming herbivores and pathogens through toxic, allelopathic, or deterring properties [Wink, 1988; Anulika *et al.*, 2016]. Similarly, pathogens have evolved mechanisms to overcome physical barriers like the cell wall and survive in presence of secondary metabolites lethal to other microorganisms. Fungal pathogens can invade plant tissue through the cuticle and cell wall by mechanical penetration or secretion of cutinases, cellulases or similar enzymes [Mendgen *et al.*, 1996; Annis & Goodwin, 1997]. Since bacteria and viruses cannot directly penetrate the epidermis, they have to rely on using either plant wounds, caused by herbivores, pests, or weather conditions, or natural openings like stomata, nectarthodes, or hydathodes [Melotto *et al.*, 2008]. The invading pathogens must then overcome the complex induced defense responses associated with the innate immune system of the plant.

1.1. Innate immunity

Unlike vertebrate animals, which have evolved an adaptive immune system based on mobile immune cells and reshuffling of immunoglobulin genes, allowing detection of an almost limitless variety of pathogens, invertebrate animals (e.g. *Drosophila melanogaster*, *Caenorhabditis elegans*) and plants both completely depend on innate immunity [Zipfel & Felix, 2005; Boller & Felix, 2009]. Even though plants are lacking mobile immune cells specialized on pathogen recognition, their innate immunity is an extraordinarily complex and efficient mechanism enabling pathogen specific immune responses.

1.1.1. Pattern-triggered immunity (PTI)

Innate immunity is initiated by recognition of specific conserved molecules, originally called elicitors [Darvill & Albersheim 1984]. Today one usually speaks of pathogen-associated molecular patterns (PAMPs) or microbe-associated molecular patterns (MAMPs), since these molecules have been associated with non-pathogenic microbes as well. PAMPs are essential molecules, being characteristic of a whole class of microbes. Bacterial flagellin, elongation factor Tu (EF-Tu), and lipopolysaccharides as well as fungal chitin are just a few common examples [Ausubel, 2005; Staal & Dixelius, 2007; Boller & Felix, 2009]. Their importance during live cycle, fitness or survival makes them difficult to mutate and, as a result, PAMPs are slowly evolving [Jones & Dangl, 2006; Zhang *et al.*, 2017a]. Aside from microbial patterns, plants can also detect so-called damage-associated molecular patterns (DAMPs), which are host-derived cell wall remains or other degradation products as well as endogenous peptides or signaling molecules that arise during pathogen attack or cell damage [Lotze & Tracey, 2005; Lotze *et al.*, 2007; Choi *et al.*, 2016; Choi & Klessig, 2016]. As far as known, all major classes of biomolecules, including proteins, carbohydrates, lipids, and nucleic acids, can be PAMPs and DAMPs. The perception of both, DAMPs, plant molecules released or changed during pathogen attack (altered-self), and PAMPs, extrinsic molecules related to the pathogen (non-self), allows recognition of a greater variety of pathogens and diversity in immune responses [Boutrot & Zipfel, 2017]. Perception of PAMPs and DAMPs is mediated by pattern recognition receptors (PRRs), localized on the surface of the plasma

membrane of all plant cells, which ultimately induce a form of defense response called pattern-triggered immunity (PTI) [Jones & Dangl, 2006; Boller & Felix, 2009]. PRRs are categorized into two distinct groups. Receptor-like kinases (RLKs) consist of three domains: an extracellular ligand-binding domain (LBD), a transmembrane domain, and an intracellular kinase domain important for signal transduction. Receptor-like proteins (RLPs) contain both, the LBD, and the transmembrane domains, but lack obvious intracellular signaling domains. Dependent on the type of ligand, LBDs feature leucine-rich-repeats (LRRs), lysin motifs (LysMs), lectin-like motifs or epidermal growth factor (EGF)-like domains [Boutrot & Zipfel, 2017; Saijo *et al.*, 2018].

A prime example of an interaction between PAMPs and PRRs are flg22 and FLS2. The PAMP flg22 is an epitope of bacterial flagellin and is able to trigger a defense response in a wide array of plants, affecting the expression of over 1000 genes in *Arabidopsis* in less than 30 minutes [Gómez-Gómez & Boller, 2002; Zipfel *et al.*, 2004]. Since the mobility of many bacteria is dependent on flagella, recognition of flg22 allows the host plant the detection of these pathogens. The LRR-RLK Flagellin Sensitive 2 (FLS2) is a structural analog to human Toll-like receptor 5 (TLR5) and the responsible PRR for flagellin recognition in *Arabidopsis thaliana* [Kopp & Medzhitov, 1999; Chinchilla *et al.*, 2006]. Plants carrying mutations in the *FLS2* gene show enhanced susceptibility to bacteria like *Pseudomonas syringae* pv. *tomato* (*Pst*) DC3000, due to impaired binding of flg22 [Zipfel *et al.*, 2004]. Similarly, perception of an 18 to 26 amino acid long domain of N-acetylated EF-Tu (elf18-elf26) is mediated by the LRR-RLK EF-Tu receptor (EFR), found only in the plant family Brassicaceae. Interfamily-transfer of EFR from *Arabidopsis thaliana* to *Nicotiana benthamiana* and *Solanum lycopersicum* confers resistance to a variety of phytopathogenic bacteria and shows the effectiveness of the expansion of the PRR repertoire of the host [Zipfel *et al.*, 2006; Lacombe *et al.*, 2010]. During signal transduction, some PRRs associate with other RLKs. It has been shown that BRI1 associated receptor kinase1 (BAK1) can associate with FLS2 or EFR in receptor complexes, with BAK1 acting as a co-receptor. Silencing *BAK1* expression affects responses to different PAMPs including flg22 [Chinchilla *et al.*, 2007; Heese *et al.*, 2007; Roux *et al.*, 2011; Sun *et al.*, 2013].

Within short time after perception of PAMPs and DAMPs, several cellular responses are triggered. An opening of ion channels in the plasma membrane leads to a rapid influx of extracellular Ca^{2+} , called the Ca^{2+} burst, which peaks at around 5 minutes. This increase in cytosolic Ca^{2+} results in the opening of other ion channels and subsequent depolarization of the plasma membrane [Jeworutzki *et al.*, 2010; Ranf *et al.*, 2011; Alhoraibi *et al.*, 2019]. Simultaneous phosphorylation events of RLK complexes lead to activation of downstream signal transduction cascades, mediated primarily by members of the CDPK (calcium-dependent protein kinases) and MAPK (mitogen-activated protein kinase) families of protein kinases [Boudsocq *et al.*, 2010; Lassowskat *et al.*, 2014; Saijo *et al.*, 2018]. During signal transduction, rapid accumulation of reactive oxygen species (ROS), like superoxide O_2^- and H_2O_2 , can be observed after phosphorylation of the NADPH oxidase RBOHD (respiratory burst oxidase homolog D) by CDPKs [Ranf *et al.*, 2011; Dubiella *et al.*, 2013; Kadota *et al.*, 2014; Alhoraibi *et al.*, 2019]. The signal

forwarded by kinase cascades ultimately culminates in the activation of transcription factors (TFs). For example, members of the WRKY family of TFs have been shown to be induced after perception of flg22 [Eulgem & Somssich, 2007; Boller & Felix, 2009; Jeworutzki *et al.*, 2010]. The following metabolic and transcriptional reprogramming results in modulation of the expression of thousands of genes, allowing for execution of an appropriate immune response tailored to the pathogen [Zipfel *et al.*, 2004; Denoux *et al.*, 2008]. This includes the induction of biosynthesis of phytoalexins, secondary metabolites accumulating after pathogen contact. Phytoalexins like camalexin from *Arabidopsis thaliana* are known to restrict growth of several pathogenic microorganisms [Glazebrook & Ausubel, 1994]. The transcriptional changes also affect the regulation of several plant hormones including ethylene (ET) [Ecker & Davis, 1987], jasmonic acid (JA) [Wasternack & Parthier, 1997] and salicylic acid (SA) [Raskin, 1992], all well known to play roles in different pathways of plant immune response. Several MAPK cascades have been proposed to be involved in SA-mediated defense gene activation, with the MPK4 cascade negatively regulating SA signaling [Petersen *et al.*, 2000; Beckers *et al.*, 2009; Alhoraibi *et al.*, 2019]. Mutants unable to synthesize SA exhibit partially impaired PTI and altered expression levels of some PAMP-triggered genes [Tsuda *et al.*, 2008 a, b]. While perception of PAMPs like flg22 or PGN can induce the expression of *pathogenesis-related gene 1* (*PR1*), which is associated with SA-mediated defense responses and an acknowledged marker of systemic acquired resistance (SAR), the same is not the case for fungal PAMPs like chitin [Gust *et al.*, 2007; Tsuda *et al.*, 2008 a, b].

1.1.2. Effector-triggered immunity (ETI)

PTI allows the plant to effectively detect the majority of microbial pathogens, which successfully penetrated or bypassed the physical barriers, and to initiate adequate defense responses (Fig. 1A). Pathogens had to adapt to the mechanisms of PTI, allowing them to colonize the plant despite intricate defense reactions. To overcome the plant immune system, pathogens evolved so called effector molecules, strain specific proteins, nucleic acids, carbohydrates, or other metabolites. These effectors function as virulence factors and mediate the infection of specific plant species. They can either be delivered directly into the plant cell (intracellular effectors) or secreted to act in the extracellular space (apoplastic effectors) [Misas-Villamil & Van der Hoorn; 2008; Hogenhout *et al.*, 2009; Alhoraibi *et al.*, 2019]. Several pathogenic Gram-negative bacteria, including *Pseudomonas syringae*, use the type III secretion system (T3SS) [Szurek *et al.*, 2002; Block *et al.*, 2008], heteromultimeric protein complexes working like nanomachines. These complexes feature needle-like structures (or injectisomes), which can penetrate the host membranes, allowing secretion of effector proteins directly into the cytoplasm of the host cell [Erhardt *et al.*, 2010; Kuhlen *et al.*, 2018]. Analysis of the *Pst* DC3000 genome alone revealed genes for 31 effectors and some additional genes important for translocation of said effectors [Buell *et al.*, 2003]. The targets of effectors are usually components of the immune response. The effector HopA11, a phosphothreonine lyase from *P. syringae*, inactivates MPK3, MPK4 and MPK6 by dephosphorylation [Zhang *et al.*, 2007]. PAMP receptors like FLS2 and EFR can also be directly targeted by effectors like AvrPtoB, which can inhibit BAK1 [Shan *et al.*, 2008]. Plants that are unable

to detect an effector have their immunity suppressed and exhibit disease symptoms. This phenomenon is also called effector triggered susceptibility (ETS, Fig. 1B) [Block *et al.*, 2008; Saijo *et al.*, 2018].

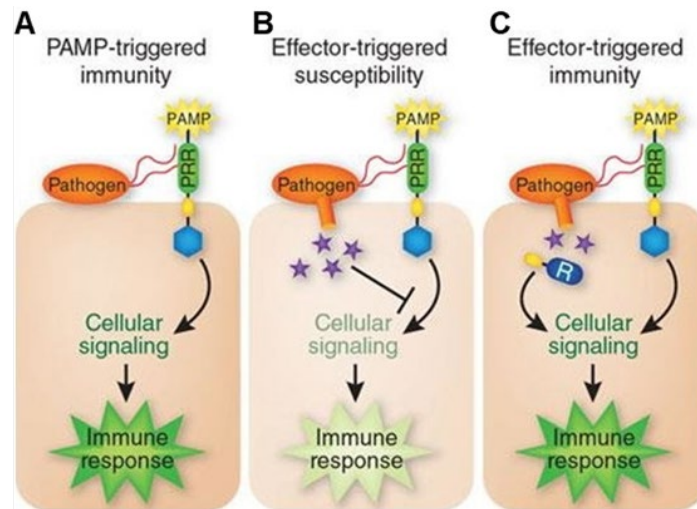


Fig. 1 Simplified schematic representation of the plant immune system. (A) In case of a pathogen attack, PAMPs activate PRRs in the host, triggering downstream signaling cascades that lead to PAMP-triggered immunity (PTI). (B) Effectors (purple stars) released by virulent pathogens suppress PTI, resulting in effector-triggered susceptibility (ETS). (C) Plants that have developed resistance (R) proteins recognizing these pathogen-specific effectors, can induce a secondary immune response called effector-triggered immunity (ETI). [Pieterse *et al.*, 2009]

To prevent ETS, plants developed intracellular receptors, encoded by so-called *resistance (R)*-genes, allowing them to specifically perceive pathogen-derived effectors. Like PRRs can trigger PTI, these receptors then induce a specific immune response in the plant called effector-triggered-immunity (ETI, Fig. 1C) [Baker *et al.*, 1997; Jones & Dangl, 2006; Katagiri & Tsuda, 2010]. Studies on the interaction between flax (*Linum usitatissimum*) and the fungal pathogen flax rust (*Malampsora lini*) laid the foundation for genetic research on ETI and led to the formulation of the gene-for-gene hypothesis. Each plant-pathogen interaction includes pairs of complementary genes: a receptor encoding R gene in the plant and an effector encoding *avrulence (Avr)* gene in the pathogen [Flor, 1942, 1971; Baker *et al.*, 1997]. A plant carrying the specific R-gene corresponding to the pathogen derived Avr-gene is resistant and can induce a defense response. The pathogen is considered avirulent and the host-pathogen interaction is referred to as incompatible. A plant lacking the R-gene corresponding to the Avr-gene of the pathogen is susceptible and will show disease symptoms. In this case, the pathogen is virulent, and the host-pathogen interaction is labeled compatible. The pathogen can spread rapidly and systemically throughout the whole plant [Hammond-Kosack & Jones, 1997]. Similar to a molecular arms race, as suggested by the zig-zag model by Jones & Dangl [2006], repeating cycles of PTI, ETS and ETI lead to a diversification of effector and receptor proteins and are a driving force behind co-evolution of plants and pathogens.

Many R-proteins belong to the nucleotide-binding site leucine-rich-repeat (NBS-LRR or NLR) family. In plants, NLR proteins are divided into two groups dependent on the N-terminal domains involved in signal transduction. CC-NLR proteins feature a coiled-coil domain, while TIR-NLR proteins possess a Toll/interleukin-1 receptor domain [Dangl & Jones, 2001; Qi & Innes, 2013]. The LRR domain represents the most polymorphic part of NLR proteins and plays an important role in effector recognition

specificity [Bonardi & Dangl, 2012; Qi & Innes, 2013]. The NBS domain is associated with activation of the NLR protein through binding and hydrolysis of ATP [Tameling *et al.*, 2002; Tameling *et al.*, 2006]. Pathogen effectors can be detected by NLRs by direct or indirect interaction. Direct physical interaction is the most straightforward type of interaction between NLR and effector proteins [Dodds *et al.*, 2006, Ravensdale *et al.*, 2012]. In flax the AvrM and AvrL567 proteins are delivered from the haustorium into the cytoplasm of infected cells and have been shown to directly interact with the M and L6 resistance protein in flax, respectively. Upon interaction AvrM and AvrL567 then trigger ETI [Dodds *et al.*, 2004; Catanzariti *et al.*, 2006; Barrett *et al.*, 2009; Rafiqi *et al.*, 2010, Catanzariti *et al.*, 2010; Barsoum *et al.*, 2019]. Dangl and Jones [2001] proposed the guard hypothesis, which suggests that indirect interaction, by recognition of effector-induced modifications in other plant proteins, allows for the detection of a large number of pathogens by a limited amount of NLR proteins. The R-protein surveils (guards) other plant proteins for possible interactions with effector proteins. These interactions in turn trigger signals detectable by the NLR [Van Der Biezen & Jones, 1998; Dangl & Jones, 2001]. In some cases, NLRs have incorporated additional so-called decoy domains by duplication or mimicry of a target gene. According to the integrated-decoy model, paired NLRs work together forming a hetero-complex receptor, in which the NLR containing the decoy acts as bait and triggers defense signaling by the second NLR upon binding of effector proteins [Van der Hoorn & Kamoun, 2008; Césari *et al.*, 2014; Wang *et al.*, 2015]. Together these modes of action show the importance of both direct and indirect interactions between effector and receptor proteins. Two recent studies by Wang *et al.* [2019a,b] described the formation of the resistosome, a funnel-shaped pentameric structure, similar to membrane pores. The inactive *Arabidopsis* CC-NLR protein HOPZ-activated resistance1 (ZAR1) is bound to the receptor-like cytoplasmic kinase (RLCK) Resistance related kinase1 (RKS1). The AvrAC effector protein from *Xanthomonas campestris* *pv. campestris* uridylylates several members of the RLCK family including PBL2, a decoy for detection of AvrAC activity. This allows recruitment of the uridylylated PBL2^{UMP} into the ZAR1-RKS1 complex [Wang *et al.*, 2015]. Conformational changes and release of ADP prime the ZAR1-RKS1- PBL2^{UMP} complex for activation, resulting in pentamerization. The resulting pore-formed resistosome is important for the association of ZAR1 to the plasma membrane and assumed to interfere with its integrity [Adachi *et al.*, 2019; Shi *et al.*, 2019; Wang *et al.*, 2019a,b].

During ETI, the signal cascade triggered by R-gene-mediated recognition of effectors elicits a versatile immune response characterized by rapid and localized emergence of programmed cell death (PCD). This phenomenon is known as the hypersensitive reaction (HR) and becomes visible by macroscopic development of necrotic lesions on pathogen infected leaves, which allow containment of local infections by restriction of pathogen spread throughout the plant [Ross, 1966; Van Loon, 1997; Jones & Dangl, 2006; Coll *et al.*, 2011]. Transcriptional changes and other aspects of ETI correlate with those observed during PTI. MAPK cascades are induced leading to transcriptional activation of a diverse set of defense related genes and an increase in intracellular Ca²⁺ triggers production of signaling molecules like ROS and nitric oxide as well as the phytohormones jasmonic acid (JA), salicylic acid (SA) and

ethylene (ET) [Lamb & Dixon, 1997; Tao *et al.*, 2003; Tsuda & Katagiri, 2010; Gao *et al.*, 2013]. Modulation of the concentration of those phytohormones and induction of their biosynthesis is important for establishment of specific immune responses and which signal is ultimately activated depends on the type of pathogen. While SA is the primary defense hormone required for protection against biotrophic and hemibiotrophic pathogens, the JA pathway mediates responses to wounding by insects and infection by necrotrophic pathogens [Thomma *et al.*, 1998; Glazebrook, 2005; Pieterse *et al.*, 2009, 2012; Yi *et al.*, 2014]. In most cases JA and SA act antagonistically and increased resistance against biotrophs correlates with susceptibility to necrotrophic pathogens and *vice versa* [Spoel *et al.*, 2007; Robert-Seilaniantz *et al.*, 2011]. Infection with a biotrophic oomycete *Hyaloperonospora parasitica*, for example, suppresses defense signaling by jasmonic acid activated by feeding caterpillars [Koornneef & Pieterse, 2008]. Compared to PTI, ETI ultimately leads to a stronger and more persistent form of immunity in tissues distal from the primary site of infection. These systemic types of resistance prevent the spread of the pathogen and protect noninfected plant tissue against subsequent infections [Tsuda & Katagiri, 2010; Ramirez-Prado *et al.*, 2018]. Induced systemic resistance (ISR) is typically induced by plant-growth promoting rhizobacteria and relies on both JA and ET as signal molecules [Yan *et al.*, 2002; Van Loon & Glick, 2004] On the other hand, systemic acquired resistance (SAR) is triggered by avirulent microbes and associated with the accumulation of SA and expression of *pathogenesis related (PR)* genes [Fu & Dong; 2013].

1.2. Systemic acquired resistance (SAR)

The idea that plants have developed a kind of immunity, which, similar to the adaptive immunity of animals, confers complete or partial resistance to reinfection following an earlier pathogen attack, goes back to the thirties [Chester, 1933]. Years later in 1961, Ross described his observations of an active and systemic resistance (*systemic acquired resistance*, SAR) triggered after infection of resistant tobacco plants with tobacco mosaic virus (TMV) [Ross, 1961, Klessig *et al.*, 2018]. As part of ETI, plants carrying the *N* resistance gene against TMV induce the HR by developing PCD at the local site of infection [Klessig *et al.*, 2018]. Furthermore, it was demonstrated that tissues in immediate vicinity of necrotic lesions caused by HR as well as systemic tissues in distal parts of the plant become highly resistant against TMV and tobacco necrosis virus (TNV) [Ross, 1961]. This increased resistance develops over several weeks following the primary infection but can already be detected 2-3 days post inoculation (dpi). This protection is long lasting, spanning weeks, months, or even sometimes for the remainder of the plant's growth period. However, it has been shown that this resistance is not passed on to the seed progeny [Ross, 1961; Lucas, 1999]. SAR-mediated resistance induction is not limited to the type or family of the pathogen that triggered it but conveys a broad-spectrum defense against a huge range of pathogenic microbes including bacteria, fungi, and viruses [Kuc, 1982].

1.2.1. Components of SAR

Establishment of SAR is generally accompanied by a considerable increase in accumulation of the phytohormone salicylic acid (SA) in both local and systemic tissues of plants displaying the HR [Malamy *et al.*, 1990; Métraux *et al.*, 1990; Dong, 2004]. Two metabolic pathways are involved in the synthesis of SA: the isochorismate synthase (ICS) pathway and the phenylalanine ammonia-lyase (PAL) pathway. Both are starting from chorismate, an intermediate product of the shikimate pathway, though their importance in different plant species varies. In Arabidopsis, biosynthesis of SA during SAR establishment is mediated by the ICS pathway. Plants containing defective mutants in the *ics1* (*isochorismate synthase1*) gene are unable to synthesize SA or accumulate SA above basal levels preventing the establishment of SAR [Nawrath & Métraux, 1999; Wildermuth *et al.*, 2001]. Likewise, plants overexpressing the *nahG* gene from *Pseudomonas putida* are unable to initiate SAR. This gene encodes a salicylate hydroxylase which converts SA into catechol (1,2-dihydroxybenzene) [Yamamoto *et al.*, 1965], which does not exhibit any inductive effects regarding plant defense and the resulting lack of SA accumulation prevents SAR establishment. Exogenous application of SA, however, has been shown to induce SAR even in plants deficient in SA accumulation [Gaffney *et al.*, 1993; Delaney *et al.*, 1994; Friedrich *et al.*, 1995]. There are functional analogues of SA mimicking its capacity to act as an inducer of SAR and acting in plant defense regulation. These functional analogues include derivatives of salicylate and benzoate, nicotinic acid, as well as benzothiadiazoles [Faize & Faize, 2018]. Prominent examples are acetylsalicylic acid [White, 1979], 2,6-dihydroxybenzoic acid [Van Loon, 1983, Xie *et al.*, 1998], 2,6-dichloro-isonicotinic-acid (INA) [Vernooij *et al.*, 1995] and Benzo-1,2,3-thiadiazole-7-carbothionacibenzolar-S-methyl ester (BTH / Bion®) [Görlach *et al.*, 1996; Lawton *et al.* 1996].

The grafting experiments conducted by Vernooij *et al.* [1994] revealed SA is required for establishment of SAR in distal tissues but does not participate in signal transduction between the local infection site and systemic tissues. Even after TMV infection, transgenic tobacco rootstocks carrying the *nahG* transgene were unable to accumulate SA. However, non-transgenic scions grafted onto those rootstocks were still able to induce PR1 gene expression [Vernooij *et al.*, 1994]. A mobile signal must be able to move from the primary infection site to uninfected tissues. The two possible routes for signal transmission are through the vasculature of the plant (xylem/phloem) or through volatile substances [Dempsey & Klessig, 2012; Shah *et al.*, 2014]. Local pathogen infection also triggers the production of other signaling molecules, including Methyl salicylate (MeSA) [Park *et al.*, 2007], glycerol-3-phosphate (G3P) [Chanda *et al.*, 2011], azelaic acid (AZA) [Jung *et al.*, 2009], Defective in induced resistance (DIR1) [Maldonado *et al.*, 2002, Lascombe *et al.*, 2008], dehydroabietinal (DA) [Chaturvedi *et al.*, 2012], and pipecolic acid (Pip), which were suggested to be involved in the long distance SAR signaling [Dempsey & Klessig, 2012; Fu & Dong, 2013; Yu *et al.*, 2013]. Recent research has established a major role of Pip and its derivate N-hydroxypipecolic acid (NHP) as key players in spreading the SAR signal. Mutants with defects in Pip biosynthesis are unable to establish SAR and show reduced accumulation of SA in systemic tissue [Návarová *et al.*, 2012; Ding *et al.*, 2016; Hartmann *et al.*, 2017]. Experiments

using SA and Pip deficient mutants revealed both, SA-dependent and SA-independent roles of Pip in priming of pathogen responses. Pip mediated defense priming is also dependent on flavin-dependent-monooxygenase1 (FMO1), which was shown to catalyze the conversion of Pip into NHP by hydroxylation. [Mishina & Zeier, 2006; Bernsdorff *et al.*, 2016; Hartmann *et al.*, 2018]. Exogenous application of NHP in lower leaves of *fmo1* plants is sufficient to rescue SAR establishment and can be detected in upper leaves indicating the ability of NHP to be transported systemically [Chen *et al.*, 2018; Hartmann & Zeier, 2019]. Taken together signaling between local and systemic leaves during SAR requires a complex interplay of different substances regulating the accumulation of SA in target tissues, with NHP being the key mobile signal.

The intracellular accumulation of SA during SAR correlates with the differential induction of *PR* genes and *de novo* synthesis of PR proteins with different biological activities and plays an important role in the resistance process allowing for a well-rounded response to different kinds of pathogens [Carr & Klessig, 1989; Uknes *et al.*, 1993; Dong, 2004; Durrant & Dong, 2004; Gruner *et al.*, 2013]. Expression of *PR* genes was first shown after TMV infection of tobacco plants carrying the N-resistance gene [Van Loon & Van Kammen, 1970]. Like SAR in general, *PR*-gene expression can also be effectively induced by exogenous application SA and functional analogs. Plants incapable of SA accumulation show no induction of *PR* genes [White, 1979; Van Huijsduijnen *et al.*, 1986; Malamy *et al.*, 1990; Nawrath & Métraux, 1999; Wildermuth *et al.*, 2001]. In both, Arabidopsis and tobacco, expression of *PR1*, *PR2*, and *PR5* genes is strongly induced by SA and the accumulation of PR1 proteins is intricately linked to SAR and can therefore be used as a molecular marker for SAR establishment [Ward *et al.*, 1991; Uknes *et al.*, 1992; Van Loon & Van Strien, 1999]. To date, a large number of PRs from different plant species have been found, which currently comprise 17 families of induced proteins [Van Loon *et al.*, 2006]. Although they are generally characterized as antimicrobial, PR proteins from different families can exhibit different kinds of enzymatic activities. In tobacco, members of the PR2 proteins show β -1,3-glucanase activity [Kauffmann *et al.*, 1987], while members of the PR3 and PR4 families feature distinctive chitinase activity [Legrand *et al.*, 1987]. Both types of enzymes can inhibit microbial growth and proliferation by hydrolyzing components of the cell wall of fungal or bacterial pathogens [Rose *et al.*, 2002]. Other families of PR proteins act as peroxidases involved in cell wall fortification, as proteinase inhibitors, or possess ribonuclease-like activities [Van Loon *et al.*, 2006]. The PR1 protein family is of particular interest. PR1 proteins are also members of a broader protein-superfamily, named the cysteine-rich secretory protein, antigen 5, and pathogenesis-related-1 (CAP) family, which share a 150 aa long domain (CAP domain) [Gibbs *et al.*, 2008; Gamir *et al.*, 2016]. It is assumed that the tobacco genome contains 16 members of this family of which only a subset of four is known to be induced upon TMV infection. This group consists of three acidic (PR1a, PR1b, PR1c) and one basic protein (PR1g) [Cornelissen *et al.*, 1987; Niderman *et al.*, 1995; Van Loon *et al.*, 2006]. After TMV infection expression of *PR1* genes is so strongly induced that these proteins can amount to up to 1 % of soluble leaf protein of the tobacco plant [Antoniw & Pierpoint, 1978; Pfitzner & Goodman, 1987]. Even though PR1

proteins were originally assumed to feature antimicrobial properties similar to other families of PR proteins, recent advances suggest a different mode of action. The CAP domain of the PR1a from tobacco and P14c from tomato were shown to possess sterol-binding activity, strongly compromising the ability of sterol-auxotroph oomycete pathogens to grow [Gamir *et al.*, 2016]. Additionally, the C-terminus of PR1 proteins features CAP-derived peptides (CAPEs). A conserved CNYx motif located N-terminally of the CAPE sequence constitutes a putative cleavage site required for release of the peptide. Exogenous application of peptides like CAPE1 from tomato or AtCAPE-PR-1 induces defense genes including PR-2 and PR-7, even in absence of an actual pathogen indicating a signal molecule like function. Together these functions of PR1 proteins suggest different mechanisms during pathogen defense [Chen *et al.*, 2014; Chien *et al.*, 2015; Breen *et al.*, 2017].

1.2.2. Regulators of SAR

To determine the mechanism by which increasing levels of SA can induce defense related gene expression, screening experiments on mutagenized Arabidopsis plants led to the discovery of two distinct groups of mutants. The first group is recognized by a constitutive activation of SAR. The *cpr* (constitutive expressor of PR genes) and *cim* (constitutive immunity) mutants exhibit elevated levels of SA accumulation and PR gene expression as well as enhanced disease resistance even in absence of chemical or biological induction [Bowling *et al.*, 1997; Clarke *et al.*, 1998]. In plants carrying *lsd* (lesion simulating disease) or *acd* (accelerated cell death) mutants, events of spontaneous necrosis in absence of avirulent pathogens can be observed, which also establishes SAR mediated resistance [Greenberg & Ausubel, 1993; Dietrich *et al.*, 1994]. The second group of mutants comprises plants characterized by an inability to activate the SAR response or induce expression of PR genes even upon chemical treatment or pathogenic infection. Using a reporter construct consisting of the promoter of the PR gene β -1,3-glucanase (*BGL2*) from Arabidopsis and the coding region of the β -glucuronidase (*GUS*) gene [Dong *et al.*, 1991], the group around Cao [1994] identified the *npr1* (*nonexpressor of PR genes1*) mutant. The *npr1* phenotype is recessive and is caused by mutation of a single nucleotide. Even after pathogen infection or exogenous application of SA or INA the affected plants were completely incapable of reporter gene induction, SAR establishment and PR gene expression [Cao *et al.*, 1994]. Independently, several groups screening for similar phenotypes identified mutants allelic to *npr1*. Like *npr1*, the *nim1* (*non-inducible immunity1*) [Delaney *et al.*, 1995], *sai1* (*salicylic acid insensitive1*) [Shah *et al.*, 1997], *eds5* (*enhanced disease susceptibility5*) and *eds53* [Glazebrook *et al.*, 1996] mutants are still able to accumulate wild type (WT) levels of SA but are completely compromised in the implementation of SA mediated responses, like expression of the PR genes *PR1*, *PR2*, and *PR5*, and did not display an increased resistance against pathogens after treatment with INA or SA. The discovery of multiple allelic mutants possessing SAR deficient phenotypes suggested an important role of NPR1/NIM1/SAI1 as a positive regulator of SAR signaling. Due to the inability of the mutants to react to salicylic acid, while maintaining normal accumulation of SA, this regulation appears to act downstream of SA accumulation but upstream of SAR mediated *PR* gene induction and establishment of resistance [Delaney *et al.*, 1995].

1.3. NONEXPRESSOR OF PATHOGENESIS RELATED GENES 1

The *NPR1/NIM1* gene from *Arabidopsis* encodes a protein consisting of 593 amino acids with a molecular weight of 66 kDa. The expression of *NPR1* is constitutive and can be increased by treatment with SA or INA, as well as by pathogen infection [Cao *et al.*, 1997; Ryals *et al.*, 1997]. Activation of NPR1 requires chemical or biological induction to mediate expression of defense related genes [Cao *et al.*, 1997]. Plants overexpressing NPR1 display an enhanced resistance against bacterial and oomycete pathogens with stronger, but not faster, induction of PR genes after infection [Cao *et al.*, 1998]. Although NPR1 has a significant influence on expression of defense-related genes, including PR genes, structural analysis revealed no DNA binding or transcriptional activation domains, making it unlikely that NPR1 could act as a transcription factor by itself. However, the protein features four ankyrin repeats in its center, as well as a BTB/POZ (Broad-complex Tramtrack, and Bric-a-brac/Pox virus and Zinc Finger) domain in the N-terminal region [Cao *et al.*, 1997; Aravind & Koonin, 1999], both of which are involved in protein-protein interactions [Bork, 1993; Bardwell & Treisman, 1994; Albagli *et al.*, 1995; Mosavi *et al.*, 2004]. Strikingly, NPR1 and the mammalian transcriptional regulator I κ B share significant homology in their amino acid sequences which is particularly high in regions containing ankyrin repeats [Ryals *et al.*, 1997]. Taken together the lack of a DNA binding domain and presence of protein-protein interaction domains in the NPR1 protein led to the assumption that NPR1 regulates the SA mediated gene expression by association with other proteins in the nucleus.

Nuclear targeting of NPR1 is mediated by a C-terminal nuclear localization sequence (NLS) between amino acids 541 and 554. Mutagenesis of this sequence results in localization of the protein exclusively in the cytoplasm [Kinkema *et al.*, 2000]. While trying to purify NPR1, Mou *et al.* [2003] found that without SAR induction NPR1 forms a cytoplasmic oligomer bound together by intermolecular disulfide bonds. It was later shown that S-nitrosylation of NPR1 at Cys¹⁵⁶ through S-nitrosoglutathione (GSNO) facilitates the oligomerization process while mutation of this cysteine inhibits efficient formation of oligomers and development of NPR1-mediated resistance [Tada *et al.*, 2008]. Two more cysteines, Cys⁸² and Cys²¹⁶, appear to play a role during NPR1 oligomerization and mutagenesis of either one leads to constitutive monomerization of NPR1 [Mou *et al.*, 2003]. Following redox changes taking place during early phases of SAR, NPR1 oligomers are reduced to monomers by disulphide-thiol exchanges catalyzed by thioredoxins (TRXs) [Mou *et al.*, 2003; Tada *et al.*, 2008; Sevilla *et al.*, 2015]. The monomerization allows transport of NPR1 into the nucleus where it can accumulate and activate PR gene expression [Kinkema *et al.*, 2000; Mou *et al.*, 2003]. Besides oligomerization, posttranslational modifications of NPR1 allow a complex but refined regulation of localization, degradation, and immune response. Nuclear import of NPR1 requires phosphorylation of C-terminal Cys⁵⁸⁹ by sucrose non-fermenting1 (SNF1)-related kinase 2.8 (SNRK2.8). SNRK2.8-mediated activation of NPR1 is dependent on only slightly elevated levels of SA enabling nuclear import of NPR1, even in distal tissues containing low levels of SA [Lee *et al.*, 2015]. In uninduced plants proteasome mediated degradation of NPR1 in the nucleus is important to prevent activation of target genes and untimely induction of defense

responses. Phosphorylation of Ser^{11/15} leads to degradation of NPR1 mediated by a Cullin3-based ligase. However, blocking the NPR1 turnover by inhibition of proteasome activity or similar means impairs transcription of NPR1-regulated genes, indicating the importance of NPR1 turnover for establishment of SAR and expression of target genes [Spoel *et al.*, 2009]. The phosphorylation of Ser^{11/15} is regulated by sumoylation of the protein with SUMO3 (*small ubiquitin-like modifier 3*). SUMO modification of NPR1 in turn is inhibited by phosphorylation of Ser^{55/59} which keeps NPR1 stable. Interaction of SUMO3 and NPR1 allows phosphorylation of Ser^{11/15} leading to Cullin3 mediated degradation [Saleh *et al.*, 2015]. NPR1 can also condensate in the cytoplasm in response to increasing intracellular SA concentrations. These SA-induced NPR1 condensates (SINCs) have been shown to be involved in the ubiquitination of stress related proteins by formation of an NPR1-Cullin3 E3 ligase complex, suggesting a role in the promotion of cell survival during plant immunity [Zavaliev *et al.*, 2020].

The genome of *Arabidopsis thaliana* contains five more genes paralogous to *NPR1*. The *NPR1*-like gene family is divided phylogenetically into three distinct clades consisting of highly similar pairs of genes which likely resulted from multiple gene duplication events during plant evolution [Shi *et al.*, 2013]. All *Arabidopsis* NPR proteins contain the conserved BTB/POZ and ankyrin-repeat domains involved in protein-protein interaction, as well as cysteine residues involved in redox based oligomerization control [Hepworth *et al.*, 2005; Shi *et al.*, 2013]. *NPR2* is the most similar to *NPR1*. Likewise, *NPR3* and *NPR4* are quite similar among each other and share a domain structure comparable to the *NPR1/NPR2* group. These four members of the *NPR* gene family are slightly induced upon pathogen infection and are assumed to take part in the SA signal transduction pathway [Canet *et al.*, 2010]. *NPR5* and *NPR6*, also known as *BOP2* (*blade-on-petiole2*) and *BOP1* (*blade-on-petiole1*) respectively, are more distant relatives of the *NPR1/NPR2* and *NPR3/NPR4* groups and are associated with developmental processes like growth asymmetry and plant architecture [Hepworth *et al.*, 2005; Khan *et al.*, 2014].

Homologs of *Arabidopsis* NPR proteins are found in all higher plants like rice [Chern *et al.*, 2005a], tobacco [Liu *et al.*, 2002; Maier *et al.*, 2011], and mustard [Ali *et al.*, 2017] and have been shown to be involved in SA-mediated defense responses as effective regulators of disease resistance. The genome of rice (*Oryza sativa* L.) contains five *NPR1*-like genes: *OsNPR1* (*NPR1* homologue 1 (*NH1*)) and *OsNPR2* (*NH2*) [Chern *et al.*, 2005a], as well as *OsNPR3*, *OsNPR4* and *OsNPR5*, with *OsNPR1* showing the highest similarity to *Arabidopsis NPR1* [Yuan *et al.*, 2007]. Overexpression of *NH1* in transgenic rice plants causes constitutive expression of defense genes and strongly enhances resistance to *Xanthomonas oryzae* pv. *oryzae*. This spontaneous activation of defense genes stands in stark contrast to *NPR1* overexpression in *Arabidopsis* where biological or chemical induction is required [Chern *et al.*, 2005a]. In tobacco there are only three known *NPR1*-like genes. Both *NtNPR1* and *NtNIMI-like* have a domain structure comparable to *AtNPR1* including a central ankyrin repeat domain and a N-terminal BTB/POZ-domain. Like *NtNPR1*, *NtNIMI-like* is expressed constitutively and shares the same binding properties. However, the transcript levels of *NtNIMI-like* are not elevated by SA [Maier *et al.*, 2011]. The *NtNPR5* (*NtBOP2*) gene encodes another BOP-protein and is involved in floral abscission [Wu *et al.*, 2012b].

1.4. NPR1 as transcriptional co-activator of bZIP TGA transcription factors

The regulation of gene expression during stress-responses in plants is strongly dependent upon specific interaction between *cis*-acting elements found in promoters of stress responsive genes and DNA-binding transcription factors (TFs). The specificity of TFs is based on distinct DNA-binding domains which differ between different families of TFs. In Arabidopsis those include ERF, Myb, TGA and WRKY transcription factors [Singh *et al.*, 2002]. In yeast, proof of interaction between the ankyrin repeat domain of NPR1 and members of the family of *activation sequence 1 (as-1)*-binding TGA transcription factors provided a connection between NPR1 and PR gene expression [Zhang *et al.*, 1999; Després *et al.*, 2000; Zhou *et al.*, 2000]. The bZIP transcription factors constitute a large and diverse family of TFs and are ubiquitous among plants and other eukaryotes and have been shown to be involved in various key processes of the plant life cycle like embryogenesis, tissue differentiation, energy metabolism, stress responses and defense against pathogens [Wei *et al.*, 2012]. Their eponymous and characteristic bZIP domain consists of 40 to 80 amino acids and contains two motifs: a basic region (b) and a leucine zipper (ZIP) [Shen *et al.*, 2016; Noman *et al.*, 2017]. The basic region consists of several basic amino acids and mediates specific binding of the TF to its target DNA at ACGT containing motifs like the CaMV 35S *as-1* element or the conserved G-Box motif [Giuliano *et al.*, 1988; Lam *et al.*, 1989; Foster *et al.*, 1994]. The leucine zipper motif is composed of at least four leucine residues separated by spacers of six amino acids each and plays an integral role in dimerization of bZIP-TFs. Hydrophobic binding of the leucine side chains of two monomers results in an interdigitated coiled-coil structure which places the two basic regions next to each other and enables DNA binding of the TFs [Landschulz *et al.*, 1988; Vinson *et al.*, 1989; Ellenberger *et al.*, 1992]. The Arabidopsis genome contains 75 bZIP-TFs, which were divided into ten groups based on sequence similarities within their basic regions. The bZIP-TGA-TFs constitute group D and are not only involved in stress responses to foreign substances (xenobiotics) and pathogens, but also in plant development [Jakoby *et al.*, 2002; Kim & Delaney, 2002; Wei *et al.*, 2012; Alves *et al.*, 2013].

Members of the TGA family bind to SA-responsive, TGACG-containing *cis-elements* like the *as-1* element found in the 35S RNA promoters from cauliflower mosaic virus (CaMV) and Arabidopsis *PR-1* [Lam *et al.*, 1989; Qin *et al.*, 1994; Lebel *et al.*, 1998; Johnson *et al.*, 2003]. Functional analysis revealed that similar so-called *as-1*-like elements can be found in the promoter region of the *PR-1a* gene from tobacco as well [Grüner & Pfitzner, 1994; Qin *et al.*, 1994; Strompen *et al.*, 1998]. The *as-1*-like region in the tobacco *PR1a*-promoter is positioned between -691 bp and -553 bp and contains two TGACG-elements in inverse orientation to each other, with six nucleotides lying between them. During expression studies, mutations in the *as-1*-like element of an *ProPR-1a:GUS* reporter gene construct were shown to decrease the SA mediated *GUS* activity [Strompen *et al.*, 1998]. The Arabidopsis *PR1*-promoter contains regulatory elements in the region between -698 bp and -621 bp including the two negative regulatory elements *linker scan4 (LS4)* and *LS5*, as well as one positive regulatory element *LS7*. The *LS5* and *LS7* elements are involved in SA mediated induction of *PR1*-gene expression and

contain the sequence ACGTCA, an *as-1*-like sequence complementary to the TGACG sequence found in the 35S promoter [Lebel *et al.*, 1998]. In tobacco Strompen *et al.* [1998] were able to prove *in vitro* interaction between the *as-1*-like element in the *PR1a*-promoter and the TGA1a transcription factor. In Arabidopsis another member of the TGA family of transcription factors, TGA2, is able to bind both *LS5* and *LS7*. The DNA binding of TGA TFs was shown to be enhanced by presence of functional NPR1 but is deregulated in *npr1* plants, suggesting a critical role of TGA TFs during NPR1-mediated *PR1*-gene induction during SAR [Després *et al.*, 2000].

Ten members of the TGA family of bZIP TFs have been described in Arabidopsis which were further divided into five groups based on sequence homologies [Jakoby *et al.*, 2002; Gatz, 2013]. Clade I comprises AtTGA1 [Schindler *et al.*, 1992] and AtTGA4 [Zhang *et al.*, 1993]. AtTGA2 [Kawata *et al.*, 1992], AtTGA5 [Zhang *et al.*, 1993] and AtTGA6 [Xiang *et al.*, 1997] form the larger clade II, and are characterized by their shorter N-termini. AtTGA3 [Miao *et al.*, 1994] and AtTGA7 [Després *et al.*, 2000] make up clade III. Clade IV consists of AtTGA9 and AtTGA10 [Murmu *et al.*, 2010]. PERIANTHIA (PAN) [Chuang *et al.*, 1999] is the single member of clade V which like clade IV is involved in flower development [Running & Meyerowitz, 1996; Murmu *et al.*, 2010]. While clades I-III play roles in plant defense [Zhang *et al.*, 2003; Foley & Singh, 2004; Choi *et al.*, 2010], only members of clade II and III have been shown to constitutively interact with NPR1 and its paralogues in untreated leaves and yeast [Zhang *et al.*, 1999; Després *et al.*, 2000; Zhou *et al.*, 2000; Hepworth *et al.*, 2005]. The interaction between AtTGA2 and NPR1 can also be stimulated by treatment with SA and INA [Subramaniam *et al.*, 2001]. Functional NPR1 protein is required for AtTGA2 and AtTGA3 binding to the *PR1* promoter. In *npr1* plants this binding is abolished even after SA treatment [Johnson *et al.*, 2003]. However, clade I TGA TFs cannot interact with NPR1 in untreated leaves. The interaction of AtTGA1 and AtTGA4 with NPR1 requires SA-mediated reduction of disulfide bonds between Cys²⁶⁰ and Cys²⁶⁶ which are only present in clade I TGA TFs. Mutagenesis of Cys^{260/266} to the corresponding residues present in TGA2 is sufficient to enable interaction of AtNPR1 and AtTGA1 and AtTGA4 [Després *et al.*, 2003]. Mutation of a single TGA factor is insufficient to produce detectable phenotypic changes and only plants containing a *tga2-1tga5-1tga6-1* triple knockout mutant, unable to express all members of clade II TGA TFs, show suppression of INA-mediated induction of SAR mediated *PR1* gene expression similar to the *npr1-1* mutant [Cao *et al.*, 1997; Zhang *et al.*, 2003]. Together these observations indicate that TGA factors can be induced by increasing levels of SA and function as positive regulators of the SAR response, with NPR1 playing the role of a transcriptional coactivator. However, TGA factors can also interact with the NPR1 paralogs NPR3 and NPR4 which feature a similar domain structure [Zhang *et al.*, 2006]. The proposed functions of NPR3 and NPR4 lie in the degradation mediated regulation of transcriptional activation applied by NPR1. Fu *et al.* [2012] proposed a function of NPR3 and NPR4 as part of Cullin3 type ubiquitin ligase complexes, requiring direct interaction between NPR1 and NPR3/NPR4. This interaction was shown to be regulated by varying levels of SA [Fu *et al.*, 2012]. However, a recent study by Ding *et al.* [2018] could neither confirm the interaction between NPR3/4

and NPR1 in yeast, nor the interaction with Cullin3A in co-immunoprecipitation assays. In contrast, this study revealed that NPR3 and NPR4 redundantly suppress basal resistance by inhibiting the expression of defense-related transcription factors like *SARD1* and *WRKY70*. This suppression is dependent on SA and requires both, an ethylene-responsive element binding factor (ERF)-associated amphipathic repression (EAR) motif, found in the C terminal half of NPR3 and NPR4 but not in NPR1 [Ohta *et al.*, 2001, Ding *et al.* 2018], as well as binding of NPR3/4 to TGA factors TGA2/TGA5/TGA6 and promoter regions of defense-related TFs. Taken together their data suggest an opposite role of NPR1 and NPR3/4 in the expression of SA-dependent genes, with NPR3/4 acting as transcriptional co-repressors.

In tobacco, there are six known members of the TGA TF family: NtTGA1a [Katagiri *et al.*, 1989] and PG13 [Fromm *et al.*, 1991] can be categorized as members of clade I and are predominantly expressed in the roots, with only moderate expression levels in leaf tissue [Katagiri *et al.*, 1989; Fromm *et al.*, 1991]. Clade II consists of NtTGA2.1 and NtTGA2.2, which show stronger expression in leaves and can bind *as-1*-like elements as part of the ASF-1 (*as-1*-binding factor-1) transcription complex [Niggeweg *et al.*, 2000 a, b]. RNAi mediated suppression of NtTGA2.1 and NtTGA2.2 consistently correlates with decreased expression of PR genes [Thurow *et al.*, 2005]. Unlike other TGA TFs in tobacco, the clade 4 member NtTGA10 is exclusively expressed in root tissue [Schiermeyer *et al.*, 2003]. The NtTGA7 protein is categorized as a clade III TGA transcription factor and is expressed differentially during plant development. In young plants NtTGA7 is expressed mostly in the stem, petioles, and roots, but accumulation of NtTGA7 mRNA has also been shown in older leaves. In yeast, NtTGA7 fused to the GAL4-DNA binding domain (GAL4BD) exhibits significant transactivation activity. NtTGA7 is very similar to NtTGA1a but, unique among TGA TFs, does bind NtNPR1 at its C-terminus instead of the N-terminus [Stos-Zweifel *et al.*, 2018]. Furthermore, only NtTGA2.1, NtTGA2.2 and NtTGA7 can interact with both, Arabidopsis and tobacco NPR1, in yeast while NtTGA1a and NtTGA10 are unable to interact with AtNPR1 [Niggeweg *et al.*, 2000b, Schiermeyer *et al.*, 2003; Stos-Zweifel *et al.*, 2018].

NPR1 is also suggested to interact with other plant transcription factors. TEOSINTE BRANCHED 1, CYCLOIDEA, PCF1 (TCP) transcription factors are usually involved in developmental processes, including seed germination, flower development, and leaf shape. TCP8, TCP14, and TCP14 were shown to physically interact with NPR1, both in yeast and *in vivo*. The triple T-DNA insertion mutant *tcp8-1 tcp14-5 tcp15-3*, but not single or double mutants, were compromised in SAR induction and induction of the defense genes *PR1*, *PR2*, and *PR5*, indicating redundant functions of those TCP transcription factors. Additionally, it was shown that TCP15 can bind to the conserved TCP binding motif of the *PR5* promoter and promotes *PR5* expression in response to exogenous SA application in an NPR1 dependent manner [Li *et al.*, 2018]. The group of Chen [2019] discovered that NPR1 can recruit the WRKY class transcription factor WRKY18 and the cyclin-dependent kinase CDK8 to its own promoter, enhancing its expression in a SA-dependent manner. Together, CDK8 and corresponding Mediator subunits enhance the expression of NPR1 and the pathogenesis-related gene *PR1* and contribute to plant immunity in a positive regulatory manner [Chen *et al.*, 2019].

1.5. NIMIN proteins

Besides different kinds of transcription factors, NPR1 has been shown to interact with members of another protein family. A yeast-two-hybrid screen of an Arabidopsis cDNA library with NPR1/NIM1 as bait revealed three novel proteins named NIM1-INTERACTING1 (NIMIN1, N1), NIMIN2 (N2) and NIMIN3 (N3). All members of the NIMIN family are small proteins with molecular masses between 13 and 17 kDa. Searching databases using sequence alignment revealed a fourth member of this family which based on its high similarity to NIMIN1 (64 %) was named NIMIN1b (N1b). In yeast, all four Arabidopsis NIMIN proteins have been shown to localize to the nucleus and are able to interact with NPR1. Of these proteins N1, N1b and N2 interact with the C-terminal moiety of NPR1, while N3 binds to the N-terminus instead [Weigel *et al.*, 2001]. Structural analysis identified several conserved domains shared among members of the NIMIN protein family (Fig. 2). N1, N1b and N2 contain highly similar nuclear localization sequences (NLS; Fig. 2, yellow bars) and even though N3 does not contain an NLS matching established consensus sequences [Raikhel, 1992], the protein is rich in lysine and arginine and features two sequences with high similarity to the NLS sequences found in N1 and N2, which might fulfill the same function [Weigel, 2000]. The DXFFK domain in the N-terminal half of N1, N1b and N2 (Fig. 2, blue bars) and an EDF domain in the central part of N1, N1b, and N3 (Fig. 2, green bars) are typically associated with the ability to interact with NPR1 [Weigel *et al.*, 2001; Chern *et al.*, 2012]. Additionally, all Arabidopsis NIMIN proteins harbor short LxLxL repeats near the C-terminus (Fig. 2, red bars) which are highly similar to the EAR motifs associated with transcriptional repression, which were first identified in ERF and zinc finger TFs [Ohta *et al.*, 2001].

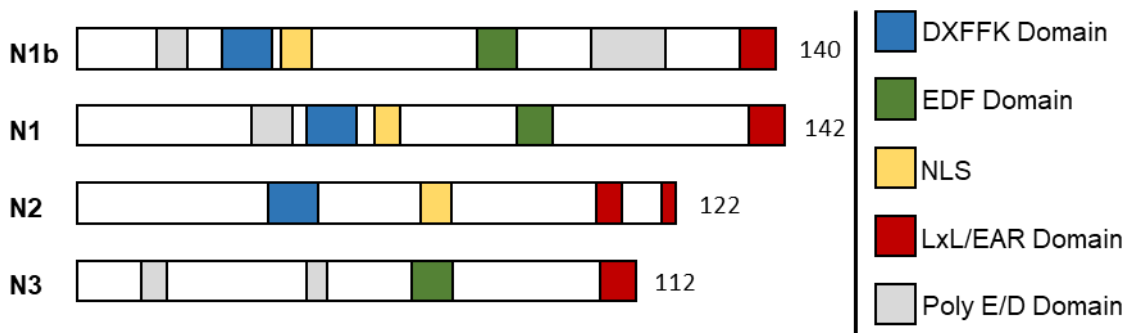


Fig. 2 Domain architecture of Arabidopsis NIMIN proteins. Schematic representation of NIMIN proteins showing their characteristic domains. The diagram is drawn approximately to scale. Conserved regions include a DXFFK motif of about 10 amino acids with high similarity (blue), an EDF domain (green), hypothetical nuclear localization signals (yellow), a short LxLxL type EAR domain (red), and stretches of at least four consecutive acidic residues (Poly E/D domain, grey). [modified after Weigel *et al.*, 2001].

While sharing many similarities on the protein level, the *NIMIN* genes are expressed differentially during SAR establishment. Salicylic acid plays a fundamental role in the regulation of *N1* and *N2* gene expression. Both genes are induced transiently before accumulation of *PR1* transcripts and *N1* and *N2* transcript levels are elevated to moderate levels in Arabidopsis plants treated with SA [Weigel *et al.*, 2001]. The sensitivity to salicylic acid observed in *NIMIN* promoters is mediated by the presence of *cis*-acting elements containing TGACG motifs. Mutations in these motifs result in reduced gene expression

in response to application of SA [Glocova *et al.*, 2005; Hermann, 2009; Fonseca *et al.*, 2010]. *NIMIN3* differs from *NIMIN1* and *NIMIN2* in that it is expressed constitutively at low levels. The *NIMIN3* gene expression is independent of the presence of functional NPR1 protein and is not responsive to SA or other plant hormones involved in defense reactions [Hermann *et al.*, 2013].

NIMIN proteins are not exclusive to the family of Brassicaceae but can be found in all higher plants. Homology comparisons revealed NIMIN-like proteins in many species including tobacco [Weigel *et al.*, 2001; Zwicker *et al.*, 2007], tomato [Zwicker *et al.*, 2007], and rice [Chern *et al.*, 2005b]. As of now, four NIMIN homologues were identified as interactors of NH1 in rice: negative regulator of resistance (NRR), NRR repressor homologue1 (RH1), RH2 and RH3, all of which share similarities with Arabidopsis N2 [Chern *et al.*, 2005b, 2012]. Like Arabidopsis NIMIN proteins, NRR localizes to the nucleus and comprises an EAR motif, though the one found in NRR contains an overlapping LDLNxxP consensus sequence [Kagale *et al.*, 2010]. Sequence alignment revealed high homology between the product of the SA-inducible *G8-1* gene from tobacco described by Horvath *et al.* [1998] and Arabidopsis NIMIN2. The *G8-1* protein contains a potential NLS, an EAR motif located close to the C-terminus and a domain similar to the DXFFK motif [Weigel *et al.*, 2001]. Besides *G8-1*, which was renamed into NtMININ2a (NtN2a), five more members of the NIMIN-protein family have been identified in tobacco. NtNIMIN2b (NtN2b) and NtNIMIN2c (NtN2c) are structurally related to NtN2a, sharing a high homology to N2, and include the same domains. Expression of *NtNIMIN2* genes, just like their Arabidopsis counterparts, can be induced by exogenous application of SA or eliciting defense response through pathogen exposure and share their temporal expression profile. Interestingly, transcripts of *NtNIMIN2* genes can be detected in older untreated leaves but are not present in leaves of younger untreated plants [Zwicker *et al.*, 2007]. This is consistent with the findings observed by Glocova *et al.* [2005] showing weak activity of *N1* and *N2* promoters in older leaves of transgenic tobacco plants carrying reporter constructs. The sequences of the three novel tobacco proteins NIMIN1-like1 (BP), NIMIN1-like2 (FG), and NIMIN2-like (FS) are available in the Genbank database and contain all characteristic structural domains of the NIMIN protein family. Unlike other NIMIN proteins from tobacco, BP and FG are more similar to NIMIN1 and also contain the EDF motif [Masroor, 2013; U. M. Pfitzner, personal communication]. In yeast, all NIMINs from tobacco have been shown to interact with tobacco NPR1 and NIM1-like and the binding of NIMIN2-proteins to Arabidopsis NPR1 could be demonstrated as well [Zwicker *et al.*, 2007; Masroor, 2013].

1.5.1. Differential interaction with NPR proteins

Although all NIMIN proteins from Arabidopsis and tobacco have been shown to interact with the respective NPR1 proteins from the same species, they do so differentially [Weigel *et al.*, 2001; Chern *et al.*, 2005b, Zwicker *et al.*, 2007; Hermann *et al.*, 2013]. The N-terminal DXFFK domain is conserved among NIMIN proteins from Arabidopsis and tobacco [Zwicker *et al.*, 2007] and is required for interaction with the C-terminal region of NPR1 [Weigel *et al.*, 2001]. In yeast, the presence of salicylic

acid in the medium significantly reduces the binding of N1, N1b and N2 to NPR1, while interaction between NPR1 and N3 or TGA TFs remains unchanged. Interactions between tobacco NIMIN and NPR proteins show the same sensitivity to SA as observed in their Arabidopsis counterparts, resulting in almost complete repression of binding activity [Maier *et al.*, 2011]. Besides Arabidopsis and tobacco NIMIN proteins, NRR can also interact with Arabidopsis NPR1. This interaction is linked to the NPR1-interacting domain consisting of 25 amino acids (NI25), which shows sequence similarity to the DXFFK domain. However, the NI25 domain is not sufficient for interaction with NH1 [Chern *et al.*, 2005b]. The interaction site of Arabidopsis and tobacco NPR1 required for binding the DXFFK domain of N1, N1b and N2 was mapped to an almost identical stretch of about 20 amino acids in the C-terminal region of the NPR proteins, ranging from position 493 to 512 in AtNPR1 and 491 to 510 in NtNPR1, respectively [Maier *et al.*, 2011]. This highly conserved N1/N2 binding domain (N1/N2BD) from AtNPR1 and NtNPR1 is also present in NtNIM1-like [Maier *et al.*, 2011] and N1 and N2 from Arabidopsis can interact with both NtNPR1 and NtNIM1-like. The N1/N2BD contains two essential phenylalanine residues (Phe^{507/508} in AtNPR1, Phe^{505/506} in NtNPR1), which when mutated to serine, completely abolish binding of N1 and N2 proteins, but do not compromise the interaction between AtNPR1 and N3 [Maier *et al.*, 2011, Hermann *et al.*, 2013]. Similarly, substitution of the conserved amino acids Tyr⁵⁰⁸ Phe⁵⁰⁹ from NtNIM-like prevents its interaction with N2 type proteins [Konopka, 2018]. Inversely, the two phenylalanine residues in the DXFFK-domain are conserved among NIMIN proteins and play a crucial role during interaction with NPR1. A NIMIN1 F49/50S mutant is completely unable to bind NPR1 in yeast and in planta [Weigel *et al.*, 2005].

Unlike N1, N1b and N2, the N3 protein does not contain a DXFFK domain and was instead shown to interact with the N-terminal part of NPR1 in a SA independent manner [Weigel *et al.*, 2001]. Studies on rice NRR revealed that, while interaction with Arabidopsis NPR1 is mediated by the NI25 domain, binding of NRR1 to NH1 is mediated by a different domain. The NH1-binding domain of NRR comprises 24 amino acids, and is located directly behind NI25 [Chern *et al.*, 2005b]. This domain, shared by RH1, RH2 and RH3, was named the EDF motif based on the WRPxFx^W/_MEDF consensus sequence deduced by sequence alignments [Chern *et al.*, 2012]. This sequence is highly similar to the eight amino acid motif P^A/_SFQPEDF which was identified within the sequences of N1, N1b, and N3 proteins from Arabidopsis and is also present in the N1-like proteins from tobacco [Weigel *et al.*, 2001; Chern *et al.*, 2012; Masroor, 2013]. The sequence similarities between EDF domains from rice NRR and Arabidopsis NIMIN proteins indicate that interaction between N3 and the N-terminus of NPR1 is most likely mediated by this motif and the insensitivity of the interaction to SA is most likely caused of the different binding site [Zwicker *et al.*, 2007; Maier *et al.*, 2011]. Despite their different binding sites, a simultaneous binding of N1/N1b/N2 and N3 to NPR1 is not possible. The data suggest that N1, N1b and N2 most likely compete for the same binding site, while binding N3 may prevent access to the binding site used by the other NIMIN proteins [Hermann *et al.*, 2013].

1.5.2. Transcriptional repression of *PR1* promoters

Transient overexpression of *NIMIN*-genes driven by the *35S* promoter in transgenic *Nicotiana benthamiana* plants revealed differential effects on the *Pro-1533PR1a:GUS* reporter gene construct [Grüner & Pfitzner, 1994; Hermann *et al.*, 2013]. When compared with a GFP control, the SA mediated reporter gene expression was repressed by overexpression of *N1* and *N3*. This observed repression of the *PR1a*-promoter activity was more pronounced for *N1* than for *N3* while overexpression of *N2* showed no significant difference compared to the controls. This differential repression was shown to not only affect reporter gene expression but also the endogenous expression of the *PR1*-gene from *N. benthamiana* [Hermann *et al.*, 2013]. Transgenic overexpression of *NIMIN1* in Arabidopsis also showed negative effects on the expression of endogenous *PR* genes and *NIMIN1*. These plants are also impaired in the establishment of SAR and development of *R*-gene mediated resistance as observed during infection with a virulent or avirulent strains of *P. syringae* after SA treatment. However, the *NIMIN1* F49/50S mutant, which is unable to bind NPR1, does not induce similar deficiencies in immunity [Weigel *et al.*, 2005]. Consistent with these results, overexpression of *NRR* in rice and Arabidopsis results in enhanced pathogen growth and repression of defense gene expression and SAR which is abolished in NPR1 binding mutants [Chern *et al.*, 2005b, 2008]. This indicates that enhanced susceptibility of *NIMIN1* overexpressing lines is directly contingent on the interaction of NIMIN1 and NPR1 [Weigel *et al.*, 2005]. In accord with these observations, both *nimin1* knockout lines, unable to generate *nimin1* mRNA, and dsRNAi (double stranded RNA interference) lines, with a strongly reduced *nimin1* expression, showed an enhanced induction of SA-mediated *PR*-gene expression [Weigel *et al.*, 2005].

The effects on SA mediated induction of *PR1* genes during SAR establishment indicated a repressive effect of NIMIN proteins on gene regulation conveyed by the NPR1-TGA transcription complex. Even though NIMIN proteins can physically interact with NPR1, no direct interaction between TGA2 or TGA6 and NIMIN proteins could be detected in yeast. However, using the yeast three-hybrid system, Weigel *et al.* [2001] were able to show that NPR1 can form a ternary complex with NIMIN proteins and TGA factors. *In vivo* this complex can bind to *cis*-regulatory elements in the *PR-1* promoter [Weigel *et al.*, 2001, 2005]. As has been shown for the binary interaction between *N1* and NPR1, ternary complexes comprising *N1* are also sensitive to SA. However, ternary complexes including *N2* remain stable under the same conditions [Hermann *et al.*, 2013]. *N1* therefore acts as a negative regulator of its own and *PR1*-gene expression by direct interaction with NPR1 and inhibition of NPR1-TGA transcription complexes [Weigel *et al.*, 2005]. The presence of EAR motifs close to the C-terminus of NIMIN proteins from Arabidopsis, tobacco, and rice, support these observations as EAR motifs negatively regulate genes involved in diverse biological functions including developmental, hormonal and stress signaling. The consensus sequence patterns typically found in EAR motifs are LxLxL, DLNxxP or a motif with overlapping LxLxL and DLNxxP [Kagale *et al.*, 2010]. Interestingly, NIMIN proteins from Arabidopsis and those from tobacco and rice contain different types of EAR motifs. In Arabidopsis EAR motifs

follow LxLxL consensus and are typically placed directly at the C-terminus with N2 carrying a bipartite EAR motif [Weigel *et al.*, 2001]. Meanwhile NIMIN proteins from tobacco and rice typically carry DLNxxP type EAR motifs [Chern *et al.*, 2005b, Zwicker *et al.*, 2007]. The Arabidopsis Interactome Mapping Consortium [2011] revealed that NIMIN proteins can interact with the transcriptional co-repressor TOPLESS (TPL) and similar interactions between TPL and Auxin/Indole-3-acetic acid (AUX/IAA) transcriptional repressors regulate the activity of auxin response factors (ARFs). Direct interaction between TPL and NIMIN proteins has later been confirmed in yeast [Späth, 2012] and supports the role of NIMIN proteins as direct negative regulators of *PR* gene repression [Weigel *et al.*, 2001, 2005].

1.5.3. Role of NIMIN proteins in perception of salicylic acid

The influence of SA as a signal to induce the establishment of SAR has been known for decades [Malamy *et al.*, 1990; Métráux *et al.*, 1990]. Even though the functions of NPR1 as a positive regulator of SAR and SA mediated induction of the *PR1* gene expression are widely accepted [Cao *et al.*, 1997; Ryals *et al.*, 1997; Shah *et al.*, 1997], the underlying mechanism behind perception of salicylic acid was not fully understood. In search of the receptor which perceives the SA signal and consequentially enables the induction of *PR1* expression, several hypotheses arose trying to explain how SAR is regulated by changing levels of SA. The research by Maier *et al.* [2011] identified a transactivation domain in the C-terminal moiety of NtNPR1, whose activity is measurably enhanced in presence of SA, confirming reports of a similar domain found in AtNPR1 [Rochon *et al.*, 2006]. Additionally, studies based on a *nim1-4* mutant [Ryals *et al.*, 1997], harboring amino acid exchanges of an arginine within a strongly conserved C-terminal LENRV pentapeptide, not only showed a loss of SA induced transcriptional activity of GAL4BD fused NtNPR1, but also inhibition of SA-mediated dissociation of N1 and N2 proteins from Arabidopsis and tobacco NPR1. These results imply a crucial role of the NPR1 C-terminus in SA perception and the regulation of NPR1-TGA transcription complexes by interaction with NIMIN proteins [Maier *et al.*, 2011]. Structure-function analysis of NPR1 alleles revealed clusters of SA-insensitive mutations in the C-terminal moiety of NPR1 in areas corresponding to the N1/N2BD and the LENRV motif [Canet *et al.*, 2010; Maier *et al.*, 2011], further supporting the importance of this region of NPR1. Based on this analysis and observations regarding differential binding of NIMIN proteins to NPR1, Hermann *et al.* [2013] proposed a model explaining the SA induced establishment of SAR, taking into account the negative regulatory function of NIMIN proteins. This model interprets the differential effects of salicylic acid on interaction of NPR1 and TGA TFs or NIMIN proteins using Arabidopsis NPR1 as an example (Fig. 3) [Hermann *et al.*, 2013]. In Arabidopsis, the *NIMIN3* gene is expressed constitutively not requiring additional induction. In unchallenged plants, without endogenous accumulation of SA, NIMIN3 can bind to the N-terminus of NPR1 repressing untimely expression of *PR* genes by inactivation of the NPR1-TGA transcription complex. During pathogen infection, low tissue levels of SA induce the *NIMIN2* promoter, allowing NIMIN2 to replace NIMIN3 and bind to the C-terminus of NPR1. The alleviation of N3 mediated repression could allow the expression of early SA

response genes like *NI* but is not sufficient to allow activation of late SAR genes including *PR1*. The transient interaction between NPR1 and N2 is dispersed by increasing levels of SA, allowing N1 to take its place on the C-terminus and once again prevent the expression of NPR1 dependent genes. Upon reaching a certain threshold of endogenous SA, N1 dissociates from the NPR1-TGA transcription complex as proposed by Maier *et al.* [2011]. The now active transcription complex can enable the expression of *PR1* and other late SAR genes. While precise regulation of *PR1* gene expression is mediated by SA dependent sequential interaction between different NIMIN proteins and NPR1, direct interaction of NPR1 and SA is required for dissociation of N1.

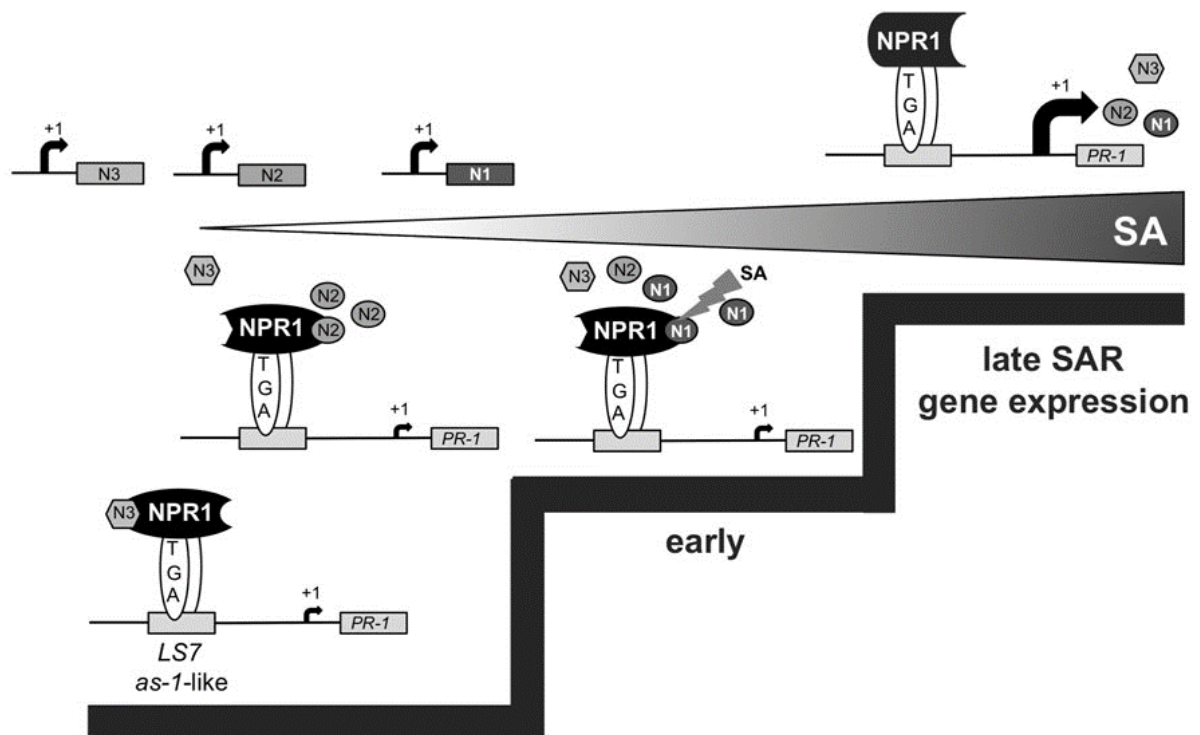


Fig. 3 Perception of salicylic acid and regulation of *PR1* gene induction through consecutive interaction of NIMIN proteins and NPR1 during SAR. This model suggests consecutive binding of different NIMIN proteins and NPR1 during SAR. Sensing of ambient SA levels is implied to be mediated by formation of regulatory NIMIN-NPR1 complexes with varying biochemical properties. This enables activation of *PR* genes at specific threshold levels of SA. In this example, the direct action of SA on the NIMIN1-NPR1 complex results in induction of the defense gene *PR1* during the later stages of SAR [Hermann *et al.*, 2013].

Other models from different research groups proposed diverging opinions on this matter. The results by Fu *et al.* [2012] were unable to show a direct interaction between NPR1 and SA. Instead, they proposed NPR3 and NPR4, both established negative regulators of SAR [Zhang *et al.*, 2006], to exert this role by degradation-dependent regulation of NPR1 availability, based on their differential affinity to SA. This is mediated by a complex consisting of AtNPR1, AtNPR4 and Cullin3, which facilitates degradation of NPR1 in presence of low levels of endogenous SA and prevents untimely activation of defense responses. After pathogen infection, increasing levels of SA interrupt the SA sensitive interaction between NPR1 and NPR4. This leads to the formation of an AtNPR1-AtNPR3-Cullin3 complex which has lower sensitivity for SA. Further degradation of NPR1 is accompanied by a hypersensitive response in the affected cells. In surrounding tissues, the level of salicylic acid is low

enough to prevent interaction between NPR1 and NPR3, but high enough that NPR4 dissociates from NPR1. The resulting accumulation of NPR1 allows the establishment of SAR and the associated defense responses [Fu *et al.*, 2012; Fu & Dong, 2013]. However, contradicting with these results, other working groups were able to prove the interaction between SA and NPR1 *in vitro* although with varying activity [Wu *et al.*, 2012; Manohar *et al.*, 2015]. Wu *et al.* [2012] proposed that this interaction requires a copper ion binding to the C-terminal Cys^{521/529} residues of NPR1. They suggest that binding of SA triggers conformational changes in NPR1 disrupting the interaction between the C-terminal transactivation domain and the N-terminal autoinhibitory BTB/POZ-domain. The Cys^{521/529} residues, however, are not conserved among NPR1 homologues from tobacco or tomato. The studies by Fu *et al.* [2012] and Wu *et al.* [2012] also do not take into account the role of NIMIN proteins despite their established role in SA dependent regulation of *PR1* gene expression during SAR.

Studies by Neeley *et al.* [2019] further expand upon the studies by Maier *et al.* [2011] and uncovered the mechanism by which the C-terminus of tobacco NPR1 is able to transduce the SAR signal. Mutational analysis regarding the conserved LENRV and N1/N2BD region not only confirmed the dependency on the conserved Arg⁴³¹ within the LENRV domain but also showed that other amino acid substitutions in this extended region can negatively affect SA sensitivity of the NtNPR1 C-terminus. Based on these results, the LENRV and N1/N2BD domains were separated and analyzed for potential interaction and direct association between both domains could be confirmed in yeast, *in vitro*, *in planta*, as well as in animal cells. This interaction is enhanced by SA and its functional analogs. Yeast three-hybrid assays confirmed that NIMIN proteins can form ternary complexes with the separated LENRV and N1/N2BD domains. This suggests a conformational change of the NtNPR1 C-terminus which is modulated by NIMIN proteins to reconstitute a functional C-terminus with transactivation activity [Neeley *et al.*, 2019]. Just recently a publication by Wang *et al.* [2020] further confirmed these observations. Using different NPR4 constructs, they were able to map the SA-binding core (SBC) to a region encompassing amino acids 373 to 516. This region encompasses the same dimensions and subregions as the NtNPR1 386/588 fragment used by Maier *et al.* [2011] to map the SA sensitivity of tobacco NPR1. By analyzing a purified crystal structure, Wang *et al.* [2020] found this domain to take up an α -helical fold, arranged in two interlocking V shapes. The complete embedment of SA into the binding pocket suggests extensive conformational changes. These alterations also weaken the interaction between NPR4 and NPR1. Even though the hormone binding residues of both proteins are nearly identical, the SA-binding activity of NPR1 is significantly lower compared to NPR4 [Wang *et al.*, 2020].

1.6. Aims and objectives

The extensive signaling network involved in mediating the defense of plants against biotic stress, including pathogen invasion, has been studied thoroughly. The establishment of SAR as a persistent defense response and expression of *PR* genes requires the interaction of the signaling molecule SA and a transcription complex consisting of NPR1 and TGA transcription factors. Since their discovery, studies regarding the expression of *NIMIN* genes and the biochemical properties of NIMIN proteins revealed their role as negative regulators of the SAR response by binding NPR1 differentially in a SA dependent manner. However, there are still various unresolved questions regarding the NIMIN protein family. Even though there were many important breakthroughs in the field during recent years, including the mechanism of SA perception by NPR proteins [Neeley *et al.*, 2019; Wang *et al.*, 2020] or the role of NPR3 and NPR4 as transcriptional co-repressors [Ding *et al.*, 2018] few studies touch upon the possible role of NIMIN proteins.

For this reason, this study aims to gain further insights into both, regulation, and function of the NIMIN protein families in Arabidopsis and tobacco. The Arabidopsis *NIMIN* genes are regulated differentially, showing varying dependency on NPR1 or availability of salicylic acid. The NIMIN proteins harbor different domains and interact differentially with NPR1. These binary interactions, as well as ternary complexes with TGA transcription factors show varying sensitivity towards SA. Therefore, it can be presumed that NIMINs serve different functions *in planta* and there are indications, that these functions might not be exclusively associated with SAR establishment. To further elucidate differences between NIMIN proteins and their role in plant defense and other processes, diverse reporter constructs encompassing promoter and coding regions from Arabidopsis and tobacco *NIMIN* genes were analyzed in transient gene expression experiments in *Nicotiana benthamiana* and in transgenic tobacco plants. Targeted mutations were introduced to study the significance of specific domains for NIMIN protein function and to obtain a deeper understanding of the underlying mechanisms.

The identification of properties and functions of NIMIN proteins, including their potential involvement in other processes, could not only enhance the current understanding of SAR establishment, but also provide new insights into the interplay of different signaling pathways during plant defense. This knowledge may help to produce plants more resistant to pathogens and provide sustenance to the growing world population.

2. Materials

2.1. Enzymes & chemicals

Standard chemicals were obtained from the companies Duchefa (Haarlem, NL), Merck (Darmstadt, GER), Roth (Karlsruhe, GER), and Sigma-Aldrich (Taufkirchen, GER). Restriction enzymes and DNA modifying enzymes were obtained from the companies New England Biolabs (Frankfurt am Main, GER) or Thermo Fisher Scientific (St. Leon-Rot, GER). Consumables were obtained from the company Sarstedt (Nümbrecht, GER). Deviations from these sources are mentioned in the text.

2.2. Biological Materials / Organisms

2.2.1. Bacteria

Escherichia coli **DH5 α** (Laboratory stock) [Hanahan, 1983]

Genotype: F ϕ 80dlacZ Δ M15 Δ (*lacZYA-argF*) U169 *deoR recA1 endA1 hsdR17* (rk-, mk+)
phoA supE44 λ - thi-1, recA1, gyrA96 relA1

Agrobacterium tumefaciens **LBA4404** (Laboratory stock) [Hoekema *et al.*, 1983]

Genotype: Ach5 pTiAch5 Δ T, Rif^R

Agrobacterium tumefaciens **GV3101** (Laboratory stock) [Holsters *et al.*, 1980]

Genotype: pMP90RK, Gen^R, Rif^R

2.2.2. Plants

Nicotiana tabacum L. var. **Samsun NN**; *Nicotiana benthamiana* (**Domin**)

Origin: Tobacco Institute, North Carolina, USA
Prof. Dr. K. W. Mundry, Universität Stuttgart

Pro-1533PR-1a:GUS Nicotiana benthamiana

Origin: Lab generated transgenic reporter line, Prof. Dr. Artur J. P. Pfitzner

ProPR1a:GUS Nicotiana tabacum L. var. **Samsun NN (Line 138)**

Origin: Lab generated transgenic reporter line, Dr. Ursula M. Pfitzner

2.2.3. Yeast

Saccharomyces cerevisiae **HF7c** (Laboratory stock) [Bartel *et al.*, 1993]

Genotype: MATa, *ura3-52, his3-200, ade2-101, lys2-801, trp1-901, leu2-3, 112, gal4-542,*
gal80-538, LYS2::GAL1-HIS3, URA3::(GAL4 17-mers)₃-CYC1-lacZ

Origin: Clontech, Heidelberg, GER

The yeast strain HF7c contains the *HIS3* and *lacZ* reporter genes.

2.2.4. Viruses

Tobacco mosaic virus (TMV) „common strain“

Origin: American Type Culture Collection, USA

2.2.5. DNA standard

To determine the size of DNA fragments after separation on agarose gels, two different DNA size standards were used, depending on the estimated fragment sizes.

GeneRuler 1 kBp DNA Ladder (Thermo Scientific #SM0313)

10000 Bp | 8000 Bp | **6000 Bp** | 5000 Bp | 4000 Bp | 3500 Bp | **3000 Bp** | 2500 Bp | 2000 Bp | 1500 Bp | **1000 Bp** | 750 Bp | 500 Bp | 250 Bp

GeneRuler 100 Bp DNA Ladder (Thermo Scientific #SM0241)

1000 Bp | 900 Bp | 800 Bp | 700 Bp | 600 Bp | **500 Bp** | 400 Bp | 300 Bp | 200 Bp | 100 Bp

2.2.6. Protein standard

To determine the molecular weight of proteins after separation on SDS-polyacrylamide gels and immunodetection the protein size standard PageRuler™ Plus Prestained Protein Ladder (Thermo Scientific #26620) was used. Reference proteins coupled to red dye are written bold, those coupled to green dye are written italic:

250 kDa | 130 kDa | 100 kDa | **70 kDa** | 55 kDa | 35 kDa | **25 kDa** | 15 kDa | *10 kDa*

2.3. Kits

2.3.1. Plasmid preparation

Plasmid DNA for use in sequencing was prepared using the NucleoSpin® Plasmid Kit produced by Macherey-Nagel (REF 740588.250).

2.3.2. DNA elution from agarose gels

Elution of DNA from agarose gels was carried out using the Silica Bead DNA Gel Extraction Kit produced by Thermo Scientific (#K0513).

2.4. Plasmids

2.4.1. pBluescriptII (pBSKS(+)) / T-vector

The pBluescript vector produced by Stratagene (La Jolla, USA) has a size of 2,961 bp. It contains a multiple cloning site located within the coding region of the β -galactosidase (*lacZ*) gene, as well as an ampicillin resistance (*Amp^R*). In *E. coli* DH5 α (see 2.2.1) α -complementation of β -galactosidase allows identification of recombinant clones by blue-white selection. The vector was modified by Dr. Bernhard Roth to enable cloning of PCR products. The plasmid was linearized by restriction with *EcoRV* and subsequently treated with terminal deoxynucleotidyl transferase (TDT) in presence of 2',3'-Dideoxythymidine-5'-Triphosphate (ddTTP). This allows the addition of desoxythymidines to the blunted 3'-OH ends of the linearized plasmid DNA. Many *Thermus aquaticus* (*Taq*) polymerases tend to add an extra adenosine to the 3'-OH ends amplified DNA. These added adenosines can hybridize with the overlapping thymidines of the modified T-vector, making it useful for cloning PCR products.

2.4.2. pGBT9

The pGBT9 vector [Bartel *et al.*, 1993] is used in the analysis of protein-protein interactions in the context of the Yeast-Two-Hybrid system. The vector has a size of 5524 bp and replicates autonomously in *E. coli* as well as in *S. cerevisiae*. It carries an ampicillin resistance for selection in bacteria and a *TRP1* marker gene allowing selection of yeast cells on minimal medium without tryptophan. The multiple cloning site is located at the 3'-end of an open reading frame encoding the GAL4 DNA binding domain (BD). The constitutive *ADHI* promoter mediates the expression of GAL4BD or possible fusion proteins. Successful expression of a GAL4BD fusion protein requires cloning in the correct reading frame.

2.4.3. pGAD424

The pGAD424 vector [Bartel *et al.*, 1993] is used in the analysis of protein-protein interactions in the context of the Yeast-Two-Hybrid system. The vector has a size of 6659 bp and replicates autonomously in *E. coli* as well as in *S. cerevisiae*. It carries an ampicillin resistance for selection in bacteria and a *LEU2* marker gene allowing selection of yeast cells on minimal medium without leucine. The multiple cloning site is located at the 3'-end of an open reading frame encoding the GAL4 transcription activation domain (AD). The constitutive *ADHI* promoter mediates the expression of GAL4AD or possible fusion proteins. Successful expression of a GAL4AD fusion protein requires cloning in the correct reading frame.

2.4.4. pUC19

The pUC19 vector [Yanisch-Perron *et al.*, 1985] has a size of 2686 bp and is a high copy replicating *E. coli* plasmid vector. The plasmid contains a multiple cloning site located within the coding region of the *lacZ* gene, as well as an ampicillin resistance (*Amp^R*). In *E. coli* DH5 α (see 2.2.1) α -complementation of β -galactosidase allows identification of recombinant clones by blue-white selection.

2.4.5. pBin19/35S

The pBin19 vector [Bevan, 1984] is a binary plant vector used for the *Agrobacterium tumefaciens*-mediated transfer of DNA sequences into plants. This large plasmid has a size of 11,777 bp and contains a modified T-DNA carrying an MCS and the neomycin-phosphotransferase (*NPTII*) kanamycin resistance (*Kan^R*) gene between the left and right border. This kanamycin resistance is used in the selection of transformed plants. Outside of the T-DNA it encodes a second *NPTII* gene for selection in bacteria. The vector has two origins of replication (*ori*) allowing its replication in *E. coli* and in *A. tumefaciens*.

The transfer of the T-DNA by excision from the binary vector and subsequent integration into the plant genome requires another plasmid containing the *vir*-region of the original Ti plasmid. The *Agrobacterium* strains LBA4404 and GV3101 (see 2.2.1.) carry a disarmed Ti plasmid which contains only the *ori* and *vir* regions but lacks the T-DNA.

2.4.6. pRK2013

The helper plasmid pRK2013 is required for bacterial conjugation during tri-parental mating (TPM) [Figurski und Helinski, 1979]. It enables the transfer of the binary vector from the *E. coli* strain DH5 α into *agrobacteria* by providing the necessary gene products.

2.5. Synthetic oligonucleotides

The oligonucleotides used in this study were obtained from the company Invitrogen (Darmstadt).

35S	5' – TCC TTC GCA AGA CCC TTC CT – 3'
NOS	3' – CAT CGC AAG ACC GGC AAC AGG – 3'
GUS-3	5' – CGC TGC GAT GGA TTC CGG C – 3'
Bax-5-BglIII	5' – GCA GAT CTT TAT GGA CGG GTC CGG GGA – 3'
Bax-3-Sma	5' – TAA CCC GGG TCA GCC CAT CTT CTT CCA G – 3'
Venus-2	5' – GAG CTC TTA GGT GAT ATA GAC GTT GTG G – 3'
Venus-4	5' – GGG AGC TCT TAC TTG TAC AGC TCG – 3'
Venus-5	5' – TTG GAT CCA TGG TGA GCA AGG GCG AGG AGC – 3'
Venus-6	5' – TTG TCG ACT TAC TTG TAC AGC TCG – 3'
Venus-7	5' – GGG GAT CCA TAT GTA TCC TAA ACA ATT TAG TTT ATA CAA TTA TTC CCT AGA GAC CAT GGT GAG CAA GGG CGA GGA GCT GTT CAC CGG G – 3'
Venus-8	5' – GGG AGC TCT TAG GTC TCT AGG GAA TAA TTG TAT AAA CTA AAT TGT TTA GGA TAC ATC TTG TAC AGC TCG TCC ATG CCG AGA G

2. Materials

N1-P6	5' – CCA AGC TTG AGG TGG GGA CAG GGT G – 3'
N1 fwd	5' – CGG GAT CCA TAT GTA TCC TAA ACA ATT TAG – 3'
N1-13	5' – AAG GAT CCT AAA GCC TTG TCT TCG TTT CGC – 3'
N1-14	5' – CCG GAT CCA TAT GCA ATT TAG TTT ATA CAA TTA TTC CCT AGA GAC C – 3'
N1-15	5' – CCG GAT CCA TAT GTA TCC TAA ACA ATT TAG TGG ATA CAA TTA TTC CCT AGA GAC C – 3'
N1-16	5' – CCG GAT CCA TAT GAA TTA TTC CCT AGA GAC C – 3'
N1-17	5' – CCG GAT CCA TCT GTA TCC TAA ACA ATT TAG TTT ATA CAA TTA TTC CCT AGA GAC C
N1b-P3	5' – CAC CAC TCC CCT CAA TAT AC – 3'
N1b-1	5' – GGG GAT CCA TAT GAA CCA AGA AGA AG – 3'
N1b-2	5' – CCG GAT CCC AAT GCA AGA TTA AGA TCT AAA CC – 3'
N1b-4	5' – GGG GAT CCA TAT GTA TCC TAA ACA ATT TAG TTT ATA CAA TTA TTC CCT AGA GAC CAT GAA CCA AGA AGA AGA AAA AAC AGA G – 3'
N1b-5	5' – CCG GAT CCA TAT GTA TCC TAA ACA ATT TGC TTT AGC CAA TGC TGC CCT AGA GAC CAT GAA CCA AGA AGA AGA AAA AAC AGA G – 3'
N1b-6	5' – CCG GAT CCT AAA CCA TTA TCT TTT CTC ATC ACC – 3'
N1b-7	5' – CCG GAT CCG GTC TCT AGG GAA TAA TTG TAT AAA CTA AAT TGT TTA GGA TAC ATC AAT GCA AGA TTA AGA TCT AAA CCA TTA TCT TTT CTC
N2-3	5' – GGG GAT CCC AAC GAT AAA CTA ACG CTG TCT GG – 3'
N2-5	5' – GGG GAT CCA TAT GTA TCC TAA ACA ATT TAG TTT ATA CAA TTA TTC CCT AGA GAC CAT GAA CAA CTC TTT GAA GAA AGA AGA ACG CG – 3'
A10-2	5' – CCG GAT CCA TAT GCT ACT TAC TAT GGA CG – 3'
N2c-9	5' – AAG GAT CCC AAA CCA CCT TTT CGC ACG – 3'
FS-1	5' – TTG GAT CCA TAT GCC GCT AAT GGA GGG TG – 3'
FS-2	5' – AAG GAT CCA ACG CCG TTA GTC TCT GG – 3'
FS-3	5' – GCG GAG GTT GAG GAG TCC TCC GCT ATT TTA CGG AGG – 3'
FS-4	5' – CCT CCG TAA AAT AGC GGA GGA CTC CTC AAC CTC CGC – 3'
FS-5	5' – GGG GAT CCT TCC AAA CCA CCA TTC CGT AAC GG – 3'

2.6. Antisera

2.6.1. GFP (FL) antiserum

For detection of GFP, Venus, and corresponding fusion proteins, the primary “GFP (FL) polyclonal IgG” antiserum (200 µg/ml) (Santa Cruz Biotechnology, # sc-8334) was used at a dilution of 1:3000 in blocking solution. This antiserum consists of polyclonal IgG from rabbit and was raised against the full length GFP protein from *Aequorea victoria* as the targeted epitope.

2.6.2. GFP (MC) antiserum

In later experiments the detection of GFP, Venus, and corresponding fusion proteins was conducted using the primary “GFP Recombinant Rabbit Monoclonal Antibody” antiserum (200 µg/ml) (Thermo Fischer Scientific, # G10362) was used at a dilution of 1:1000 in blocking solution. This antiserum consists of recombinant monoclonal IgG from rabbit and was raised against the full length GFP protein from *Aequorea victoria* as the targeted epitope. For differences between GFP (FL) and GFP (MC) antisera, see Appendix I.

2.6.3. GST-N1 antiserum

For detection of untagged N1 protein, the primary “α-GST-N1” antiserum (U. M. Pfitzner, personal communication) was used at a dilution of 1:2000 in the blocking solution. This antiserum consists of polyclonal IgG from rabbit and was raised against *E. coli* expressed GST-N1 protein as the targeted epitope.

2.6.4. PR1 antiserum

For detection of PR1 proteins from plant protein extracts, the primary “α-PR1a” antiserum [Pfitzner & Goodman, 1987] was used at a dilution of 1:500 in blocking solution. This antiserum consists of polyclonal IgG from rabbit and was raised against purified PR1a protein from *N. tabacum* as the targeted epitope. The antiserum was provided by U. M. Pfitzner.

2.6.5. GAL4BD antiserum

For detection of proteins fused to the GAL4 DNA binding domain, the primary “α-GAL4BD” antiserum (200 µg/ml) (Santa Cruz Biotechnology, # sc-577) was used at a dilution of 1:500 in blocking solution. This antiserum consists of polyclonal IgG from rabbit and was raised against the amino acids 1-147 within the N-terminal DNA binding domain of GAL4 as the targeted epitope.

2.6.6. Anti rabbit IgG-HRP conjugate

For the detection of primary antibodies produced from rabbits, a secondary anti rabbit IgG antiserum (Rockland, USA) coupled to horseradish peroxidase was used at a dilution of 1:10.000 in the blocking solution.

3. Methods

3.1. Standard molecular biological methods

Standard methods in molecular biology were conducted according to the instructions published by Sambrook *et al.* [1989]. Enzymatic reactions and kits were used according to the instructions provided by the respective manufacturer, unless stated otherwise. The pH values of all solutions were adjusted using acetic acid (C₂H₄O₂), hydrochloric acid (HCl), potassium hydroxide (KOH) or sodium hydroxide (NaOH). In all cases deionized (dH₂O) water was used for preparation of solutions unless stated otherwise.

3.1.1. Growth of *E. coli*

<u>LB medium [1 l]</u>		<u>Antibiotics concentration</u>	
10 g	Peptone	50 µg/ml	Ampicillin (Amp)
5 g	Yeast extract	50 µg/ml	Kanamycin (Kan)
10 g	NaCl		
ad 1 l dH ₂ O		<u>Additives used in blue-white screening</u>	
<u>pH 7.5 (1 M NaOH)</u>		10 µg/ml	IPTG (Isopropyl-β-d-1-thiogalactopyranoside)
autoclaved		40 µg/ml	2 % X-Gal (5-bromo-4-chloro-3-indolyl-β-D-galactopyranoside) in dimethylformamide (DMFA)

LB Agar plates were produced by addition of 15 g micro-agar per liter of medium before autoclaving. The respective amount of antibiotics was added after the temperature of the medium cooled down to not more than 50 °C, immediately before pouring the agar plates.

The cultivation of *E. coli* in liquid medium containing the corresponding antibiotics was carried out overnight (o/n) at 37 °C and 250 rpm. Culturing on solid medium containing the required antibiotics, with or without the addition of X-Gal and IPTG for blue-white screening (see 3.1.4.), was carried out in the incubator at 37 °C.

3.1.2. Preparation of chemically competent *E. coli* DH5a cells

<u>Tfb I</u>		<u>Tfb II</u>	
30 mM	KOAc	10 mM	Na-MOPS pH7
50 mM	MnCl ₂	75 mM	CaCl ₂
100 mM	KCl	10 mM	KCl
10 mM	CaCl ₂	15 %	Glycerol
15 %	Glycerol	autoclaved	
sterile filtrated			

E. coli DH5a cells from a frozen glycerol stock were streaked out on a LB agar plate without antibiotics and incubated o/n at 37°C. A single colony from the plate was cultivated for two hours at 37 °C and 250 rpm in a 5 ml starter culture of LB medium containing 10 mM MgSO₄. This culture was used to

inoculate 100 ml LB medium containing 10 mM MgSO₄, which was incubated for another two to three hours at 37 °C and 250 rpm. At a cell density of 0.6 at OD₆₀₀ the culture was placed on ice and the cells were harvested by centrifugation at 6000 rpm for 10 min at 4 °C in a cooled centrifuge. The following steps were conducted exclusively under sterile conditions using pre-cooled reagents and materials. The supernatant was discarded, and the cell pellet was resuspended in two times 40 ml TfbI. The suspension was incubated on ice for 5 min before repeating the centrifugation step. The supernatant was discarded again, and the cells were resuspended in a total of 8 ml TfbII. The suspension was divided into 200 µl aliquots and snap frozen in liquid nitrogen. The cells could be stored at a temperature of -70 °C until used.

3.1.3. Transformation of chemically competent *E. coli* DH5α cells

In this protocol adapted from Inoue *et al.* [1990], 10 µl of ligation mixture were mixed with 100 µl of ice thawed competent *E. coli* DH5α cells and incubated on ice for 30 min. The transformation mixture was then subjected to a heat shock of 42 °C in a water bath for 30 seconds and immediately afterwards incubated on ice for 2 min. After addition of 900 µl of pre-warmed liquid LB medium, the cells were incubated at 37 °C and 250 rpm for 1 hour. 100 µl (10%) of the transformation mixture was directly plated out on a selective LB agar plate. The residual bacteria suspension was pelleted by centrifugation and the supernatant was discarded leaving behind approximately 100 µl of the supernatant. The pellet was resuspended and plated onto a second selective LB agar plate. The plates were incubated o/n at 37 °C. Colonies were picked with sterile tips and grown in an o/n culture of 5 ml LB containing the appropriate antibiotics at 37 °C and 250 rpm.

3.1.4. Blue-white screening of *E. coli* DH5α

Blue-white screening is used to select recombinant bacterial colonies resulting from ligation of DNA fragments into pBluescript or related vectors like the T-vector (see 2.4.1.). The MCS of these vectors is located within the coding region of the *lacZ* gene and encodes the N-terminal α-fragment of an IPTG inducible β-galactosidase. This fragment complements a C-terminal α-fragment of β-galactosidase contained in the genome of *E. coli* DH5α cells. The complemented β-galactosidase can convert the indicator X-Gal (5-bromo-4-chloro-3-indolyl-β-D-galactopyranoside) contained in the agar plates used for this purpose into 5-bromo-4-chloro-indoxyl, which can spontaneously dimerize to produce an insoluble blue pigment. The resulting colony is dyed blue, and the cloning is shown to be negative. Successful integration of a DNA fragment into the MCS of the vector interrupts the fragment encoded by the *lacZ* gene which stops the gene expression. The β-galactosidase is not complemented which renders the enzyme inoperative. The indicator is not converted, and the positive colony remains white.

3.1.5. Preparation of stock cultures

For long-term storage of bacteria cultures, glycerol stock cultures were created. 850 µl from a freshly grown o/n liquid culture were mixed with 150 µl of sterile glycerol in a screwable 2 ml micro tube and stored at -70 °C.

3. Methods

3.1.6. Growth of *A. tumefaciens*

The agrobacterium strain LBA4404 [Hoekema *et al.*, 1983] was cultivated in MinA medium at 30 °C for 3 days. The Strain GV3101 [Holsters *et al.*, 1980] was cultivated o/n in LB Medium (see 3.1.1.) at 30°C. Strain LBA4404 harbors the rifampicin resistance gene (rif), while strain GV3101 additionally contains the gentamycin resistance gene on its Ti plasmid.

MinA Agar plates were produced by addition of 15 g micro-agar per liter of medium before autoclaving. MgSO₄, Glucose, as well as the appropriate amount of antibiotics was added after the temperature of the medium cooled down to not more than 50 °C, immediately before pouring the agar plates.

<u>5x MinA salts</u>		<u>MinA medium [1 l]</u>		<u>Antibiotics concentration</u>	
52.5 g	K ₂ HPO ₄	200 ml	5x MinA salts	50 µg/ml	Gentamycin (Gent)
22.5 g	KH ₂ PO ₄	800 ml	dH ₂ O	50 µg/ml	Kanamycin (Kan)
5.0 g	(NH ₄) ₂ SO ₄	autoclaved		50 µg/ml	Rifampicin (Rif)
2.5 g	Sodium citrate x 2 H ₂ O	1 ml	20 % MgSO ₄ x 7 H ₂ O (sterile filtrate)		
<u>ad 1 l dH₂O</u>		10 ml	20 % Glucose (sterile filtrate)		
autoclaved					

3.1.7. Triparental mating

Triparental mating describes the conjugative transfer of binary vector constructs from *E. coli* to *A. tumefaciens* as described by Bevan [1984]. The conjugation is made possible by the helper plasmid pRK2013 (see 2.4.6.) [Figurski & Helinski, 1979]. *A. tumefaciens* LBA4404 cells from a frozen glycerol stock were inoculated into two 5 ml MinA liquid cultures containing rifampicin and incubated for two days at 30 °C and 250 rpm. After one day the *E. coli* strain MM294 containing the helper plasmid pRK2013 and *E. coli* strains with the respective binary vector constructs were inoculated into a 5 ml LB liquid culture containing kanamycin. These cultures were incubated o/n at 37 °C at 250 rpm. 1 ml from each culture (a total of 2 ml for *A. tumefaciens* LBA4404) were centrifuged for 3 min in a tabletop centrifuge to pellet the cells. The supernatant was discarded, and the *E. coli* strains were suspended in 1 ml of sterile 10 mM MgSO₄ each. The Agrobacterium cells were suspended in 400 µl of sterile 10 mM MgSO₄. 50 µl of each bacterial suspension (*A. tumefaciens* LBA4404, *E. coli* with pRK2013, and *E. coli* with binary vector construct) were pipetted onto the middle of an LB agar plate without antibiotics, mixed together and spread evenly. A plate where Agrobacteria were mixed only with the helper strain only was used as a negative control. All plates were incubated o/n at 30 °C. On the next day, the cells were scraped from the plates using a sterilized Drigalski spatula and 2 ml of LB medium. The harvested cell solution was diluted 1:1000 and 50 µl were spread on a selective MinA agar plate containing kanamycin and rifampicin. The plates were incubated at 30 °C for 3-5 days. For use in restriction analysis, Agrobacterium clones were grown for two days in 5 ml MinA liquid cultures containing rifampicin and kanamycin at 30°C and 250 rpm. 4.5 ml of the culture were used to prepare plasmid DNA (see 3.1.8.).

3.1.8. Plasmid preparation from bacterial cells

Solution I		Solution II		1x TE	
50 mM	Glucose	0.2 M	NaOH	10 mM	Tris/HCl pH 8.0
25 mM	Tris/HCl pH 8.0	1 %	SDS	1 mM	EDTA pH 8.0
10 mM	EDTA pH 8.0	Solution III			
autoclaved		3 M	Sodium acetate, pH 4.8		
100 µg/ml RNase A		adjusted with glacial acetic acid			

For isolation of plasmid DNA, 1,5 ml from a 5 ml o/n culture were transferred into a reaction tube and centrifuged for 3 min at room temperature. After discarding the supernatant, the cells were resuspended in 100 µl of Solution I. Thereafter, 200 µl of Solution II were added to start cell lysis and the suspension was mixed gently by inverting the tube. The suspension was neutralized by addition of 150 µl ice-cold Solution III and again mixed gently as described above. The reaction tubes were then centrifuged for 10 min at 15.300 rpm to precipitate genomic DNA and proteins. The supernatant was carefully transferred into a new reaction tube containing 1 ml of cold ethanol (99,6 % (v/v), p.a.) and mixed by inverting the tube. The DNA was left to precipitate for 30 min at -20 °C. The reaction tube was centrifuged for 3 min to collect the DNA. The supernatant was discarded, and the DNA precipitate was resuspended in 100 µl 1x TE. After addition of 50 µl 7.5 M ammonium acetate and 200 µl of cold ethanol (99,6 % (v/v), p.a.), the DNA was precipitated for another 30 min at -20 °C. The reaction tube was again centrifuged for 3 min and the supernatant was discarded. The DNA precipitate was washed in cold ethanol (70 % (v/v), p.a.). After another 3 min centrifugation step the supernatant was discarded and the DNA was dried for 10 min using a vacuum centrifuge (speedvac, Bachhofer Laboratoriumsgeräte, Reutlingen, GER). The DNA was dissolved in 50 µl of 1x TE buffer and stored at -20 °C until used.

A. tumefaciens cells are used to transiently express or transfer the gene of interest contained in a binary plasmid (pBin19, see 2.4.5.) in plants. Plasmid preparation from *A. tumefaciens* is difficult compared to preparation from *E. coli* cells since *A. tumefaciens* is more resistant to cell lysis and its plasmids are characterized by their low copy number [Chen *et al.*, 2003]. Therefore, 3x 1.5 ml from the same o/n culture were spun down in the same reaction tube. Afterwards the protocol was carried out as described above for *E. coli*.

3.1.9. Sequence specific restriction of DNA

Plasmid DNA or PCR products were restricted using specific restriction enzymes following the instructions from the company and using the recommended restriction buffers. 0.2 to 2 µg of DNA in a final volume of 20 µl were digested using 5-10 units of the enzyme. The DNA was digested for at least 2 hours at the recommended temperature. For cloning procedures, twice the amount of DNA was used in a final volume of 40 µl and digested for at least 4 h. When performing a double digestion, the optimal buffer for both enzymes was chosen using the NEB buffer activity chart for endonucleases. In case that the restricted DNA was not used for subsequent gel electrophoresis the restriction enzymes were inactivated according to the manufacturer's specifications.

3.1.10. Dephosphorylation of DNA fragments

To prevent the religation of linearized plasmid DNA digested using a single restriction enzyme, the free 5'-phosphate residues were hydrolyzed (dephosphorylated) using the calf intestine alkaline phosphatase (CIAP) enzyme. CIAP was added to the linearized DNA according to the manufacturer's specifications and the reaction was incubated for 15 min at 37 °C.

3.1.11. Separation of DNA fragments (Gel electrophoresis)

<u>50x TAE buffer</u>		<u>5x Loading buffer</u>	
242 g	Tris	50 %	Glycerin
100 ml	0,5 M EDTA pH 8.0	1 mM	EDTA
57.1 ml	Acetic acid (100 %)	0.25 %	Bromophenol blue
ad 1 l dH ₂ O		0.25 %	Xylene cyanol

Agarose gel electrophoresis was performed to determine the size of DNA fragments from PCR products or digested plasmids and to purify said fragments. Depending on the estimated size of the fragments 1-2% agarose was dissolved in 1x TAE buffer and boiled. After the solution cooled down to below 55 °C, 10 µg/ml ethidium bromide (EtBr) was added to allow detection of DNA under ultraviolet (UV) light. The agarose solution was cast into a gel casting tray and a comb was placed. After polymerization, the gel was placed in the chamber and covered in 1x TAE buffer. Thereafter, the comb was removed, and the samples mixed 1:5 with the 5x Loading buffer were pipetted into the wells. To determine the fragment sizes, a DNA ladder was loaded onto the gel as well. Electrophoretic separation of DNA was performed at 80 to 120 Volts. The DNA was visualized under UV light.

3.1.12. Elution of DNA Fragments from agarose gels

To purify DNA fragments of specific sizes for use in cloning, PCR products or digested plasmid DNA were subjected to agarose gel electrophoresis. The elution of agarose embedded DNA was carried out using the Silica Bead DNA Gel Extraction Kit (Thermo Scientific, #K0513) according to the manufacturer's specifications.

3.1.13. Ligation of DNA Fragments

<u>Reaction [20 µl]</u>	
x µl	Insert-DNA
y µl	Vector-DNA
2 µl	10x T4 DNA Ligase buffer
1 µl	T4 DNA Ligase
z µl	dH ₂ O

The ligation of DNA fragments into plasmids was performed using the T4 DNA ligase. This enzyme catalyzes the formation of phosphodiester bonds between 5'-phosphate and 3'-hydroxyl groups in linear double stranded DNA-molecules. A reaction batch includes a fivefold excess of insert DNA compared to vector DNA and was incubated o/n at 4 °C or at least one hour at room temperature. After incubation, the ligation could be used directly for transformation into competent *E. coli* DH5α cells (see 3.1.3.).

3.1.14. PCR amplification

Amplification of specific DNA fragments was performed by using polymerase chain reaction (PCR) [Saiki *et al.*, 1988; Bej *et al.*, 1991]. A small amount of template DNA is multiplied through repeated cycles of strand separation by heat denaturation and subsequent DNA replication by hybridization of the separated DNA strands with specific synthetic oligonucleotides (primers) during annealing, and synthesis of a complementary strand by means of a thermally stable DNA polymerase (*Taq* polymerase) during elongation. Primers can be designed to produce DNA fragments harboring introduced restriction sites or mutations. Reaction mixtures were prepared on ice in sterile 0.5 ml Thermowell™ tubes (Corning Incorporated, UK). A PCR reaction containing dH₂O instead of DNA was used as a negative control. When available a positive control containing DNA able to hybridize with the primers was used as well. The reactions were carried out in a programmable thermocycler (Mastercycler® personal, Eppendorf AG, Hamburg, GER) using the PCR standard program outlined below. PCR products were verified by agarose gel electrophoresis and, if required for cloning purposes, eluted from the gel.

Reaction mixture [20 µl]		PCR standard program			
2 µl	10x PCR buffer	1 min	94 °C	Denaturation	
2 µl	MgCl ₂ (25 mM)	30 s	94 °C	Denaturation	10 cycles
2 µl	dNTPs (2 mM)	30 s	60 °C	Annealing	
2 µl	Primer 5' (10 mM)	90 s	72 °C	Elongation	
2 µl	Primer 3' (10 mM)	30 s	94 °C	Denaturation	20 cycles
0.2 µl	<i>Taq</i> DNA polymerase	30 s	60°C	Annealing	
8.8 µl	dH ₂ O	90 s + 10 s/cycle	72 °C	Elongation	
1 µl	Template DNA	7 Min.	72 °C	final Elongation	
		∞	8 °C	Hold	

3.1.15. PCR site directed mutagenesis

Site-directed mutagenesis as described by Ho *et al.* [1989] allows the introduction of a specific mutation into any known sequence by performing PCR via mismatching oligonucleotides. The resulting DNA fragments containing the mutation can be cloned afterwards. In this study, PCR site directed mutagenesis was used to substitute, delete, or insert single or multiple amino acids in a target sequence to characterize the role of specific amino acid residues or domains in a protein of interest. To introduce mutations further away from the ends of the sequence, the PCR overlap extension method was used. This method requires four primers, the first two of which are flanking the sequence, while the mutation is incorporated into the other two internal primers. A targeted mutagenesis using this method requires three PCR reactions. The first and second PCR reactions were used to amplify two PCR fragments, each using one flanking primer binding to one end of the target sequence and one internal primer, containing the mismatched oligonucleotides, which hybridizes at the target site of the mutation. The third PCR was performed using the overlapping products of the first two PCR reactions as template and the two flanking primers to generate a complete DNA fragment including the mutation.

3.1.16. Screening bacterial colonies using PCR

In the case that a large number of bacterial colonies had to be tested for successful transformation, the presence of the transgene was verified by screening the colonies using PCR. PCR reaction tubes containing 10 µl dH₂O were prepared beforehand. Using a new sterile pipette tip for each, single colonies were picked and transferred to a separate labeled sector on a new selective agar plate. The plate was incubated o/n at 37 °C for *E. coli* or at 30 °C for *A. tumefaciens*. The rest of the bacteria on the tip were suspended in the prepared reaction tubes, three colonies per tube. The resuspended bacteria cells were disrupted using a thermocycler applying the following conditions:

Disruption of bacterial cells

5 min	96 °C
90 s	50 °C
90 s	96 °C
1 min	45 °C
1 min	96 °C
1 min	40 °C
∞	8 °C

The disrupted bacterial cells were used as template in a standard PCR reaction (see 3.1.14.) utilizing primers specific for the transgene. The PCR products were separated and analyzed using agarose gel electrophoresis. For each sample showing the desired fragment size, the colonies from the labeled selective agar plate were grown in o/n liquid culture for DNA isolation to secure the right clones.

3.1.17. Cloning of PCR products

During a PCR reaction, the *Taq* DNA polymerase enzyme leads to the addition of an adenine residue to the 3' ends of both strands of the dsDNA molecule. This reaction is caused by non-template dependent terminal transferase activity of the enzyme. A PCR product with 3' adenine overhangs can be ligated into a vector having complementary 3' thymidine overlaps as seen in the T-vector (see 2.4.1.).

3.1.18. Estimation of nucleic acids concentration

To determine the concentration of nucleic acids, 5 µl of the DNA solution were diluted 1:10 using dH₂O for a final volume of 50 µl. A dilution of each sample was added to a plastic cuvette (Eppendorf UVette[®], GER). A cuvette containing 50 µl dH₂O without DNA was used as a reference. The measurements were executed in an Ultrospec[™] 3000 spectrophotometer (Pharmacia Biotech, Cambridge, UK). The concentration of nucleic acids was determined using the following formula:

$$\text{Concentration} = [(\text{Absorption } \lambda \text{ 260 nm}) - (\text{Absorption } \lambda \text{ 320 nm})] \times F \times \text{dilution factor}^{-1}$$

$$F[\mu\text{g/ml}] = 50 \text{ (DNA)} \text{ or } 40 \text{ (RNA)} \quad \lambda \text{ 320 nm} = \text{background absorption (Wavelength)}$$

$$\text{Dilution factor} = 1:10$$

3.1.19. DNA sequencing

The DNA sequence of positive clones was confirmed by sequencing. To achieve purity required for the sequencing reaction, plasmid DNA was isolated using the NucleoSpin®Plasmid Kit produced by Macherey-Nagel (REF 740588.250). 1.5 µg purified DNA were sent to the companies specialized in DNA sequencing using the chain termination method described by Sanger *et al.* [1977]. The sequencing reactions were carried out by the companies Eurofins MWG Operon (Ebersberg, GER) or Microsynth Seqlab (Göttingen, GER).

3.2. Experimental methods using *Saccharomyces cerevisiae*

3.2.1. Yeast media

SD medium [200ml]:		YPAD medium [1 l]	
0,425 g	Yeast nitrogen base without amino acids	20 g	Peptone
		5 g	Yeast extract
1,25 g	(NH ₄) ₂ SO ₄	40 mg	Adenine hemisulfate
		ad 950 ml dH ₂ O	
ad 200 ml dH ₂ O		pH 5,8 (KOH)	
pH 5,8 (KOH)		autoclaved	
autoclaved		50 ml	40 % Glucose (sterile)

Before use in the standard minimal (SD) medium, the 100x Drop-In solutions of the necessary amino acids were diluted 1:10 with dH₂O and the volume was adjusted to 25 ml. Then 25 ml of sterile 20 % glucose was added, and the resulting 50 ml 10x Drop-In solution was mixed with 200 ml SD medium. For agar plates, 1.5 % micro agar was added before autoclaving (3.75 g in 250 ml SD medium (final volume), 1.5 g in 100 ml YPAD medium).

100x Drop-In Solutions

Adenine hemisulfate	2 mg/ml
L-Histidine monohydrochloride monohydrate	2 mg/ml
L-Leucine	10 mg/ml
L-Lysine dihydrochloride or	3,6 mg/ml
L-Lysine monohydrochloride	3 mg/ml
L-Methionine	2 mg/ml
L-Tryptophan	2 mg/ml
Uracil	2 mg/ml
	in dH ₂ O

Sterile filtrated

3.2.2. Cultivation of yeast cells

Yeast cells were cultured at 30 °C and liquid cultures were shaken at 250 rpm. Yeast cells from strain HF7c (see 2.2.3.) are auxotrophic for specific amino acids essential for their metabolism and cannot grow on minimal medium lacking adenine, histidine, lysine, leucine, tryptophan, and uracil. Analogous to using antibiotic resistance selection markers in *E. coli*, yeast cells can be selected by transformation of plasmids which complement the auxotrophy. These plasmids can also contain a foreign gene of interest.

3.2.3. Preparation of competent yeast cells (HF7c)

Solution A:

10 mM Bicine
1 M Sorbitol
3 % Ethylene glycol (w/v)

pH 8,35 (KOH)

autoclaved

A 5 ml overnight culture of HF7c yeast cells was grown in YPAD medium. The culture was centrifuged for 10 min at 3000 rpm and most of the supernatant was discarded. The cells were carefully resuspended in about 500 µl of the remaining supernatant and used to inoculate 100 ml of YPAD medium. The culture was incubated at 30 °C and 250 rpm until an OD₆₀₀ of 0.6 was reached. The cells were harvested by centrifugation for 10 min at 3000 rpm and 4°C in a cooled centrifuge, and washed in 20 ml of Solution A. After another centrifugation step using the same parameters, the supernatant was discarded, and the yeast cells were resuspended in 4 ml of Solution A. The competent cells were aliquoted to 100 µl and frozen slowly at -20 °C before being stored at -70 °C.

3.2.4. Transformation of yeast cells

Solution B:

200 mM Bicine
40 % Polyethylene glycol 1000 (w/v)

pH 8,35 (KOH)

autoclaved

Solution C:

10 mM Bicine
150 mM NaCl

pH 8,35 (KOH)

autoclaved

Selective SD agar plates containing the appropriate drop-in solutions were dried in a laminar flow cabinet for 1 hour. The plasmid DNA and carrier DNA (salmon sperm DNA, 10 mg/ml in TE) were thawed at room temperature. The carrier DNA was boiled for 5 min at 100 °C in a heating block and thereafter cooled on ice. Competent yeast cells (see 3.2.3.) were taken from the -70 °C freezer and directly placed on ice. 5 µl carrier DNA was pipetted onto the wall of the reaction tube. Depending on the concentration, 3-6 µl of plasmid DNA was pipetted into the droplet of carrier DNA. The reaction tube was then incubated in a water bath at 37 °C for 3 min. After adding 1 ml of Solution B the tube was carefully mixed by inversion and incubated at 30 °C for 1 h. The tube was then centrifuged for 20 s at 15.300 rpm in a tabletop centrifuge and the supernatant was discarded. The yeast cells were carefully

resuspended in 800 μ l of Solution C by pipetting up and down. The tube was centrifuged as above, and the supernatant was discarded. The yeast cells were carefully resuspended in 100 μ l of Solution C and plated on the prepared SD agar plates. Finally, the plates were wrapped in parafilm and incubated at 30 °C for 3-4 days.

3.2.5. The yeast two-hybrid system for characterization of protein-protein interactions

The yeast two-hybrid (Y2H) system is a method devised to identify and characterize specific protein-protein interactions [Fields & Song, 1989]. This study utilizes the MATCHMAKER two-hybrid system from Clontech (Heidelberg, GER). This system is based on the GAL4 transcription factor from yeast and the *lacZ* reporter gene integrated into the genome of the yeast strain HF7c, which is under control of a promoter regulated by GAL4. The two functional domains are encoded by two different plasmids. The DNA binding domain (GAL4BD) and the GAL4 activation domain (GAL4AD) are included in the pGBT9 (2.4.2.) and pGAD424 (2.4.3.) vectors, respectively. cDNA sequences of the proteins to be tested for interaction are fused to the C-terminus of the respective domains. Both plasmids are transformed into the yeast strain HF7c (see 3.2.4.). In case of an interaction between the two proteins, the GAL4AD and GAL4BD come into close spatial proximity which enables reconstitution of the GAL4 transcription factor. The GAL4 regulated *lacZ* reporter gene is activated, allowing quantitative measurement of the interaction based on the activity of the β -galactosidase enzyme (see 3.2.6.).

3.2.6. Quantitative Test of protein-protein interaction in yeast

The *lacZ* reporter gene contained in the genome of the yeast strain HF7c was used to quantify protein-protein interactions using the Y2H system mentioned above. The activity of the β -galactosidase enzyme stands in a direct proportion to the affinity of the interaction partners. *o*-Nitrophenyl- β -galactoside (oNPG) was used as a substrate for the β -galactosidase and hydrolysis of the colorless oNPG converts it into the yellow-colored *o*-Nitrophenol.

<u>Z buffer</u>		<u>oNPG substrate solution</u>	
60 mM	Na ₂ HPO ₄ x 7H ₂ O (sterile)	4 mg/ml	<i>o</i> -Nitrophenyl- β -galactoside
40 mM	NaH ₂ PO ₄ x H ₂ O (sterile)		in Z buffer
10 mM	KCl (sterile)		
1 mM	MgSO ₄ (sterile)		
pH 7,0		Storage at -20 °C; protected from light	
For Z buffer/ β -Mercaptoethanol (MSH) add 135 μ l MSH per 50 ml of Z buffer			

From each yeast transformation (see 3.2.4.), three independent colonies were grown in a 5 ml overnight SD medium liquid culture at 30 °C and 250 rpm. As a negative control, 5 ml of non-inoculated medium was incubated under the same conditions. From each overnight culture 2x 1 ml were transferred into individual reaction tubes. To keep the cells suspended the cultures were shaken before pipetting. Another 1 ml was transferred into a cuvette to measure the OD₆₀₀ against the negative control in a spectrophotometer. The OD₆₀₀ of the yeast cultures should be between 1.0 and 1.5 for optimal results.

The reaction tubes were centrifuged for 3 min in a tabletop centrifuge to harvest the cells. The supernatant was discarded, and the cells were resuspended in 100 µl Z buffer using a vortex mixer. The cell suspension was snap frozen for 1 min in liquid nitrogen and then thawed at 37 °C in a water bath for 80 s. This process was repeated two more times to disrupt the cells. 750 µl of Z buffer containing β-Mercaptoethanol (MSH) were added. To start the reaction 150 µl of the oNPG substrate was added and the reaction tubes were mixed by inversion. The reaction tubes were incubated at 30 °C and 250 rpm until a yellow coloration became visible. Depending on activity of the enzyme this could take from a few minutes up to three hours. The reaction was stopped by adding 400 µl 1 M Na₂CO₃. The reaction tubes were centrifuged for 3 min in a tabletop centrifuge and the supernatant was transferred into cuvettes. The OD₄₂₀ was measured against the negative control. In case the OD₄₂₀ exceeds 1.5 the samples had to be diluted. The Miller units were measured using the following formula:

$$\text{Miller units} = \frac{1000 \times OD_{420}}{t \times V \times OD_{600}}$$

OD₆₀₀ = cell density of the overnight culture

t = incubation time

OD₄₂₀ = absorption of o-nitrophenol

V = volume of the cell suspension (1ml)

3.2.7. Protein extraction from yeast cells

To determine the accumulation of GAL4AD or GAL4BD and related fusion proteins single colonies from a yeast transformation were grown o/n in a 5 ml SD medium liquid culture containing the required amino acids. The entire volume was centrifuged for 5 min at 4 °C and 3000 rpm. After discarding the supernatant, the cell pellet was washed in 1 ml cold dH₂O. The suspension was centrifuged once more under the same conditions and the supernatant was discarded again. The cells were snap frozen for 1 min in liquid nitrogen and stored at -70 °C. Before the proteins could be separated using SDS-PAGE (see 3.4.2.), the cells had to be resuspended in 100 µl 1x SDS loading dye (with DTT) and boiled for 5 min at 100 °C in a heating block to denature the proteins. The sample was then centrifuged for 5 min in a tabletop centrifuge at maximum rotational speed. From the supernatant, 20 µl were applied to the gel and the remainder was stored at -20 °C.

3.3. Experimental methods using plants

3.3.1. Cultivation of plant seeds on MS Medium

MS medium

1,15 g Murashige & Skoog (MS) Basal salt mixture
 4 g Phyto agar (0,8%)
 ad 500 ml dH₂O
 pH 5,7 (KOH oder NaOH)

autoclaved

400 µg/ml Kanamycin

Antibiotic resistances introduced into plants allow preselection of transgenic seedlings for successful transformants. The seeds had to be sterilized before sowing them on MS medium agar plates. For this purpose, the seeds were placed into a sterile reaction tube and 1 ml of 70 % technical grade ethanol was added to the seeds. After an exposure of 30 s, the ethanol was carefully removed and discarded. The seedlings were then incubated in 1 ml of 5 % sodium dichloroisocyanurate dihydrate for 20 min under constant shaking and occasional inversion of the tube. After the sterilization, the seeds were centrifuged, and the supernatant was discarded. After three washing steps using sterile dH₂O, the seeds were then spread on MS medium agar plates containing no antibiotics for non-transgenic plants or kanamycin for transgenic plants. In experiments studying salicylic acid sensitivity of germination and development, 0.3 mM of SA was added to the medium before pouring the plates. The plates were incubated for about 4 weeks under standard conditions of 22 °C and 16 h of light in a light cabinet until the seedlings were large enough to be picked and planted into trays.

3.3.2. Plant cultivation and growth in the greenhouse

Cultivation of plants took place in the greenhouse. The plants were exposed to 16 h of natural or artificial illumination per day and kept at temperatures between 22 °C and 28 °C. Seedlings (see 3.3.1.) were grown in small trays containing moist standard soil. Once large enough, the plants were transferred into individual pots containing autoclaved soil.

3.3.3. Isolation of genomic DNA from plants

DNA extraction buffer

0.35 M Sorbitol
 0.1 M Tris
 5 mM EDTA
 pH 7.5

Lysis buffer

0.2 M Tris
 50 mM EDTA
 2 M NaCl
 2 % Hexadecyltrimethylammonium bromide

Sarcosyl solution

5 % N-Lauroylsarcosine
 sodium salt

Microprep buffer (freshly prepared, RT)

2.5 volumes DNA extraction buffer
 2.5 volumes Lysis buffer
 1 volume Sarcosyl solution
 0.3–0.5 g/100 ml NaHSO₃ or Na₂S₂O₅

Extraction of genomic DNA from plants was performed as described by Fulton *et al.* [1995]. Two fresh leaf discs of about (\varnothing 10 mm, 50-100 mg plant tissue) with 200 μ l freshly prepared microprep buffer were grinded in a reaction tube using a plastic pestle. Then, another 550 μ l of microprep buffer was added and mixed gently by inverting the tube. The suspension was incubated for 60 min at 65 °C in a water bath. After the incubation, 800 μ l chloroform:isoamyl alcohol (24:1) were added to the suspension. After careful mixing by inversion of the tube, the suspension was centrifuged for 5 min at 10.000 rpm in a tabletop centrifuge. The upper water phase (about 0.5 ml) was transferred into a new reaction tube and mixed with 0.5 ml of cold isopropanol. As soon as the DNA precipitates the tube was centrifuged for another 5 min at 10.000 rpm. The supernatant was discarded, and the precipitate was washed using cold ethanol (70 % (v/v), p.a.). After another centrifugation step, the ethanol was discarded, and the precipitate was air-dried for 1 hour. 50 μ l 1x TE were added and the precipitate was dissolved during an incubation for 15 min at 65 °C in a water bath. The suspension was centrifuged once more for 10 min at 10.000 rpm and the supernatant containing the genomic DNA was transferred into a new reaction tube. The isolated plant DNA could be stored at -20 °C or be used for PCR analysis. A standard PCR reaction (see 3.1.14.) requires 1 μ l of undiluted genomic plant DNA.

3.3.4. Virus inoculation of *N. tabacum*

Tobacco mosaic virus (TMV) can easily be transmitted by mechanical damage and invade the tobacco plant through wounds in epidermal cells. A small amount of graphite dust (silicon carbide) was applied to the epidermis of a leaf. 50 μ l of *TMV* suspension (1:50 in 50 mM Tris/HCl, pH 7.5) were evenly distributed in the form of small droplets. The virus suspension was then carefully spread on the leaf surface, rubbing it in using a finger. In doing so the graphite dust damages the epidermal cells and allows the virus to penetrate the cells. The infected leaves were monitored for phenotypical effects and protein extracts were used to observe possible changes in protein expression.

3.3.5. Agroinfiltration-based transient gene expression in *Nicotiana benthamiana*

The *Agrobacterium* strain LBA4404 containing binary vector (pBin19) constructs with the genes of interest under control of the 35S promoter from Cauliflower mosaic virus (CaMV) was incubated in 5 ml MinA medium with the required antibiotics for 3 days at 30 °C and 250 rpm. Constructs in the *Agrobacterium* strain GV3101 like the one containing the p19 silencing suppressor from Tomato bushy stunt virus (TBSV) were incubated under the same conditions for only one day in 5 ml LB medium containing the required antibiotics. The concentrations of all cultures were determined by measuring the OD₆₀₀ using a spectrophotometer. To achieve the same starting conditions after infiltration, the OD₆₀₀ values were used to calculate the volume of bacterial suspension needed, adjusted to an OD₆₀₀ of 0.5. As a guideline, the agroinfiltration of three leaf halves on three independent plants each requires about 6 ml of bacterial suspension. The cells were centrifuged for 3 min in a tabletop centrifuge and the supernatant was discarded. The pelleted cells were resuspended in 10 mM MgCl₂ containing 150 μ M acetosyringone. The cell suspensions were incubated for at least 2 h in the dark at room temperature.

After the incubation, the bacterial suspensions were mixed depending on the experimental setup. To prevent plant-mediated silencing, a strain overexpressing the p19 silencing suppressor from *Tomato bushy stunt virus* was added in a 1:1 ratio. The cell suspensions were infiltrated into the underside of the leaves of four- to six-week-old *N. benthamiana* plants using 1 ml needleless syringes (Omnifix®-F, Brain, Melsungen, GER). Infiltration of the left and the right leaf halves with agrobacteria containing different constructs allowed direct comparison of phenotypic effects. Noninfiltrated plants were used as negative controls while plants infiltrated with agrobacteria overexpressing GFP were used as positive controls. For each experiment, the infiltration procedure was performed on three adjacent leaves on three independent plants. Four days post inoculation (dpi) the expression of GFP in control plants was examined using ultraviolet light. In case of a strong expression, the plants could be used to extract proteins (see 3.3.7.). The phenotypic condition of infiltrated leaves was examined and documented daily.

3.3.6. Induction of the *GUS* reporter gene activity in transgenic plants

To analyze the induction of different *GUS* reporter gene constructs two fresh leaf discs (Ø 10 mm) were harvested 4-5 dpi from the upmost agroinfiltrated leaves from *N. benthamiana* plants containing *Pro-1533PR1-a:GUS* or analogous reporter constructs. When using *N. tabacum* four leaf discs (Ø 14 mm) were used instead. The induction of the reporter gene was carried out on 6 ml 1 mM SA, 0.3 mM BTH, or analogous substances in six well culture plates. As negative controls, leaf discs were incubated on the same amount of dH₂O. After two to four days the leaf discs were dried on absorbent paper towels und used for protein extraction (see 3.3.7.).

3.3.7. Protein extraction from plant cells

1 M Sodium phosphate buffer pH 7.0		GUS lysis buffer	
57.5 ml	1 M Disodium hydrogen phosphate	50 mM	Sodium Phosphate buffer pH 7
42.3 ml	1 M Sodium dihydrogen phosphate	10 mM	EDTA
		0.1 %	Triton-X 100
		0.1 %	Lauroylsarcosine
		10 mM	β-Mercaptoethanol

For protein extraction from *N. benthamiana*, two fresh leaf discs (Ø 10 mm) with 150 µl *GUS* lysis buffer were grinded in a reaction tube using a plastic pestle. For protein extraction from *N. tabacum*, four leaf discs (Ø 14 mm) were macerated in 200 µl *GUS* lysis buffer as described above. The cell lysate was centrifuged for 10 min at 4 °C and 15.300 rpm. The supernatant containing free proteins was transferred into a new reaction tube and was centrifuged again for 10 min using the same conditions. The supernatant was again transferred to a new tube and centrifuged again. The supernatant was then used for further experiments e.g., *GUS* enzyme assays, protease assays or immunodetection. The protein extracts were stored at -70 °C for extracts used in *GUS* enzyme assays and at -20 °C for extracts used for protease assays or immunodetection. After thawing of stored extracts, the tubes were centrifuged once using the same conditions as described above.

3.3.8. GUS Reporter gene assay

1 M Sodium phosphate buffer pH 7.0		GUS Lysis buffer	
57.5 ml	1 M Sodium hydrogen phosphate	50 mM	Sodium phosphate buffer pH 7.0
42.3 ml	1 M Sodium dihydrogen phosphate	10 mM	EDTA
		0.1 %	Triton X-100
		0.1 %	Lauroylsarcosine
		10 mM	β -Mercaptoethanol
10 mM MUG Solution			
0.35 g	4-Methylumbelliferyl β -D-glucuronide in 100 ml GUS lysis buffer		

MU Stock solution

100 μ M 4-Methylumbelliferone
in 96 % EtOH

Storage: in darkness at -20°C

To determine the activity of the induced GUS reporter gene, plant extracts prepared from the appropriate leaf material were used in a modified GUS reporter gene assay [Jefferson, 1987]. 20 μ l of protein extract were mixed in a reaction tube with 70 μ l of GUS lysis buffer and 10 μ l of 10 mM MUG solution as a substrate. The reaction tube was incubated at 37 °C. The GUS assay allows quantification of the activity of the β -glucuronidase enzyme encoded by the GUS reporter gene. β -glucuronidase converts the substrate 4-Methylumbelliferyl β -D-glucuronide (MUG) into 4-methylumbelliferone (MU) and glucuronic acid. MU is a fluorescent indicator stimulated by UV radiation. As a reference, a reaction tube containing 90 μ l GUS lysis buffer and 10 μ l of 10 mM MUG solution was used. After 30 min of incubation and regularly every 15 min thereafter, reaction tubes were checked under UV light to evaluate fluorescence intensity. The reactions were stopped by addition of 400 μ l of 0.2 M Na₂CO₃ and the incubation time was documented. The stopped reaction tubes could be stored at 4 °C until further use.

MU fluorescence was quantified using a fluorometer (Spectraflour; Tecan, Crailsheim, GER). MU emits blue light at a wavelength of 455 nm when excited by UV light of 365 nm wavelength. To quantify the data a calibration curve in the range between 0 and 5000 pMol MU was determined. The reactions were compared to the calibration curve under UV light and, if required, diluted using 0.2 M Na₂CO₃. The dilution factors were considered when calculating enzyme activity. 250 μ l from each reaction sample and from the calibration samples were applied to flat-bottom 96-well plates (Costar, Bodenheim, GER). The calibration curve was pipetted into the top row of the plate and used to calculate the calibration curve factor. GUS enzyme activity (in pMol MU/ μ g Protein x h) was calculated using the measured values from the fluorometer, the calibration curve factor, incubation time of the GUS enzyme assay, as well as the protein concentration of the original protein extracts (see 3.4.1.).

Fluorometer measurement parameters

Excitation filter	360 nm
Emission filter	455 nm
Shaking time	0 s
Shaking	off
Gain	60
Number of flashes	3
Start of integration	0 μ s
Time of integration	40 μ s
Plate type	CO96K_T

3.3.9. Protease assay on protein extracts from *N. benthamiana***Proteinase K (Roth, #7528.1)**

Stock	20 mg/ml in 50 mM Tris, 15 mM Calcium acetate, pH 8.0
Work	50 μ g/ml

Trypsin (Roth, #2193.1)

Stock	1 mg/ml in 0,037 % HCl, pH 2.0
Work	1: 50 enzyme:substrate

10x Proteinase K reaction buffer

300 mM	Tris-HCl
pH 8.0	

Reaction temperature 37 °C

10x Trypsin reaction buffer

500 mM	Tris-HCl
200 mM	CaCl

pH 8.0

Reaction temperature 37 °C

Papaine (Roth, #8933.1)

Preparation	10 mg/ml in 0.05 M Sodium acetate pH 4.5
Activation	diluted 1:100 in buffer containing 5 mM L-Cysteine
Work	1:2000 enzyme:substrate

10x Papain reaction buffer

100 mM	Sodium phosphate buffer
pH 5.7	

Reaction temperature 55 °C

The concentration of protein extracts was determined after Bradford (see 3.4.1.). For each reaction 20 μ g of protein were adjusted to 20 μ l in GUS lysis buffer (see 3.3.7.). Stock aliquots of proteinase K and trypsin were thawed at room temperature and kept on ice. Papain solution was freshly prepared in 0.05 M sodium acetate buffer. For activation of papain, the solution was diluted 1:100 in buffer containing additional 5 mM L-Cysteine and incubated for 30 min at RT. For each reaction tube, the enzyme was added in the required working concentration together with 2.5 μ l of the respective 10x reaction buffer. The volume was adjusted to 25 μ l using dH₂O. Reactions using proteinase K or Trypsin

were incubated at 37 °C in a heat cabinet. Reactions using papain were incubated at 55 °C in a programmable thermocycler with a heated lid to prevent evaporation. The incubation time was between multiple hours to several days. As negative controls, samples without enzyme were incubated as well. After incubation, the samples were mixed with 5 µl 5x SDS loading buffer and 1.25 µl 20x reducing agent (2M Dithiothreitol (DTT)) and boiled for 5 min at 100 °C in a heating block. After a short centrifugation in a tabletop centrifuge to collect the evaporated liquid, the samples were stored at -20°C until all samples were available for SDS-PAGE.

3.3.10. Subcellular localization studies using fluorescence microscopy

To determine the subcellular localization of a protein of interest in plant cells GFP and Venus fusion constructs were overexpressed using agroinfiltration. The expression of GFP in control plants was checked using ultraviolet light. In case of a strong expression, leaves with infiltrated tissue were collected. A noninfiltrated leaf was used as a control. To obtain a leaf epidermal peel the leaf was bent or torn from the edge. Using a tweezer, a transparent thin layer of epidermal cells was peeled from the leaf and placed in a drop of water on a microscope slide. A coverslip was placed on the sample which could then be viewed under epifluorescence and bright field conditions under the appropriate magnification (x100 to x400) using a Nikon Eclipse TS100 microscope (Nikon GmbH, Düsseldorf, GER). GFP and Venus fusion proteins were visualized with a filter block limiting fluorescence excitation in a range of 450-490 nm, which also allows low pass emission detection above 515 nm [Maier *et al.*, 2011]. Images were captured using an Olympus C7070 camera (Olympus Imaging Europa GmbH; Hamburg, GER). The images were processed and merged using Adobe Photoshop and ImageJ.

3.4. Standard protein biochemical methods

3.4.1. Protein concentration determination after Bradford

The protein concentration in extracts from plant material was measured using the colorimetric assay devised by Bradford [Bradford *et al.*, 1976]. 2 µl of protein extract was pipetted into a reaction tube and mixed with 798 µl dH₂O and 200 µl Bradford reagent (Roti®-Quant solution, Roth). As a reference dH₂O was used instead of protein extract. All samples were incubated for 5 min at room temperature. Following the incubation, the absorbance of each reaction mixture was measured at OD₅₉₅ in a spectrophotometer. The protein concentration was calculated using the following formula:

$$\text{Protein concentration } [\mu\text{g}/\mu\text{l}] = \frac{\text{OD}_{595} \times 15,7}{2}$$

3.4.2. SDS-polyacrylamide gel electrophoresis (SDS-PAGE)

Separation of proteins was performed using SDS-PAGE after Laemmli [Laemmli *et al.*, 1970]. SDS-PAGE allows the separation of denatured proteins based on polypeptide length. The polyacrylamide gel consists of a separation gel and a stacking gel layered on top of it. The separation gel makes up two thirds of the full polyacrylamide gel. After preparation, the separation gel had to be poured quickly into a contraption consisting of a glass plate and an aluminum plate, separated by two 1 mm thick spacers. The gel was immediately overlaid with 500 μ l H₂O to obtain an even upper edge. After polymerization of the separation gel, the water was removed using filter paper. The comb was inserted into the contraption and the stacking gel was cast on top of the separation gel. After polymerization, the wells were marked on the glass plate and the gel was securely clamped into a protein gel electrophoresis apparatus (Mighty Small II SE250/260, Hoefer Scientific Instruments, San Francisco, USA). The comb was removed, and the apparatus was filled with 1x electrode buffer until the gel was covered completely.

<u>Solution I</u>	<u>Solution II 10%</u>	<u>Solution II 15%</u>	
18,3 g Tris	20 g Acrylamide	30 g Acrylamide	
115 μ l TEMED	0,5 g Bisacrylamide	0,75 g Bisacrylamide	
pH 8,9 (HCl)	0,2 g SDS	0,2 g SDS	
ad 100 ml dH ₂ O	ad 100 ml dH ₂ O	ad 100 ml dH ₂ O	
<u>Solution III</u>	<u>Solution IV</u>	<u>Solution V</u>	
0,6 g Ammonium persulfate (APS)	6,1 g Tris	12 g Acrylamide	
ad 100 ml dH ₂ O	230 μ l TEMED	0,3 g Bisacrylamide	
	pH 6,8 (HCl)	0,4 g SDS	
	ad 100 ml dH ₂ O	ad 100 ml dH ₂ O	
<u>Separation gel</u>	<u>Stacking gel</u>	<u>10x Electrode buffer</u>	<u>5x Loading buffer</u>
1 part Sol I	1 part Sol IV	30 g Tris	0,313 M Tris/HCl pH 8
2 parts Sol II	1 part Sol V	144 g Glycine	10 % SDS
1 part Sol III	1 part dH ₂ O	10 g SDS	50 % Glycerol
	1 part Sol III	ad 1 l dH ₂ O	0,05 % Bromophenol blue

To denature proteins from plant extracts (see 3.3.7.) for use in SDS-PAGE, 20 μ l of each protein extract were mixed with 4 μ l 5x loading buffer and 1 μ l 20x reducing agent (2M Dithiothreitol (DTT)) and boiled for 5 min at 100 °C in a heating block. After a short centrifugation in a tabletop centrifuge to collect evaporated liquid, the samples were loaded into the gel. The pretreatment of yeast extracts is described above (see 3.2.7.). The standard protein molecular weight marker (see 2.2.6.) was loaded in parallel to the protein samples to allow estimation of the relative molecular weight of the protein via immunodetection. The separation of proteins was carried out at 120 V. After the gel electrophoresis, the gel was used in a western transfer (see 3.4.3.) with subsequent immunodetection (see 3.4.4.).

3.4.3. Western Transfer

After SDS-PAGE (see 3.4.2.) the proteins were transferred to a nitrocellulose membrane (porablot NCP; Macherey Nagel, Düren, GER). The stacking gel was separated from the separation gel, which was then transferred into a western transfer cassette (peQlab; Erlangen, GER) following the schema described below. Before assembling the transfer cassette, the sponges, Whatman 3M chromatography paper and nitrocellulose membranes were soaked in western transfer buffer. During assembly, any air bubbles trapped between the components were removed by rolling a glass tube on the sandwich. The western transfer cassette was closed using locker clips on both sides of the cassette and inserted into the blotting apparatus (MiniTank™ Elektrobloetter VEP-2, PeQLab; Erlangen, GER). The apparatus was filled with western transfer buffer until the transfer cassettes were completely covered. The proteins were transferred from the separation gel to the nitrocellulose membrane for at least 2 hours in the cooling chamber at 4 °C using a constant voltage of 50 V.

Assembly of the transfer sandwich	Western transfer buffer	
Western transfer cassette (cathode)	5,45 g	Tris
Sponge	25,9 g	Glycine
Two layers Whatman 3 M chromatography papers	1620 ml	dH ₂ O
Separation gel	180 ml	Methanol
Nitrocellulose membrane		
Two layers Whatman 3 M chromatography papers		
Sponge		
Western transfer cassette (anode)		

3.4.4. Immunodetection of Proteins with specific antibodies

After transferring the proteins from the separation gel to the nitrocellulose membrane using western transfer (see 3.4.3.), the membrane was taken from the transfer cassette. To saturate nonspecific binding sites, the nitrocellulose membrane was incubated in blocking solution for at least two hours at 4 °C. All blocking, hybridization and washing steps were performed under continuous shaking. The membrane was incubated with the primary antiserum overnight at 4 °C to allow hybridization. Thereafter, the membrane was washed three times for 10 min with TTBS at room temperature and incubated for two hours with 25 ml secondary antiserum solution for at least 2 hours at room temperature. Both primary and secondary antibody solutions were prepared in blocking solution using the concentrations described in section 2.6. The membrane was then washed three times for 10 min with TTBS and three times with TBS. The secondary antibody was coupled to horseradish peroxidase allowing the detection of the peroxidase activity of the protein-antibody-complex using a chemiluminescence reaction. For this purpose, the membrane was completely covered with enhanced chemiluminescence (ECL) solution and incubated for 2 min. After removing the solution, the membrane was placed between two layers of transparent film and placed in an exposition cassette with an x-ray film (Fuji Super RX; Fuji, Düsseldorf,

GER) placed on top. The duration of the exposition varies depending on the strength of signal. The film was then developed.

TBS		TTBS [1 l]		Blocking solution	
20 mM	Tris/HCl pH 7,5	1 l	TBS	5 %	Skimmed milk powder in TTBS
500 mM	NaCl	0,5 ml	Tween 20		

Solution A		Solution B [10 ml]		ECL solution	
0,1 M	Tris/HCl pH 8,6	11 mg	p-coumaric acid	2 ml	Solution A
250 mg/l	Luminol		in dimethyl sulfoxide (DMSO)	0,6 µl	H ₂ O ₂ (30 %)
				200 µl	Solution B

3.4.5. Ponceau S staining of nitrocellulose membranes.

After immunodetection the nitrocellulose membrane was washed for 10 min in TTBS. Then the membrane was incubated for 10 min in 0.1 % Ponceau S staining solution containing 5 % acetic acid under constant shaking. Following the incubation, the membrane was washed multiple times with H₂O to remove residual staining solution. The proteins stained by the red azo dye Ponceau S were used as loading control and the membrane was scanned for documentation.

4. Results

4.1. Expression of Arabidopsis *NIMIN* genes

The NIMIN family of proteins was initially discovered by our working group as interactors of the NPR1 (NIM1/SAI1) protein from *Arabidopsis thaliana*, the central regulator of systemic acquired resistance (SAR) [Weigel *et al.*, 2001] and homologs have been found throughout the plant kingdom like in important model organisms such as tobacco and rice [Chern *et al.*, 2005b; Zwicker *et al.*, 2007]. The Arabidopsis genome contains four *NIMIN* genes: *NIMIN1*, *NIMIN1b*, *NIMIN2*, and *NIMIN3* [Weigel *et al.*, 2001]. These *NIMIN* genes have been shown to be expressed differentially regarding their expression patterns and sensitivity to SA stimuli. While *NIMIN1* and *NIMIN2* are expressed transiently after induction by SA, *NIMIN3* is expressed constitutively at low levels independent of the presence of functional NPR1 [Hermann *et al.*, 2013]. It is yet unknown under which circumstances the *NIMIN1b* gene is expressed.

To further define differential activities of Arabidopsis *NIMIN* genes, the sensitivity of *NIMIN* promoter constructs was tested, observing reporter activity in response to defense related signaling molecules with special emphasis on the *N1b* promoter. In addition, the cellular localization of NPR1, NPR3 and NIMIN fusion proteins was determined.

4.1.1. Subcellular localization of NIMIN1 and NPR fusion proteins

Both NPR1 and NIMIN proteins have to localize in the nucleus to regulate the expression of defense related genes during SAR. The known NIMIN proteins contain NLS sequences matching or being highly similar to established consensus sequences [Weigel, 2000; Weigel *et al.*, 2001]. Likewise, NPR proteins from both, Arabidopsis and tobacco, contain NLS sequences close to their C-terminus. The NLS of both AtNPR1 and NtNPR1 are bipartite and share high similarity, although they are not fully conserved [Kinkema *et al.*, 2000; Liu *et al.*, 2002; Shi *et al.*, 2013]. In contrast to NtNPR1, which accumulates strongly in the nucleus, AtNPR1 initially accumulates in the cytoplasm [Kinkema *et al.*, 2000; Maier *et al.*, 2011]. Without prior activation, AtNPR1 forms a cytoplasmic oligomer bound together by disulfide bonds. Three cysteine residues, Cys⁸², Cys¹⁵⁶, and Cys²¹⁶, have been shown to be involved in this S-nitrosylation mediated oligomerization process [Mou *et al.*, 2003; Tada *et al.*, 2008]. Only after SAR induction the AtNPR1 protein translocates into the nucleus and nuclear-localized AtNPR1-GFP fusion protein activates *PR* gene expression [Kinkema *et al.*, 2000; Mou *et al.*, 2003]. Together, this indicates that AtNPR1 and NtNPR1 follow different regulatory processes.

To get a more precise understanding of the cellular localization of NPR and NIMIN proteins and to determine if members of the NIMIN family of proteins can colocalize with members of the NPR family in the nucleus, agroinfiltration-based transient overexpression of fluorescent fusion proteins was used. The gene of interest was fused to the N-terminus of the yellow fluorescent protein Venus [Rekas *et al.*, 2002]. The constructs were under control of the constitutively active 35S promoter from CaMV to allow accumulation of a sufficient amount of fusion protein. A construct containing the Arabidopsis NIMIN1 (N1) open reading frame fused to the N-terminus of the Venus protein was already available [Lehmann, 2014]. AtNPR1-Venus, and AtNPR3-Venus fusion constructs were generated during this study (see Appendix V; Fig. 4A). *Nicotiana benthamiana* plants were infiltrated using *Agrobacterium* strains containing the respective fusion genes, together with a strain expressing the silencing suppressor p19. Accumulation of the resulting fusion proteins was confirmed via immunodetection. The N1-Venus fusion protein accumulates strongly as a 44 kDa band, with the signal being almost as strong as in control tissue overexpressing GFP. Interestingly, the immunodetection shows two more signals below the full length N1-Venus fusion protein at 35 kDa and at 27 kDa corresponding to the molecular weight of GFP. On the other hand, the AtNPR1- and AtNPR3-Venus fusion proteins show much weaker overall accumulation as 93 kDa bands, with AtNPR3-V exhibiting a slightly stronger signal than AtNPR1-V (Fig. 4B).

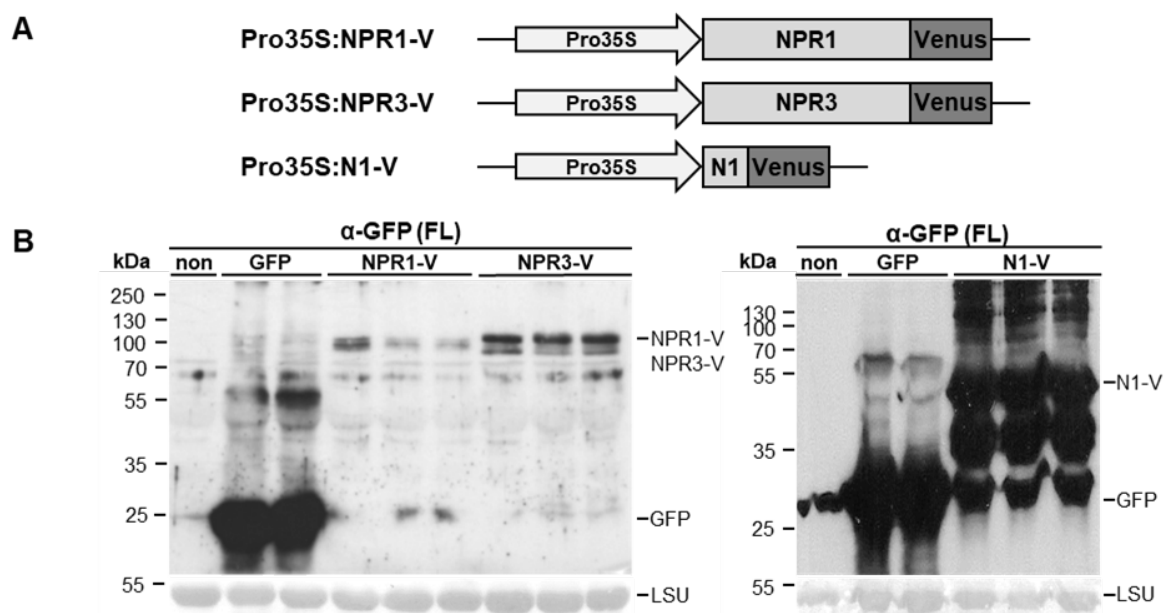


Fig. 4 Accumulation of Arabidopsis NPR1, NPR3 and NIMIN1 as Venus fusion proteins in *N. benthamiana*. (A) Schematic representation of gene constructs. Arabidopsis *N1*, *NPR1* and *NPR3* were fused to the N-terminus of the *Venus* reporter gene and placed under control of the 35S promoter from CaMV. (B) Immunodetection of Venus fusion proteins in leaf extracts of *N. benthamiana* using the α -GFP (FL) antiserum. Mixtures of *Agrobacterium* suspensions harboring the indicated gene constructs were infiltrated into *N. benthamiana* leaf tissue for transient overexpression. Protein extracts were prepared 4 dpi from three independent plants inoculated for each construct. Ponceau S staining of the RuBisCO large subunit (LSU) was used as loading control.

4. Results

To determine the subcellular localization of N1-, AtNPR1- and AtNPR3-Venus, infiltrated *Nicotiana benthamiana* plants were observed using fluorescence microscopy (Fig. 5). The GFP (Fig. 5A) and Venus (Fig. 5A,B) proteins used as controls accumulate unspecifically in the whole cell and a strong fluorescence signal can be observed in the cytoplasm. The N1-Venus fusion protein accumulates almost exclusively in the nucleus with only weak fluorescence visible in the cytoplasm (Fig. 5A). Likewise, AtNPR1-Venus and AtNPR3-Venus (Fig. 5B) both accumulate in the nucleus with AtNPR3-Venus showing slightly stronger accumulation, confirming the observations from the immunodetection assay.

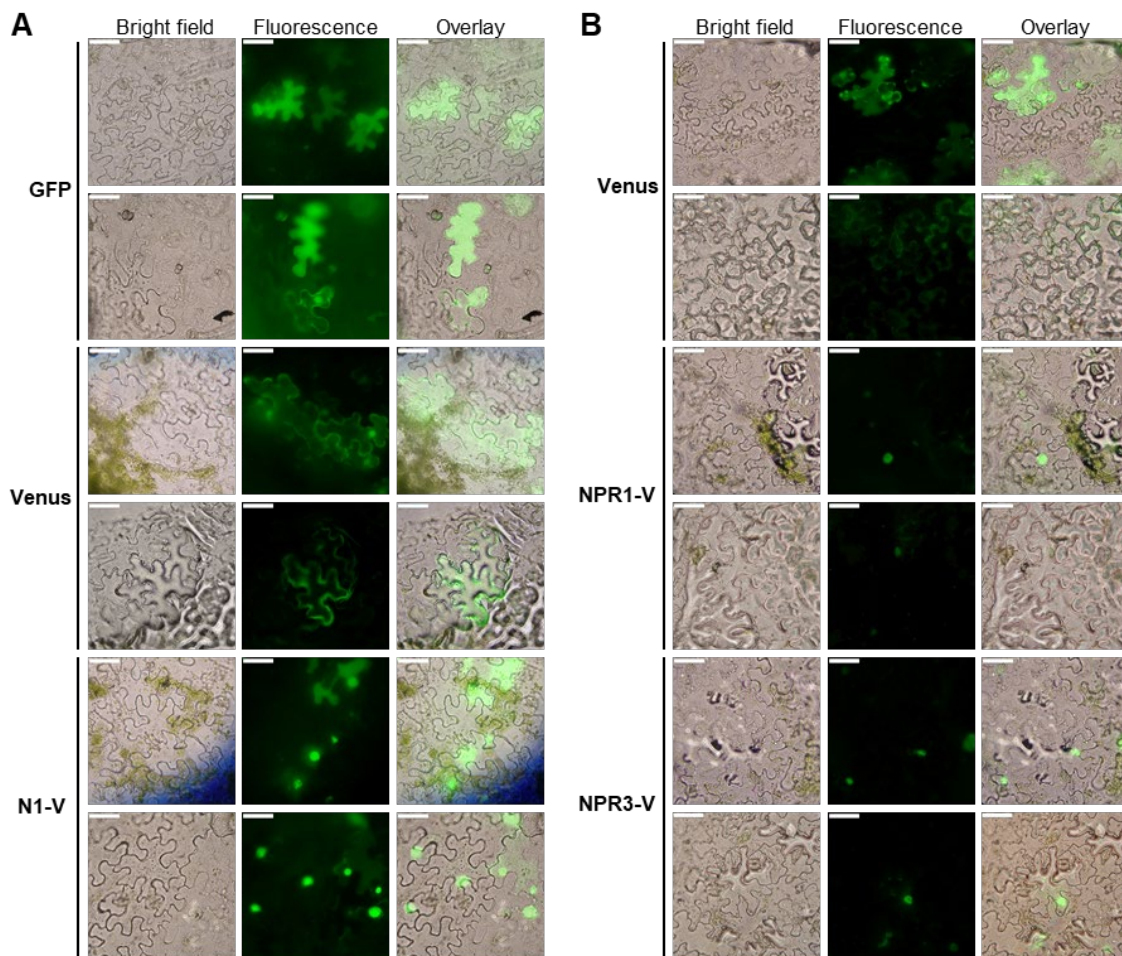


Fig. 5 Subcellular localization of Arabidopsis NIMIN1, NPR1 and NPR3 as Venus fusion proteins in *N. benthamiana*. Mixtures of *Agrobacterium* suspensions harboring the indicated gene constructs under control of the 35S promoter from CaMV were infiltrated in *N. benthamiana* leaf tissue. Epidermal peels from two independent plants were observed 5-6 days post infiltration depending on fluorescence intensity of *Pro35S:GFP* infiltrated control plants under UV light. The cells were viewed under epifluorescence and bright field conditions. The scale bar represents 50 μm . (A) Subcellular localization of GFP and Venus and NIMIN1-Venus (B) Subcellular localization of Venus, NPR1-Venus, and NPR3-Venus.

4.1.2. Chemical induction of *NIMIN1* and *NIMIN2* promoters

The *NIMIN* genes are expressed differentially during the establishment of the SAR response. In leaves of *Arabidopsis thaliana*, *N3* is constitutively expressed at low levels. This expression is unaffected by phytohormone or pathogen induction, suggesting the *NIMIN3* protein is most likely involved in the repression of the immune response in unchallenged plants [Hermann *et al.*, 2013]. Opposed to *N3*, the *N1* and *N2* genes are transiently expressed after SA application. Studies on transgenic tobacco seedlings harboring the GUS reporter gene under control of the *PR1a*, *N1*, *N2* and *N3* promoters revealed that unlike the promoters of *PR1a* and *N3*, which are primarily active in leaf tissue, the expression from the *N1* and *N2* promoters takes place in leaf and root tissues [Hermann *et al.*, 2013]. This expression pattern was also observed for GFP expression from the *N1* promoter in *Arabidopsis* plants [Fonseca *et al.*, 2010]. The expression of the *N1* gene, like *PR-1*, is dependent on the presence of functional NPR1 protein. In *npr1-1* and *npr1-2* plants, unable to express functional NPR1, both the *PR-1* and *N1* genes are inactive. Meanwhile, *N2* expression is still detectable in NPR1 deficient plants, although at lower levels, suggesting an only partial dependency on NPR1 [Glocova *et al.*, 2005; Hermann, 2009; Hermann *et al.*, 2013]. The *NIMIN2* gene was classified as an immediate early SA responsive gene as transcripts could be detected as early as 0.5 h after SA treatment reaching an early maximum after 1 h which is maintained for 24 h. *NIMIN1* transcripts become abundant 2 h after application of SA. Expression of *NIMIN1* however, is even more transient than *NIMIN2* expression and is already shut down when *PR-1* transcripts begin to accumulate after around 10 h. This successive induction by SA suggests that SAR establishment is regulated dependent on the accumulation and concentration of SA in the cell [Maier *et al.*, 2011; Hermann *et al.*, 2013].

The promoters of the *Arabidopsis NIMIN* genes have already been analyzed regarding their structure and their temporal and spatial expression patterns, as well as their sensitivity to SA and other phytohormones [Hermann *et al.*, 2013]. As observed for the *PR-1* promoter from tobacco and *Arabidopsis*, the SA inducibility of the *N1* and *N2* promoters is mediated by the presence of SA responsive *as-1*-like sequences. The *N2* promoter region extends to 1251 bp upstream of the translation initiation codon and contains a TGACG motif at the positions -210 to -217 from the start codon [Glocova, 2003]. The slightly shorter *N1* promoter region extends to 1042 bp upstream of the translation initiation codon and contains two TGACG motifs at positions -360 to -364 and -424 to -428. These lie much further away from each other and mutation in one of those motifs (-360 to -364) did not affect the SA sensitivity of the promoter [Glocova, 2003]. The studies by Hermann [2009] localized the SA responsive element of the *N1* promoter to the region between -436 and -402. Mutation within one TGATG repeat within this region results in complete loss of TGA factor binding but no loss of the SA sensitivity of the promoter [Hermann, 2009]. While the 1135 bp promoter region of *N1b* also contains one TGACG motif close to the 5' end of the promoter region between positions -1033 and -1038, no SA mediated induction of the promoter has yet been observed.

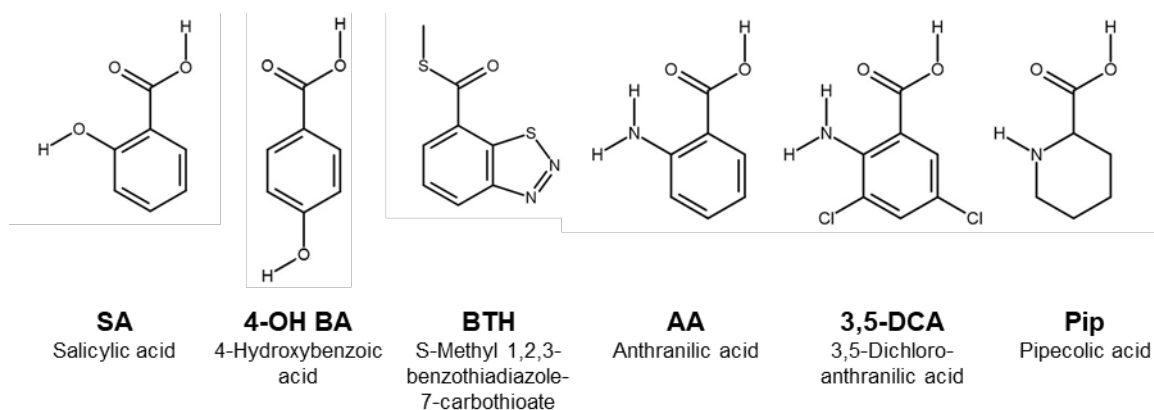


Fig. 6 Structural formulas of salicylic acid analogs. Structural formula of Salicylic acid (SA; PubChem CID 338); Structural formula of 4-Hydroxybenzoic acid (4-OH BA; PubChem CID 135); Structural formula of S-Methyl 1,2,3-benzothiadiazole-7-carbothioate (BTH; PubChem CID 86412); Structural formula of Anthranilic acid (AA; PubChem CID 227); Structural formula of 3,5-Dichloroanthranilic acid (3,5-DCA; PubChem CID 76036); Structural formula of Pipelicolic acid (Pip; PubChem CID 849).

Salicylic acid (SA, 2-hydroxy-benzoic acid, Fig. 6) is the canonical signaling molecule required for the induction of defense responses and expression of *PR* genes during SAR. Recent studies revealed SA to be directly perceived by NPR proteins [Neeley *et al.*, 2019; Wang *et al.*, 2020]. Besides pathogen defense, SA is also involved in regulation of developmental processes like seed germination and flower development [Raskin, 1992]. In plants, the two metabolic pathways for SA synthesis are the ICS and the PAL pathway, both starting from chorismate. These pathways are of varying importance in different plant species. While in *Arabidopsis* SA synthesis is predominantly mediated by the ICS pathway [Nawrath & Métraux, 1999; Wildermuth *et al.*, 2001], the PAL pathway is prevalent in rice [Chen *et al.*, 2009] but equal contribution is also possible as observed in soybean [Shine *et al.*, 2016; Lefevere *et al.*, 2020]. ICS facilitates the conversion of chorismate into its constitutional isomer isochorismate [Wildermuth *et al.*, 2001; Strawn *et al.*, 2007; Garcion *et al.*, 2008; Chen, 2009]. Rekhter *et al.* [2019] recently discovered the involvement of two proteins in the SA biosynthesis in *Arabidopsis*. Isochorismate is exported from the plastid into the cytosol by Enhanced Disease Susceptibility5 (EDS5) where the amidotransferase *avrPphB* Susceptible3 (PBS3) converts glutamate and isochorismate into isochorismate-9-glutamate [Rekhter *et al.*, 2019]. By either spontaneous decomposition or enzymatic activity of the acyltransferase enhanced pseudomonas susceptibility1 (EPS1), isochorismate-9-glutamate is then converted into SA and N-pyruvoyl-L-glutamate [Torrens-Spence *et al.*, 2019]. In the PAL pathway chorismate is converted into prephenate via Chorismate Mutase (CM), which over several steps is converted to phenylalanine (Phe) [Maeda *et al.*, 2011]. The PAL enzyme mediates the conversion of Phe into trans-cinnamic acid (tCA). Abnormal Inflorescence Meristem1 (AIM1) as a beta-oxidation enzyme then catalyzes the conversion of tCA to benzoic acid (BA) [Richmond & Bleecker, 1999; Lefevere *et al.*, 2020]. The final step of the PAL pathway, the conversion of BA to SA, is suggested to be catalyzed by a benzoic acid 2-hydroxylase. However, the exact enzyme has yet to be identified. [Leon *et al.*, 1995; Lefevere *et al.*, 2020].

Throughout the years several other substances have been identified which can induce SAR signaling and influence the expression of *PR* genes or are otherwise involved in immune responses against biotrophic or hemibiotrophic pathogens. There are several structural analogs of SA, including benzoic acid (BA) or 2,6-dihydroxy-benzoic acid (2,6-OH BA) sharing properties with SA. BA is an intermediate of the SA biosynthesis by phenylalanine ammonia lyase (PAL) pathway and can induce the expression of *PR1*-genes and increase resistance against *TMV* [White, 1979; Xie *et al.*, 1998; Maier *et al.* 2011]. In contrast other similar substances like 4-hydroxy-benzoic acid (4-OH BA, Fig. 6) are ineffective in the induction of SAR. S-Methyl 1,2,3-benzothiadiazole-7-carbothioate (BTH, Fig. 6)), the active component of the crop protection agent Bion® [Schurter *et al.*, 1987, 1993], is another known activator of SAR. Application of BTH achieves the same extensive protection against pathogens as SA- or pathogen-mediated induction of immune responses resulting in the accumulation *PR1* transcripts independent of the presence of SA [Friedrich *et al.*, 1996, Lawton *et al.*, 1996]. Like SA and INA, BTH is unable to induce defense reactions or pathogen resistance in the SA insensitive *A. thaliana npr1* mutant [Cao *et al.*, 1994; Delaney *et al.*, 1995].

During screening experiments searching for synthetic defense elicitors using an oomycete responsive *ProCaBP22:GUS* reporter construct 3,5-dichloroanthranilic acid (3,5-DCA, Fig. 6) was identified [Knoth *et al.*, 2009]. 3,5-DCA can induce potent immune responses against phylogenetically distinct pathogens like the oomycete *Hyaloperonospora parasitica*, as well as against the bacterium *Pseudomonas syringae*. It has been shown that exogenous application of 3,5-DCA, like SA, BA or BTH, is able to induce defense responses in *nahG* plants and therefore acts independent of innate SA accumulation. However, in contrast to those substances, 3,5-DCA induces more transient defense reactions. Interestingly, 3,5-DCA is partially inhibited in *npr1* as well as *wrky70* mutant plants, suggesting functions in WRKY70 dependent pathways [Knoth *et al.*, 2009; Bektas & Eulgem, 2015]. The structural analog anthranilic acid (AA, 2-aminobenzoic acid, Fig. 6) - although structurally closer to SA - is inactive concerning defense induction [Knoth *et al.*, 2009].

Pipecolic acid (Pip, piperidine-2-carboxylic acid, Fig. 6), as well as its derivate N-hydroxypipecolic acid (NHP) have been shown to be the signaling molecules required for systemic spreading of the SAR signal. AGD2-like defense response protein1 (ALD1) and SAR-deficient4 (SARD4) both are key enzymes required for conversion of lysine to pipecolic acid. An impaired Pip biosynthesis inhibits SA accumulation and prevents establishment of SAR in systemic tissues [Návarová *et al.*, 2012; Ding *et al.*, 2016; Hartmann *et al.*, 2017]. Flavin-dependent-monooxygenase1 (FMO1) catalyzes the conversion of Pip into NHP by hydroxylation and is important for Pip mediated defense priming [Mishina & Zeier, 2006; Bernsdorff *et al.*, 2016; Hartmann *et al.*, 2018]. Even in *fmo1* deficient plants, exogenous application of NHP is sufficient to rescue SAR establishment and can be detected in distant leaves, making NHP the systemic signal of SAR [Chen *et al.*, 2018; Hartmann & Zeier, 2019].

To further elucidate the differences in promoter activity between *NIMIN1* and *NIMIN2*, several substances were tested for their ability to induce GUS reporter constructs containing the *N1* and *N2* promoters (Fig. 7A). The promoter regions of the *N1* and *N2* genes from *A. thaliana* fused to the *GUS* gene were already available, stably integrated into the genome of *N. tabacum* via Agrobacterium mediated transformation [Glocova *et al.*, 2005]. As a control a GUS reporter construct under control of the *PR1a* promoter was used [Grüner *et al.*, 2003]. Four leaf discs each, from three independent plants, were incubated for three days on the respective substance. Reporter activity was strongly induced after treatment with 1 mM SA for both the *Pro-1533PR1a:GUS* (line 138-3) and *ProN1:GUS* (line 342-4) reporter constructs, while *ProN2:GUS* (line 322-7/1) showed only weak activity (Fig. 7B,C,D). Likewise, 0.3 mM BTH was sufficient to induce comparable levels of reporter activity. As expected, 4-OH BA was unable to induce reporter activity for any of the used reporter constructs (Fig. 7B). Similarly, neither 0.1 mM AA nor 0.1 mM 3,5-DCA were able to significantly induce the reporter constructs (Fig. 7C,D). Interestingly Pip was able to considerably induce *Pro-1533PR1a:GUS* activity while only slightly raising the activity of the *ProN1:GUS* and *ProN2:GUS* constructs above background levels (Fig. 7D). Together, while all the *PR1a*, *N1*, and *N2* promoters share similar expression profiles with clear responsiveness to SA and BTH and inactivity to the same structural SA analogs, only Pip seems to preferentially affect *PR1a* promoter activity.

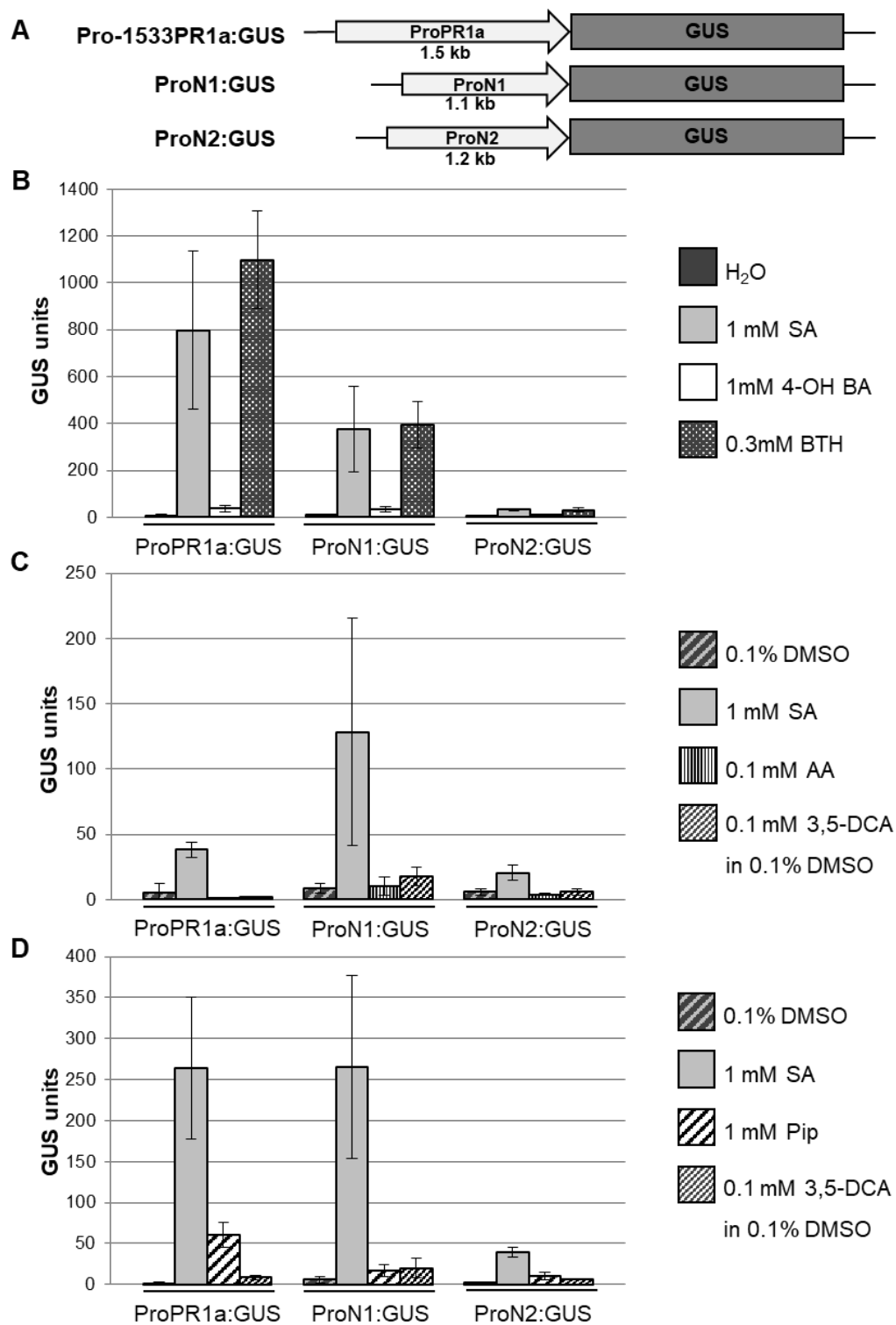


Fig. 7 Chemical induction of *PR1a*, *NIMIN1* and *NIMIN2* promoter constructs in transgenic tobacco plants after chemical induction using salicylic acid (SA), 4-hydroxybenzoic acid (4-OH BA), S-Methyl 1,2,3-benzothiadiazole-7-carbothioate (BTH), Anthranilic Acid (AA), 3,5-Dichloroanthranilic acid (3,5-DCA) and Pipecolic acid (Pip). (A) Schematic representation of gene constructs. The GUS reporter gene was placed under control of the promoters from the tobacco *PR1a* (line 138-3) and Arabidopsis *NI* (line 342-4) and *N2* (line 322-7/1) genes. (B-D) GUS reporter gene activity measured from leaf disc extracts from three independent plants per line after 3 days of floating on the specified chemicals. (B) H₂O, 1 mM SA, 1 mM 4-OH BA and 0.3 mM BTH. (C) 0.1 % DMSO, 1mM SA, 0.1 mM AA and 0.1 mM 3,5-DCA in 0.1 % DMSO. (D) 0.1 % DMSO, 1 mM SA, 1 mM Pip and 0.1 mM 3,5-DCA in 0.1 % DMSO.

4.1.3. Expression from the *NIMIN1b* promoter

Unlike *NI*, *N2* and *N3*, whose expression has been described extensively, *N1b* remains a mystery. The analysis of endogenous expression patterns of *N1b* in Arabidopsis plants did not result in the detection of *N1b* transcripts. Even after exogenous application of SA or JA, transcripts of *N1b* could not be detected. A *ProN1b:GUS* reporter construct containing the 1135 bp 5' region created to allow easier detection of promoter activity did not show expression in transgenic tobacco plants. Based on these results it was assumed that *NIMIN1b* could be an inoperative pseudogene which lost its activity at some time during evolution [Hermann, 2009]. On the other side, however, the *ProN1b:GUS* construct produces clear reporter enzyme activity in transient gene expression assays (U. M. Pfitzner, personal communication). In another attempt to identify possible expression of the *N1b* gene during development a different, more directly visible reporter gene had to be used. One such gene is the human *Bax* gene, which is a pro-apoptotic member of the Bcl-2 family of proteins involved in the regulation of cell death [Kroemer, 1997]. When expressed in plants, the resulting phenotype is highly similar to the cell death during HR when induced by TMV in tobacco plants carrying the *N* gene. Moreover, it has been shown that the promotion of cell death mediated by *Bax* expression correlates with the accumulation of PR proteins in affected tissues [Lacomme & Santa Cruz, 1999]. Glocova *et al.* [2005] were able to show that reporter constructs expressing *Bax* under control of the *NI* and *N2* promoters do not induce cell death in untreated tobacco plants suggesting these genes to be inactive unless induced by increasing levels of SA. This confirms the expression profiles published by Hermann *et al.* [2013]. To gain insight of *N1b* expression during development a *ProN1b:Bax* reporter construct was compared to a *ProNI:Bax* construct.

4.1.3.1. Transient expression of *ProNIMIN1b:Bax* in *N. benthamiana*

To examine if the *ProN1b:Bax* construct can be expressed in a transient context, agrobacteria containing *ProNI:Bax* [Glocova *et al.*, 2005] or *ProN1b:Bax* [U. M. Pfitzner, personal communication] (Fig. 8) were infiltrated into *N. benthamiana* leaves. As a control, agrobacteria containing a *Pro35S:NIMINI* construct were used, which were shown to elicit cell death during transient overexpression assays [Masroor, 2013]. The phenotype of infiltrated leaves was documented to monitor the development of cell death. Plant tissue in which the *NI* gene is overexpressed shows small patches of visible cell death at only 6 dpi which intensifies over the following days (Fig. 8B,C). Tissues overexpressing the *Bax* constructs show more rapid development of cell death with leaf halves expressing the *ProN1b:Bax* construct showing large patches of dead tissue at 6 dpi (Fig. 8C) and those expressing *ProNI:Bax* showing strong cell death after only 4 dpi (Fig. 8B). These results indicate that the 1135 bp upstream region of *N1b* does act as a promoter and is active under the conditions prevalent during Agrobacterium mediated transient overexpression.

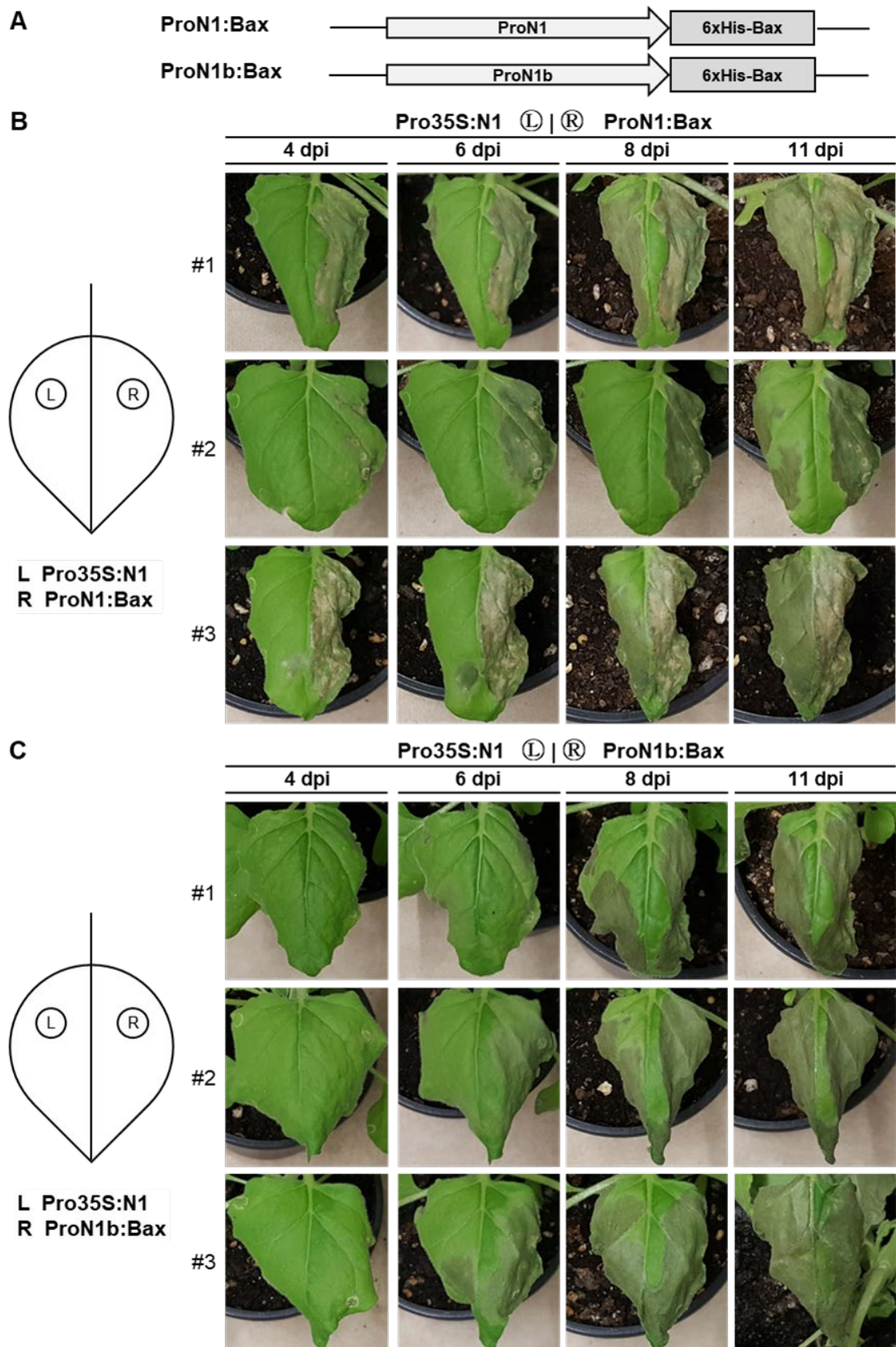


Fig. 8 Phenotypic effects of transient overexpression of *NIMIN1* and *Bax* constructs in *N. benthamiana* plants. (A) Schematic representation of the gene constructs expressed by the infiltrated agrobacteria strains. *N1* was expressed under control of the 35S promoter from CaMV. *6xHis-Bax* was expressed under control of the *N1* and *N1b* promoters from *Arabidopsis thaliana*. (B) and (C) Phenotype of infiltrated *N. benthamiana* leaves during transient overexpression. Left leaf half: *Pro35S:N1*; Right leaf half: *ProN1:Bax* (B) or *ProN1b:Bax* (C) respectively. Symptom development was documented from three independent plants at 4, 6, 8 and 11 dpi.

4.1.3.2. Germination of tobacco seeds harboring *ProNIMIN1b:Bax*

To determine if the *NIMIN1b* promoter exhibits activity during seed germination, seeds of stably transformed transgenic plants containing *ProNI:GUS*, *ProNI:Bax*, and *ProN1b:Bax* constructs (U. M. Pfitzner, personal communication) were sown onto selective agar plates containing kanamycin (Kan) with or without supplementation of 0.3 mM SA (see 3.3.1.). After four weeks in a light cabinet the germination was documented (Fig. 9).

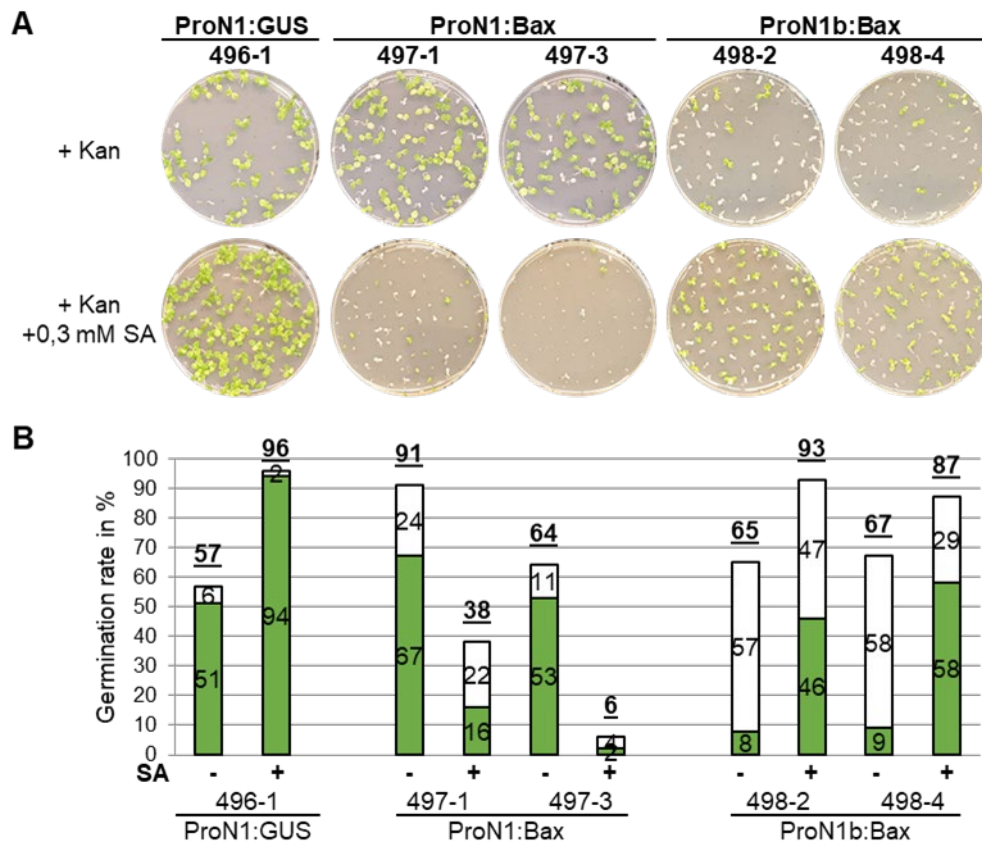


Fig. 9 Influence of salicylic acid on the germination of transgenic tobacco seeds. Seeds containing *6xHis-Bax* under control of the *NI* (Transgenic line 497-1 and 3) and *N1b* (Transgenic line 498-2 and 4) promoters from *Arabidopsis thaliana* were placed on MS medium agar plates containing kanamycin with or without addition of 0.3 mM SA. Seeds containing the *GUS* reporter gene under control of the *NI* promoter were used as a control (transgenic line 496-1). (A) Documentation of agar plates after 4 weeks of incubation in a light cabinet. (B) Germination rate in percent showing green seedlings (green bar) and discolored seedlings (white bar).

The germination of seedlings containing the *ProNI:GUS* construct (line 496-1) was used as negative control. These seeds are largely unaffected by presence of SA during germination showing only slightly reduced growth compared to seedlings without SA supplementation. The germination of seeds containing the *ProNI:Bax* constructs (lines 497-1 and 3) are strongly affected by the presence of SA in the medium resulting in a reduction in germination rate of over 80 % (Fig. 9A,B). Seeds containing the *ProN1b:Bax* (lines 498-2 and 4) appear to show enhanced germination in presence of SA. To confirm these results the experiment was repeated using different *ProNI:Bax* and *ProN1b:Bax* lines (Fig. 10).

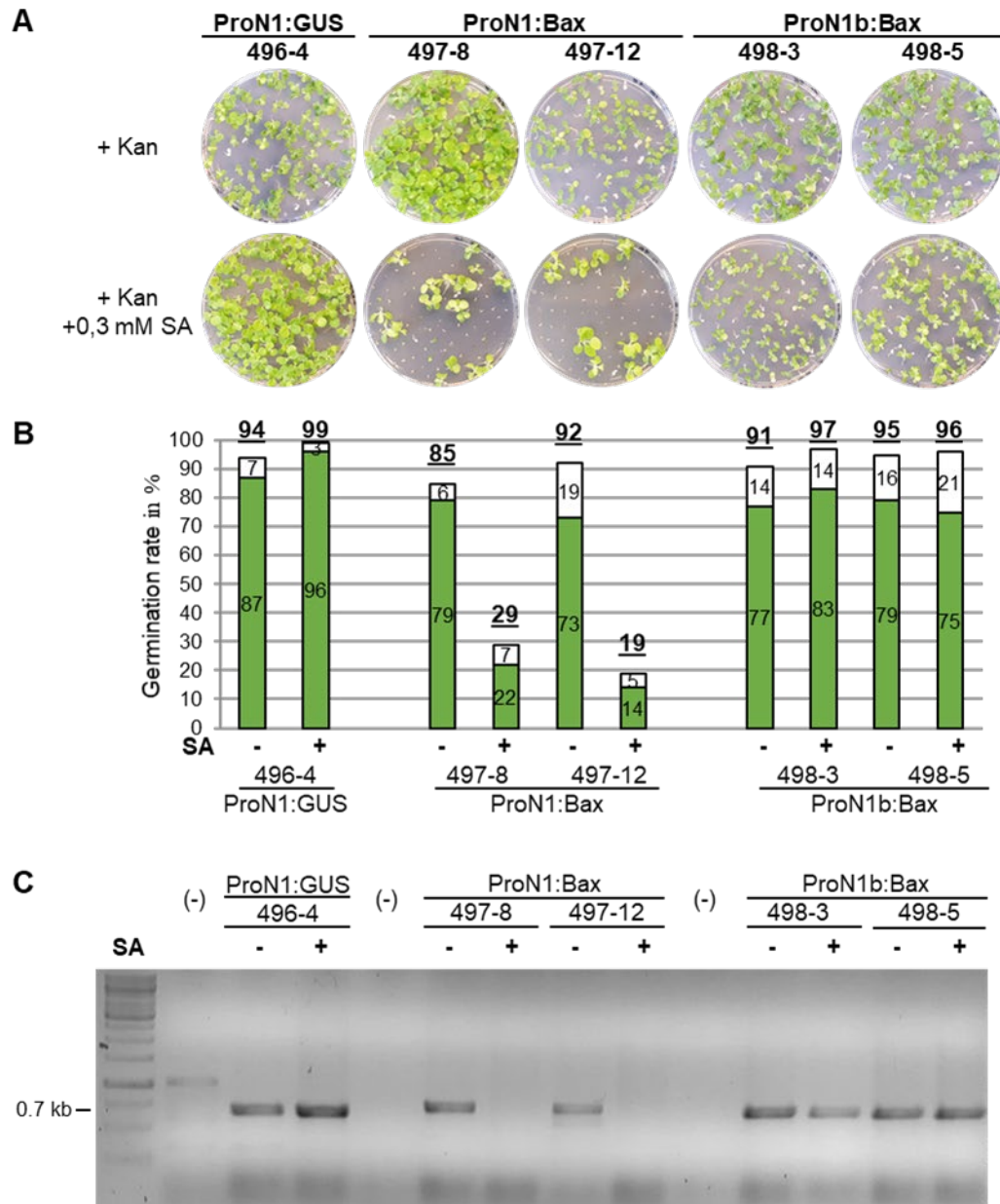


Fig. 10 Influence of salicylic acid on the germination of transgenic tobacco seeds. Seeds containing *6xHis-Bax* under control of the *N1* (Transgenic line 497-8 and 12) and *N1b* (Transgenic line 498-3 and 5) promoters from *Arabidopsis thaliana* were placed on MS medium agar plates containing kanamycin with or without addition of 0.3 mM SA. Seeds containing the *GUS* reporter gene under control of the *N1* promoter (transgenic line 496-4) were used as a control. (A) Documentation of agar plates after 4 weeks of incubation in a light cabinet. (B) Germination rate in percent showing green seedlings (green bar) and discolored seedlings (white bar). (C) PCR amplification of reporter constructs using specific primers: N1-P6/*GUS*-3 for *ProN1:GUS*, N1-P6/*Bax*-3-Sma for *ProN1:Bax*, and N1b-P3/*Bax*-3-Sma for *ProN1b:Bax* respectively. Genomic DNA isolated from 10 green seedlings growing on selection plates with or without SA was used as template. H₂O used as negative control (-).

The germination of seeds containing the *ProN1:Bax* construct (lines 497-8 and 12) is strongly decreased in presence of SA (Fig. 10A, B), confirming the observations made in the previous experiment (Fig. 9). However, deviating from that, *ProN1b:Bax* seedlings from the transgenic lines 498-3 and 498-5 are not affected by the presence of SA in the medium like lines 498-2 and 498-4. To determine if this is caused by a lack of the transgenic constructs a PCR reaction using specific primers was executed on genomic DNA from seedlings. The resulting fragment sizes consist of approximately 100 bp promoter region

4. Results

plus the complete *Bax* ORF (579 bp) or the N-terminal part of the *GUS* ORF (~600 bp) respectively (Fig. 10C). Interestingly, no PCR product could be detected from *ProN1:Bax* seedlings growing on SA containing agar plates suggesting seedlings with the transgene are unable to germinate in presence of SA. Meanwhile the *ProN1b:Bax* construct can be detected in all seedling extracts, suggesting that in *ProN1b:Bax* lines *Bax* is not expressed from the *N1b* promoter in SA-exposed seedlings.

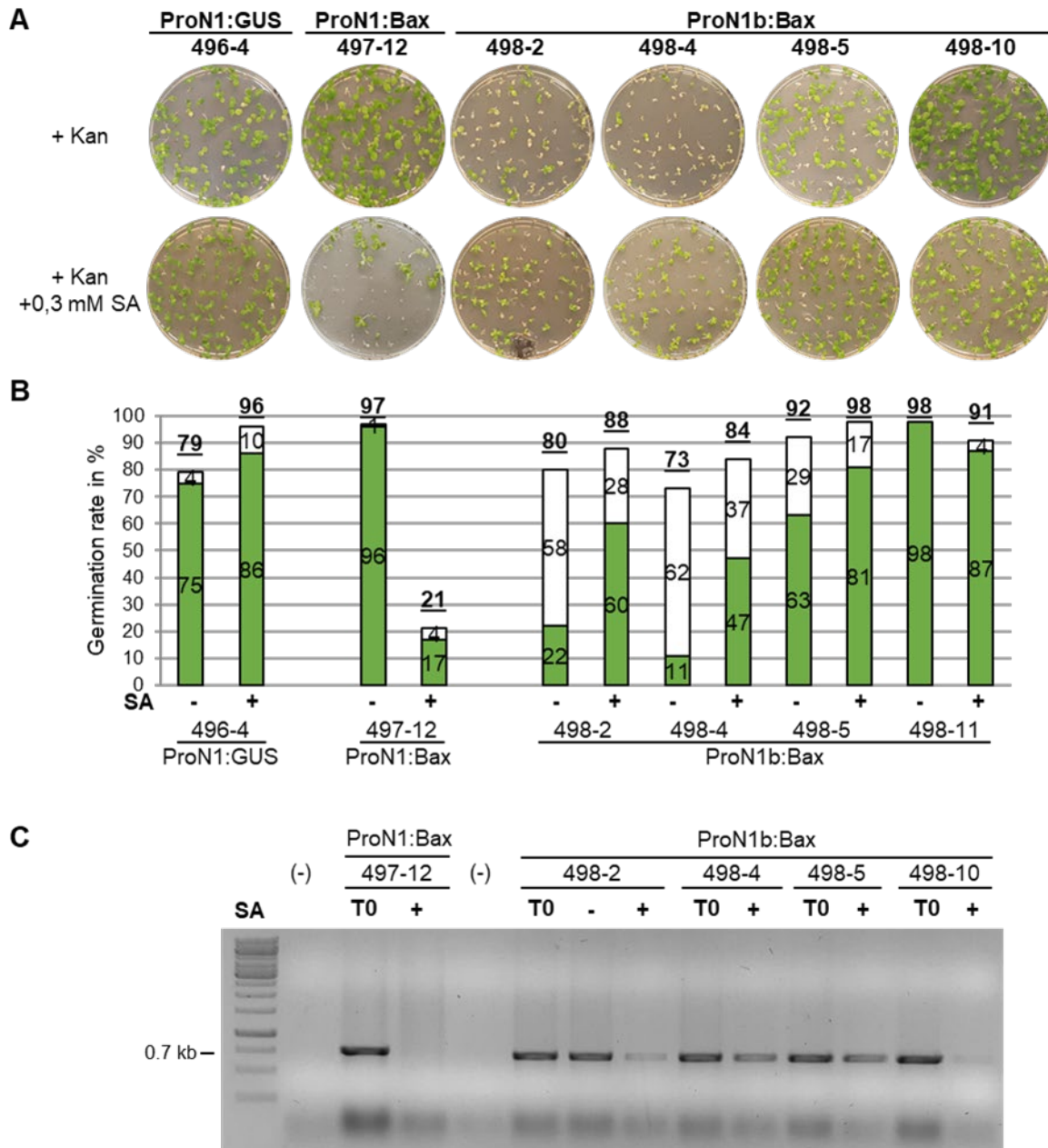


Fig. 11 Influence of salicylic acid on the germination of transgenic tobacco seeds. Seeds containing *6xHis-Bax* under control of the *N1* and *N1b* promoters from *Arabidopsis thaliana* were placed on MS medium agar plates containing kanamycin with or without addition of 0.3 mM SA. Seeds containing the *GUS* reporter gene under control of the *N1* promoter were used as a control. (A) Documentation of agar plates after 4 weeks of incubation in a light cabinet. (B) Germination rate in percent showing green seedlings (green bar) and discolored seedlings (white bar). (C) PCR amplification of reporter constructs using specific primers N1-P6/Bax-3-Sma for *ProN1:Bax* and N1b-P3/Bax-3-Sma for *ProN1b:Bax* respectively. Genomic DNA isolated from 10 green seedlings growing on selection plates with or without SA was used as template. H₂O used as negative control (-). Genomic DNA from the respective primary transformants (T0 plants) was used as a positive control.

The results shown for the germination of the transgenic lines 498-2, 3, 4 and 5 (Fig. 9, 10) were inconsistent. Therefore, the experiment was repeated. Four transgenic lines containing the *ProN1b:Bax* construct were compared: 498-2 and 498-4, the two lines which appear to grow better on SA containing agar plates (Fig. 9), 498-5, which does not show this effect (Fig. 10), and the previously untested line 498-10. One line each, containing the *ProN1:GUS* and *ProN1:Bax* constructs, were used as controls (Fig. 11). As observed before, *ProN1:GUS* seedlings are unaffected by the presence of SA and *ProN1:Bax* seedlings show a drastically reduced germination rate (Fig. 11 A,B). The seeds containing *ProN1b:Bax* show inconsistencies among those four lines, with lines 498-2 and 498-4 showing more green seedlings unaffected by Kan on SA plates, while lines 498-5 and 498-10 show no significant effect of the SA supplementation of the medium. PCR amplicons of *ProN1b:Bax* using the primer combination N1b-P3/Bax-3-Sma can be detected with genomic DNA isolated from seedlings and from the respective primary transformants in all four lines (Fig. 11C). As expected, the results show that seedlings containing the *ProN1:Bax* construct are unable to grow on medium supplemented with SA as the *N1* promoter is strongly induced by SA. Seedlings containing the *ProN1b:Bax*, however, show no reduction in germination rates.

4.1.3.3. Phenotype of tobacco plants harboring *ProN1b:Bax*

The remaining seedlings from lines 496-1 (*ProN1:GUS*), 497-3 (*ProN1:Bax*) and 498-3 (*ProN1b:Bax*) taken from the selective agar plates used for the germination experiment (Fig. 9) containing only kanamycin were grown in the greenhouse (3.3.2.). To examine if the *N1b* promoter can be induced in any tissue, whole plants were sprayed using 1 mM SA or 0.3 mM BTH (BION). Plants sprayed with water served as negative controls (Fig. 12A). After 8 days the control plants containing *ProN1:GUS* are mostly unaffected by SA and BTH, showing only minimal amounts of cell death on leaves sprayed with 1 mM SA (Fig. 12A, line 496-1). Both SA and BTH induce strong cell death in *ProN1:Bax* plants (Fig. 12A, line 497-3) confirming the strong inducibility of the *N1* promoter (4.1.2., Fig.7). Like the negative control, the *ProN1b:Bax* plants only exhibit tiny patches of cell death (Fig. 12, line 498-2), which are most likely unrelated to the reporter construct. To confirm that the plants contain the *Bax* transgene, genomic DNA was extracted from leaf discs and amplified using PCR using the primer combination Bax-5-BglII/Bax-3-Sma. All PCR products from *ProN1:Bax* and *ProN1b:Bax* plants treated with SA or BTH contain the 600 bp *Bax* ORF (Fig. 13B). These observations indicate that unlike the promoter of *N1*, the *N1b* promoter cannot be induced in any plant tissue using SA or BTH. Plants of the same lines were monitored during their whole life cycle till maturity. None of the plants developed visible cell death suggesting both the *N1* and the *N1b* promoters to be inactive during normal plant growth.

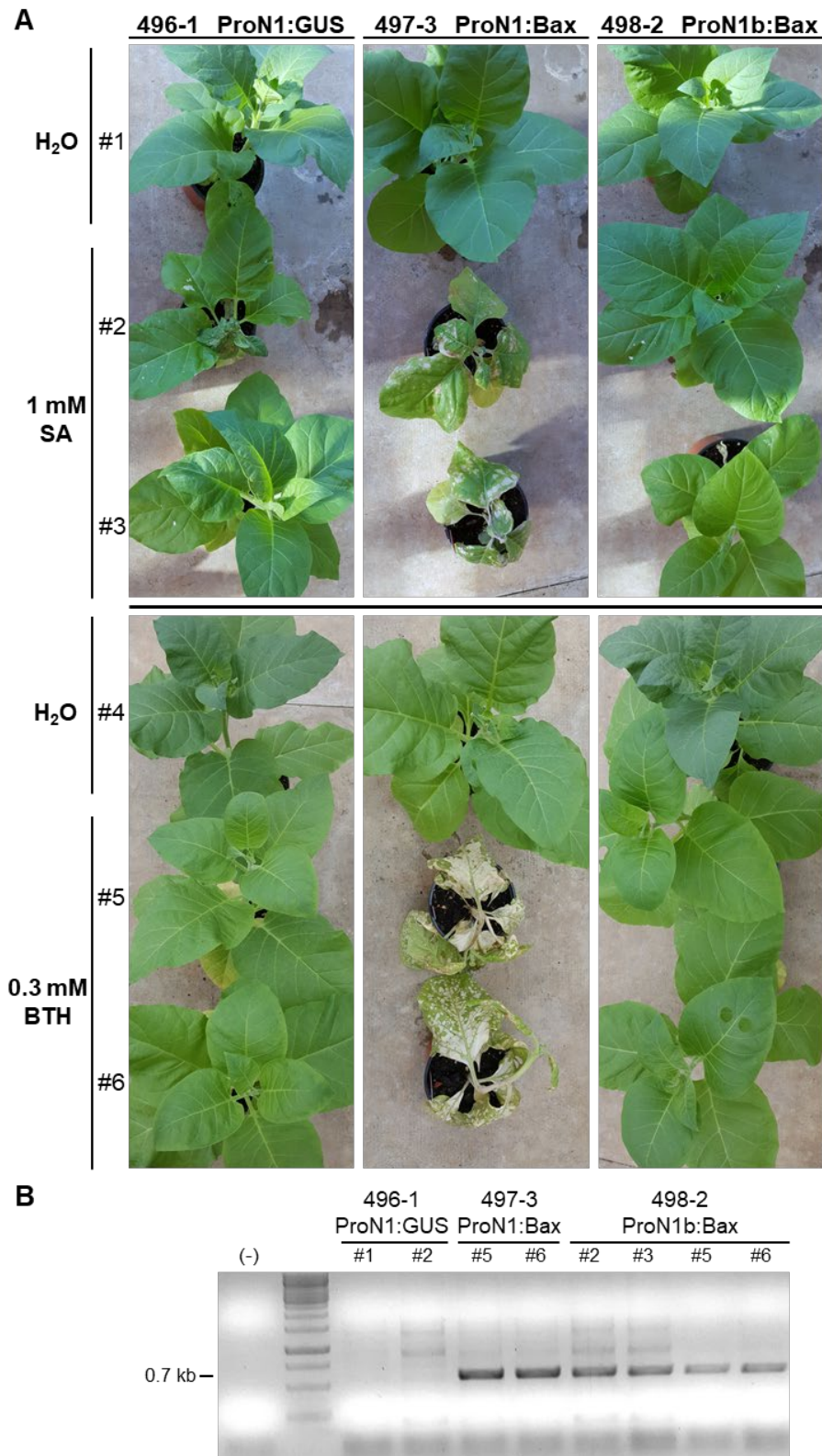


Fig. 12 Effects of SA and BTH on tobacco plants containing *ProN1:Bax* and *ProN1b:Bax* reporter constructs. Transgenic *Nicotiana tabacum* plants containing the *ProN1:Bax* or *ProN1b:Bax* were treated with SA or BTH. *ProN1:GUS* plants were used as controls. (A) Plants sprayed with H₂O, 1 mM SA or 0.3 mM BTH were documented 8 days post treatment. (B) PCR amplification of reporter constructs using specific primers: Bax-5-BglII/Bax-3-SmaI. Genomic DNA from plant extracts was used as template. H₂O and genomic DNA from *ProN1:GUS* plants was used as negative control. The size of the amplicons is around 600 bp.

4.2. Phenotypic effects of overexpression of Arabidopsis and tobacco *NIMIN* genes in *N. benthamiana* and *N. tabacum*

In addition to the negative regulatory effects the NIMIN proteins exert on NPR1-mediated gene induction during SAR establishment, Ashir Masroor described another striking effect of NIMIN proteins [Masroor, 2013]. During Agrobacterium mediated transient overexpression of *NIMIN1* and *NIMIN3* in *N. benthamiana*, infiltrated leaf tissues began to develop necrotic areas while there was no observable emergence of cell death during overexpression of *NIMIN1b* or *NIMIN2*. This observation is remarkable, as SAR establishment is not commonly associated with the emergence of cell death. Further experiments showed that this phenomenon is not exclusive to Arabidopsis *NIMIN* genes but can also be observed for the tobacco *NIMIN* genes *NtN2a* and *NtN2c* [Masroor, 2013; Jung, 2019]. Unlimited bacterial growth in plants overexpressing the *NIMIN1* gene has been excluded as no difference in bacterial growth could be detected in comparison to control plants overexpressing *GFP* or *NIMIN2* [Wagner, 2016].

To gain a better understanding which of the known NIMIN proteins exhibit cell death promoting activity and to identify common properties causing this phenomenon, *NIMIN-Venus* fusion constructs under control of the CaMV *35S* promoter were used in overexpression studies. This approach allows easy detection of different NIMIN proteins using a single antiserum. Initially, *NIMIN1* overexpression was directly compared to *NIMIN1-Venus* overexpression. Phenotypic effects of overexpression of *NIMIN1-Venus* and other Arabidopsis and tobacco *NIMIN-Venus* fusion constructs were monitored in transient expression assays in *N. benthamiana* and in transgenic tobacco plants.

4.2.1. Phenotypic effects of overexpression of Arabidopsis *NIMIN* genes in *N. benthamiana*

The Arabidopsis *NIMIN1* protein is the prime example of cell death promoting activity of NIMIN proteins and was besides *NIMIN3* the first NIMIN protein to be shown to exhibit this sort of phenotype [Masroor, 2013]. To replicate the results observed by Ashir Masroor, Agrobacterium mediated expression of *NIMIN1* was compared to *GFP*. Both genes were expressed under control of the *35S* promoter from CaMV to guarantee a high constitutive level of DNA transcription. The *GFP* protein was chosen as negative control as it plays no role during SAR or pathogen defense in general and does not affect the expression of the *PR1* gene. To exclude plant specific effects, the agrobacteria strains containing either the *Pro35S:GFP* [Hermann, 2013] or the *Pro35S:NI* [Weigel, 2001] construct (Fig. 13A) were infiltrated into the left and right leaf halves of three independent *N. benthamiana* plants, respectively. The phenotypic characteristics of infiltrated leaves were observed over a period of 2 weeks and pictures were taken for documentation (Fig. 13B). Consistent with the observations by Ashir Masroor, overexpression of *Pro35S:NI* leads to development of visible necrosis around 6 days post infiltration (see also Fig. 8). During the following days, the necrotic area spreads with increasing intensity until the whole infiltrated area died off 11 days post infiltration. Meanwhile, leaf halves infiltrated with *Pro35S:GFP* show no development of cell death during this time. Only after 12 or more days post infiltration the *GFP* overexpressing leaf halves show rather limited visible cell death.

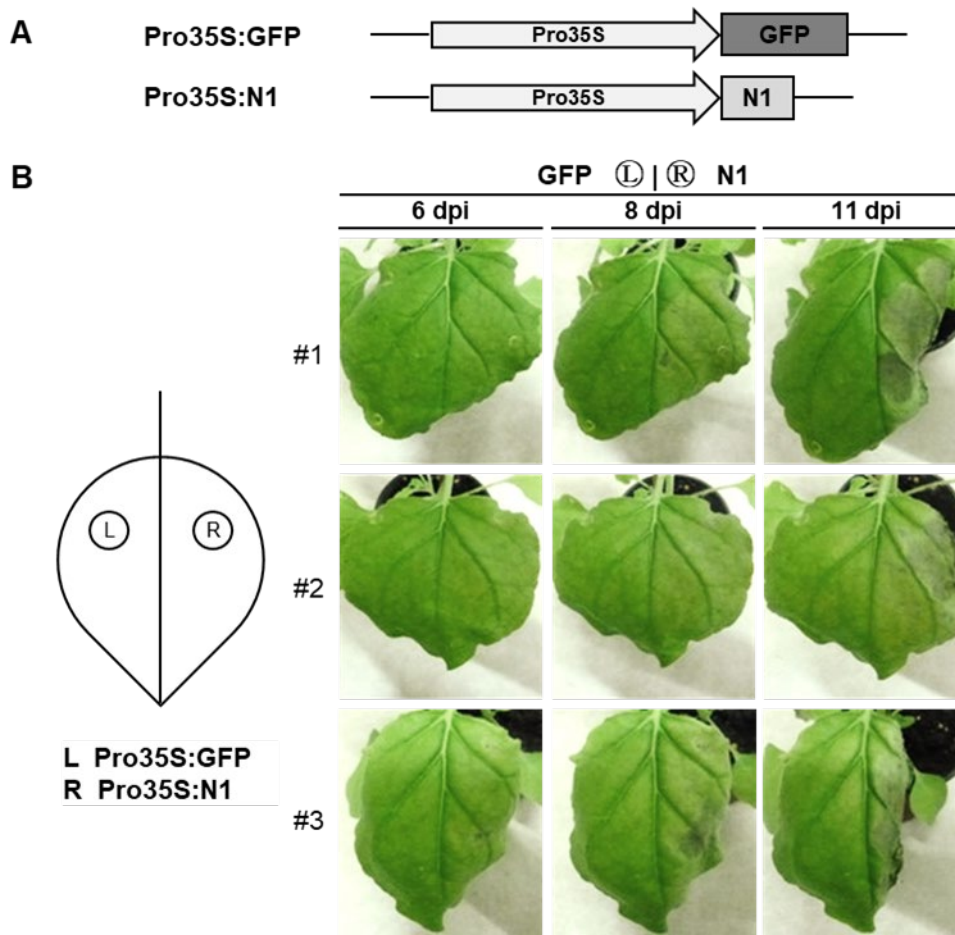


Fig. 13 Phenotypic effects of transient overexpression of *NIMINI* in *N. benthamiana* plants. (A) Schematic representation of the gene constructs expressed by the infiltrated agrobacteria strains. *GFP* and *NI* were expressed under control of the 35S promoter from CaMV. (B) Phenotype of infiltrated *N. benthamiana* leaves. Left leaf half: *Pro35S:GFP* ; Right leaf half: *Pro35S:NI*. Symptom development was documented from three independent plants at 6, 8 and 11 dpi.

4.2.1.1. Comparison of *NIMINI* and *NIMINI-Venus* overexpression

One problem while working with NIMIN proteins is the lack of an antiserum capable of detecting all of them with a clear and distinct signal. Therefore, to enable easy detection of NIMIN protein accumulation using the α -GFP antiserum, NIMIN-Venus fusion proteins were used. Venus is a yellow fluorescent variant of GFP containing several mutations to enhance both protein maturation and stability. In Arabidopsis the N1 protein binds to the highly conserved N1/N2 binding domain in the C-terminal part of NPR1. This interaction is strongly suppressed by the presence of SA [Maier *et al.*, 2011]. To determine if fusion of Venus to the N1 C-terminus interferes with the interaction between N1 and NPR1 a quantitative yeast two-hybrid assay was used (Fig. 14A). *HF7c* yeast cells were co-transformed with a pGAD424 plasmid, harboring a *GAL4AD* fusion of *AtNPR1*, and a pGBT9 plasmid, harboring a *GAL4BD* fusion of *NI* [Weigel *et al.*, 2001], *NI-Venus* (*NI-V*) or *Venus* (see Appendix V). pGAD424 and pGBT9 plasmids without inserts expressing only *GAL4AD* and *GAL4BD* respectively were used as negative controls.

Indeed, Gal4BD fusions of N1-V, like N1, strongly interact with AtNPR1 in yeast. The strength of this interaction is greatly reduced if 0.3 mM SA is added to the medium showing that N1-V behaves like N1 regarding its NPR1 binding properties. As expected, the Venus protein alone is unable to interact with NPR1 in yeast. The expression of Venus and N1-Venus as GAL4BD fusions in yeast cells was proven by using the α -GAL4BD antiserum on protein extracts from yeast cells (Fig. 14B). The fusion proteins have a size of 49 kDa for GAL4BD-Venus and 66 kDa for GAL4BD-N1-V, respectively.

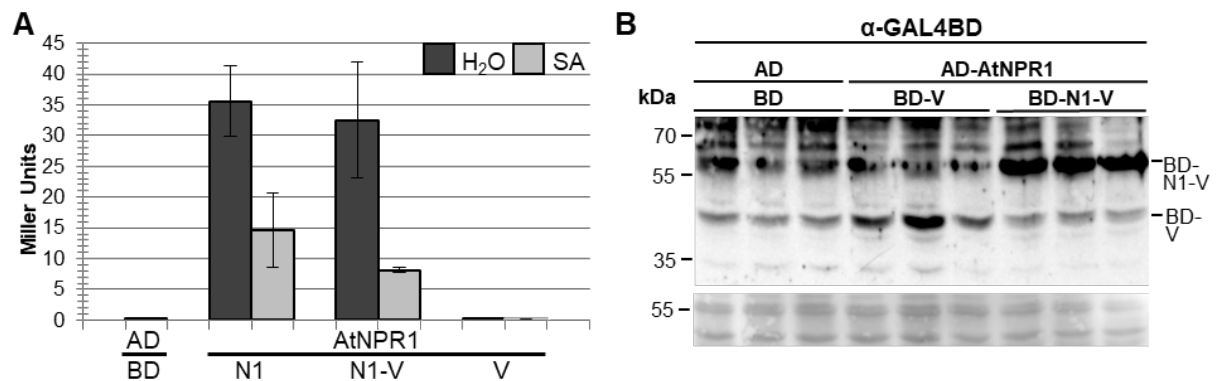


Fig. 14 Interaction of NIMIN1, NIMIN1-Venus and Venus with AtNPR1 in yeast. (A) Quantitative Y2H assay for interaction of GAL4BD fusion proteins of N1, N1V and Venus with GAL4AD-AtNPR1. The assays were performed under standard conditions in presence (light bar) and absence (dark bar) of 0.3 mM SA using three independent colonies with two replicates for each colony. (B) Immunodetection GAL4BD-Venus (BD-V, 49 kDa) and GAL4BD-N1V (BD-N1V; 66 kDa) from yeast protein extracts using the α -GAL4BD antiserum. Ponceau S staining was used as loading control.

To ensure that the Venus protein like GFP does not trigger the development of necrotic tissue and that N1-Venus fusion proteins behave like wildtype N1, a *Pro35S:NI-Venus* [Lehmann, 2014] construct was transiently overexpressed in *N. benthamiana* leaves of three independent plants in direct comparison with *Pro35S:Venus* [Neeley *et al.*, 2019] and *Pro35S:GFP* (Fig. 15). Similar to leaf halves overexpressing *Pro35S:GFP* (Fig. 13B, Fig. 15A, left leaf halves), leaf halves infiltrated with agrobacteria containing the *Pro35S:Venus* (Fig. 15B) display no necrotic tissues. This indicates that the Venus protein behaves like GFP and does not promote accelerated cell death. Overexpression of *Pro35S:NI-Venus* results in development of cell death with the first visible necrotic patches appearing around 6 days post infiltration and gradually increasing in intensity and spread (Fig. 15A,B, right leaf halves). As previously shown (4.4.1., Fig. 4B) immunodetection reveals strong accumulation of the N1-Venus fusion protein at 44 kDa with two lower bands at 35 kDa and 27 kDa respectively.

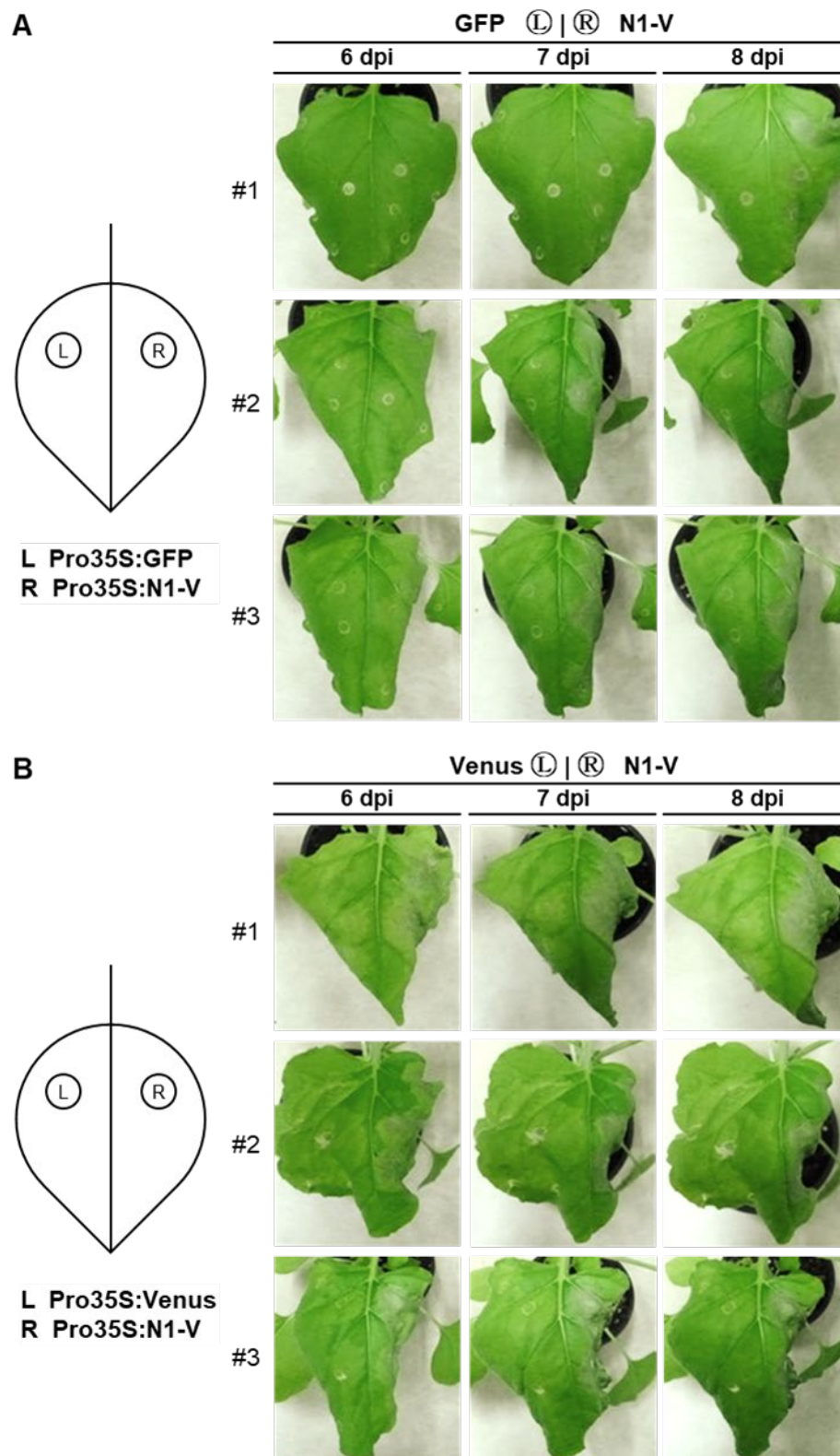
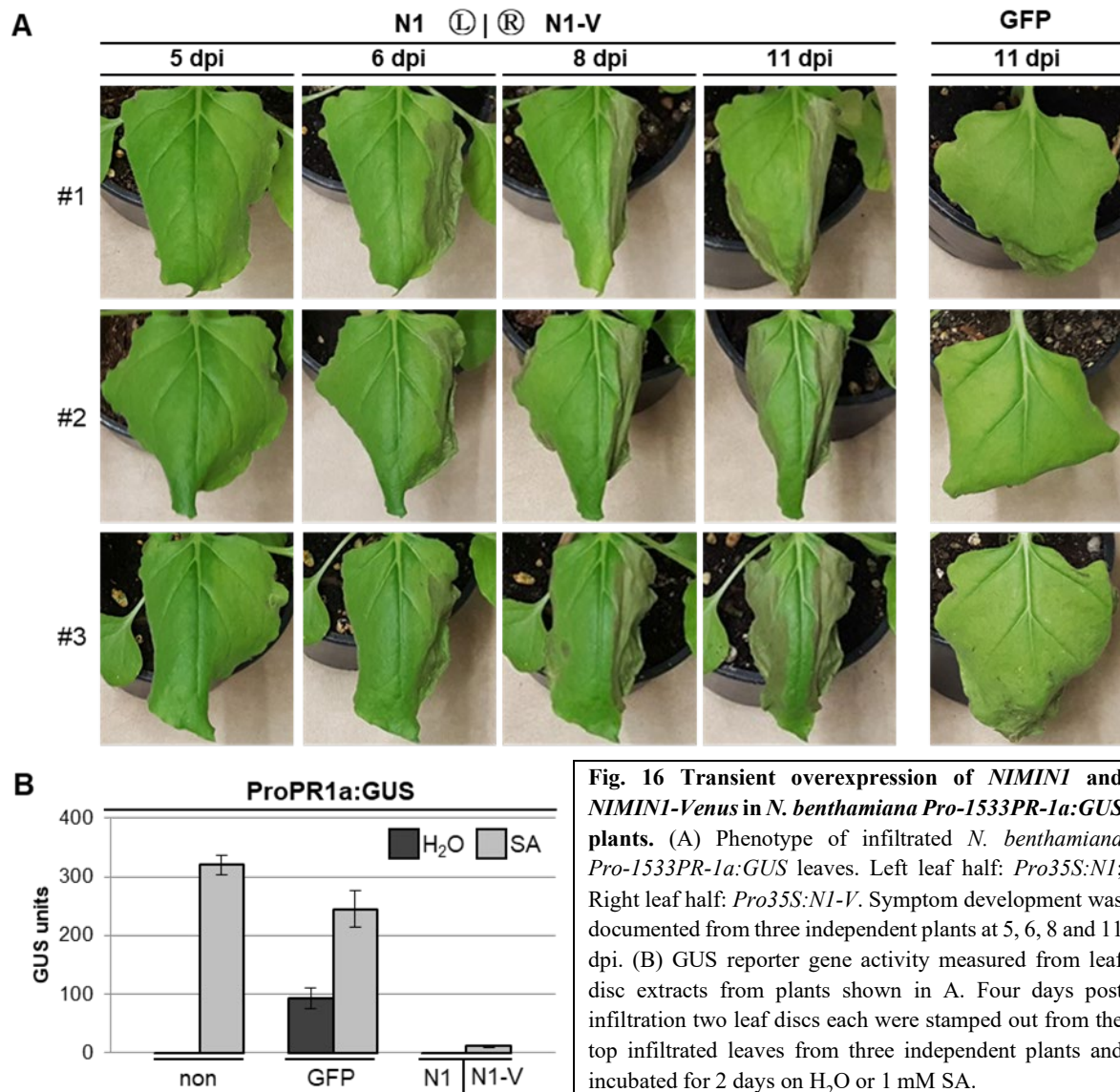


Fig. 15 Phenotypic effects of transient overexpression of *NIMINI-Venus* in *N. benthamiana* plants. *GFP*, *Venus*, and *NI-Venus* were expressed under control of the 35S promoter from CaMV. (A) and (B) Phenotype of infiltrated *N. benthamiana* leaves. Left leaf half: *Pro35S:GFP* (A) or *Pro35S:Venus* (B); Right leaf half: *Pro35S:NI-V*. Symptom development was documented from three independent plants at 6, 7 and 8 dpi.

To achieve a more direct comparison of *N1* and *N1-Venus*, agrobacteria containing the *Pro35S:N1* and *Pro35S:N1-Venus* constructs were infiltrated into the respective left and right leaf halves of *N. benthamiana* plants containing the *Pro-1533PR-1a:GUS* reporter construct (Fig. 16).



Side-by-side comparison revealed that overexpression of *N1-Venus* actually promotes cell death even more strongly than *N1*. (Fig. 16A) with visible necrosis emerging two days earlier. Four days post infiltration, before the emergence of visible cell death, two leaf discs were stamped out and incubated for three days on H₂O or 1 mM SA. During this time *N1* and *N1-V* infiltrated leaf discs developed small brown spots correlating with the development of cell death on the respective leaf halves. A GUS reporter assay on protein extracts from those leaf discs revealed that both, *N1* and *N1-Venus* overexpression, completely abolishes the SA mediated induction of the *Pro-1533PR-1a:GUS* reporter construct (Fig. 16B), indicating that the Venus fusion does not interfere with the negative regulatory properties of *N1* during the induction of *PR1a* gene expression. Taken together these results indicate that fusion to the Venus protein does not interfere with the binding properties (Fig. 14) or regulatory functions of *NIMIN1* regarding *PR1* gene expression (Fig. 16).

4.2.1.2. Phenotypic effects of overexpression of *NIMIN1b*, *N2*, and *N3-Venus* fusion genes

N1 shares a similar domain architecture with the three other members of the NIMIN protein family found in *Arabidopsis thaliana*, N1b, N2, and N3, which differs primarily in the presence of the two NPR1 interaction domains, the DXFFK motif and the EDF motif (see 1.5., Fig. 2) [Weigel *et al.*, 2001; Hermann *et al.*, 2013]. To identify common features among cell death-promoting NIMIN proteins the effects of *NI-V* overexpression were compared to equivalent *NIMIN-Venus* fusion constructs for *N1b*, *N2*, and *N3*. As shown in the previous section (4.2.1.1.), N1-Venus behaves like N1 regarding its biochemical properties and phenotypic effects while producing strong signals using the α -GFP (FL) antiserum. While *Pro35S:NI-Venus* and *Pro35S:N3-Venus* constructs were already available [Lehmann, 2014], analogous constructs were generated for *N1b* and *N2* as part of this thesis (see Appendix V).

Of all NIMIN proteins from *Arabidopsis*, N1 and N1b share the highest sequence similarity with each other (38 % identity, 67 % similarity) and an almost identical domain structure. While N1b was shown to be an equally strong suppressor of *PR1a* reporter gene activation as N1, development of cell death during transient overexpression could not be observed [Masroor, 2013]. To reproduce these results, *Agrobacteria* containing *Pro35S:NI-Venus* or *Pro35S:N1b-Venus* were infiltrated into opposite halves of leaves from three independent *N. benthamiana* plants containing the *Pro-1533PR-1a:GUS* reporter construct (Fig. 17). Tissue overexpressing *NI-Venus* exhibits rapid development of necrosis, the first signs of which were becoming visible at 6 days post infiltration (Fig. 17A). Like the GFP control, tissue overexpressing N1b-Venus does not show any signs of cell death even 12 days post infiltration. Immunodetection assays using the α -GFP (FL) antiserum revealed that N1b-Venus does not accumulate in significant amounts showing only vague signal at 44 kDa (Fig. 17B). Four days post infiltration, two leaf discs from each leaf half from all three plants were stamped out and incubated for two days on H₂O or 1 mM SA. A GUS reporter assay from leaf disc extracts shows a reduction in *PR1a* promoter activity for tissue overexpressing *NI* to the background levels observed in GFP infiltrated control tissue incubated on H₂O. This effect is less pronounced for overexpression of *N1b* (Fig. 17C). However, the high background in this experiment does not allow an accurate assessment of N1b mediated *PR1a* repression.

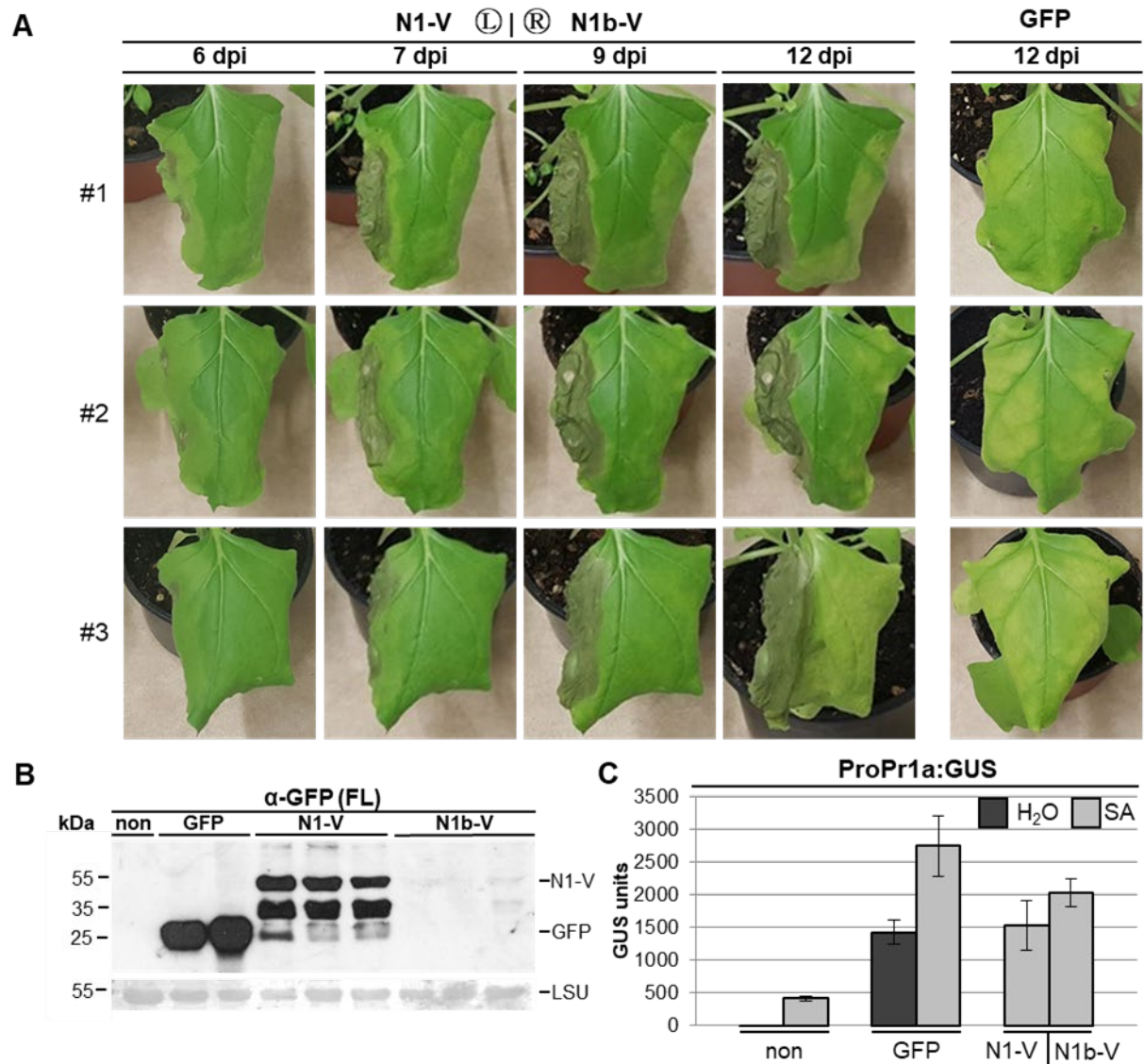


Fig. 17 Transient overexpression of *NIMIN1-Venus* and *NIMIN1b-Venus* in *N. benthamiana Pro-1533PR-1a:GUS* plants. (A) Phenotype of infiltrated *N. benthamiana* leaves. Left leaf half: *Pro35S:N1-V*; Right leaf half: *Pro35S:N1b-V*. Symptom development was documented from three independent plants at 6, 7, 9 and 12 dpi. Plants infiltrated with *Pro35S:GFP* were used as a control. (B) Immunodetection of Venus fusion proteins from protein extracts prepared 4 dpi from three independent plants, using the α -GFP (FL) antiserum. Ponceau S staining of the RuBisCO large subunit (LSU) was used as loading control. (C) GUS reporter gene activity measured from leaf disc extracts. Four days post infiltration two leaf discs each were stamped out from the top infiltrated leaves from three independent plants and incubated for 2 days on H₂O or 1 mM SA.

N2 differs from other Arabidopsis NIMIN proteins in the lack of an EDF motif. *Pro35S:N2-V* and *Pro35S:N1-V* Agrobacteria were infiltrated side by side into the opposing leaf halves of three independent *N. benthamiana* halves carrying the *Pro-1533PR-1a:GUS reporter* construct (Fig. 18). Like *N1b-Venus* (Fig. 17A), overexpression of *N2-Venus* does not induce the development of cell death (Fig. 18A). Using the α -GFP (FL) antiserum on protein extracts from infiltrated leaves revealed no visible accumulation of the proposed 40 kDa full-length N2-Venus protein. Only several lower bands between 25 and 30 kDa could be detected (Fig. 18B). Consistent with the results by Masroor observed for N2 [2013], overexpression of *N2-Venus* has no repressive effect on the SA mediated induction of the *PR-1a* promoter (Fig. 18C), confirming that N2, unlike N1 or N1b, is a non-suppressive protein.

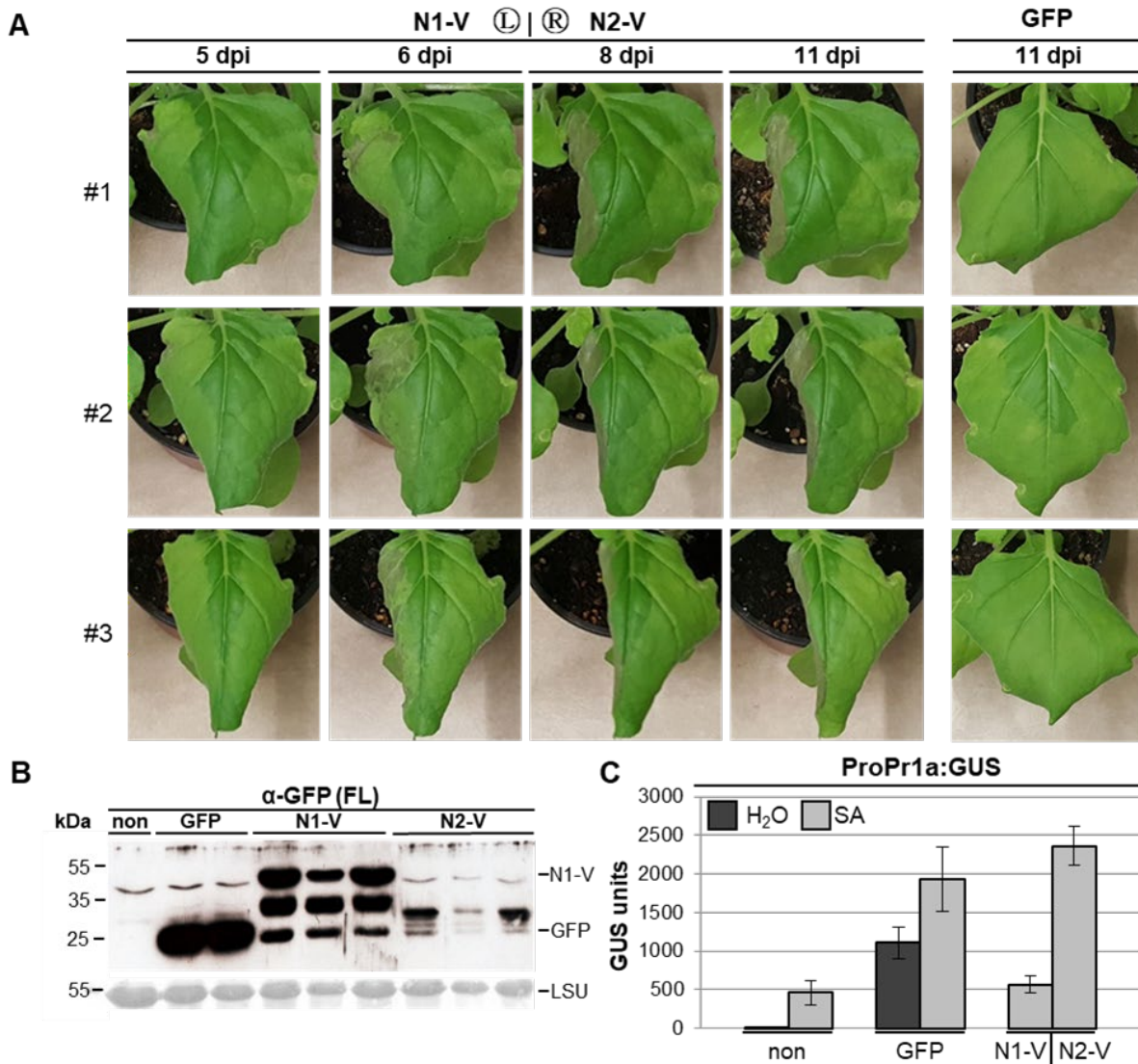


Fig. 18 Transient overexpression of NIMIN1-Venus and NIMIN2-Venus in *N. benthamiana* Pro-1533PR-1a:GUS plants. (A) Phenotype of infiltrated *N. benthamiana* leaves. Left leaf half: *Pro35S:N1-V*; Right leaf half: *Pro35S:N2-V*. Symptom development was documented from three independent plants at 5, 6, 8 and 11 dpi. Plants infiltrated with *Pro35S:GFP* were used as a control. (B) Immunodetection of Venus fusion proteins from protein extracts prepared 4 dpi from three independent plants, using the α-GFP (FL) antiserum. Ponceau S staining of the RuBisCO large subunit (LSU) was used as loading control. (C) GUS reporter gene activity measured from leaf disc extracts. Four days post infiltration two leaf discs each were stamped out from the top infiltrated leaves from three independent plants and incubated for 2 days on H₂O on 1 mM SA.

N3 differs from other Arabidopsis NIMIN proteins in several characteristics. Unlike N1, N1b and N2, N3 interacts with the N-terminus of NPR1, rather than its C-terminus [Weigel *et al.*, 2001]. Furthermore, N3 does not contain a NLS canonical consensus sequence but the protein is rich in lysine and arginine and contains similar sequences to the NLSs from N1 and N2 which could serve the same purpose [Weigel, 2000]. During Agrobacterium mediated transient overexpression, *Pro35S:N3-V* is able to promote the development of cell death (Fig. 19A). The necrotic tissue, however, becomes visible later than for the *Pro35S:N1-V* construct infiltrated into the opposing leaf halves. Immunodetection revealed that the N3-V protein, like N1-V, accumulates strongly in infiltrated leaf tissue (Fig. 19B). The signal of the full-length protein is detected at 40 kDa, only slightly below the 44 kDa signal of N1-V and both proteins have a similar band pattern.

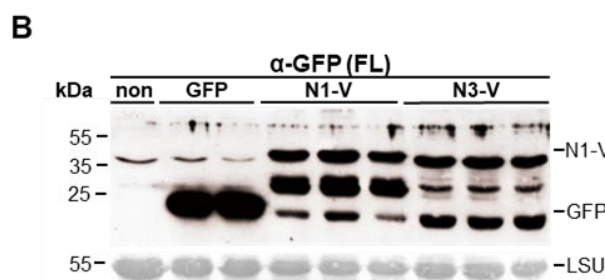
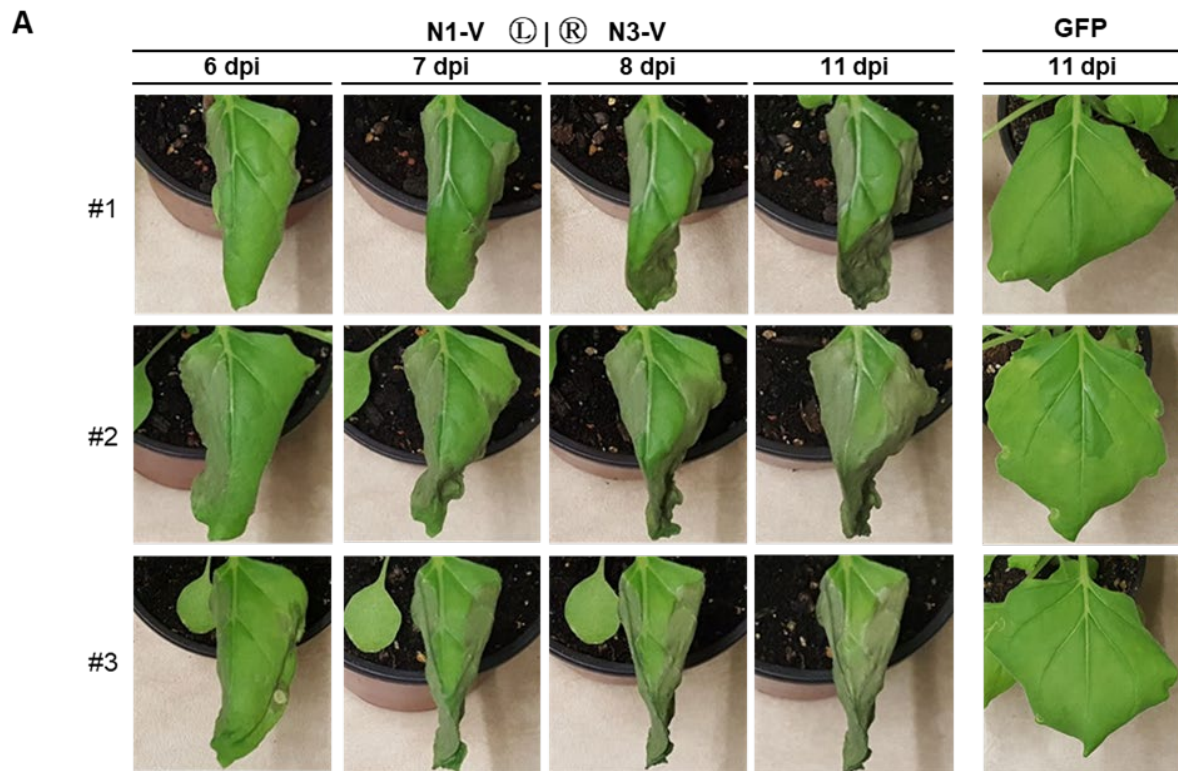


Fig. 19 Transient overexpression of *NIMIN1-Venus* and *NIMIN3-Venus* in *N. benthamiana* plants.

(A) Phenotype of infiltrated *N. benthamiana* leaves. Left leaf half: *Pro35S:N1-V*; Right leaf half: *Pro35S:N3-V*. Symptom development was documented from three independent plants at 6, 7, 8 and 11 dpi. Plants infiltrated with *Pro35S:GFP* were used as a control. (B) Immunodetection of Venus fusion proteins from protein extracts prepared 4 dpi from three independent plants, using the α-GFP (FL) antiserum. Ponceau S staining of the RuBisCO large subunit (LSU) was used as loading control.

The results suggest a correlation between the development of cell death observed in plants overexpressing certain NIMIN proteins and the accumulation of said proteins. N1-V and N3-V accumulate strongly and lead to fast spreading necrosis in infiltrated tissues (Fig. 19), while neither full-length N1b-V nor N2-V can be detected, and infiltrated tissues do not differ from those overexpressing *GFP* regarding induction of cell death (Fig. 17, 18).

4.2.1.3. Effects of *NI*- and *N2-Venus* overexpression on *N1* and *N2* promoter activity

As shown in the previous section, overexpression of NIMIN proteins affects the expression from the *PR1a* promoter differentially. While Arabidopsis *N1* and *N1b* are repressors of *PR1a* promoter activity (Fig. 16, 17), Arabidopsis *N2* does not affect the expression from this promoter significantly (Fig. 18). Like the *PR1a* promoter, the promoters of the *N1* and *N2* genes also contain SA responsive *as-1*-like elements with TGACG motifs. However, while the *N1* promoter is dependent on the presence of functional NPR1, the *N2* promoter shows only partial dependency [Glocova *et al.*, 2005; Hermann, 2009; Hermann *et al.*, 2013]. To test whether overexpression of *N1* or *N2* affects the activity of the *N1* and *N2* promoters in a similar manner as the *PR1a* promoter, agroinfiltration-based transient overexpression was used.

Transgenic *N. benthamiana* plants containing *ProN1:GUS* (line 475-2/3) or *ProN2:GUS* (line 476-2/2 and -5/5, U. M. Pfitzner personal communication) reporter constructs were infiltrated using *Agrobacterium* strains containing *Pro35S:NI-V* or *Pro35S:N2-V* constructs (Fig. 20A). Leaf halves overexpressing *NI-V* show emergence of necrosis 6 days post infiltration while leaf halves overexpressing *N2-V* do not (Fig. 20E), confirming earlier observations (Fig. 18). Leaf discs were stamped out 4 days post infiltration, before the emergence of visible cell death and incubated for three days on H₂O or 1 mM SA. A GUS reporter assay on protein extracts from those leaf discs revealed much weaker overall induction of the *N2* promoter (Fig. 20C,D) compared to the *N1* Promoter (Fig. 20B), consistent with the observations from tobacco plants (see 4.1.2., Fig. 7). The *ProN1:GUS* reporter construct can be induced by SA in noninfiltrated plants, as well as in plants overexpressing *GFP* or *N2-Venus*. However, overexpression of *NI-Venus* inhibits SA mediated induction of the *N1* promoter (Fig. 20B). This effect appears less pronounced for the *N2* promoter, but the high background activity makes these results less reliable (Fig. 20C,D).

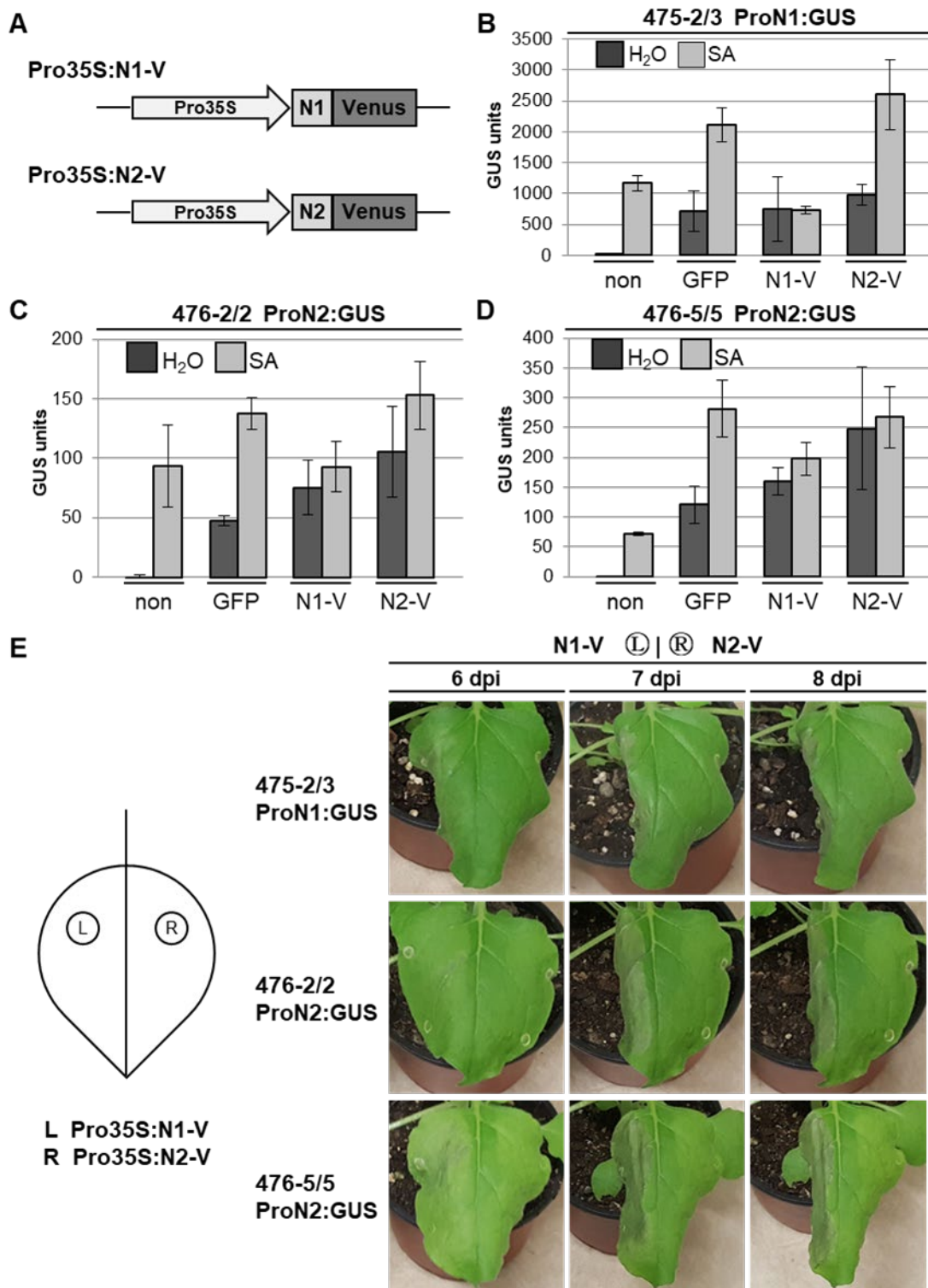


Fig. 20 GUS reporter gene activity of *NIMIN1* and *NIMIN2* promoter constructs and phenotype of *Nicotiana benthamiana* plants after chemical induction during NIMIN protein overexpression. (A) Schematic representation of the gene constructs expressed by the infiltrated agrobacteria strains. *N1* and *N2* were fused to the N-terminus of the *Venus* reporter gene and placed under control of the 35S promoter from CaMV. (B-D) GUS reporter gene activity measured from leaf disc extracts. Transgenic *N. benthamiana* plants containing *ProN1:GUS* (475-2/3, B) or *ProN2:GUS* (476-2/2, C; 476-5/5, D) reporter constructs were infiltrated using *Agrobacterium* suspensions harboring the indicated gene constructs. Five days post infiltration two leaf discs each were stamped out from three independent plants and incubated for 3 days on H₂O or 1 mM SA. (E) Phenotype of infiltrated leaves. The same plants were used for phenotypic studies. Symptom development was documented at 6, 7 and 8 dpi.

4.2.2. Phenotypic effects of overexpression of tobacco *NIMIN-Venus* fusion genes in *N. benthamiana*

The tobacco genome contains four *N2*-like genes which contain a DXFFK but not an EDF domain and were shown to repress the induction of the *PR-1* genes during the early stages of SAR. Besides *NtNIMIN2a* (*NtN2a*, also called *G8-1*), *NtN2b* and *NtN2c* [Horvath *et al.*, 1998; Zwicker *et al.*, 2007], BLAST search of the Genbank database for NIMIN-like sequences led to the identification of one more *N2*-like gene named *NtN2-like* (*FS*, EST FS401103) [Masroor, 2013], as well as two *N1*-like genes: *NtN1-like1* (*BP*, EST BP531936) [Masroor, 2013] and *NtN1-like2* (*FG*, EST FG635992) [U.M. Pfitzner, personal communication]. While both, tobacco *N1*-like and *N2*-like proteins, share a similar domain architecture as those found in Arabidopsis (Fig. 21), no equivalent for *N3* has been found in tobacco so far. This suggests a different sequence of events during the SAR mediated defense gene activation in tobacco than proposed in Arabidopsis. However, like their Arabidopsis counterpart the *N1*-like proteins BP and FG contain an EDF domain, which could allow to compensate the lack of a *N3*-like protein. Unlike Arabidopsis NIMIN proteins, which contain LxLxL type EAR motifs, tobacco NIMINs feature DLNxxxP type EAR motifs near their C-termini with only the FS protein containing an EAR motif with overlapping LxLxL and DLNxxxP sequences.

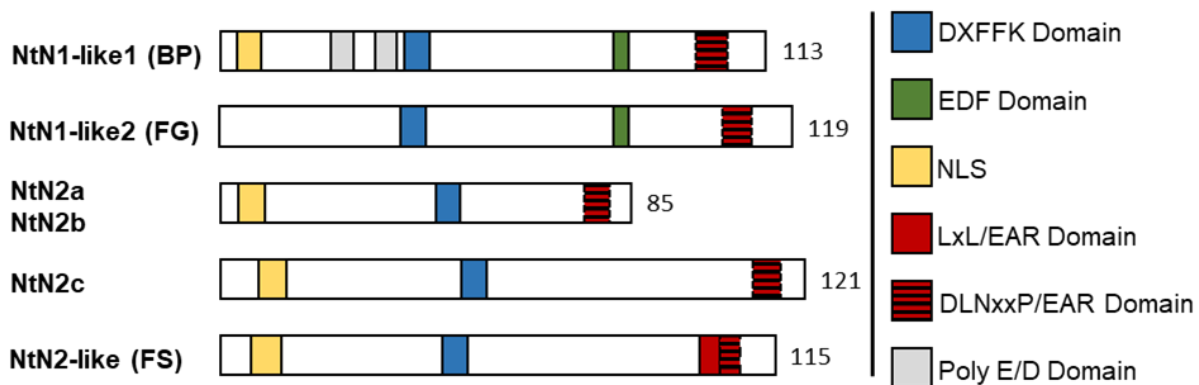


Fig. 21 Domain architecture of tobacco NIMIN proteins. Schematic representation of NIMIN proteins from tobacco showing their characteristic domains. The diagram is drawn approximately to scale. Conserved regions include a DXFFK motif of about 10 amino acids with high similarity (blue), an EDF domain (green), hypothetical nuclear localization signals (yellow), LxL (red) and/or DLNxxxP type EAR domains (red striped), and stretches of at least four consecutive acidic residues (Poly E/D domain, grey).

The works by Zwicker *et al.* [2007], Maier *et al.* [2011] and Masroor [2013] showed that tobacco NIMIN proteins NtN2a, NtN2b, NtN2c, BP and FS interact with the NPR1 proteins from tobacco, NtNPR1 and NtNIM1-like1 (NtNPR3), in a SA dependent manner. To confirm these results and to learn if the new FG protein shares this property with the other tobacco NIMIN proteins quantitative yeast two-hybrid assays were used (Fig. 22). *HF7c* Yeast cells were co-transformed with a pGAD424 plasmid, harboring a *GAL4AD* fusion of *NgNPR1* [Zwicker, 2002] or *NtNIM1-like1* [Maier *et al.*, 2011], and a pGBT9 plasmid, harboring a *GAL4BD* fusion of *NtN2a*, *NtN2c* [Zwicker *et al.*, 2007], *BP*, *FS* [Masroor, 2013] or *FG* [U.M. Pfitzner, personal communication]. pGAD424 and pGBT9 plasmids without inserts expressing only *GAL4AD* and *GAL4BD* respectively were used as negative controls.

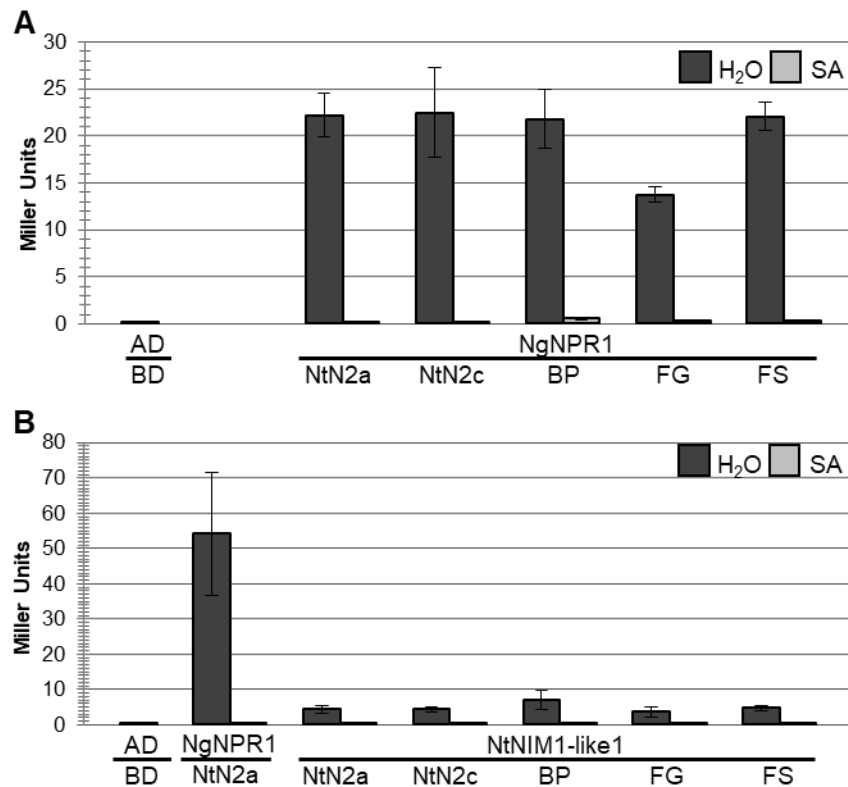


Fig. 22 Interaction of tobacco NIMIN and NPR proteins in yeast. Quantitative Y2H assay for interaction of GAL4BD fusion proteins of NtN2a, NtN2c, BP, FG and FS with GAL4AD-*NgNPR1* (A) or GAL4AD-*NtNIM1-like1* (B). The assays were performed under standard conditions in presence (light bar) and absence (dark bar) of 0.3 mM SA using three independent colonies with two replicates for each colony.

All tested tobacco NIMIN proteins show a strong interaction with *NgNPR1* with only FG showing about 35 % weaker interaction (Fig. 22A). However, when the yeast growth medium was supplemented with SA these interactions were almost completely abolished. FG also interacts with *NtNIM1-like1*, but this interaction is much weaker, comparable to other tobacco NIMIN proteins (Fig. 22B). These results confirm that N1-like and N2-like proteins from tobacco, like their *Arabidopsis* counterparts, interact with NPR1 proteins in a SA dependent manner.

As tobacco contains N1-like and N2-like proteins with similar biochemical properties as *Arabidopsis*, it was of great interest to see if they act like their counterparts regarding cell death promoting activity. For this purpose, *NIMIN-Venus* fusion gene constructs analogous to the *Arabidopsis* constructs were created for the N1-like genes *BP* and *FG*, as well as for the N2-like genes *NtN2c* and *FS* (see Appendix V). Surprisingly, during transient overexpression in leaves of *N. benthamiana* *Pro-1533PR-1a:GUS* plants, neither *Pro35S:BP-V* nor *Pro35S:FG-V*, unlike *Pro35S:N1-V*, led to the development of cell death in agroinfiltrated tissues (Fig. 23A). A GUS reporter assay revealed that overexpression of *BP* only slightly reduces the activity of the *PR1a* promoter while overexpression of *FG* does not induce any significant reduction in reporter gene activity (Fig. 23B).

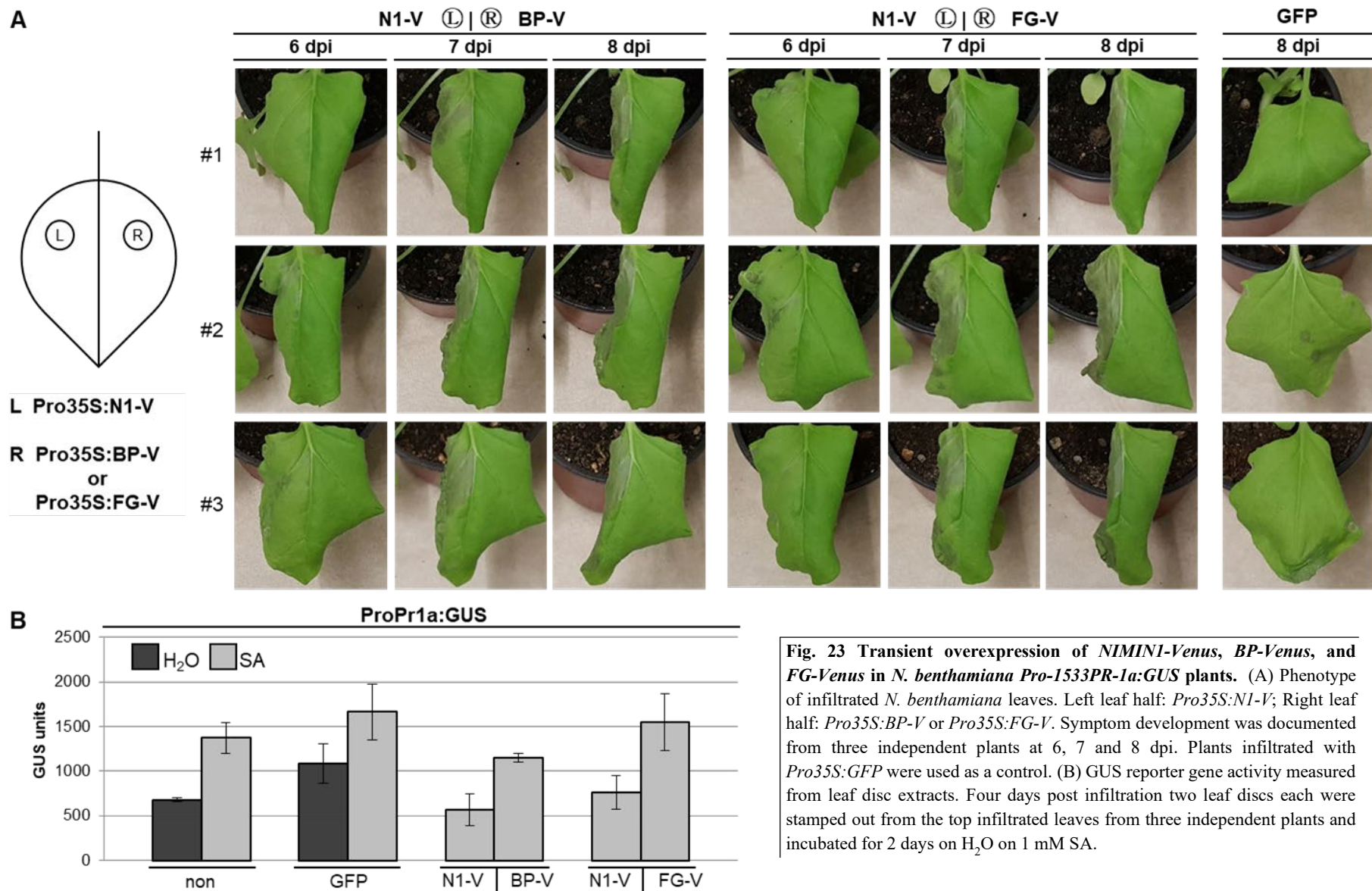
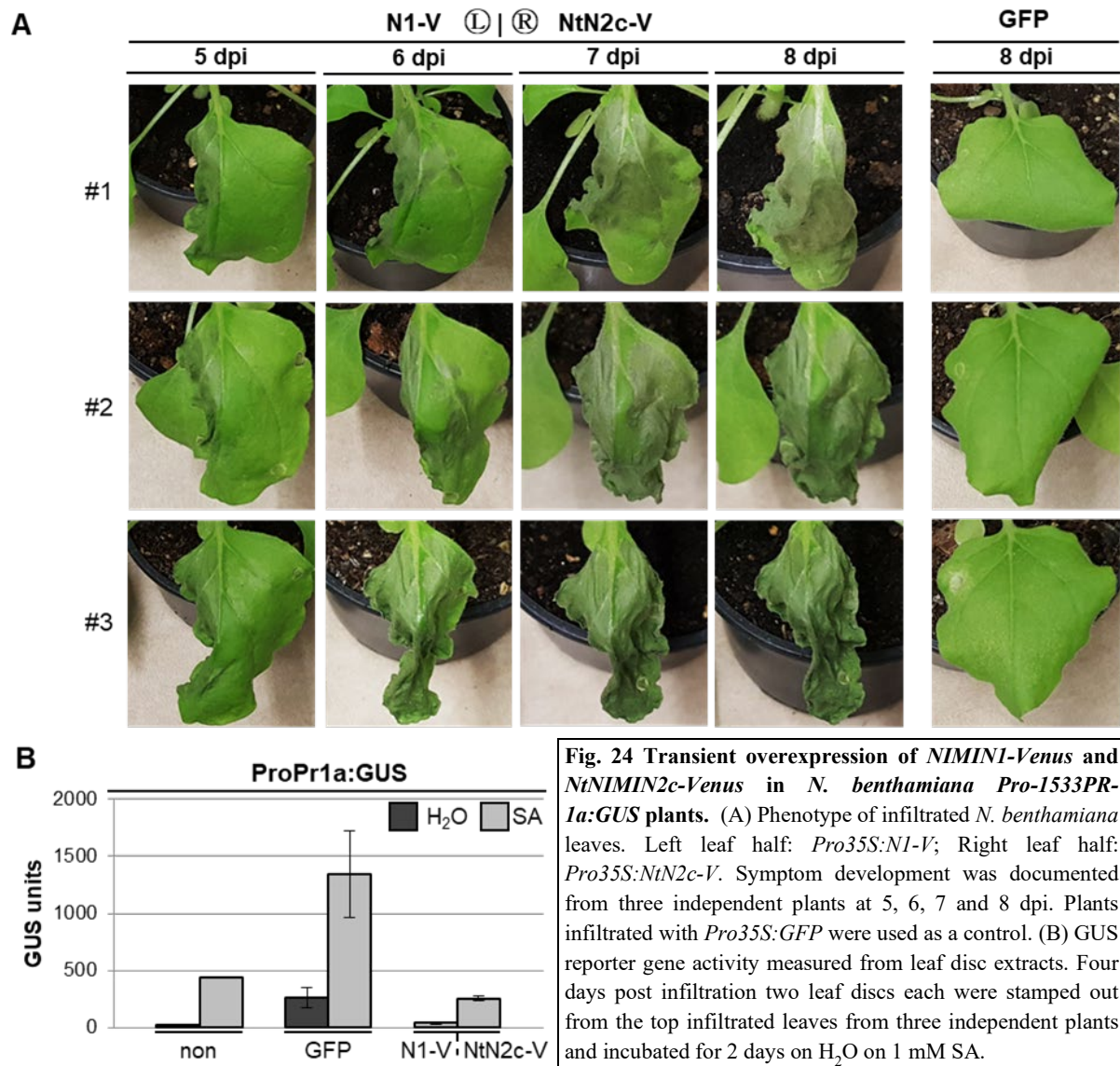


Fig. 23 Transient overexpression of *NIMIN1-Venus*, *BP-Venus*, and *FG-Venus* in *N. benthamiana* *Pro-1533PR-1a:GUS* plants. (A) Phenotype of infiltrated *N. benthamiana* leaves. Left leaf half: *Pro35S:N1-V*; Right leaf half: *Pro35S:BP-V* or *Pro35S:FG-V*. Symptom development was documented from three independent plants at 6, 7 and 8 dpi. Plants infiltrated with *Pro35S:GFP* were used as a control. (B) GUS reporter gene activity measured from leaf disc extracts. Four days post infiltration two leaf discs each were stamped out from the top infiltrated leaves from three independent plants and incubated for 2 days on H₂O on 1 mM SA.

Unlike the N1-like proteins from tobacco, infiltration of an *Agrobacterium* strain overexpressing a *Pro35S:NtN2c-V* construct led to equally strong, although slower, development of necrosis when compared to *Pro35S:NI-V* (Fig. 24A). A reporter assay for induction of GUS expression after SA-mediated induction of the *PR1a* promoter demonstrated almost equally strong repression of the promoter activity by *NtN2c-V* as observed for *NI-V* (Fig. 24B).



Similar results were observed for FS, another N2 like protein. Overexpression of *Pro35S:FS-V* appears to promote cell death more strongly than *Pro35S:NtN2c-V* as the first visible spots of necrotic tissue arise at 6 days post infiltration, at the same time as for *Pro35S:NI-V* (Fig. 25A). Likewise, this overexpression results in strong repression of the *PR1a* promoter (Fig. 25B).

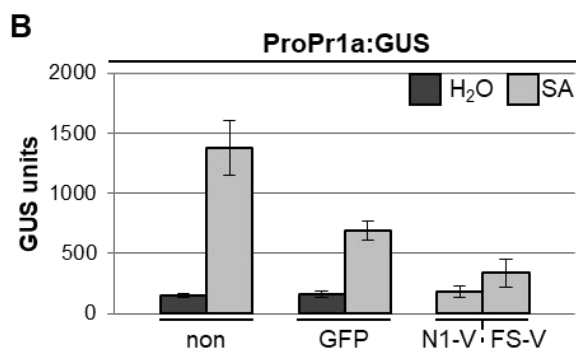
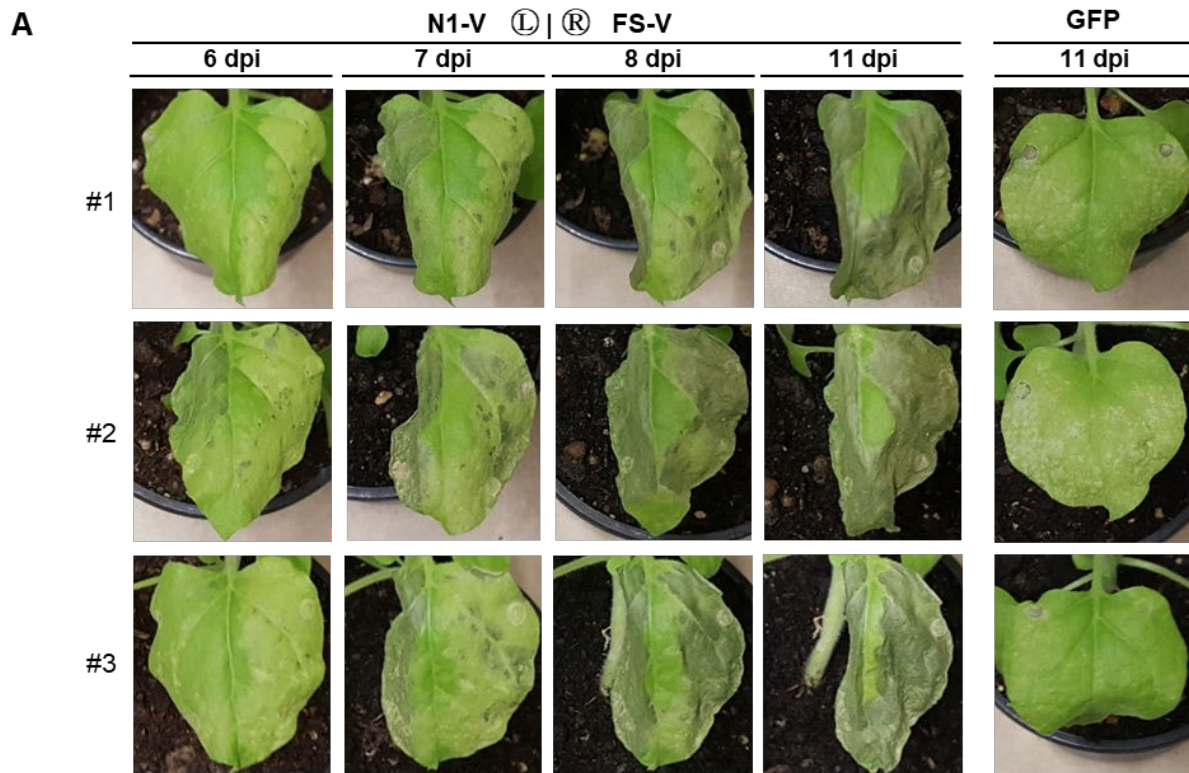


Fig. 25 Transient overexpression of *NIMIN1-Venus* and *FS-Venus* in *N. benthamiana Pro-1533PR-1a:GUS* plants. (A) Phenotype of infiltrated *N. benthamiana* leaves. Left leaf half: *Pro35S:N1-V*; Right leaf half: *Pro35S:FS-V*. Symptom development was documented from three independent plants at 6, 7, 8 and 11 dpi. Plants infiltrated with *Pro35S:GFP* were used as a control. (B) GUS reporter gene activity measured from leaf disc extracts. Four days post infiltration two leaf discs each were stamped out from the top infiltrated leaves from three independent plants and incubated for 2 days on H₂O on 1 mM SA.

The results for transient overexpression of the N1-like proteins BP-V and FG-V and the N2-like proteins NtN2c-V and FS-V suggest that, like in the NIMIN protein family from Arabidopsis, there are differences among NIMIN proteins regarding their cell death promoting activity. The results from Arabidopsis indicate a correlation between protein accumulation and development of necrosis (Fig. 17, 18, 19). To examine if this is also the case in tobacco, protein extracts from wildtype *N. benthamiana* leaf tissue infiltrated with agrobacteria carrying the respective overexpression constructs were analyzed using immunodetection. Using the α -GFP (FL) antiserum it was observed that the tobacco NIMIN-Venus fusion proteins accumulate differentially (Fig. 26). Both N2-like proteins, NtN2c-V (Fig. 26A) and FS-V (Fig. 26B), accumulate strongly, both showing signals at 40 kDa for the full length-protein and a secondary signal at around 30 kDa. Meanwhile the N1-like proteins BP-V (Fig. 26A) and FG-V (Fig. 26B) share much lower overall accumulation. For FG-V there is a weak 40 kDa signal slightly below an unspecific signal, which most likely represents the full-length protein, while no such band is detected for BP-V. However, BP-V and FG-V share a secondary band below 35 kDa, which is stronger for FG-V, but its significance is still unclear.

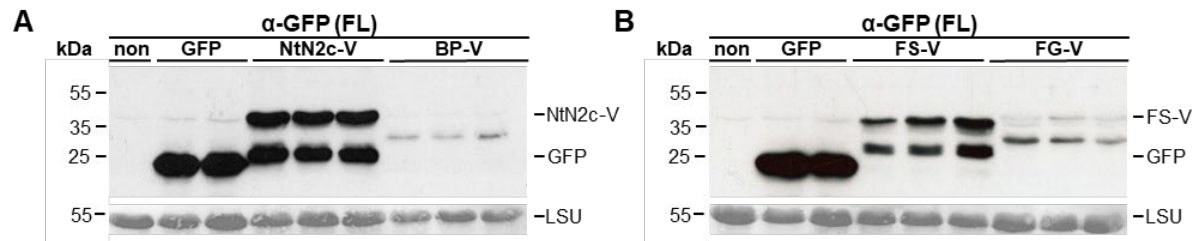


Fig. 26 Accumulation of NIMIN-Venus fusion proteins from tobacco during transient overexpression in *N. benthamiana* plants. Immunodetection of Venus fusion proteins from protein extracts prepared 4 dpi from three independent *N. benthamiana* wildtype plants, using the α -GFP (FL) antiserum. Ponceau S staining of the RuBisCO large subunit (LSU) was used as loading control. (A) Extracts from infiltrated *N. benthamiana* leaves expressing *Pro35S:NtN2c-V* and *Pro35S:BP-V*. (B) Extracts from infiltrated *N. benthamiana* leaves expressing *Pro35S:FS-V* and *Pro35S:FG-V*.

The results regarding tobacco NIMIN proteins clearly confirm the observations made for Arabidopsis NIMIN proteins. Only NIMIN proteins which accumulate strongly, N1-V and N3-V for Arabidopsis and NtN2c-V and FS-V for tobacco, clearly promote the development of cell death.

4.2.3. Phenotypic effects of overexpression of *NIMIN* genes in *N. tabacum*

Even though the establishment of SAR is not commonly associated with the development of cell death like symptoms, the transient expression of certain members of the NIMIN protein family from both Arabidopsis and tobacco in *N. benthamiana* clearly revealed cell death promoting activity. These observations raised the question if NIMIN proteins may also have other functions than their regulatory effects during the defense response associated with SAR. While transient overexpression has several experimental upsides, like not affecting the host genome and not requiring regeneration of transformed cells, it only allows for the observation of gene effects during a limited period of the plant life. Constitutive overexpression can help to identify the effects of a gene product during the full life cycle of the plant and could therefore help to provide further insight into cell death promoting activity of NIMIN proteins. For this purpose, stably transformed tobacco plants containing gene constructs overexpressing Arabidopsis and tobacco *NIMIN* fusion constructs under control of the constitutively active 35S promoter from CaMV were used. These plants were monitored during their growth and PR1 protein expression was observed after chemical and biological induction over several generations.

4.2.3.1. Phenotypes of tobacco plants harboring *Pro35S:N1-Venus* and *Pro35S:N1 F49/50S*

The negative regulatory activity of NIMIN proteins on the induction of defense related genes during SAR establishment is typically mediated by their SA sensitive interaction with NPR1. To determine whether this interaction is also involved in the cell death promoting activity of N1 and is required for the development of the resulting phenotypes, N1 was compared to N1 F49/50S. The N1 F49/50S mutant contains a mutation in the strongly conserved DXFFK motif, one of the two protein-protein interaction domains associated with NPR1 binding. Here the two Phe residues (Phe-49 and Phe-50) are exchanged for Ser which was previously shown to prevent interaction between N1 F49/50S and AtNPR1 [Weigel *et al.*, 2005]. To ensure that N1 F49/50S is indeed unable to interact with NPR1 proteins a quantitative yeast two-hybrid assay was used (Fig. 27). Indeed, a Gal4BD fusion of N1 F49/50S, unlike N1, is unable

4. Results

to interact with GAL4AD fusions of AtNPR1 or NgNPR1, confirming the observations by Weigel *et al.* Additionally, mutation in the EDF motif (N1 E94A D95V) [Masroor, 2013], which mediates the interaction between N3 and NPR1 has no effect on the interaction between N1 and NPR1 proteins indicating the DXFFK motif to be the primary NPR1 interaction site for N1.

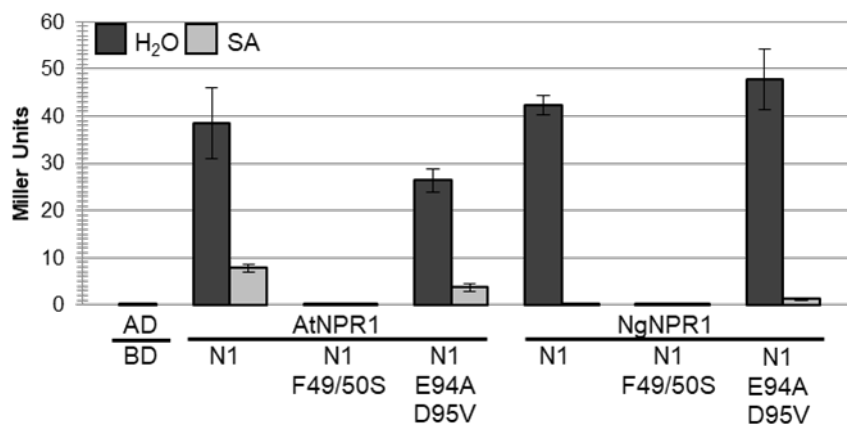


Fig. 27 Interaction of NIMIN1 mutants in the DXFFK and EDF motifs and NPR1 proteins in yeast. Quantitative Y2H assay for interaction of GAL4BD fusion proteins of N1, N1 F49/50S and N1 E94A D95V with GAL4AD fusions of AtNPR1 and NgNPR1. The assays were performed under standard conditions in presence (light bar) and absence (dark bar) of 0.3 mM SA using three independent colonies with two replicates for each colony.

Nicotiana tabacum cv Samsun NN (SNN) plants transformed after the method described by Horsch *et al.* [1985], containing either *Pro35S:N1-V* (Line 493) or *Pro35S:N1 F49/50S* (Line 494) and a control line containing *Pro35S:GUS* (Line 492) (U. M. Pfitzner, personal communication), were used for the following experiments (Fig. 28A). The primary transformants had to be confirmed to be transgenic to select plants suitable to produce seeds. Line 492, harboring *Pro35S:GUS*, was tested for GUS expression by performing a GUS assay on protein extracts isolated from leaf tissue. As expected only extracts from line 492 plants, but not plants from lines 493 and 494 exhibit strong activity of the GUS enzyme (Fig. 28B). For line 493, immunological detection of accumulation of the N1-Venus fusion protein expressed from *Pro35S:N1-V* was performed using the α -GFP (FL) antiserum. Several plants (493-3, 13, 17, and 19) show strong accumulation of N1-V and were selected for seed production (Fig. 28C). As N1 F49/50S was not translationally fused to Venus, it could not easily be detected using the α -GFP (FL) antiserum. Therefore, genomic DNA of line 494 plants was extracted and analyzed using PCR. Unfortunately, the primer combination 35S/NOS, which bind within the 35S promoter and the NOS terminator of the *Pro35S:N1 F49/50S* gene construct respectively, yields an unspecific band pattern even in the water control with a strong band at around 700 bp (Fig. 28D). Using a 1 % agarose gel for better separation of DNA fragments revealed a second band, which is not found on the negative control, slightly below the unspecific band. This lower band corresponds to the *Pro35S:N1 F49/50S* construct and plants 494-3, 5, 6, 8, and 9, whose DNA shows strong PCR bands, were chosen for seed production.

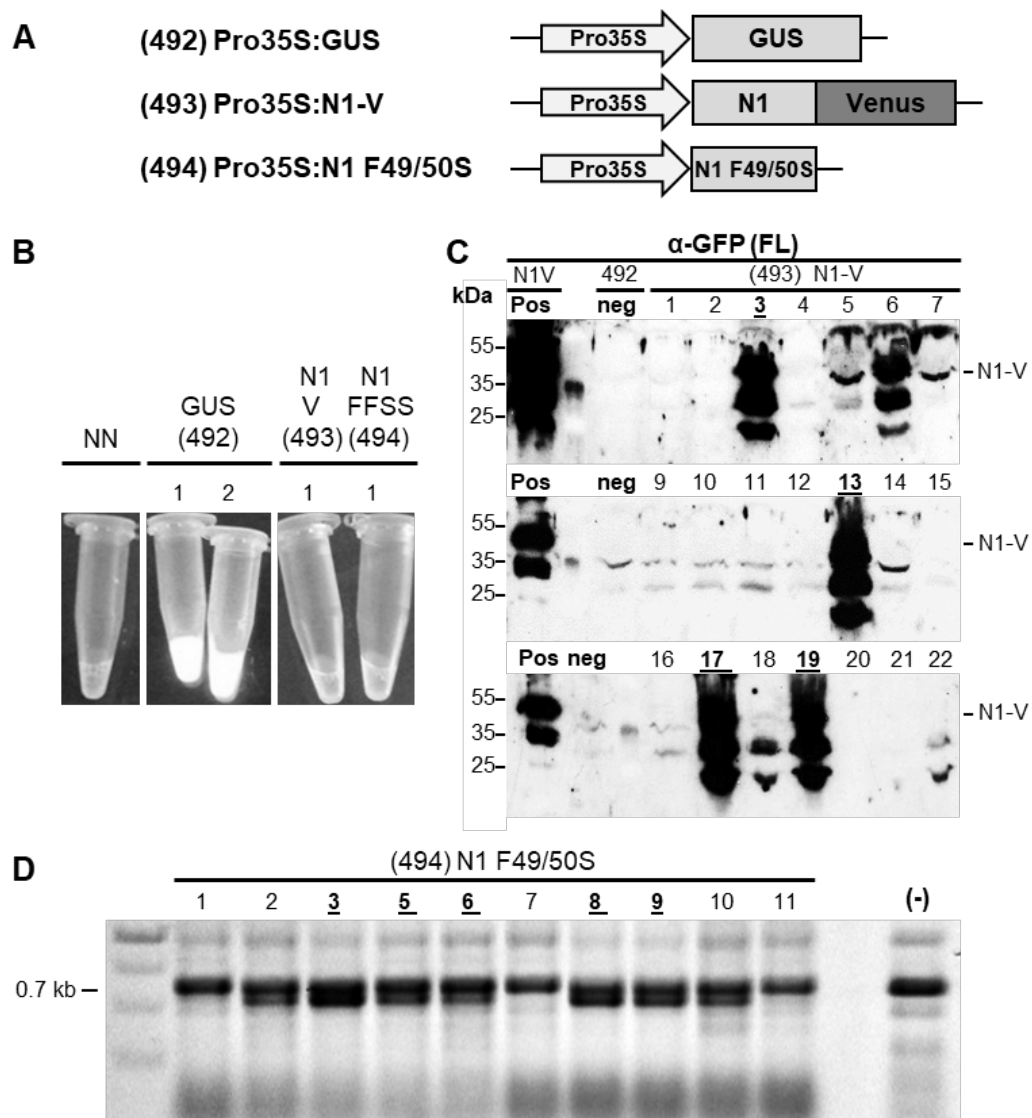


Fig. 28 Characterization of primary tobacco transformants (T0 generation) harboring *Pro35S:N1MIN1-Venus* and *Pro35S:N1 F49/50S*. (A) Schematic representation of gene constructs. *GUS*, *N1-V*, and *N1 F49/50S* were expressed under control of the 35S promoter from CaMV. (B) GUS Assay for reporter activity of the *Pro35S:GUS* transformants (492), Samsun NN and *Pro35S:N1-V* (493) and *Pro35S:N1 F49/50S* (494) plants were used as controls. (C) Immunodetection of N1-V accumulation from line 493 plants. Four leaf discs from each plant were stamped out and N1-V accumulation was detected from protein extracts using the α -GFP (FL) antiserum. A protein extract from line 492 was used as negative control. A protein extract from transient overexpression of N1-V was used as a positive control. (D) PCR amplification the transgene of line 494 using the primer combination 35S/NOS. Genomic DNA from leaf extracts was used as template. H₂O used as negative control (-). The size of the amplicons is around 700 bp.

T0 plants tested positive for containing *Pro35S:N1-V* (Lines 493-3, 13, 17, and 19) and *Pro35S:N1 F49/50S* (Lines 494-3, 5, 6, 8, and 9) were monitored until seed harvesting, but did not show phenotypic anomalies during growth in the vegetative stage. However, after development of inflorescences and self-pollination it could be observed that flowers and seed capsules from line 493 and 494 plants fall off easily. Additionally, seed capsules from those plants contain relatively few seeds when compared to the control line containing *Pro35S:GUS* (Line 492).

construct, showed some of those phenotypes, most of which are categorized as moderate to weak symptoms. T1 plants from line 494, harboring the *Pro35S:NI F49/50S* construct, are even more severely affected with over 95 % showing symptoms and over 35 % showing strong manifestation of those phenotypes with lines 494-3 and 494-9 being most strongly affected.

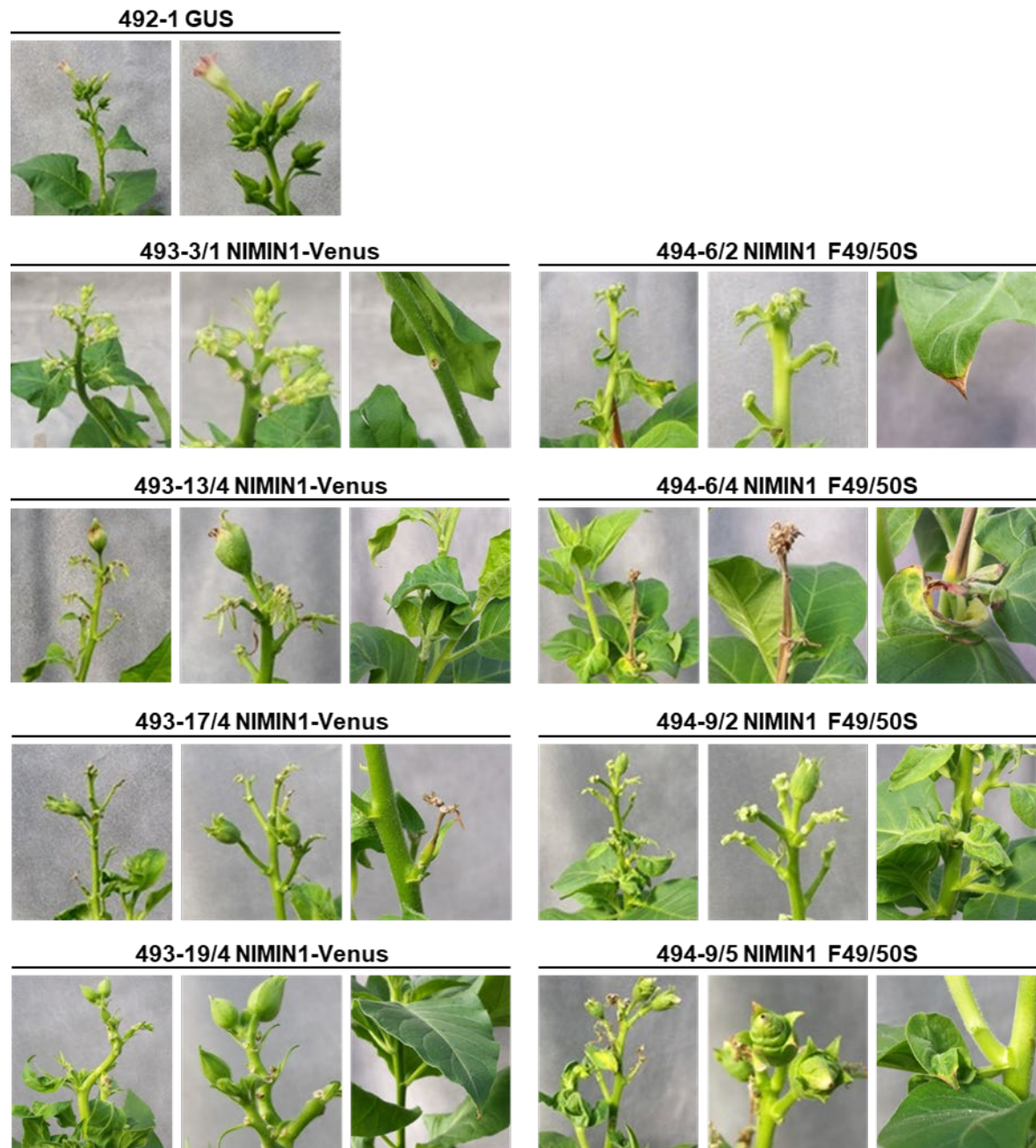


Fig. 30 Phenotype development during flower formation of T1 tobacco plants harboring *Pro35S:NIMIN1-Venus* and *Pro35S:NI F49/50S*. The phenotype of transgenic tobacco plants containing *Pro35S:NI-V* (line 493) or *Pro35S:NI F49/50S* (line 494) was monitored during flower formation and maturation of seed capsules. The plant numbers indicate the number of the T0 ancestor and the number of the respective T1 plant separated by a slash. A *Pro35S:GUS* plant (line 492) was used as a control. Pictures were chosen to represent typical phenotypes with the first picture giving a general overview of the shoot phenotype, the second picture giving detail on inflorescences and the third picture varying by plant giving detail on other anomalies.

4. Results

Table 1: Symptom severity in T1 tobacco plants overexpressing *NI-Venus* or *NI F49/50S*

Transgenic line	# of plants	Weak symptoms	Moderate symptoms	Strong symptoms
<i>493 Pro35S:NI-V</i>				
493-3	6	2	2	0
493-13	8	0	3	1
493-17	8	1	4	1
493-19	8	1	3	0
Total	30	4	12	2
		13 %	40 %	7 %
<i>494 Pro35S:NI F49/50S</i>				
494-3	10	6	4	0
494-6	8	3	1	4
494-9	15	4	2	8
Total	33	13	7	12
		39 %	21 %	36 %

When compared to the T0 generation of *Pro35S:NI-V* and *Pro35S:NI F49/50S* plants, the T1 yielded even fewer seeds after self-pollination with many seed capsules being empty or necrotic. While the plants 493-13/3, 493-19/3 and 493-19/4 yielded enough seeds for further experiments in the T2 generation, plants belonging to the 494 lines did not provide enough seed material for experimental procedures.

To gain further insight into the development of these phenotypes, plants of the T2 and T3 generations were monitored for the emergence of similar symptoms as observed in the T1 generation. Seeds from 493-13/3, 493-19/3 and 493-19/4 were sown onto selective agar plates containing Kan incubated in a light cabinet for four weeks until after germination. As observed for the T1 generation, there was only a small number of Kan sensitive seedlings in the T2 generation, indicating that most seeds contain the transgene. The seedlings were then grown in seed trays until reaching a sufficient size. T2 plants of all three lines harboring the *Pro35S:NI-V* construct showed similar symptoms as those observed in the T1 generation, most prominently necrotic seed capsule stems and side shoots, as well as deformed leaves with necrotic lesions at the tips or the center (Fig. 31A). Interestingly none of the symptoms classified as strong were observed in those plants while leaf deformations, ranging from sharp bends in the leaf blade to discolored patches of tissue and narrow and asymmetric leaf blades, appeared even more common than in T1 plants with line 493-19/4 being most strongly affected (Fig. 31B).

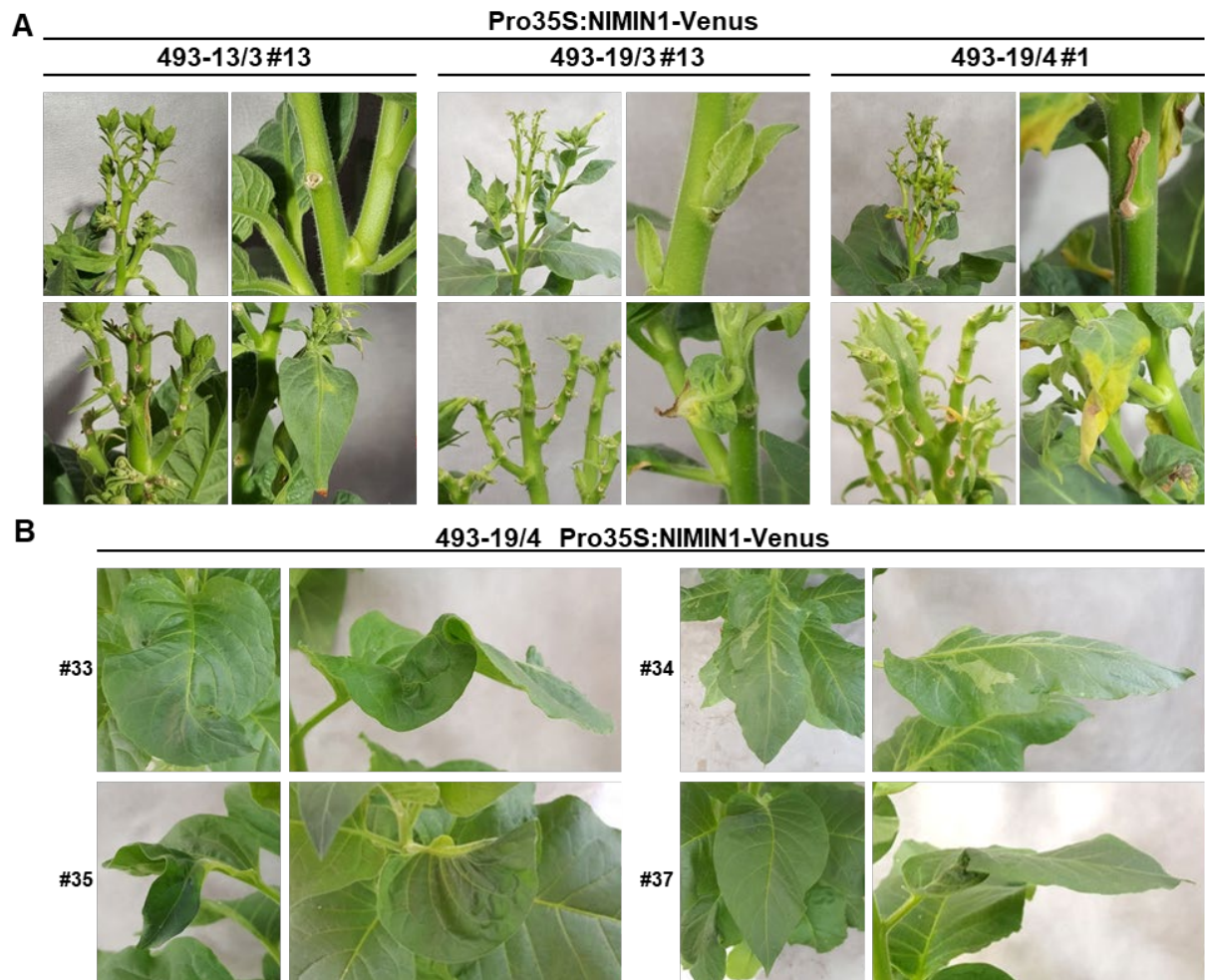


Fig. 31 Phenotype development during flower formation of T2 tobacco plants harboring Pro35S:NIMIN1-Venus. Phenotype of transgenic tobacco plants containing *Pro35S:NI-V* (lines 493-13/3, 19/3, and 19/4). (A) Overall phenotype of N1-V transgenic plants monitored during flower formation and maturation of seed capsules. Pictures were chosen to represent typical phenotypes. (B) Leaf deformation phenotype observed in mature plants. Line 493-19/4 was chosen as an example.

This trend of an increase in morphological defects of the leaves was continued in the T3 generation. Fifteen plants from the T3 lines 493-13/3/1, 493-19/3/7 and 493-19/4/7 lines were monitored for those morphological studies. Plants containing the *ProPRIa:GUS* construct (Line 138-3) were used as controls. While only one control plant showed a noticeable dent in the blade of one leaf, the *Pro35:NI-V* plants showed a much higher frequency of defects, including deformed leaves with asymmetric leaf blades and in some instances a forked midrib (Fig. 32A). Four plants from line 493/13/3/1 (27 %) and seven plants from line 493-19/3/7 (47 %) were affected. As observed in the T2 generation for line 493-19/4, the descending line 493-19/4/7 showed the highest rate of leaf phenotypes, with nine out of fifteen affected plants (60 %). During maturation plants of those lines also showed a stocky stature and were much shorter than the control plants from line 138-3 (Fig. 32 C). Tobacco leaves are usually arranged in a staggered spiral pattern around the stem (Fig. 32B, line 138-3). This alternating pattern is lost in the F3 plants of the N1-V overexpressing lines with several leaves originating on the same height of the stem (line 493-19/3/1 #7 and 19/4/7 #2, 14). Additionally, some plants displayed very narrow blades covering even the petioles up to the stem (line 493-19/3/7 # 7 and 19/4/7 #2, 14).

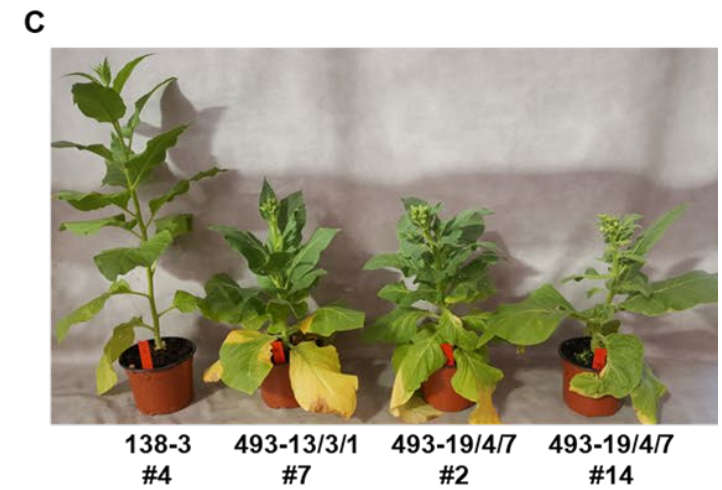
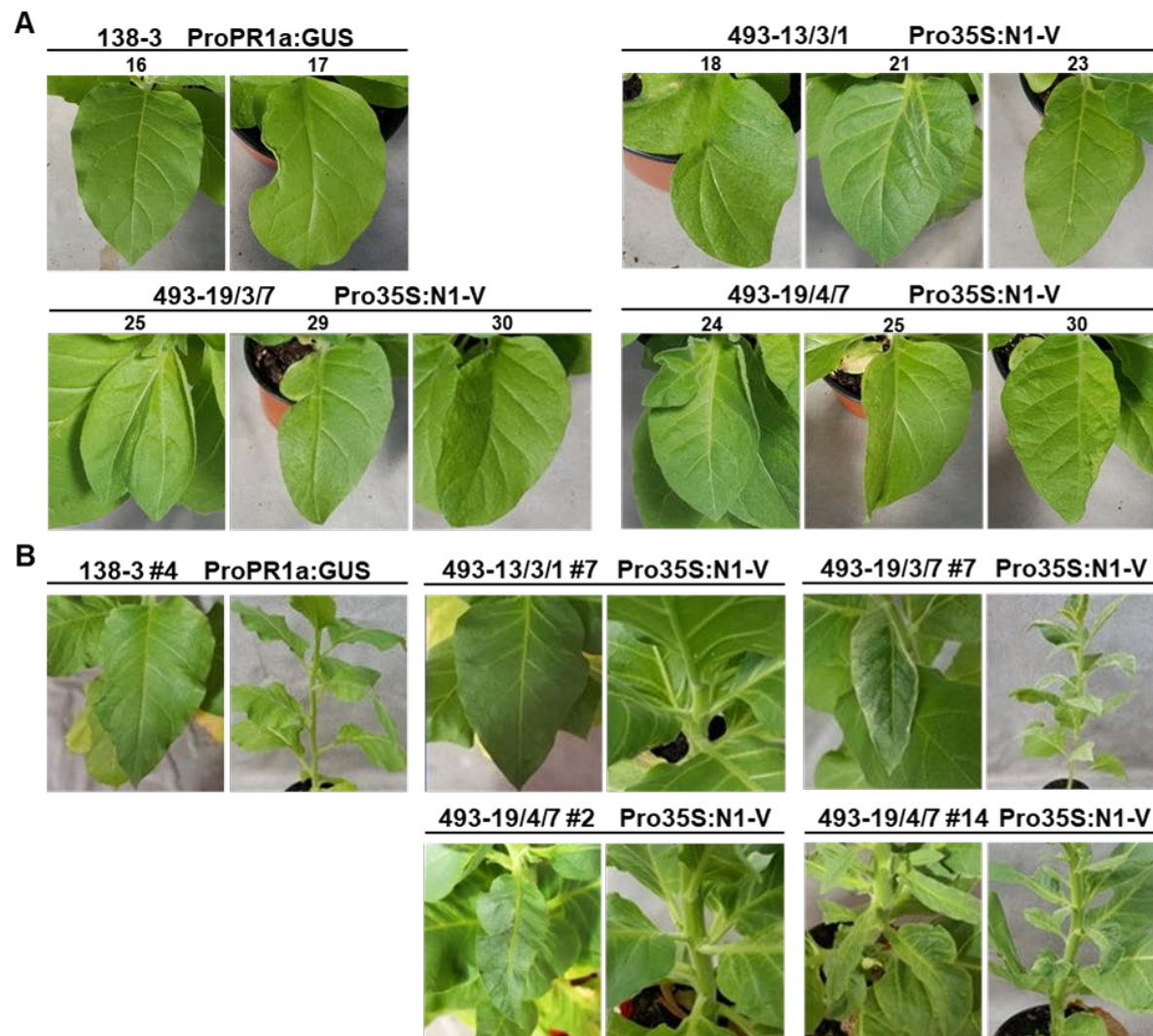


Fig. 32 Leaf morphology and growth phenotype of T3 tobacco plants harboring Pro35S:NIMINI-Venus. Phenotypes of young transgenic tobacco plants containing *Pro35S:N1-V* (lines 493-13/3/1, 19/3/7, and 19/4/7). *ProPR1a:GUS* plants (line 138-3) were used as controls. (A) Leaf anatomy of young plants. Photos were taken five weeks after repotting from seed trays. (B) Leaf anatomy and arrangement in N1-V transgenic plants. Leaves originate much closer to each other and show narrow blades often connected to the petiole. (C) Growth phenotype of N1-V transgenic plants. Plants are much shorter than controls.

Taken together, constitutive overexpression of *NI-V* and *NI F49/50S* in transgenic plants leads to the development of interesting phenotypes most often involving leaf anatomy and flower development, which coincide with low seed production during the reproductive phase.

4.2.3.2. Effects of *NI-Venus* and *NI F49/50S* overexpression on PR1 accumulation in *N. tabacum*

As shown before (see section 4.2.1.), transient overexpression of *NI-Venus* in *N. benthamiana* results in strong repression of the *PR1a* promoter and significantly reduces the expression of the *GUS* gene from the *Pro-1533PR-1a:GUS* reporter construct. To determine how the constitutive overexpression of NIMIN proteins can affect the accumulation of PR1 proteins in transgenic tobacco plants, the same transgenic lines from section 4.2.3.1. were used.

Leaf discs from several plants from the *NI-V* overexpression lines 493-3, 13, 17 and 19, as well as the *NI F49/50S* overexpression lines 494-3 and 494-9 were incubated for three days on 1 mM SA to allow chemical induction of the *PR1* promoter. Leaf discs from plants from the *GUS* overexpression line 492 were used as controls. Protein extracts from leaf discs were analyzed for accumulation of PR1 proteins by immunodetection using the α -PR1a antiserum (Fig. 33).

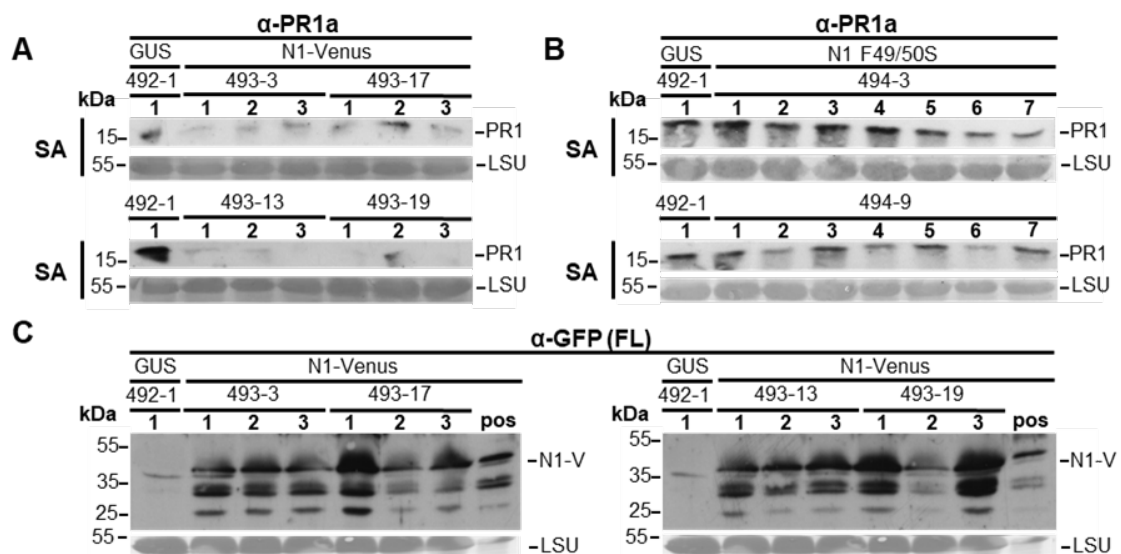


Fig. 33 Accumulation of PR1 proteins after SA mediated induction in T1 tobacco plants harboring *Pro35S:NIMINI-Venus* and *Pro35S:NI F49/50S*. Immunodetection from protein extracts prepared from transgenic T1 plants containing *Pro35S:NI-V* (Line 493, A,C) or *Pro35S:NI F49/50S* (Line 494, B). Plants containing *Pro35S:GUS* (Line 492) were used as controls. Ponceau S staining of the RuBisCO large subunit (LSU) was used as loading control. (A) and (B) Immunodetection of PR1 accumulation. Four leaf discs from each plant were incubated on H₂O or 1 mM SA for 3 days and PR1 accumulation was detected from protein extracts using the α -PR1a antiserum. (C) Immunodetection of N1-V accumulation from the same protein extracts used in A using the the α -GFP (FL) antiserum.

In the *GUS* overexpressor plants of line 492 the PR1 proteins accumulate clearly after induction by SA being visible as a 15 kDa band on the western blot. Compared to the control line, PR1 accumulation is considerably reduced in transgenic lines constitutively overexpressing N1-Venus (Fig. 33A). While this reduction is already strong in the lines 493-3 and 493-17, it appears even more pronounced in lines 493-13 and 493-19. Immunodetection using the α -GFP antiserum revealed strong accumulation of N1-Venus in all tested plants from line 493 (Fig. 33C). On the contrary the transgenic lines

overexpressing N1 F49/50S, 494-3 and 494-9 show no to only slight reduction of PR1 accumulation compared to the control.

To gain more data on N1-V mediated repression of the PR1a promoter several experiments were conducted in the T2 generation to analyze the accumulation of PR1 proteins after chemical or biological induction of SAR. Lines 493-13/3 and 19/3 were chosen because of their strong accumulation of the N1-V protein and repression of PR1 accumulation (Fig. 33A,C) while line 493-19/4 belonged to those plants exhibiting the strongest necrotic phenotypes among N1-V overexpression lines (Fig. 30). From each of those lines, leaf discs were incubated for three days on 1 mM SA or 0,3 mM BTH (Bion®). Afterwards, protein extracts were generated and analyzed for accumulation of PR1 and N1-V using immunodetection (Fig. 34). Chemical induction by both SA and BTH can induce strong accumulation of PR1 proteins in the wildtype tobacco plants used as controls. Only few of the *Pro35S:N1-V* lines show visible accumulation of the 44 kDa full-length N1-V protein but lower signals at 35 kDa and 27 kDa can still be detected. After SAR induction most of the plants with detectable accumulation of N1-V display reduced accumulation of PR1 protein, including the SA treated plants 493-13/3 #1 and #2, 493-19/3 #3; and 493-19/4 #1 and #4 (Fig. 34A), and the Bion treated plants 493-13/3 #6, 493-19/3 #7 and #8; and 493-19/4 #5, #6, #7 and #8 (Fig. 34B). However, some plants with similarly strong signals for N1-V, including the SA treated plant 493-19/3 #4 and the Bion treated plant 493-13/3 #6, show no proportionate reduction of PR1 accumulation while the BION treated plant 493-19/3 #5 shows strong reduction in PR1 accumulation without visible accumulation of N1-V.

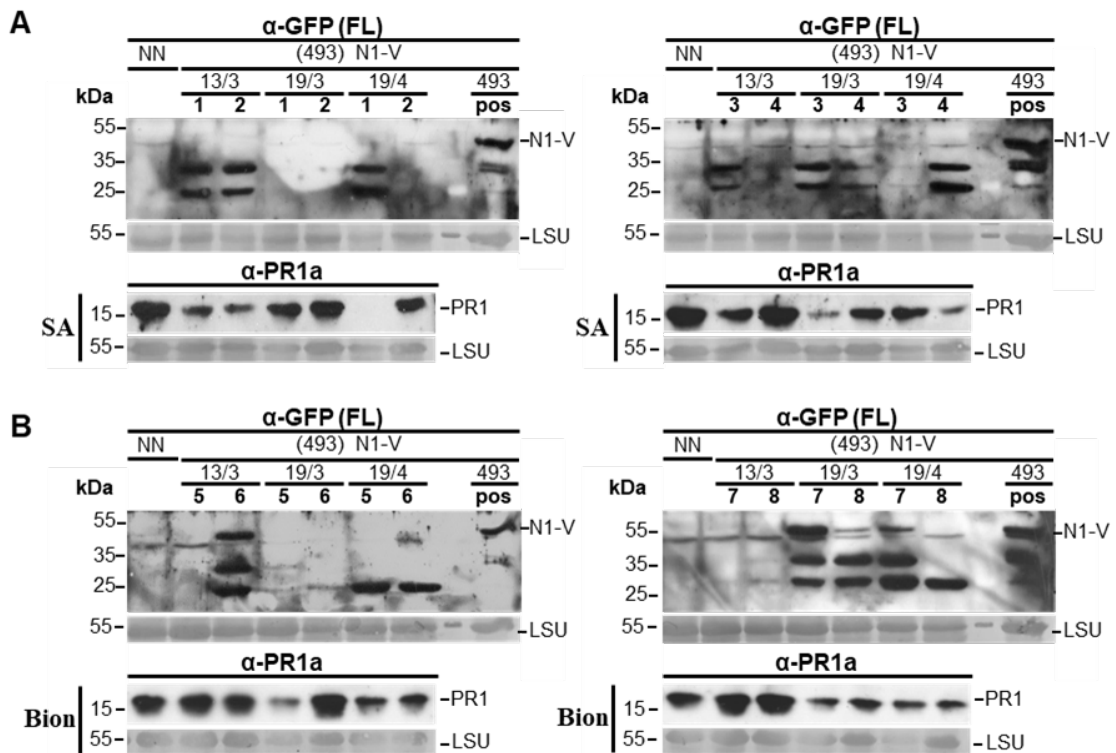


Fig. 34 Phenotype and accumulation of PR1 proteins after chemical induction in transgenic T2 tobacco plants expressing *N1-Venus*. Immunodetection from protein extracts prepared from transgenic F2 plants containing *Pro35S:N1-V*. Four leaf discs from each plant were incubated on 1 mM SA (A) or 0.3 mM BTH (Bion, B) for 3 days. Accumulation of PR1 protein was detected using the α -PR1a antiserum. Wild-type tobacco plants were used as controls for PR1 accumulation. Accumulation of N1-V protein was detected using the α -GFP (FL) antiserum. A protein extract from the T0 generation was used as a positive control. Ponceau S staining of the RuBisCO large subunit (LSU) was used as loading control.

As the results from chemical induction were rather inconclusive, the question was brought up whether repression of PR1 during actual defense responses after pathogen infection behaves similarly. Therefore, four plants from the transgenic lines 493-13/3, 19/3 and 19/4 were infected using TMV. Wild-type *Nicotiana tabacum* SNN plants were used as controls. After six days leaf discs with necrotic lesions were stamped out to generate protein extracts. Immunodetection of N1-V and PR1 protein accumulation was performed using the α -GFP (FL) and α -PR1a antibodies, respectively (Fig. 35). The pattern of protein bands detected for N1-V using the α -GFP (FL) antiserum matches the one observed in previous experiments with only few plants showing no detectable accumulation of N1-V (Fig. 35A). Meanwhile accumulation of PR1 proteins is strongly reduced in all infected *Pro35S:N1-V* plants, independent of N1-V accumulation, when compared to the WT control plants. While the number of necrotic lesions varied between WT controls which averaged at 224 and N1-V overexpressing plants which averaged at 113 when monitored six days post infection, the necrotic lesions on transgenic plants appeared to be larger in size. The leaves were observed for five more days and the size of the necrotic lesions was documented 11 days post infection (Fig. 35B). When compared to a size indicator (orange circle, \varnothing 8 mm) plants from lines 493-13/3, 19/3 and 19/4 with strong accumulation of the N1-V protein exhibit larger lesions with more uneven borders than the wild type control plants (Fig. 35B, upper row, marked with +). Interestingly, when compared to the lesions observed on plants without detectable accumulation

4. Results

of the N1-V protein (Fig. 35B, lower row), the lesions on plant 493-13/3 #12 and 493-19/3 #11 appear just as large. These results show that the influence of N1-V overexpression in leaf material showing HR mediated cell death is also not entirely clear.

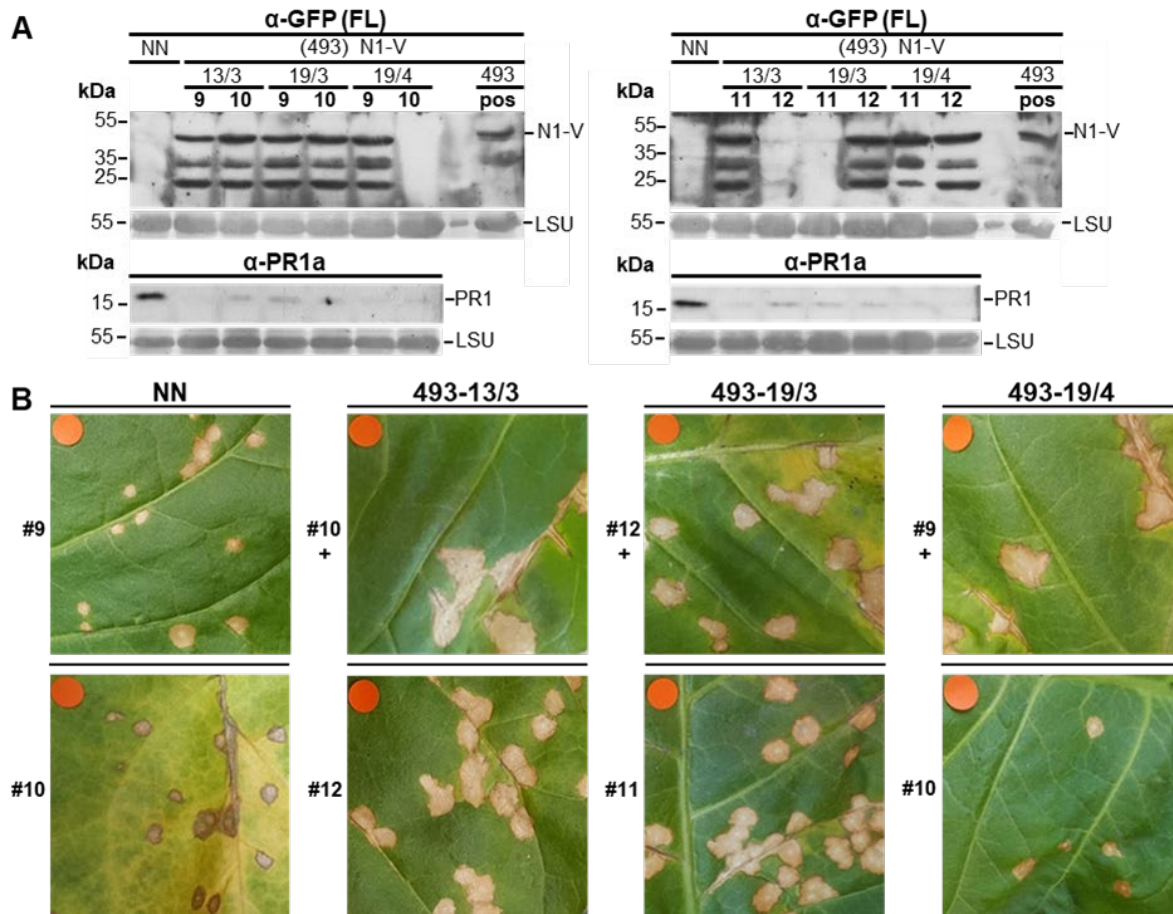


Fig. 35 Accumulation of PR1 proteins after TMV infection in transgenic T2 tobacco plants expressing *NI-Venus*. Leaf tissue from transgenic F2 plants containing *Pro35S:NI-V* was infected with TMV. *Nicotiana tabacum* SNN plants were used as controls (A) Immunodetection from TMV infected leaf tissue. At 6 dpi four leaf discs from each plant including necrotic lesions were used to create protein extracts. Accumulation of PR1 protein was detected using the α -PR1a antiserum. Accumulation of N1-V protein was detected using the α -GFP (FL) antiserum. A protein extract from the T0 generation was used as a positive control. Ponceau S staining of the RuBisCO large subunit (LSU) was used as loading control. (B) Phenotype of necrotic lesions. At 11 dpi infected leaves were documented including an \varnothing 8 mm size indicator (orange circle).

To find out if the repression of PR1 accumulation is apparent in noninfected tissue in the context of SAR establishment another TMV infection experiment was devised. Three plants each, from the transgenic lines 493-13/3, 19/3 and 19/4, were infected using TMV. Wild-type *Nicotiana tabacum* SNN plants were used as controls. Four times two nested leaf discs of different sizes were stamped out from infected leaves (outer circle \varnothing 2.0 cm, inner circle \varnothing 1.6 cm) 18 days post infection, with the inner circle containing a necrotic lesion and the outer circle containing only uninfected tissue. Immunodetection on protein extracts created from those leaf discs using the α -GFP (FL) antiserum revealed accumulation of N1-V in all plants with the usual band pattern (Fig. 36A) but weaker signal strength compared to the previous experiment (Fig. 35A). The accumulation of PR1 proteins was compared between protein extracts from the two nested leaf discs (Fig. 36B), with the inner ring consisting of HR affected tissue and the outer ring consisting of uninfected tissues where PR genes are induced during SAR

establishment. PR1 accumulation is not significantly reduced in protein extracts of HR affected tissue when compared to the *N. tabacum* SNN control plants, with only plant 493-19/3 #24 showing a visibly weaker signal which, however, can also be attributed to lower overall protein levels apparent in the Ponceau S staining used as loading control. The same can be observed for PR1 accumulation in uninfected tissues. While no other plants from lines 493-19/3 and 19/4 show similar strong effects on the PR1 protein levels, plants 493-13/3 #24 and #25 show visible reduction in PR1 accumulation when compared to #23 even though all three plants show similar levels of N1-V accumulation. To ensure the induction of PR1 accumulation is not caused by the spread of TMV virus particles the same extracts were analyzed using the α -TMV-CP antiserum, which detects the coat protein of TMV (Fig. 36C). While protein extracts containing tissues with necrotic lesions show a strong signal corresponding to the 18 kDa TMV coat protein (inner ring), the same is not true for extracts from the surrounding healthy tissue (outer ring). Only seemingly healthy tissue from plant 493-19/4 #25 shows a signal for the TMV CP suggesting unprecise excision of the leaf discs.

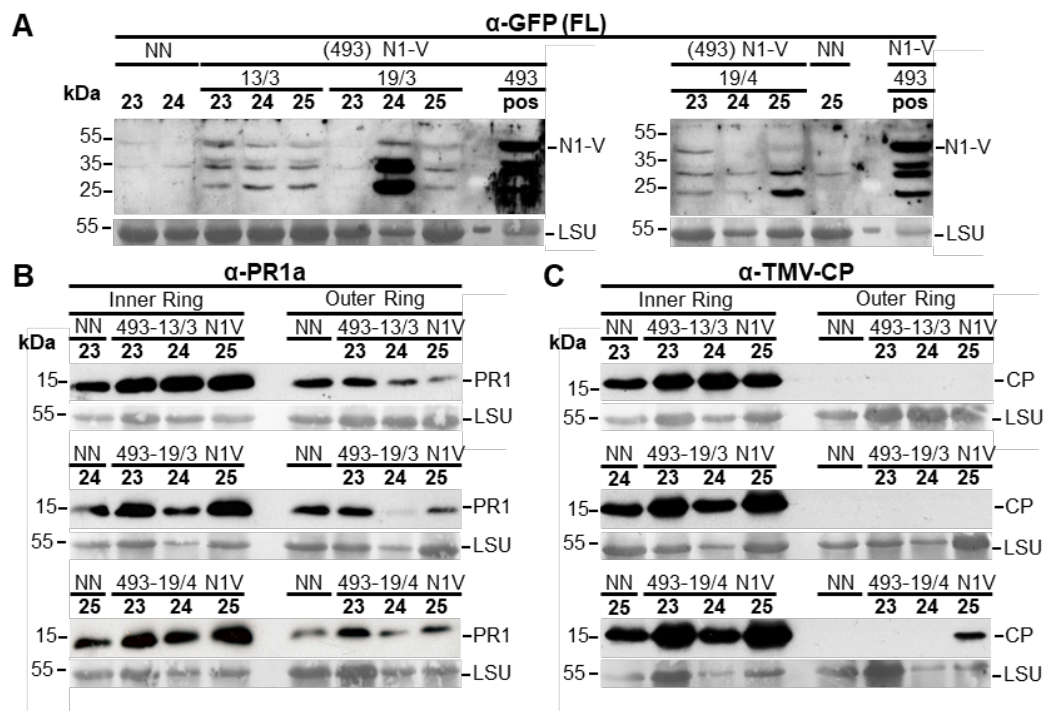


Fig. 36 Accumulation of PR1 proteins during SAR establishment after TMV infection in transgenic T2 tobacco plants expressing *NI-Venus*. Leaf tissue from transgenic F2 plants containing *Pro35S:NI-V* was infected with TMV. *Nicotiana tabacum* SNN plants were used as controls. Four nested pairs of leaf discs, with the inner one containing a necrotic lesion (\varnothing 1.6 cm), and the outer one comprising healthy leaf tissue (\varnothing 2.0 cm), were excised 18 days post infection and analyzed using immunodetection. Ponceau S staining of the RuBisCO large subunit (LSU) was used as loading control. (A) Accumulation of N1V protein was detected using the α -GFP (FL) antiserum. A protein extract from the T0 generation was used as a positive control. (B) Accumulation of PR1 proteins was detected using the α -PR1a antiserum. (C) Accumulation of TMV coat protein (CP) was detected using the α -TMV-CP antiserum.

Taken together the results from both chemical induction (Fig. 33, 34) and biological induction within the frame of HR (Fig. 35) and SAR (Fig. 36) are inconclusive. While plants overexpressing *NI-V* show a tendency to reduced accumulation of PR1 proteins, no direct correlation to the actual accumulation of the N1-V protein could be observed.

4.2.3.3. Phenotypes of tobacco plants harboring *Pro35S:NtN2c-Venus* and *Pro35S:FS-Venus*

As shown before (4.2.3.1.) overexpression of both *NI-V* and *NI F49/50S* results in the emergence of specific phenotypes affecting leaf morphology, growth, and cell death like symptoms during the flowering stage. To find out whether similar effects apply to NIMIN proteins from tobacco, two transgenic *Nicotiana tabacum* SNN lines constitutively expressing *NtN2c-Venus* (line 505) and *FS-Venus* (line 506) fusion constructs under control of the 35S promoter from CaMV were used. *NtN2c-V* and *FS-V* were chosen because of their ability to promote cell death during transient overexpression in *N. benthamiana* (see 4.2.2.) which is similar to Arabidopsis N1. Plants containing *Pro35S:Venus* (line 503) were used as controls. The primary transformants (T0 generation) were initially tested via PCR using the primer combination 35S/Venus-2 amplifying a fragment of about 550 bp for the *Pro35S:Venus* construct and about 900 bp for *Pro35S:NtN2c-V* and *Pro35S:FS-V*. For the control line, five out of six tested plants produced a PCR fragment of the right size (83 %) and in four of those the 27 kDa Venus protein band could be detected using the α -GFP (FL) antiserum (67 %) (Fig. 37). For lines 505 and 506 it was difficult to find successfully transformed and regenerated plants. For line 505 (*NtN2c-V*) only four out of nine available plants were able to produce a PCR fragment of the right size (44 %) and in only two of those (22 %) protein accumulation could be detected. For line 506 (*FS-V*) out of 26 available plants only six produced the appropriate PCR fragment (23 %) and in only four of those (15 %) protein accumulation could be detected. Furthermore, the protein signal detected from line 505 and 506 was not detected at 40 kDa as expected, but at 30 kDa corresponding to the lower band observed during transient overexpression (Fig. 26). Plants 3 and 9 from line 505 and plants 10 and 12 from line 506 were chosen to generate seeds.

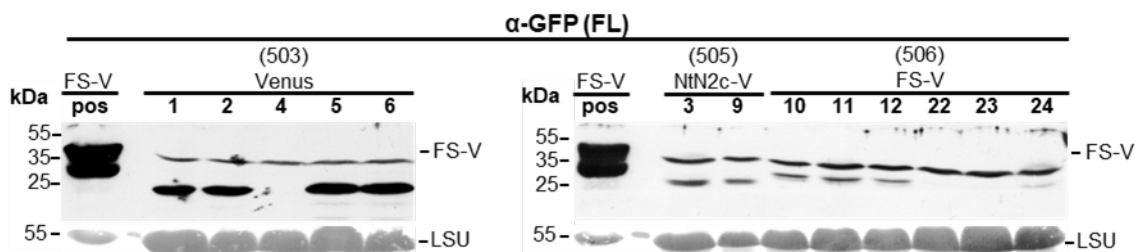
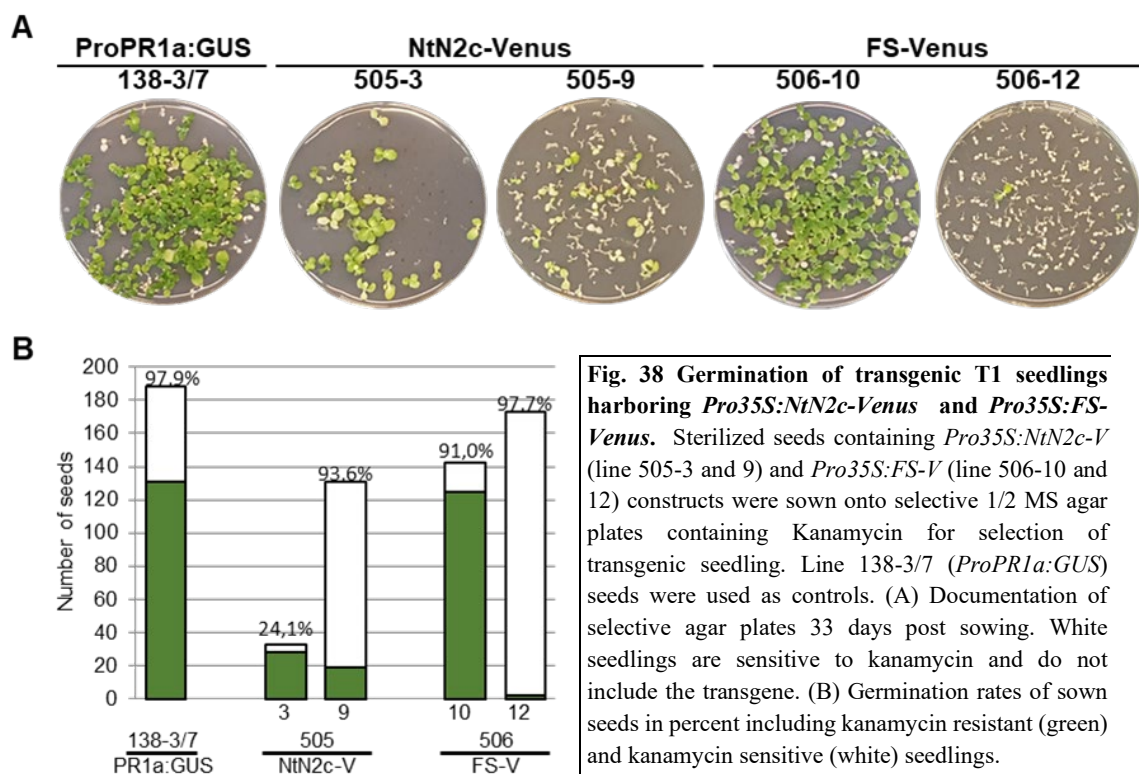


Fig. 37 Accumulation of NtN2c-Venus and FS-Venus fusion proteins in primary tobacco transformants (T0 generation).

Immunodetection of protein accumulation in primary transformants of transgenic *Nicotiana tabacum* SNN plants containing *Pro35S:NtN2c-V* (line 505) and *Pro35S:FS-V* (line 506). Four leaf discs from each plant were stamped out and protein accumulation was detected from protein extracts using the α -GFP (FL) antiserum. Protein extracts from line 503 (*Pro35S:Venus*), was used as control. Protein extracts from transient overexpression of *FS-V* was used as a positive control.

Seeds from the chosen lines were sown into selective agar plates containing kanamycin, using seeds containing a *ProPR1a:GUS* construct (line 138-3/7) as a control. The agar plates were documented 33 days post sowing (Fig. 38A) and germination rates in percent were calculated for each line from the total number of sown seeds (Fig. 38B). While over 90 % of seeds from the control line as well as both *FS-V* overexpression lines and the *NtN2c-V* overexpression line 505-9 germinated only 24 % seeds of the *NtN2c-V* line 505-3 produced seedlings. However, most seeds from line 505-9 are kanamycin sensitive indicating a lack of the co-transformed Kan resistance. Likewise, almost all germinated seeds from the *FS-V* line 506-12 are kanamycin sensitive. Only seeds from the control line and from line 506-10 mostly retain their color and can be assumed to inherit the transgene.



After five weeks of incubation in a light cabinet, the seedlings were transferred into seedling trays. Even green seedlings from line 505-9 died off after a few weeks so only seedlings from lines 505-3 and 506-10 made it to maturity. When analyzing protein extracts from those plants by immunodetection using the α -GFP (FL) antiserum, no accumulation of the *NtN2c-Venus* and *FS-Venus* fusion proteins could be detected. Interestingly, those plants display similar phenotypes as observed for the T3 generation of *N1-V* overexpressing plants, being visibly shorter than the control plants with a stocky stature (Fig. 39A). Likewise, leaves of plants from lines 505-3 and 506-10 originate much closer to each other often on the same height of the stem (Fig. 39B). Leaf morphology observed for those plants also includes asymmetric and bent, sometimes narrow blades which in some cases extend over the petiole. Together these results indicate that *NtN2c-V* and *NtFS-V* affect tobacco plants in a similar manner as *N1-V*.

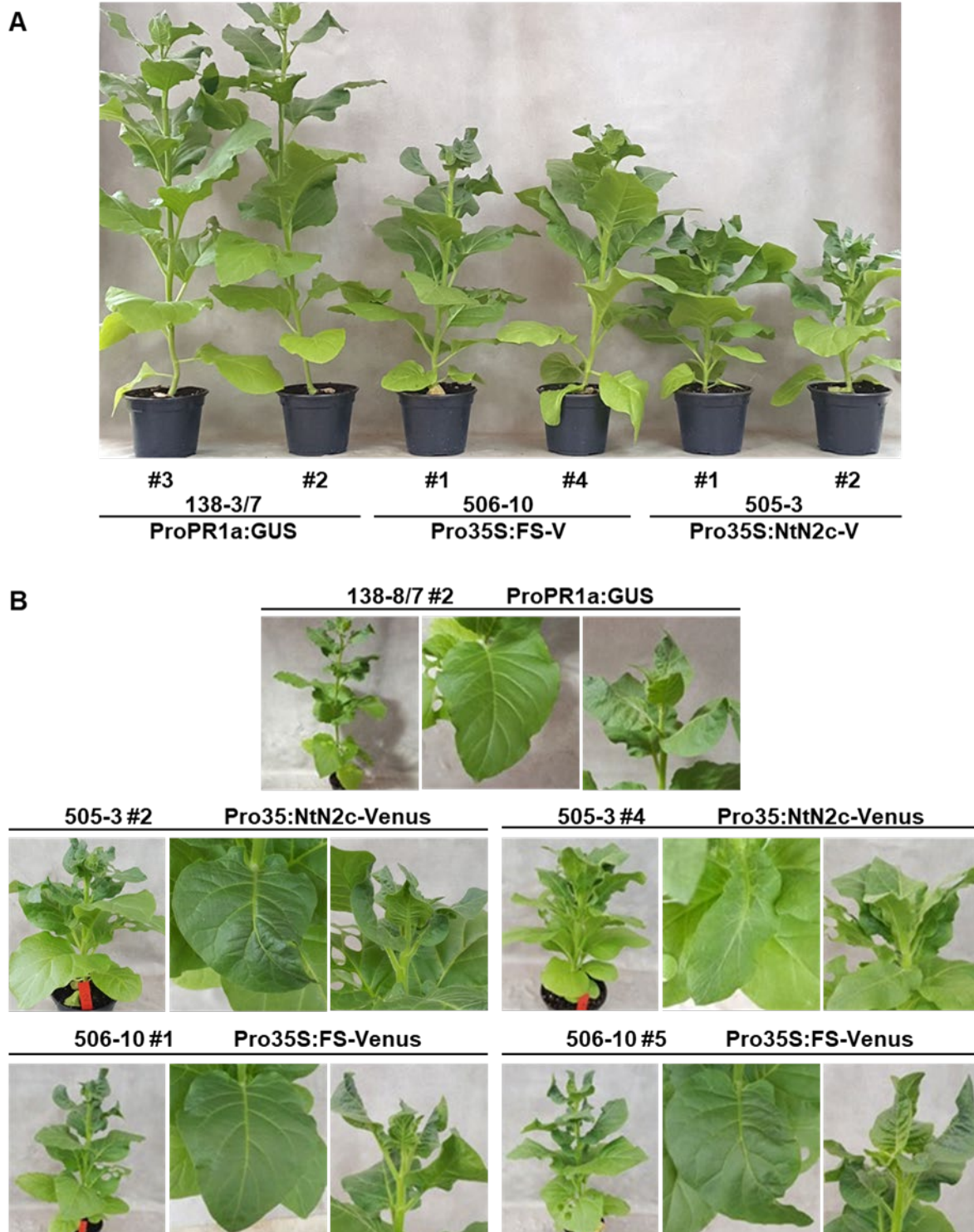


Fig. 39 Phenotype development of transgenic tobacco plants expressing *NtN2c-Venus* and *FS-Venus* in the T1 generation. Phenotype of transgenic tobacco plants containing *Pro35S:NtN2c-V* (lines 505-3) and *Pro35S:FS-V* (line 506-10). Plants containing *ProPR1a:GUS* (line 138-8/7) were used as controls. (A) Growth phenotype of *NtN2c-V* and *FS-V* transgenic plants. Plants are much shorter than control (B) Leaf anatomy and arrangement in N1-V transgenic plants. Leaves originate much closer to each other and show deformed narrow blades sometimes connected to the petiole.

4.3. Phenotypic effects of overexpression of Arabidopsis and tobacco *NIMIN* mutant genes in *N. benthamiana*

The fact that some NIMIN proteins promote cell death in transient overexpression and lead to various morphological phenotypes in transgenic plants has raised the question how they can cause these effects. As NIMIN proteins contain various conserved structural motifs it can be assumed that one or more may be involved in the emergence of those phenotypes. The general structure of NIMIN proteins has been shown in Fig. 2 for Arabidopsis and Fig. 21 for tobacco. The two most prominent types of structural motifs observed in NIMIN proteins are two different NPR1 binding domains, the DKFFK motif and the EDF motif, located in the central part of the proteins, and the C-terminal EAR motif, which is supposed to be involved in transcriptional repression [Weigel *et al.*, 2001; Kagale *et al.*, 2010]. Mutations in these motifs could help to understand the underlying mechanism behind the cell death promoting activity of NIMIN proteins during transient overexpression.

4.3.1. Analysis of NIMIN1 mutants in the NPR1 binding motifs

The two NPR1 binding motifs are differentially represented among NIMIN proteins. The DXFFK motif is located in the N-terminal moiety of N1 and N2 type proteins from both Arabidopsis and tobacco and is part of a 10 aa region with over 80 % overall similarity (Fig. 40). It has been shown previously that mutation in the DXFFK motif of N1, replacing the two consecutive hydrophobic Phe residues with Ser (F49/50S), prevents interaction with NPR1 (see Fig. 27) [Weigel *et al.*, 2005]. Meanwhile, the EDF motif is located in the C-terminal moiety of N1 type proteins from Arabidopsis and tobacco, as well as N3, comprising a highly conserved stretch of eight amino acids including the eponymous EDF sequence. This sequence is largely identical to the NH1-binding domain of the rice NIMIN homolog NRR1 [Chern *et al.*, 2005b, 2012]. The research of Ashir Masroor suggests a role of the EDF motif in the interaction between N3 and the N-terminus of AtNPR1 [Masroor, 2013].

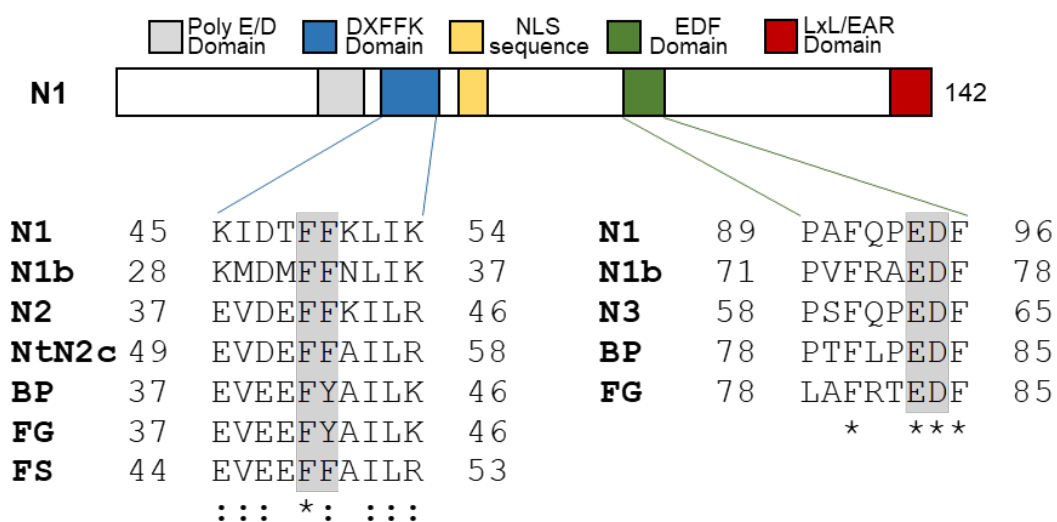


Fig. 40 Conservation of NPR1 binding domains from Arabidopsis and tobacco NIMIN proteins. Schematic representation of NIMIN proteins, using N1 as an example. The amino acid sequences of NPR1 binding domains of NIMIN proteins from Arabidopsis and tobacco are compared among each other. A star (*) indicates perfect alignment, while a colon (:) indicates strong and a period (.) indicates weak similarity.

When transiently overexpressed, *NI-V* clearly promotes the emergence of cell death in infiltrated leaf tissue. A comparison of *NI-V* with mutants in the NPR1 binding motifs should help to determine if the ability to bind NPR1 is involved in this process and required for the emergence of cell death. Therefore NIMIN-Venus fusion constructs were transiently overexpressed in leaves of *N. benthamiana*. Agrobacteria containing *Pro35S:NI-V* or *Pro35S:NI F49/50S-V* (U.M. Pfitzner, personal communication, Fig. 41A) were infiltrated into the left and right leaf halves of three independent *N. benthamiana* plants. Leaf halves overexpressing *NI F49/50S-V* exhibit visible necrosis about two days after those overexpressing *NI-V*, although with no loss in intensity (Fig. 41B). Immunodetection in this experiment was facilitated using the monoclonal α -GFP (MC) antiserum (see 2.6.2.). While the polyclonal α -GFP (FL) antiserum produces a stronger signal for GFP than for Venus, the α -GFP (MC) antiserum detects similar signals of similar intensity for both (see Appendix I), indicating that some antibodies within the α -GFP (FL) antiserum cannot bind to Venus. The immunodetection revealed an equivalent accumulation of both *NI-V* and *NI F49/50S-V* fusion proteins at 44 kDa, with the typical lower signals visible at 35 kDa and 27 kDa (Fig. 41C), indicating this delay in cell death emergence is not caused by differential protein accumulation. Additionally, despite the inability of *NI F49/50S* to interact with NPR1 (Fig. 27), overexpression of *NI F49/50S-V*, like *NI-V*, leads to repression of the PR1a promoter measured from the GUS activity mediated by the *ProPR1a:GUS* construct (Fig. 41D). These results show, that even while unable to interact with AtNPR1, the mutant *NI F49/50S-V* protein is still able to accumulate and promote the emergence of cell death, albeit with a small delay.

To determine if the EDF motif is involved in the cell death promoting activity of *NI* another mutant was used. The *NI E94A D95V* mutant was originally created by Ashir Masroor [Masroor, 2013]. In the resulting protein the negatively charged Glu and Asp residues at positions 94 and 95 are replaced by smaller and non-polar Ala and Val residues (Fig. 42A). Agrobacteria carrying a *Pro35S:NI E94A D95V-V* construct (U.M. Pfitzner, personal communication) were infiltrated into *N. benthamiana* leaf tissue, side by side with agrobacteria containing *Pro35S:NI-V*. During overexpression of *NI E94A D95V-V*, cell death emerges in the same time frame as for *NI-V*, without the delay observed for *NI F49/50S-V* (Fig. 42B). The mutant protein accumulates to the same levels as *NI-V* and displays the same banding pattern (Fig. 42C). Also, like *NI F49/50S-V*, *NI E94A D95V* displays the same repression of the PR1a promoter (Fig. 42D).

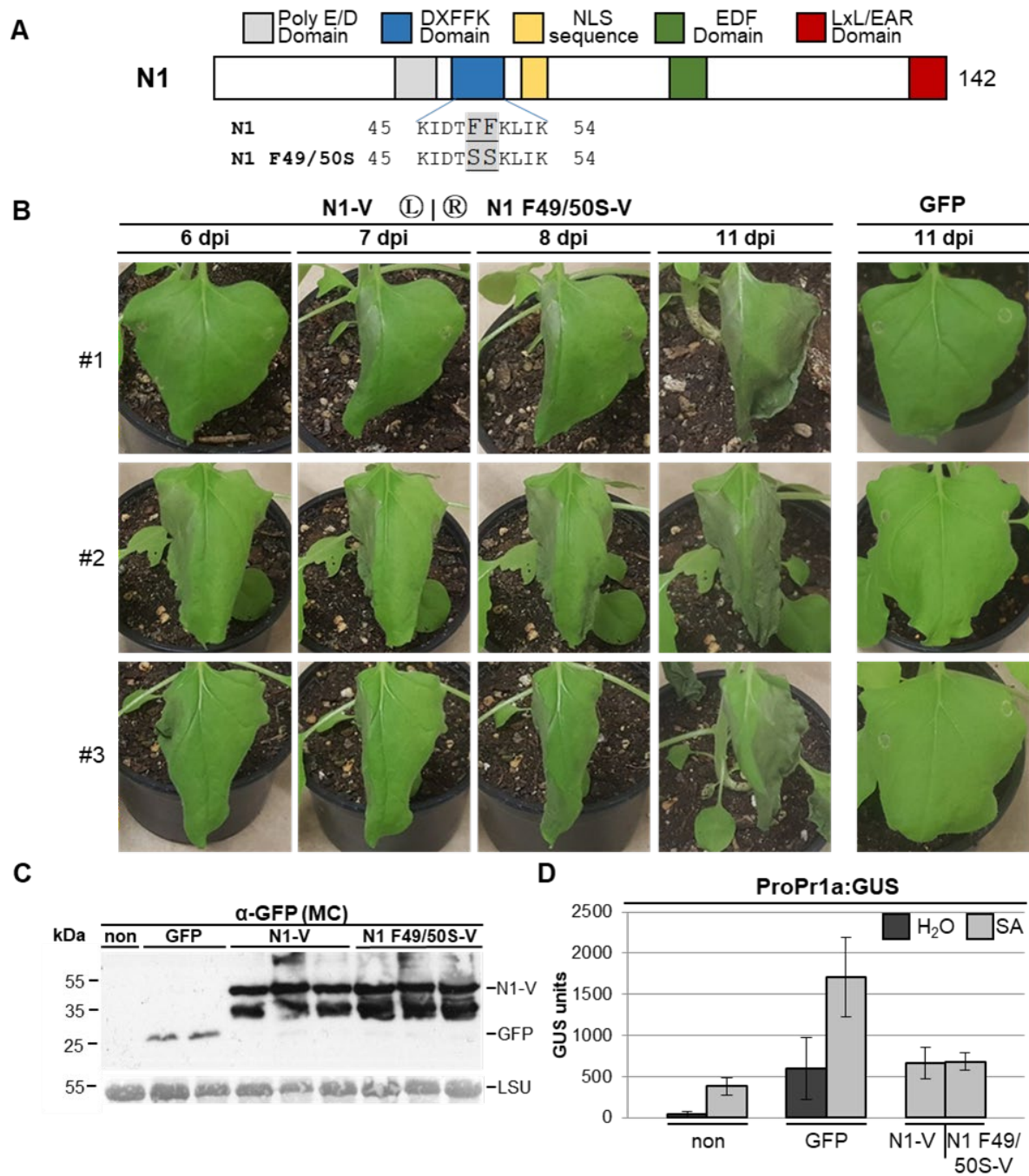


Fig. 41 Transient overexpression of *NIMIN1-Venus* and *NIMIN1 F49/50S-Venus* in *N. benthamiana Pro-1533PR-1a:GUS* plants. (A) Schematic representation of NIMIN1 indicating amino acid changes in the mutant. (B) Phenotype of infiltrated *N. benthamiana* leaves. Left leaf half: *Pro35S:N1-V*; Right leaf half: *Pro35S:N1 F49/50S-V*. Symptom development was documented from three independent plants at 6, 7, 8 and 11 dpi. Plants infiltrated with *Pro35S:GFP* were used as a control. (C) Immunodetection of Venus fusion proteins from protein extracts prepared 4 dpi from three independent plants, using the α -GFP (MC) antiserum. Ponceau S staining of the RuBisCO large subunit (LSU) was used as loading control. (D) GUS reporter gene activity measured from leaf disc extracts. Four days post infiltration two leaf discs each were stamped out from the top infiltrated leaves from three independent plants and incubated for 2 days on H₂O on 1 mM SA.

4. Results

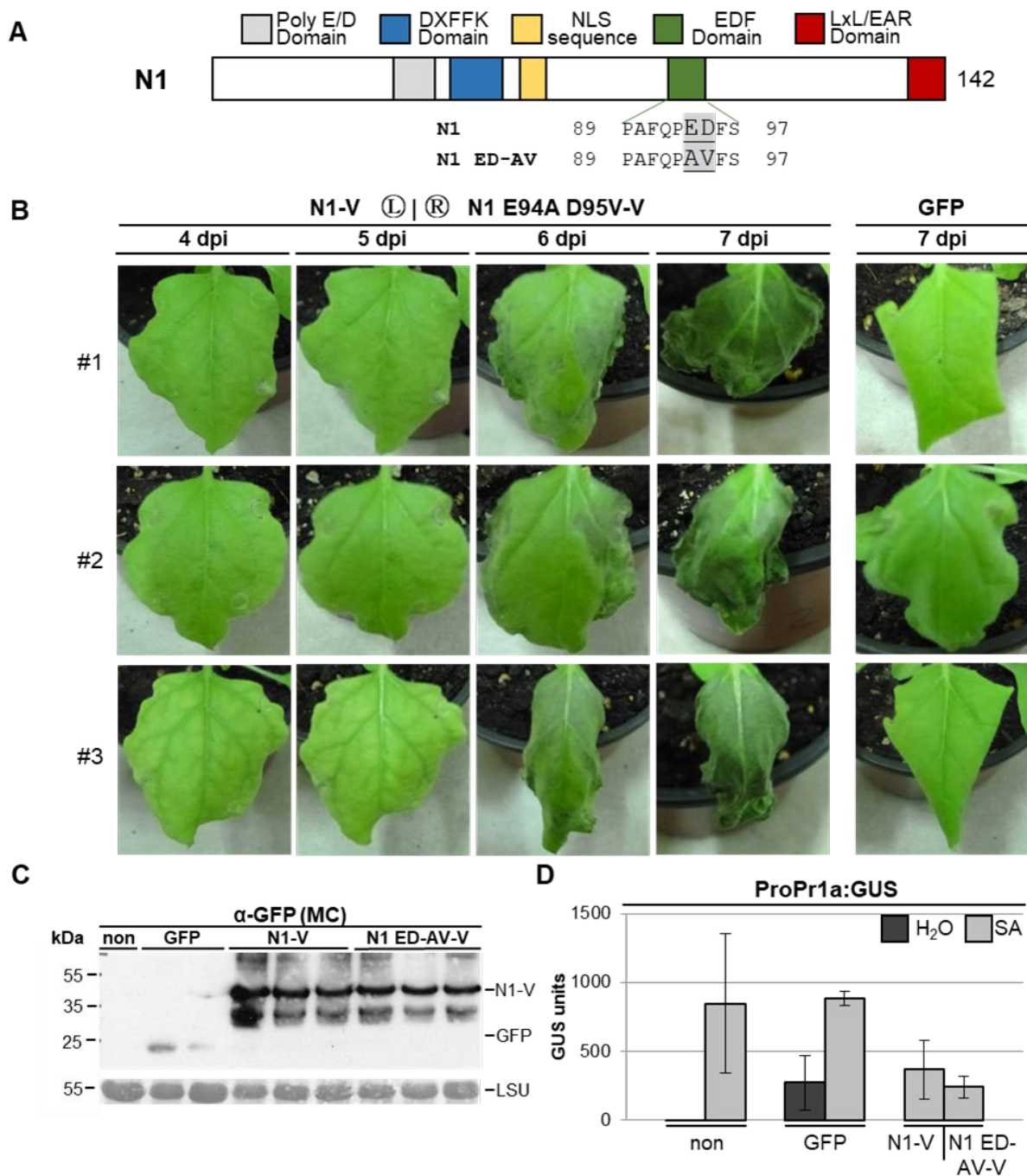


Fig. 42 Transient overexpression of *NIMINI-Venus* and *NIMINI E94A D95V-Venus* in *N. benthamiana* *Pro-1533PR-1a:GUS* plants. (A) Schematic representation of NIMIN1 indicating amino acid changes in the mutant. (B) Phenotype of infiltrated *N. benthamiana* leaves. Left leaf half: *Pro35S:N1-V*; Right leaf half: *Pro35S:N1 E94A D95V-V*. Symptom development was documented from three independent plants at 4, 5, 6 and 7 dpi. Plants infiltrated with *Pro35S:GFP* were used as a control. (C) Immunodetection of Venus fusion proteins from protein extracts prepared 4 dpi from three independent plants, using the α -GFP (MC) antiserum. Ponceau S staining of the RuBisCO large subunit (LSU) was used as loading control. (D) GUS reporter gene activity measured from leaf disc extracts. Four days post infiltration two leaf discs each were stamped out from the top infiltrated leaves from three independent plants and incubated for 2 days on H₂O on 1 mM SA.

To determine if mutation of both the DXFFK motif and the EDF motif in one protein has any additional effects on the phenotype caused by *NI-V* overexpression, a double mutant carrying the amino acid exchanges from the F49/50S and the E94A D95V mutant was created (Fig. 45A; see Appendix V). This N1 F49/50S E94A D95V mutant was tested for its NPR1 binding activity using a quantitative Y2H

assay (Fig. 43B). As expected, like the N1 F49/50S mutant, the N1 F49/50S E94A D95V is unable to interact with NPR1 in presence or absence of SA in the growth medium. Markus Späth was able to show that N1 is also able to interact with an N-terminal fragment of the transcriptional corepressor TOPLESS (TPL) using the C-terminal LxLxL type EAR motif found in all Arabidopsis NIMIN proteins [Späth, 2012]. In the same Y2H experiment as in Fig. 43B, the interaction between N1 and the N-terminal TPL 1/333 fragment is much weaker than with NPR1 (Fig. 43C). Interestingly, mutations in the NPR1 binding domains also negatively affect the N1-TPL1/333 interaction but are not sufficient to completely abolish it as the interaction strength is still considerably higher than background activity.

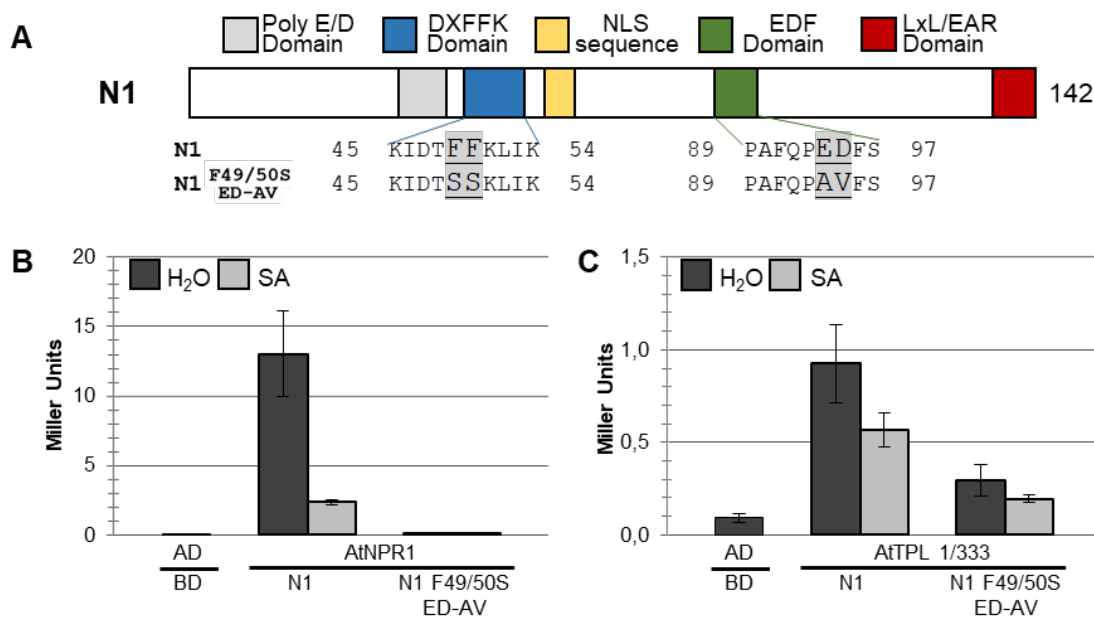


Fig. 43 Interaction of N1 and N1 F49/50S E94A D95V with AtNPR1 and AtTPL 1/333 in yeast. (A) Schematic representation of NIMIN1 indicating amino acid changes in the mutant. (B) and (C) Quantitative Y2H assay for interaction of GAL4BD fusion proteins of N1 and N1 F49/50S E94A D95V with GAL4AD fusions of AtNPR1 (B) and AtTPL 1/333 (C). Due to considerably different quantitative interaction strength, results are shown in separate diagrams. The assays were performed under standard conditions in presence (light bar) and absence (dark bar) of 0.3 mM SA using three independent colonies with two replicates for each colony.

During Agrobacterium mediated transient overexpression under control of the 35S promoter the *N1 F49/50S E94A D95V-Venus* mutant promotes cell death only slightly slower than *N1-V* (Fig. 44A). Immunodetection using the α -GFP (FL) antiserum revealed that the mutant protein accumulates to the same levels as N1-V showing the typical banding pattern (Fig. 44B). The activity of the *ProPR1a:GUS* reporter constructs is reduced during N1 F49/50S E94A D95V overexpression even though the protein is unable to interact with NPR1 (Fig. 44C).

4. Results

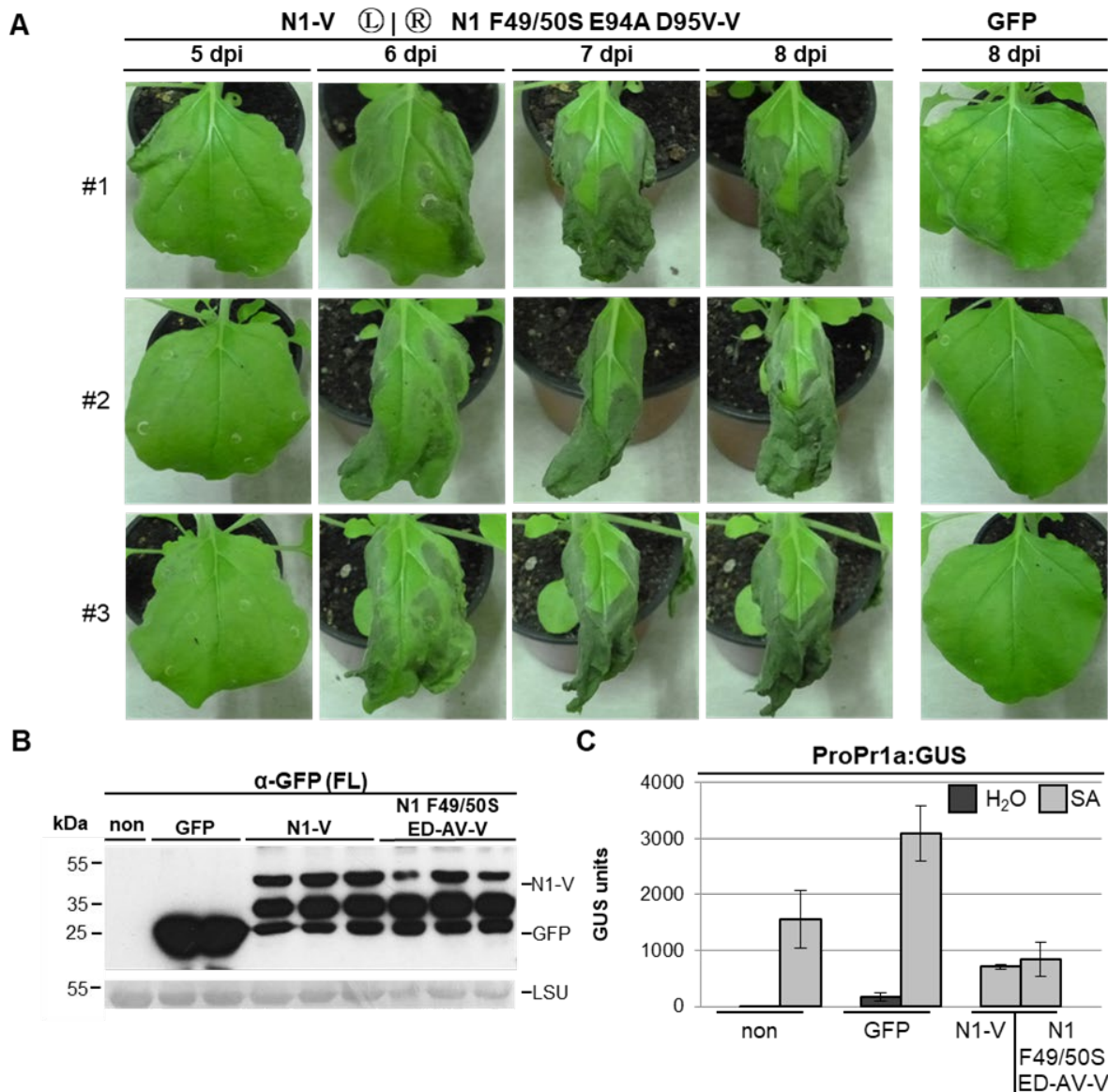


Fig. 44 Transient overexpression of *NIMINI-Venus* and *NIMINI F49/50S E94A D95V-Venus* in *N. benthamiana* *Pro-1533PR-1a:GUS* plants. (A) Phenotype of infiltrated *N. benthamiana* leaves. Left leaf half: *Pro35S:N1-V*; Right leaf half: *Pro35S:N1 F49/50S E94A D95V-V*. Symptom development was documented from three independent plants at 5, 6, 7, and 8 dpi. Plants infiltrated with *Pro35S:GFP* were used as a control. (B) Immunodetection of Venus fusion proteins from protein extracts prepared 4 dpi from three independent plants, using the α-GFP (FL) antiserum. Ponceau S staining of the RuBisCO large subunit (LSU) was used as loading control. (C) GUS reporter gene activity measured from leaf disc extracts. Four days post infiltration two leaf discs each were stamped out from the top infiltrated leaves from three independent plants and incubated for 2 days on H₂O on 1mM SA.

The results from NPR1 binding mutants in the DXFFK and/or the EDF motif show that neither mutation is sufficient to significantly affect the emergence and promotion of cell death during transient overexpression of N1-V (Fig. 41, 42, 44). The slight delay in manifestation of necrosis observed during *N1 F49/50S E94A D95V-V* overexpression (Fig. 44) coincides with a reduced interaction between N1 and TPL1/333 (Fig. 43), which makes the EAR domain the next most likely motif involved.

4.3.2. Analysis of EAR motif mutants regarding their cell promoting activity

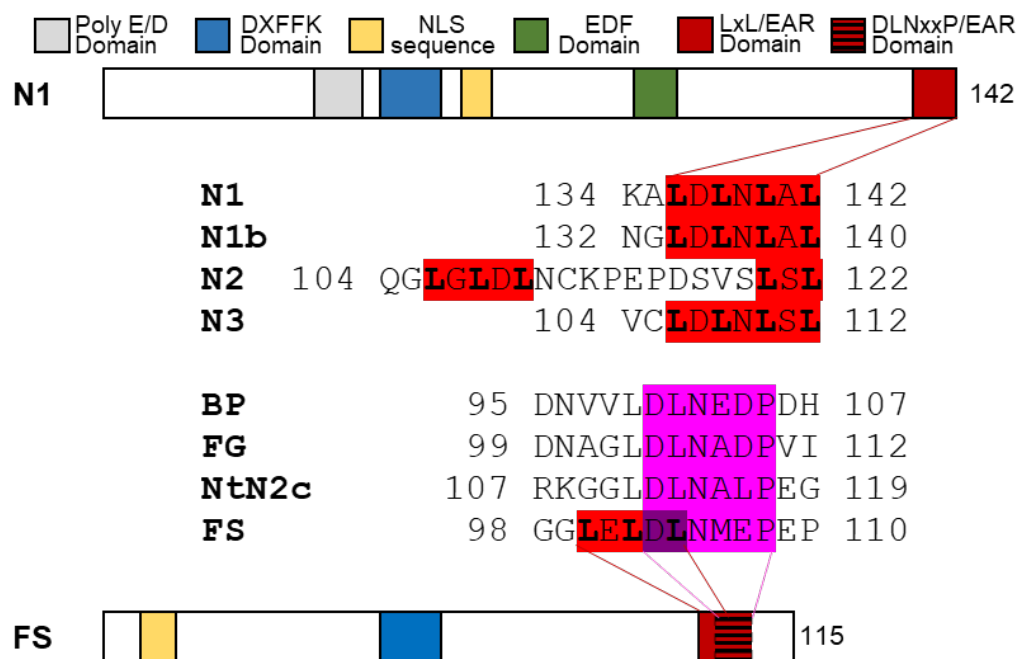


Fig. 45 EAR motifs domains from Arabidopsis and tobacco NIMIN proteins. Schematic representation of NIMIN proteins, using N1 as an example for Arabidopsis and FS as an example for tobacco. The amino acids sequences of EAR motifs of NIMIN proteins from Arabidopsis and tobacco are compared among each other. LxL type EAR motifs are highlighted in red, DLNxxP type EAR motifs are highlighted in magenta.

All known NIMIN proteins from Arabidopsis and tobacco contain an EAR motif in close proximity to their C-terminus (Fig. 45). Arabidopsis NIMIN proteins contain LxLxL type EAR motifs with N1, N1b and N3 having three LxL repeats directly at their C-terminus and N2 having a bipartite EAR motif with a single LxL repeat directly at the C-terminus and two LxL repeats from amino acid 105 to 109. Meanwhile, NIMIN proteins from tobacco typically contain a DLNxxP type EAR motif with only FS containing a hybrid motif of two LxL repeats blending into the following DLNxxP sequence. The Arabidopsis Interactome Mapping Consortium [2011] suggested an involvement of the transcriptional corepressor TPL in the SAR pathway. The N-terminal CTLH (C-terminal to LisH) domain of TPL is known to interact with LxLxL type EAR motifs like those found in several Auxin/Indole-3-acetic acid (AUX/IAA) transcriptional repressors, Pseudo Response Regulators modulating circadian transcription [Szemenyei *et al.*, 2008; Wang *et al.*, 2013; Martin-Arevallo *et al.*, 2017], as well as Arabidopsis NIMIN proteins. Direct interaction of an N-terminal fragment of TPL, encompassing the first 333 amino acids including the CTLH region (TPL 1/333), with N1 and N3 was shown in yeast. However, this interaction could not be verified for the full-length TPL protein [Späth, 2012]. To verify these results TPL and TPL1/333, as well as TPL1/196, a shorter TPL fragment encompassing the first 196 amino acids still including the CTLH region (see Appendix V), were tested for interaction with N3 using a quantitative yeast two-hybrid assay. N3 was chosen as earlier experiments revealed a stronger interaction with TPL1/333 as observed for N1. Indeed, N3 interacts with both TPL 1/333 and TPL 1/196 while there is no visible interaction with the full-length topless protein (Fig. 46A). Mutants in which the two central leucines of the LxLxLxL motif of N3 are replaced

4. Results

with alanine residues (*N3 L108/110A*) [Masroor, 2013] or deletion of the five C-terminal amino acids of N3, including three leucine residues of the EAR motif (*N3ΔEAR*) [Wöhrle, 2014] are both sufficient to abolish interaction between N3 and TPL1/333 (Fig. 46B). Interestingly, the interaction between N1 and TPL1/333 is compromised after C-terminal fusion of Venus (Fig. 46C).

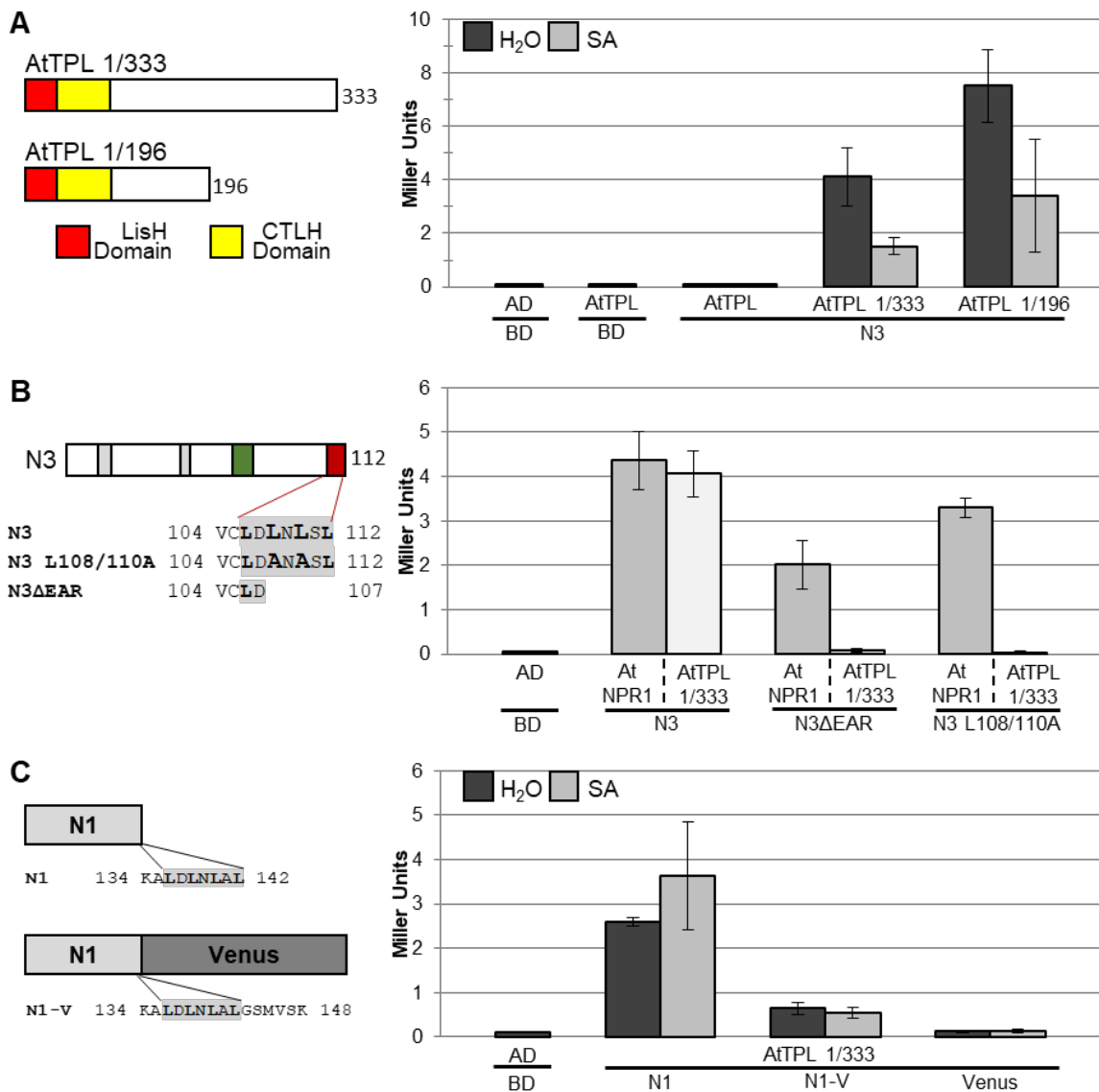


Fig. 46 Interaction Arabidopsis NIMIN proteins and AtTPL fragments in yeast. Quantitative Y2H assays for interaction of GAL4BD fusions of NIMIN proteins with GAL4AD fusions of TPL fragments. The assays were performed under standard conditions using three independent colonies with two replicates for each colony. Where indicated the assays were performed in presence (light bar) and absence (dark bar) of 0.3 mM SA. (A) Quantitative Y2H assay for interaction of N3 and AtTPL fragments of different size. (B) Quantitative Y2H assay for interaction of EAR motif mutants of N3 and AtNPR1 and AtTPL 1/333. (C) Quantitative Y2H assay for interaction of N1, N1-V and Venus with AtTPL1/333.

To analyze if the EAR motif is involved in the cell death promoting activity of NIMIN1, EAR motif mutants were analyzed during transient overexpression. Ashir Masroor produced two N1 mutants, *NI L138/140A*, in which the two central leucines of the LxLxLxL are replaced with alanine residues, and *NI 1/137 (NIΔEAR)*, in which the last five amino acids of the EAR motif are deleted [Masroor, 2013]. The *NI L138/140A* mutant (Fig. 47A) was also available as a Venus fusion construct which allowed to determine if reduced TPL 1/333 binding of N1-V has any effect on phenotype development during transient overexpression of EAR motif mutants. Agrobacteria carrying *NI* and *NI L138/140A* or their respective Venus fusions under control of the 35S promoter were infiltrated into the left and right leaf halves of *N. benthamiana* plants carrying the *ProPRIa:GUS* reporter construct, respectively.

As shown before (Fig. 16) *NI-V* overexpression promotes cell death slightly faster than *NI* with necrotic tissues becoming visible five or six days post infiltration, respectively (Fig. 47B,C). However, both *NI L138/140A* and *NI L138/140A-V* show much slower development of cell death after infiltration. Seven days post infiltration no development of necrotic tissue could be observed and even 11 days post infiltration the intensity of cell death development is strongly reduced in EAR mutants when compared to *NI* or *NI-V*.

4. Results

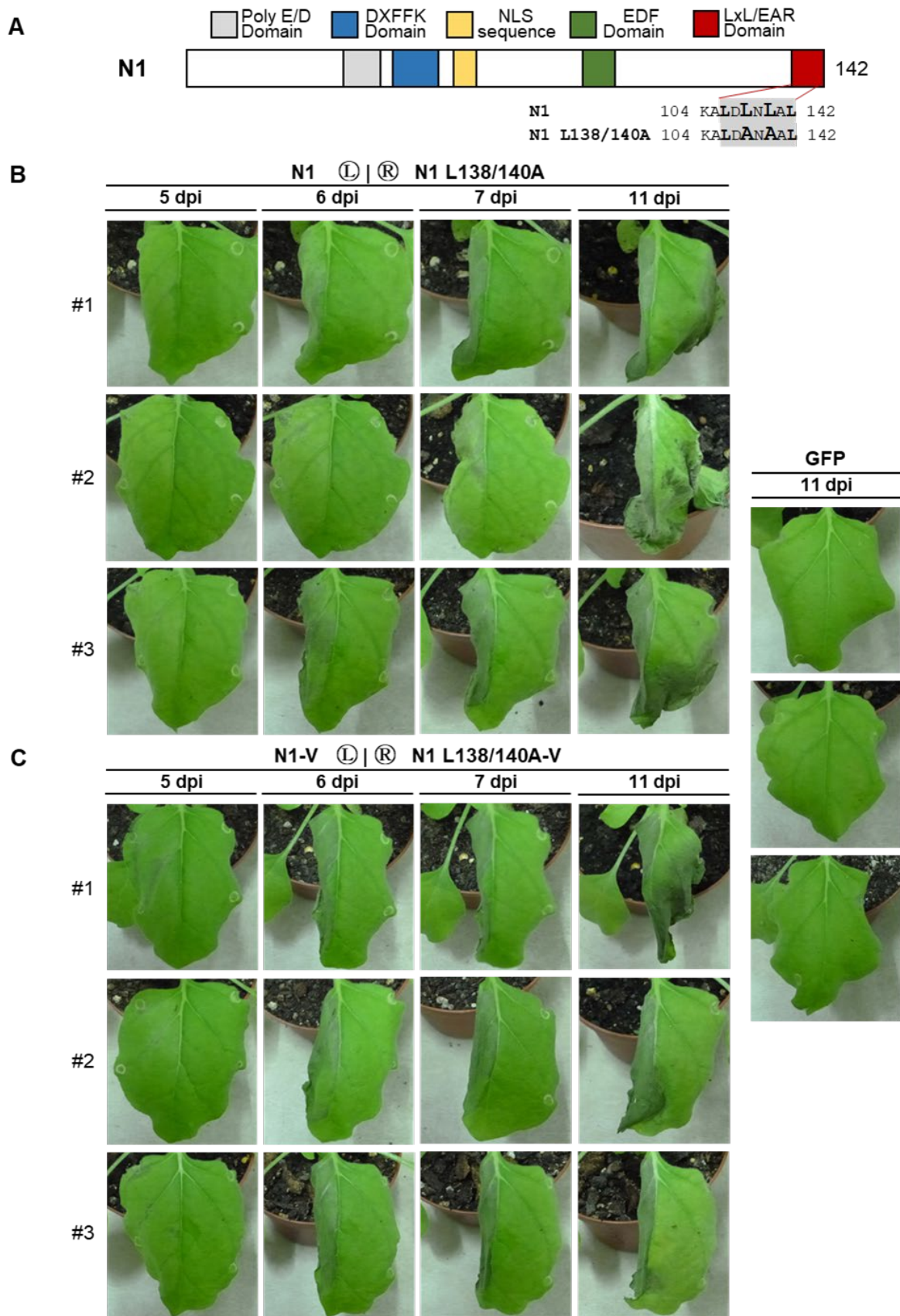


Fig. 47 Transient overexpression of *NIMINI*, *NIMINI L138/140A* and Venus fusions in *N. benthamiana* *Pro-1533PR1a:GUS* plants. (A) Schematic representation of *NIMINI* indicating amino acid changes in the mutant. (B) and (C) Phenotype of infiltrated *N. benthamiana* leaves. Symptom development was documented from three independent plants at 5, 6, 7 and 11 dpi. Plants infiltrated with *Pro35S:GFP* were used as a control. Left leaf half: *Pro35S:N1*; Right leaf half: *Pro35S:N1 L138/140A* (B), Left leaf half: *Pro35S:N1-V*; Right leaf half: *Pro35S:N1 L138/140A-V* (C).

The results from transient overexpression of Arabidopsis and tobacco *NIMIN* genes (see 4.2.1. and 4.2.2.) suggest a correlation between NIMIN protein accumulation and the manifestation of cell death. To examine whether the decreased emergence of cell death in the *NI L138/140A* mutant is actually caused by mutation in the EAR motif and not by reduced accumulation of the N1 L138/140A-V protein, protein extracts from the same plants used in Fig. 47C were analyzed by immunodetection using the α -GFP (MC) antiserum (Fig. 48A). N1 L138/140A-V accumulates to the same levels as N1-V, exhibiting the typical banding pattern at 44 kDa, 37 kDa and 27 kDa, showing that reduced emergence of cell death during *NI L138/140A-V* overexpression is not caused by a decrease in protein accumulation. Observation of SA mediated induction of the *ProPR1a:GUS* reporter construct showed a reduction in PR1a promoter activity in tissue overexpressing *NI L138/140A* and *NI L138/140A-V*. This decrease in reporter activity is only slightly weaker when compared with *NI* and *NI-V* (Fig. 48B).

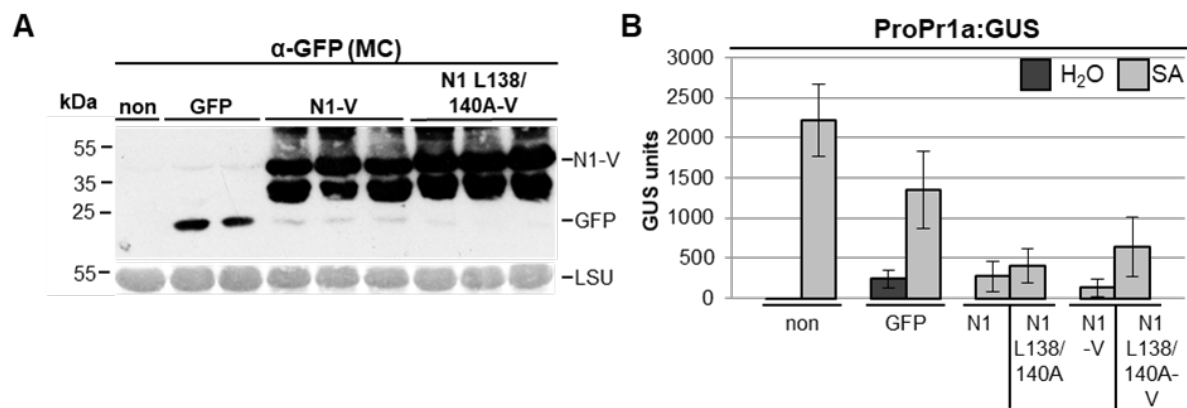


Fig. 48 Accumulation and PR1a promoter repression of *NIMIN1*, *NIMIN1 L138/140A* and Venus fusions in *N. benthamiana Pro-1533PR1a:GUS* plants during transient overexpression. (A) Immunodetection of N1-V and N1 L138/140A-V from protein extracts prepared 4 dpi from three independent plants, using the α -GFP (MC) antiserum. Ponceau S staining of the RuBisCO large subunit (LSU) was used as loading control. (B) GUS reporter gene activity measured from leaf disc extracts. Four days post infiltration two leaf discs each were stamped out from the top infiltrated leaves from three independent plants and incubated for 2 days on H₂O on 1 mM SA.

4. Results

To examine if deletion of the EAR motif has similar effects as amino acid exchanges, the *N1ΔEAR* mutant (Fig. 49A) was transiently overexpressed in *N. benthamiana* leaf tissue. As observed for *N1* *L138/I40A*, during *N1ΔEAR* overexpression cell death emerged much later than for *N1* (Fig. 49B). Similarly, *N1ΔEAR* was still able to reduce the activity of the *PR1a* promoter (Fig. 49C).

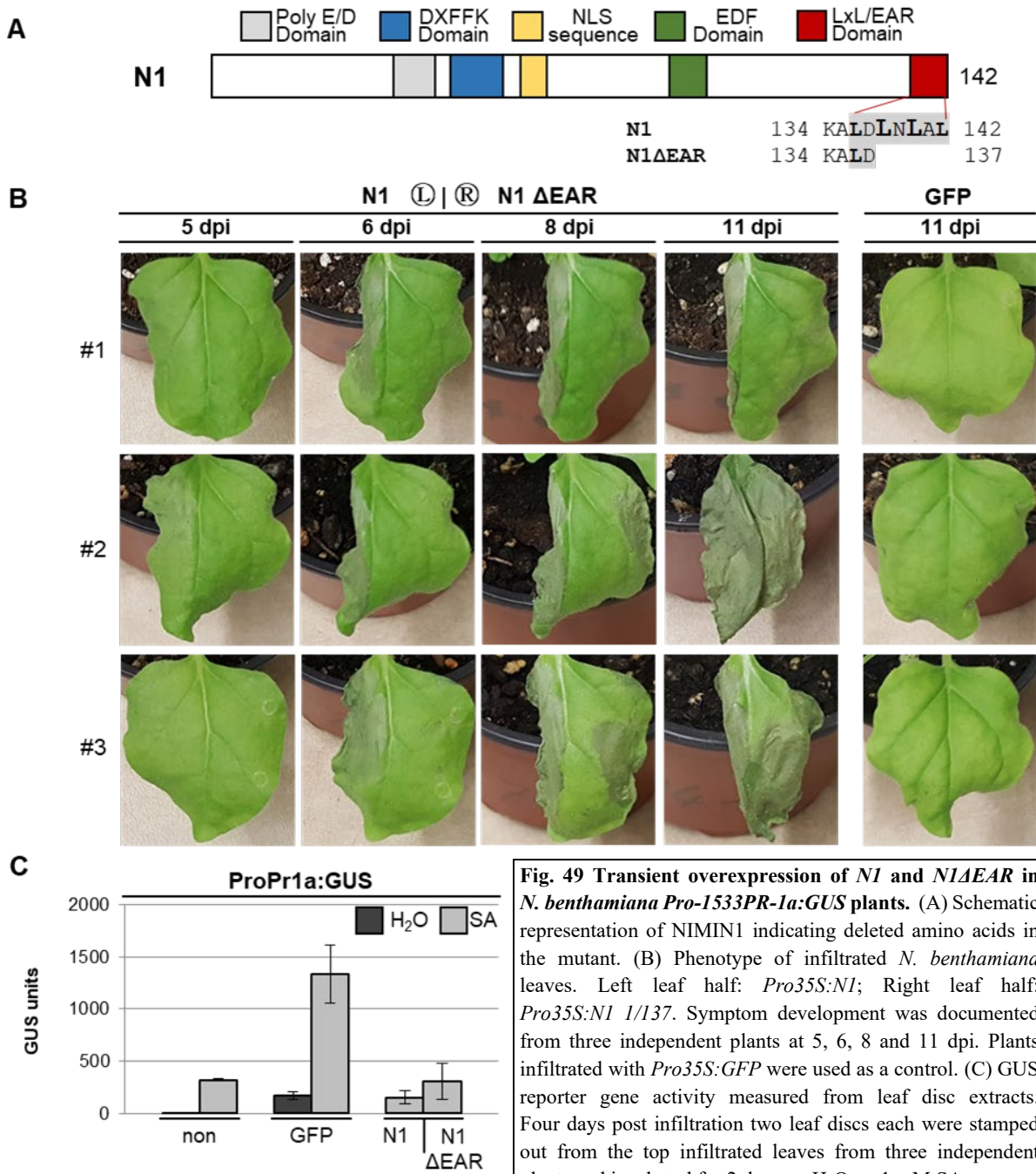


Fig. 49 Transient overexpression of *N1* and *N1ΔEAR* in *N. benthamiana* *Pro-1533PR-1a:GUS* plants. (A) Schematic representation of NIMIN1 indicating deleted amino acids in the mutant. (B) Phenotype of infiltrated *N. benthamiana* leaves. Left leaf half: *Pro35S:N1*; Right leaf half: *Pro35S:N1 I/137*. Symptom development was documented from three independent plants at 5, 6, 8 and 11 dpi. Plants infiltrated with *Pro35S:GFP* were used as a control. (C) GUS reporter gene activity measured from leaf disc extracts. Four days post infiltration two leaf discs each were stamped out from the top infiltrated leaves from three independent plants and incubated for 2 days on H₂O on 1 mM SA.

The strong deceleration of cell death emergence in both EAR motif mutants suggests that the EAR motif could play a major part of the cell death promoting activity of NIMIN proteins. As cell death also developed slightly later during transient overexpression of NPR1 binding mutants the next step was to combine both types of mutants. The resulting *NI F49/50S E94A D95V ΔEAR* mutant (*NI****; Fig. 50A; see Appendix V) contains mutations in both NPR1 binding motifs and a deletion of the six C-terminal amino acids including three leucine residues from the EAR motif. In yeast, this mutant is unable to interact with either NPR1 or the TPL1/333 fragment (Fig. 50B). Accumulation of the GAL4BD-*NI**** fusion protein was detected at slightly below the 38 kDa band of GAL4BD-*NI* using the α -GAL4BD antiserum (Fig. 50C).

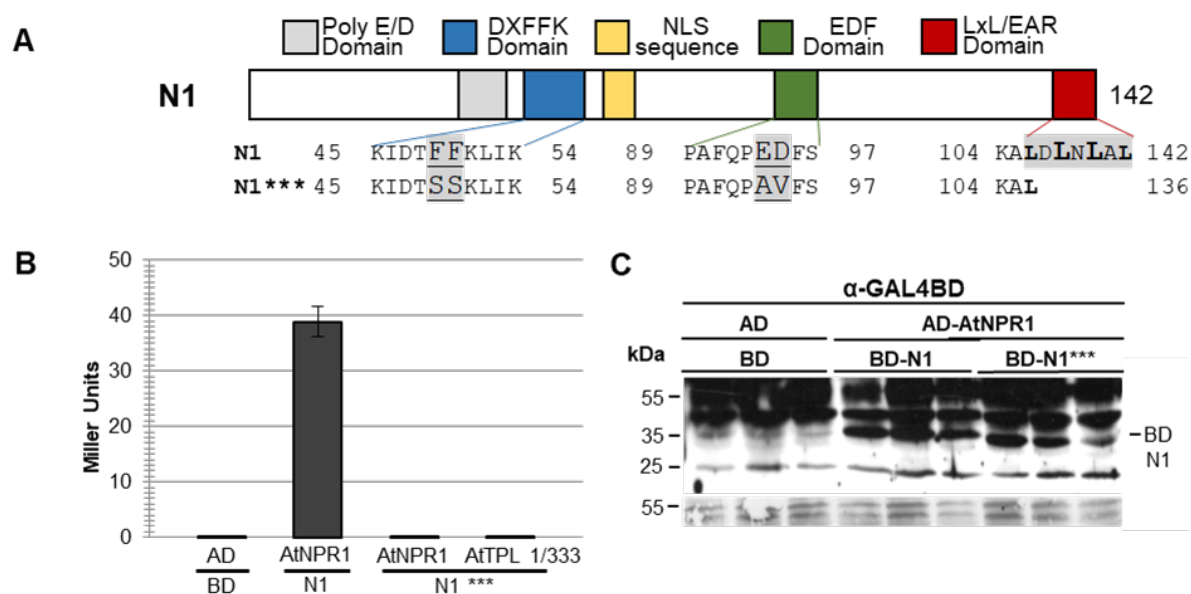


Fig. 50 Interaction of *N1 F49/50S E94A D95V ΔEAR* with *AtNPR1* and *AtTPL 1/333* in yeast. (A) Schematic representation of NIMIN1 indicating amino acid changes and deletions in the mutant. (B) Quantitative Y2H assay for interaction of GAL4BD fusion proteins of *N1 F49/50S E94A D95V ΔEAR* (*N1****) with GAL4AD fusions of *AtNPR1* and *AtTPL 1/333*. Interaction between Gal4BD-*N1* and GAL4AD-*AtNPR1* was used as a positive control. The assays were performed under standard conditions using three independent colonies with two replicates for each colony. (C) Immunodetection of GAL4BD fusion proteins from protein extracts prepared from three independent yeast liquid cultures, using the α -GAL4BD antiserum. Ponceau S staining was used as loading control.

When transiently overexpressed side by side with *NI-V* the *NI F49/50S E94A D95V ΔEAR-V* triple mutant produces no visible cell death even 10 days post infiltration (Fig. 51A). Protein extracts show the typical banding pattern and a similar accumulation of both proteins even though the loading control reveals reduced overall protein abundance in tissue overexpressing *NI-V*, probably caused by the emergence of necrosis (Fig. 51B). Surprisingly, unlike *NI-V*, the *NI F49/50S E94A D95V ΔEAR-V* mutant is unable to suppress SA mediated *PR1a* promoter activity (Fig. 51C).

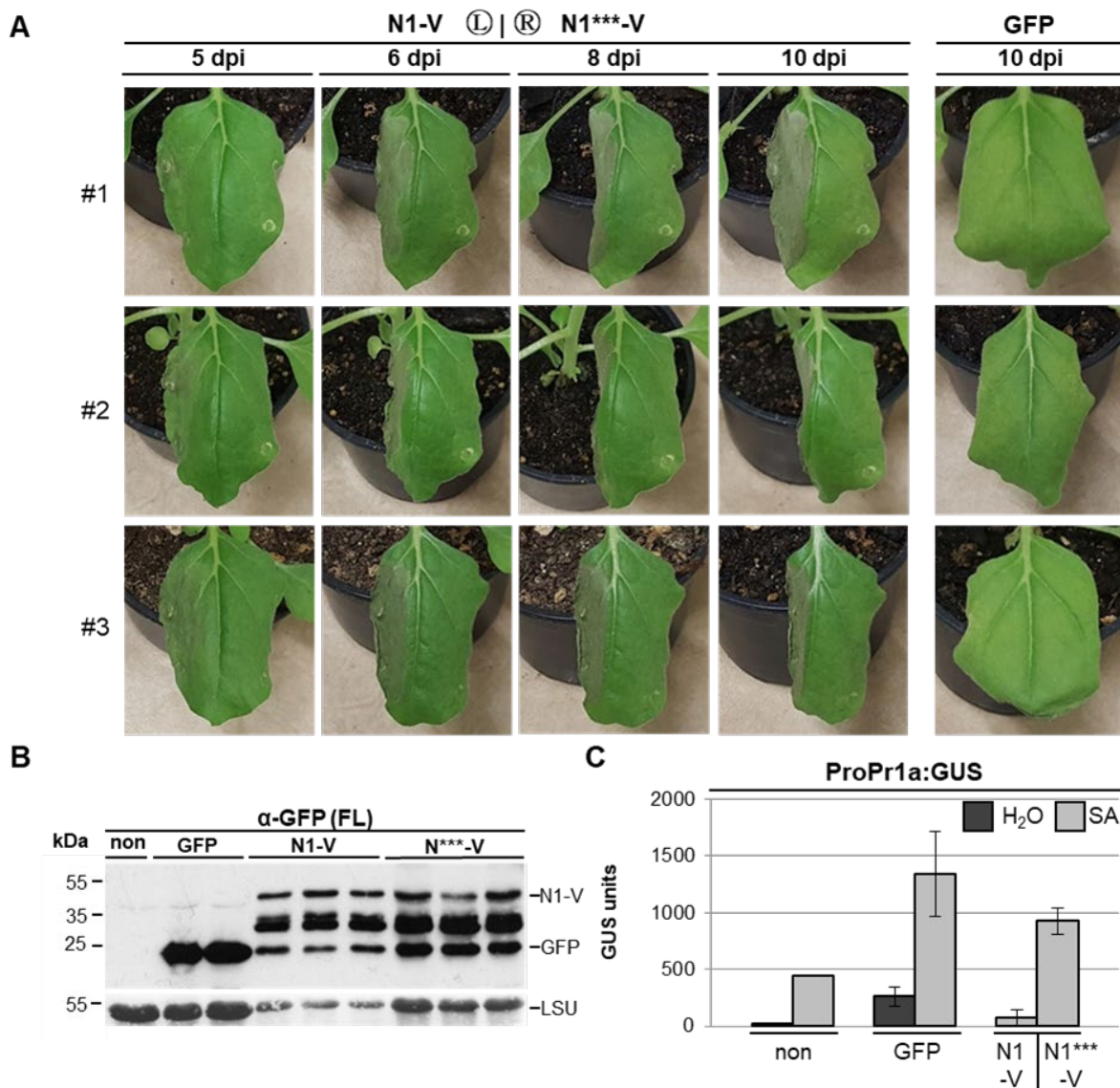


Fig. 51 Transient overexpression of *NIMINI-Venus* and *NIMINI F49/50S E94A D95V ΔEAR-Venus* in *N. benthamiana* *Pro-1533PR-1a:GUS* plants. (A) Phenotype of infiltrated *N. benthamiana* leaves. Left leaf half: *Pro35S:N1-V*; Right leaf half: *Pro35S:N1 F49/50S E94A D95V ΔEAR-V (N1***-V)*. Symptom development was documented from three independent plants at 5, 6, 8 and 10 dpi. Plants infiltrated with *Pro35S:GFP* were used as a control. (B) Immunodetection of Venus fusion proteins from protein extracts prepared 4 dpi from three independent plants, using the α-GFP (FL) antiserum. Ponceau S staining of the RuBisCO large subunit (LSU) was used as loading control. (C) GUS reporter gene activity measured from leaf disc extracts. Four days post infiltration two leaf discs each were stamped out from the top infiltrated leaves from three independent plants and incubated for 2 days on H₂O on 1mM SA.

These results from the analysis of EAR motif mutants show that both, the exchange of conserved leucine residues within the EAR motif (Fig. 47, 48) or deletion of it (Fig. 49, 51), are sufficient to significantly reduce the cell death promoting activity of N1 during transient overexpression without affecting protein accumulation. Interestingly, while neither NPR1 binding mutants (see 4.3.1.) nor EAR motif mutants (Fig. 48, 49) on their own have any significant effect on N1 mediated repression of the *PR1a* promoter, the *N1 F49/50S E94A D95V ΔEAR-V* triple mutant is unable to mediate the same level of suppression.

4.3.3. Analysis of tobacco NIMIN2 mutants in the NPR1 binding and EAR motifs

The results from N1 (see 4.3.2.) suggest the EAR motif to play a major role in N1-mediated cell death promotion during transient overexpression. Therefore, the question arose if NIMIN proteins from tobacco respond accordingly. As shown above (Fig. 45) tobacco NIMIN proteins feature a different kind of EAR motif. To test whether the DLNxxP type EAR motif is also able to interact with the TPL1/333 fragment a quantitative yeast two-hybrid assay was used. Both *NtN2c-V* and *FS-V* have been shown to promote the emergence of cell death during transient overexpression (Fig. 24,25) and EAR motif mutants of both, *NtN2cΔEAR* and *FSΔEAR* (Fig. 52A; see Appendix V) were created to investigate its influence. Additionally, a NPR1 binding mutant of *FS* was created to observe the effect of this interaction on tobacco NIMIN promoted cell death.

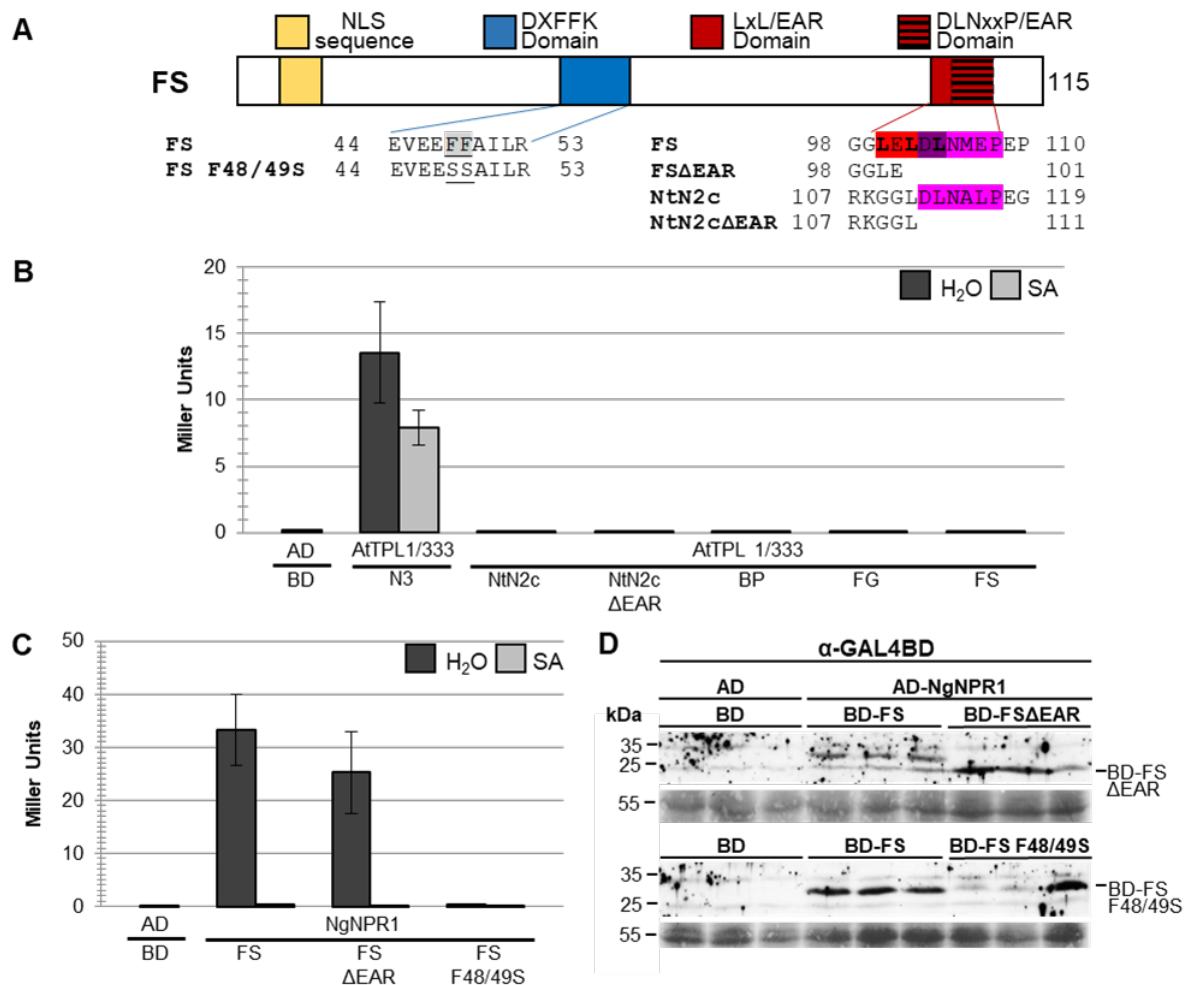


Fig. 52 Interaction of tobacco NIMIN proteins and mutants in the NPR1 binding and EAR motifs with *AtTPL1/333* or *NgNPR1* in yeast. (A) Schematic representation N2-like tobacco NIMINs using *FS* as an example, indicating amino acid changes and deletions in the mutants. (B) and (C) Quantitative Y2H assay for interaction of GAL4BD fusion proteins of tobacco NIMIN proteins and their mutants with GAL4AD fusions *AtTPL 1/333* or *NgNPR1*. The assays were performed under standard conditions using three independent colonies with two replicates for each colony. (B) Interaction of *NtN2c*, *NtN2cΔEAR*, BP, FG and *FS* with a GAL4AD fusion *AtTPL 1/333* using the interaction between GAL4BD-N3 and GAL4AD-*AtTPL1/333* as a positive control (C) Interaction of *FS*, *FSΔEAR*, and *FS F48/49S* with a GAL4AD fusion *NgNPR1*. (D) Immunodetection of GAL4BD fusion proteins from protein extracts prepared from three independent yeast liquid cultures, using the α -GAL4BD antiserum. Ponceau S staining was used as loading control.

None of the tobacco NIMIN proteins tested were able to interact with the AtTPL1/333 fragment in yeast (Fig. 52B) indicating that this N-terminal fragment of TPL can only interact with LxLxL type EAR motifs. Compatible with the results obtained from N1 mutants, deletion of the EAR motif does not affect the interaction between FS and NgNPR1 while mutation in the DXFFK motif completely abolishes this interaction (Fig. 52C). In protein extracts from yeast, a GAL4BD fusion of wildtype FS, as well as FS F48/49S, can be detected at the expected 34 kDa when using the α -Gal4BD antiserum (Fig. 54D). However, GAL4BD-FS Δ EAR accumulates at about 25 kDa, below the 32 kDa calculated for the fusion protein.

Agrobacteria containing *Pro35S:FS F48/49S-V* and *Pro35S:FS Δ EAR-V* constructs (see Appendix V) were used for transient overexpression side by side with *Pro35S:FS-V*. In accordance with the results from N1 (Fig. 41), mutation in the DXFFK motif in *FS F48/49S-V* delays the emergence of cell death only slightly with necrotic tissue becoming visible 6 days after infiltration rather than 5 days as observed for *FS-V* (Fig. 53A). Meanwhile, the emergence of cell death could not be observed during overexpression of *FS Δ EAR-V* even at 8 days post infiltration. Measurement of GUS activity from H₂O and SA floated leaf discs revealed, that even in absence of cell death the SA mediated activity of the *PR1a* promoter is repressed in plants overexpressing *NtFS Δ EAR* (Fig. 53B).

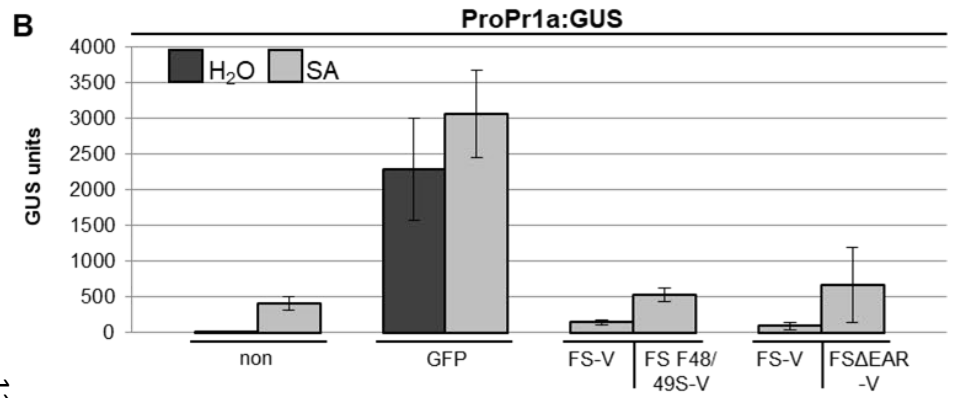
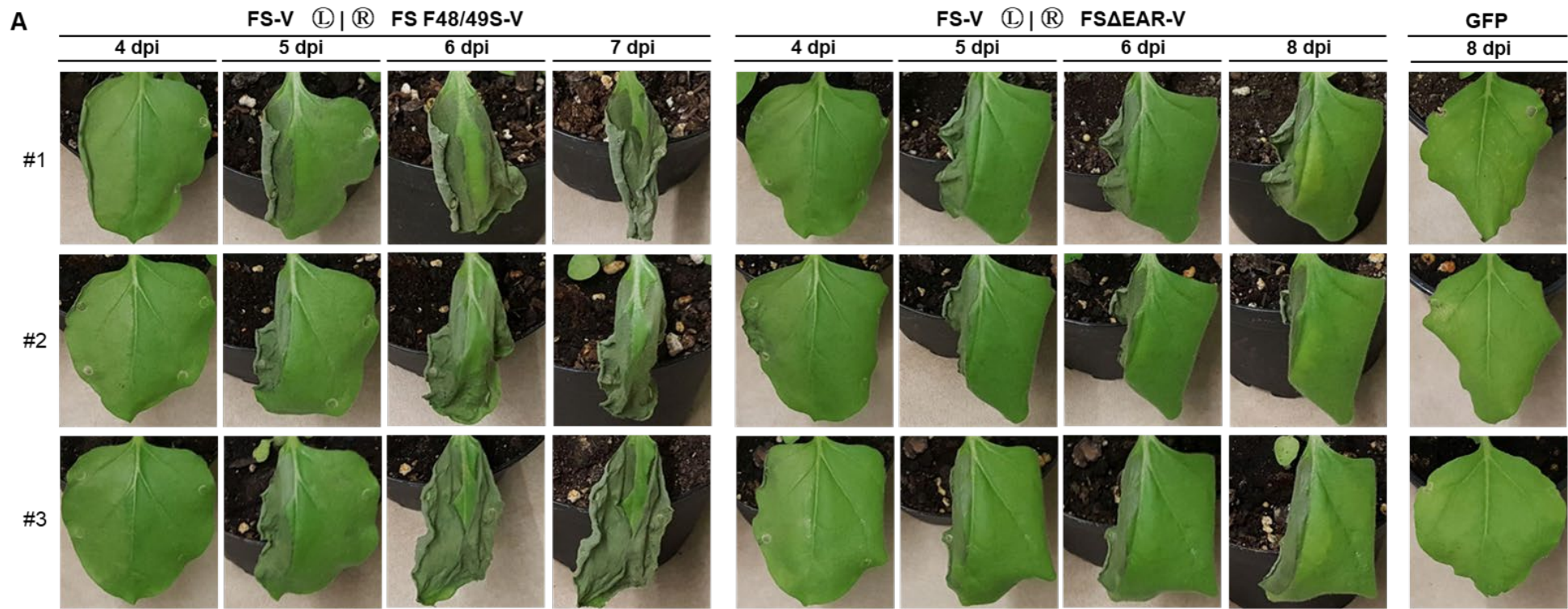


Fig. 53 Transient overexpression of *FS-Venus*, *FS F48/49S-Venus* and *FSΔEAR-Venus* in *N. benthamiana* *Pro-1533PR-1a:GUS* plants. (A) Phenotype of infiltrated *N. benthamiana* leaves. Left leaf half: *Pro35S:FS-V*; Right leaf half: *Pro35S:FS F48/49S-V* (left) or *Pro35S:FSΔEAR-V* (right). Symptom development was documented from three independent plants at 4, 5, 6 and 7 or 8 dpi. Plants infiltrated with *Pro35S:GFP* were used as a control. (B) GUS reporter gene activity measured from leaf disc extracts. Four days post infiltration two leaf discs each were stamped out from the top infiltrated leaves from three independent plants and incubated for 2 days on H₂O or 1 mM SA.

4. Results

Accumulation of both FS mutants could be detected using the α -GFP (FL) antiserum on protein extracts from plants transiently overexpressing *FS F48/49S-V* or *FS Δ EAR-V* (Fig. 54). However, while *FS F48/49S-V* like *FS-V* can be detected as a 40 kDa band with a secondary 30 kDa band below it (Fig. 54A), the 40 kDa band for the full length *FS Δ EAR-V* is only faintly visible with several lower bands down to a 27 kDa band, the size of the Venus protein (Fig. 54B). This hints at possible degradation of the *FS Δ EAR-V* fusion protein preventing the promotion of cell death.

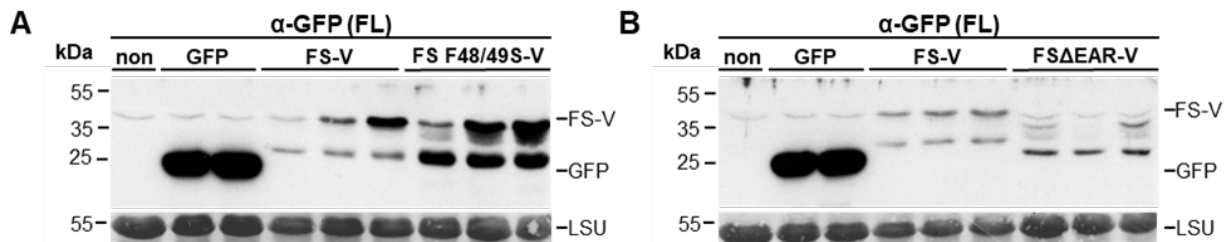


Fig. 54 Protein accumulation of FS-Venus, FS F48/49S-Venus and FS Δ EAR-Venus in *N. benthamiana Pro-1533PR-1a:GUS* plants during transient overexpression. Immunodetection of Venus fusion proteins from protein extracts prepared 4 dpi from three independent plants, using the α -GFP (FL) antiserum. Ponceau S staining of the RuBisCO large subunit (LSU) was used as loading control. (A) Immunodetection of *FS-Venus* and *FS F48/49S-Venus*. (B) Immunodetection of *FS-Venus* and *FS Δ EAR-Venus*.

To observe if this instability of the *FS Δ EAR-V* protein is shared by the analogous *NtN2c Δ EAR-V* protein, agrobacteria containing *Pro35S:NtN2c-V* and *Pro35S:NtN2c Δ EAR-V* constructs were infiltrated side by side into *N. benthamiana* leaf tissue. Overexpression of *NtN2c Δ EAR-V* produces no visible necrosis even 10 days post infiltration (Fig. 55A). Immunodetection showed that the *NtN2c Δ EAR-V* protein accumulates just below the 40 kDa signal observed for *NtN2c-V* with a similarly shifted lower band below the 30 kDa signal of the secondary *NtN2c-V* band (Fig. 55B).

In summary, these results show that mutations in tobacco NIMIN proteins shown to promote cell death have similar effects on the emergence of cell death as equivalent mutations in Arabidopsis N1. NPR1 binding mutants of both N1 and FS have a weak delaying effect on the development of necrotic tissue while EAR motif mutants show a much stronger impact.

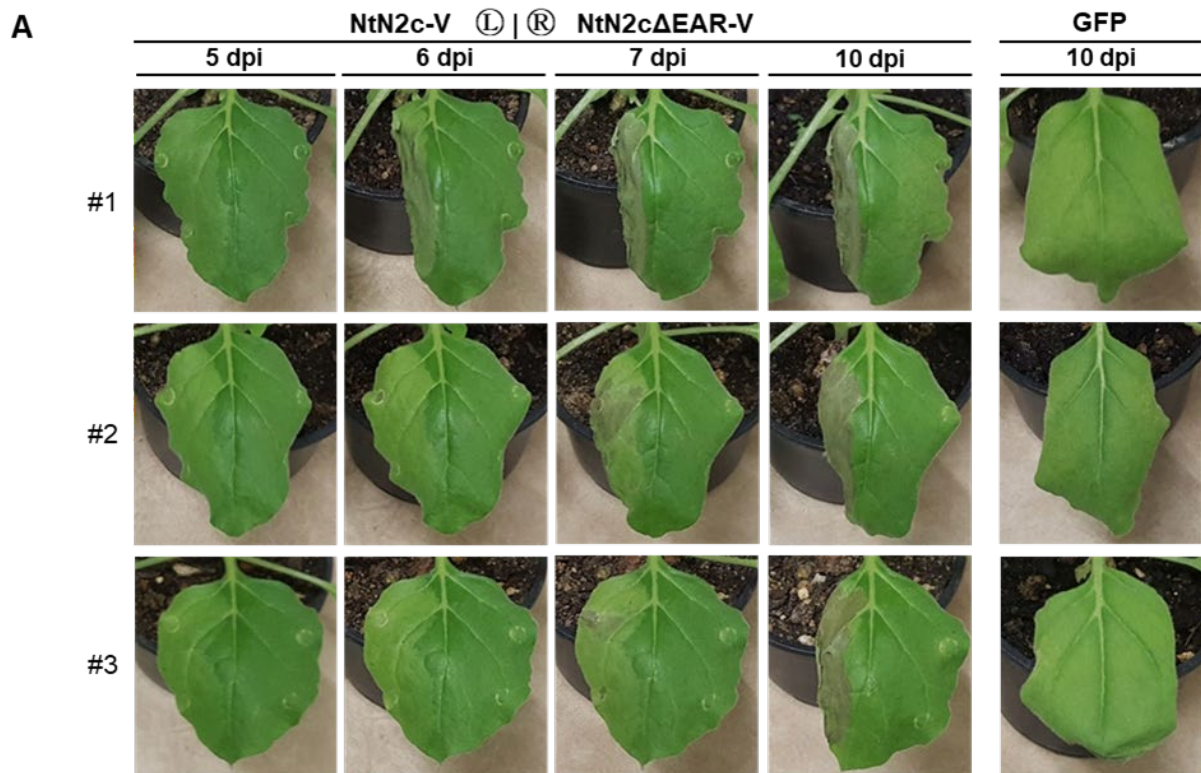
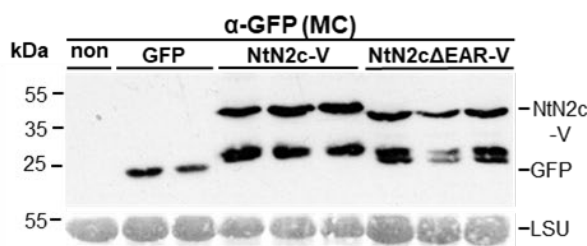
**B**

Fig. 55 Transient overexpression of *NtN2c-V* and *NtN2cΔEAR-V* in *N. benthamiana* WT plants. (A) Phenotype of infiltrated *N. benthamiana* leaves. Left leaf half: *Pro35S:NtN2c-V*; Right leaf half: *Pro35S:NtN2cΔEAR-V*. Symptom development was documented from three independent plants at 5, 6, 7 and 10 dpi. Plants infiltrated with *Pro35S:GFP* were used as a control. (B) Immuno-detection of Venus fusion proteins from protein extracts prepared 4 dpi from three independent plants, using the α -GFP (MC) antiserum. Ponceau S staining of the RuBisCO large subunit (LSU) was used as loading control.

4.3.4. Phenotypic effects of overexpression of TOPLESS in *N. benthamiana*

The data collected during mutant analysis (see 4.3.2. and 4.3.3.) suggest that the EAR motif plays a key role during the NIMIN mediated emergence of cell death. Confirming the results from previous studies [Späth, 2012; Wöhrle, 2014], both, *Arabidopsis* N1 and N3, are able to interact with an N-terminal fragment of TPL (TPL 1/333, Fig. 46). EAR motif-containing proteins are known for their ability to exert transcriptional repression through their interaction with transcriptional co-repressors like TOPLESS (TPL) [Kagale *et al.*, 2010]. One of the most studied groups of TPL interactors are the AUX/IAA transcriptional repressors, which are involved in the regulation of auxin signaling [Szemenyei *et al.*, 2008]. AUX/IAA proteins are involved in several processes with roles in developmentally regulated programmed cell death [Denbigh *et al.*, 2020] and, like NIMIN proteins, interact with TPL through an LxLxL type EAR motif [Tiwari *et al.*, 2004]. Interestingly, observations during transient overexpression of *TPL 1/333* in *N. benthamiana* leaf tissues showed cell death like symptoms comparable to those observed for N1 [U.M. Pfitzner, personal communication]. These facts suggest a possible connection between NIMIN mediated cell death and the interaction between NIMIN proteins

4. Results

and TPL. Therefore, to gain a deeper understanding of underlying mechanism behind EAR motif mediated cell death special attention was given to the interaction between NIMIN proteins and the N-terminal TPL1/333 fragment. The first step in this direction was taken by monitoring the effects of *TPL1/333* during transient overexpression. To achieve a direct comparison, agrobacteria containing *Pro35S:NI-V* or *Pro35S:TPL1/333* (UPf, personal communication) were infiltrated into the left and right leaf halves of *N. benthamiana* plants, respectively. *TPL1/333* overexpression promotes cell death in a similar pace as observed for *NI-V* (Fig. 56) indicating that both proteins can induce cell death.

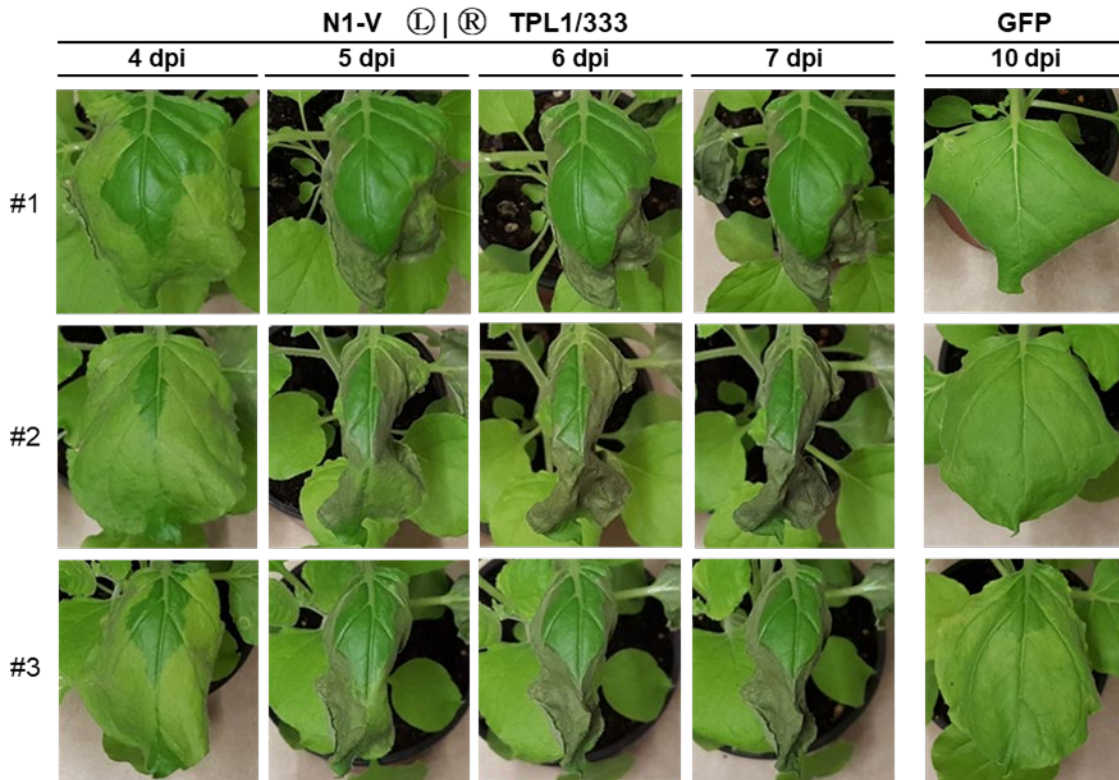


Fig. 56 Transient overexpression of *NIMINI-Venus* and *TPL1/333* in *N. benthamiana* plants. Phenotype of infiltrated *N. benthamiana* leaves. Left leaf half: *Pro35S:NI-V*; Right leaf half: *Pro35S:TPL1/333*. Symptom development was documented from three independent plants at 4, 5, 6 and 7 dpi. Plants infiltrated with *Pro35S:GFP* were used as a control.

To establish whether both proteins act synergistically to mediate the emergence of cell death, *TPL1/333* and different Arabidopsis *NIMIN* genes were transiently co-expressed. To ensure an equivalent bacteria titer, bacteria suspensions of the same OD were mixed. The left leaf half was infiltrated with agrobacteria carrying the *Pro35S:TPL1/333* construct with an equal amount of LBA4404 agrobacteria without a binary vector construct for gene expression, while in the right leaf half agrobacteria containing *Pro35S:NI*, *Pro35S:N2*, or *Pro35S:N3* were co-infiltrated instead (Fig. 57). Interestingly, the simultaneous overexpression of *TPL1/333* and *NI* or *N3*, rather than accelerating the emergence of cell death, leads to a visible deceleration of necrosis development in infiltrated leaf halves when compared to tissues only overexpressing *TPL1/333* (Fig. 57 A,C). Meanwhile, coexpression of *TPL1/333* and *N2* does not cause similar effects (Fig. 57B). Unlike *N1* or *N3*, *N2* cannot interact with *TPL1/333* in yeast [Späth, 2012] indicating that interaction between *TPL1/333* and *NIMIN* proteins affects cell death emergence in transient co-expression experiments.

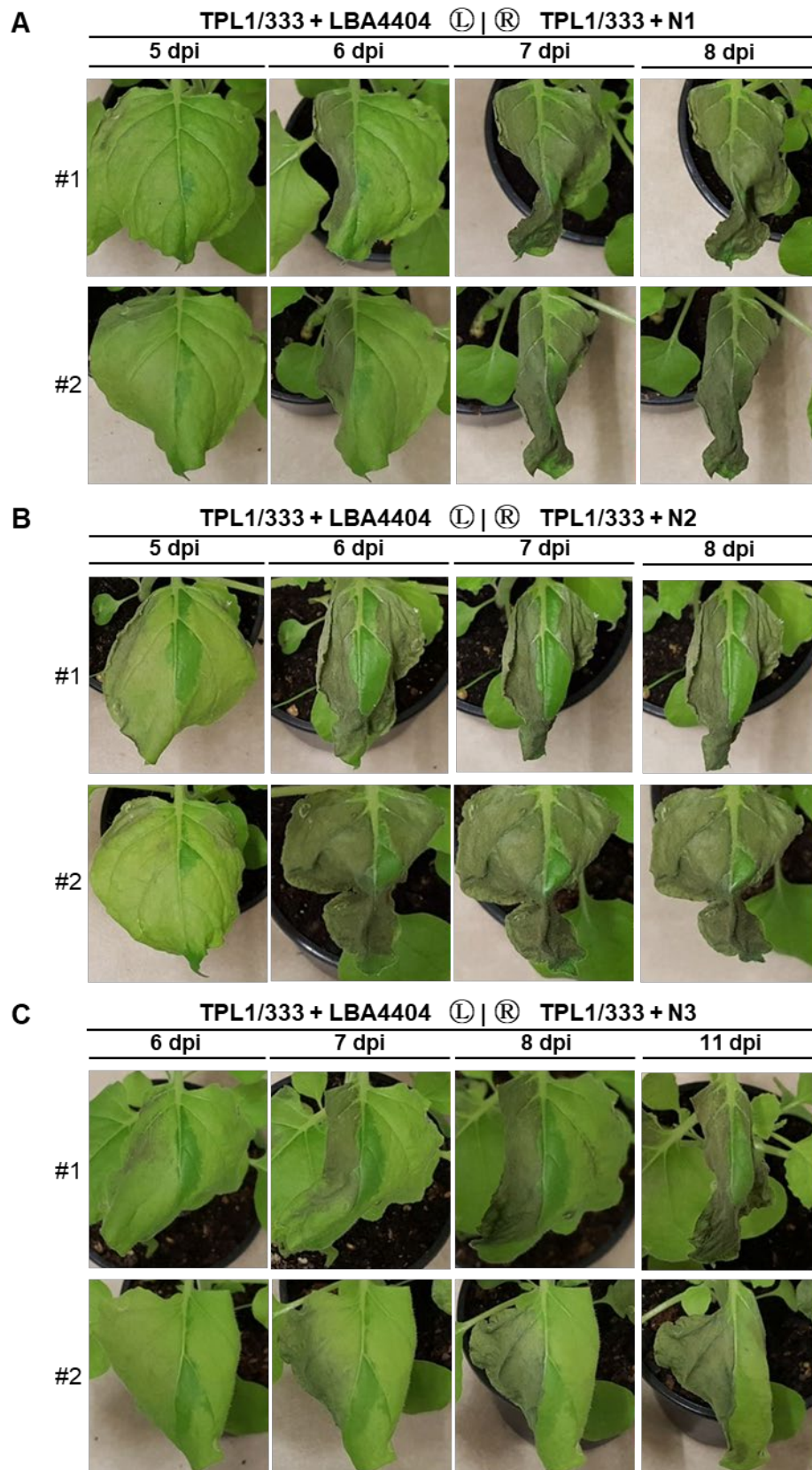


Fig. 57 Transient coexpression of *TPL1/333* with *NIMIN1*, *NIMIN2* or *NIMIN3* in *N. benthamiana* plants. Phenotype of infiltrated *N. benthamiana* leaves. Left leaf half: *Pro35S:TPL1/333* and LBA4404 Agrobacteria without binary vector; Right leaf half: *Pro35S:TPL1/333* and *Pro35S:N1* (A), *Pro35S:N2* (B), or *Pro35S:N3* (C). Symptom development was documented at 5, 6, 7 and 7 dpi for *N1* and *N2* (A&B) or 6, 7, 8 and 11 dpi for *N3* (C).

4.3.5. Phenotypic effects of overexpression of Bax

Previous reports demonstrated that overexpression of certain NIMIN proteins represses transcription from the *PR1a* promoter [Weigel *et al.*, 2005; Zwicker *et al.*, 2007; Chern *et al.*, 2008]. NIMIN-mediated induction of cell death was not observed in these experiments. However, in this study, cell death correlated, in many cases, with repression of the *PR1a* promoter, for example during overexpression of *NI-V* and *FS-V* (Fig. 25), as well as their associated NPR1 binding mutants (Fig. 41, 42, 44 and 53), even though the mutant proteins are unable to interact with NPR1 proteins in yeast (Fig. 27, 43 and 52). There were however a few exemptions including *Nib-V* (Fig. 17) and the EAR motif mutants *NI L138/I40A-V* (Fig. 48), *NIΔEAR* (Fig. 49), and *FSΔEAR* (Fig. 53) which despite showing no or strongly delayed visible emergence of cell death are able to suppress *PR1a* promoter activity. Samples for *PR1a* promoter induction were typically taken between four to six days after agroinfiltration, depending on GFP accumulation in the control plants, when cell death was not yet visible on infiltrated leaves. Leaf discs were floated for 2 days on 1 mM SA and sometimes developed visible discoloration or cell death symptoms. It can therefore not be excluded that tissues programmed for later cell death emergence became inapt to induce the *ProPR1a:GUS* reporter construct early after agroinfiltration.

To determine if there is a correlation between the intensity of cell death and repression of the *PR1a* promoter which can be observed for overexpression of NIMIN proteins, the *ProNib:Bax* construct was chosen. Bax mediated cell death is not associated with the processes taking place during SAR and can therefore be used as an independent control. As shown before, during transient overexpression of *Bax* cell death is elicited only slightly faster than during overexpression of *NI* (Fig. 8). To further adjust this for comparable levels of cell death, the *ProNib:Bax* containing agrobacteria strains used for infiltration were diluted 1:2 and 1:4 using Agrobacterium strain LBA4404 without the plasmid containing a foreign gene for overexpression. The infiltration was carried out in *N. benthamiana* plants containing the *Pro-1533PR-1a:GUS* reporter construct. When overexpressed side by side with *Pro35S:NI-V*, the 1:2 dilution of *ProNib:Bax* elicits comparable amounts of cell death at 5dpi while the 1:4 dilution exhibits cell death slightly slower (Fig. 58A). Four days post infiltration leaf discs were stamped out of infiltrated leaves and incubated on H₂O or 1 mM SA for three days. A GUS reporter assay revealed that the overexpression of *Pro35S:NI-V* completely abolishes reporter induction and measurable GUS activity as does *ProNib:Bax* in 1:2 dilution. However, under stronger dilution GUS activity is only partially inhibited (Fig. 58B). This supports the hypothesis that GUS reporter activity is reduced even before appearance of visible amounts of cell death. This indicates that the measurement of GUS reporter gene expression is not a viable method for determining the suppressive effect on the *PR1a* promoter mediated by cell death promoting NIMIN proteins, as these results are distorted even before necrotic tissues become visible to the naked eye.

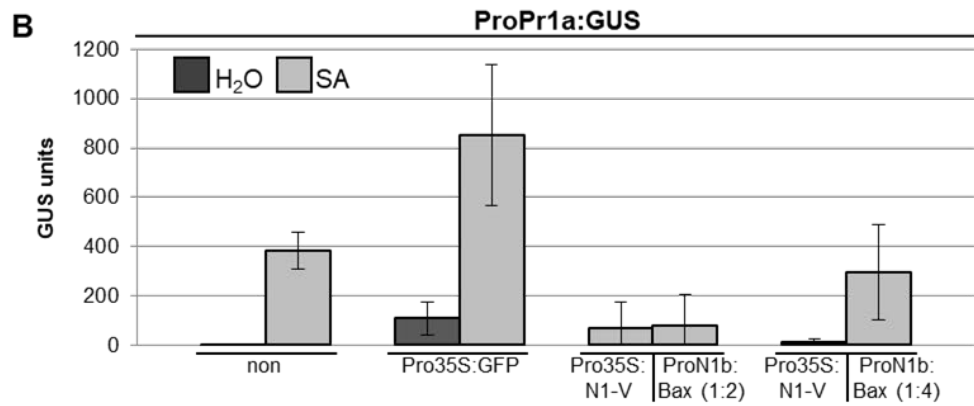
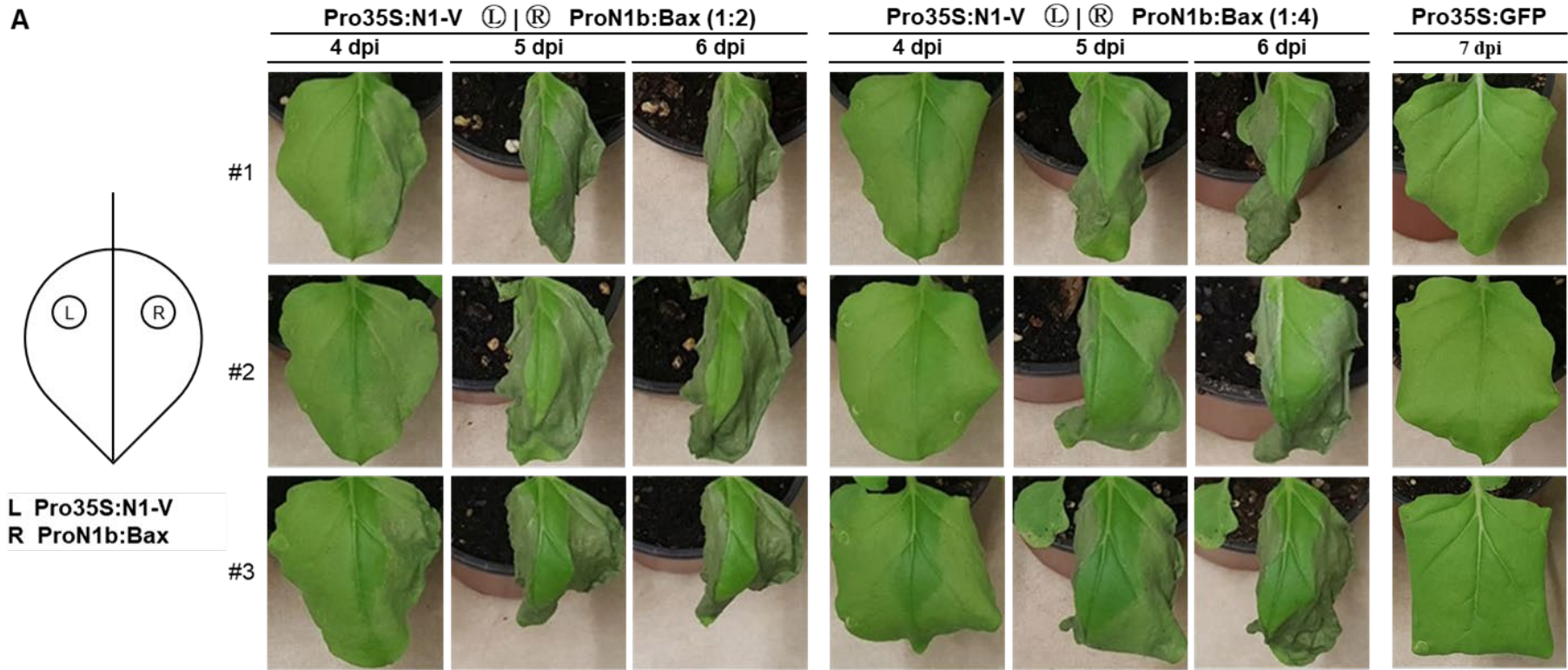


Fig. 58 Concentration dependent effects of transient overexpression of a *ProN1b:Bax* reporter constructs in *N. benthamiana* plants. *6xHis-Bax* was expressed under control of the *N1b* promoter from *Arabidopsis thaliana*. (A) Phenotype of infiltrated *N. benthamiana* leaves. Left leaf half: *Pro35S:N1-V*; Right leaf half: *ProN1b:Bax* diluted 1:2 or 1:4 respectively. Plants infiltrated with *Pro35S:GFP* were used as a control. Symptom development was documented from three independent plants at 4, 5 and 6 dpi. (B) GUS reporter gene activity measured from leaf disc extracts from the same plants. Four days post infiltration two leaf discs each were stamped out from three independent plants. and incubated for 3 days or H₂O or 1 mM SA.

4.4. Identification of a novel domain in NIMIN1 important for protein accumulation

The results obtained during transient overexpression of *NIMIN* genes in *N. benthamiana* revealed differential accumulation of the respective NIMIN-Venus fusion proteins (see 4.2.2. and 4.2.3.). Some NIMIN proteins, N1 and N3 from Arabidopsis and NtN2c and FS from tobacco, accumulate strongly during Agrobacterium mediated transient overexpression, while other proteins from the same family, N1b and N2 from Arabidopsis and BP and FG from tobacco, show only very weak accumulation under the very same conditions. Furthermore, the cell death promoting activity of NIMIN proteins appears to be strongly associated with available NIMIN protein levels as only during overexpression of NIMIN proteins with strong detectable accumulation, like N1 (Fig. 4B, Fig. 13), N3 (Fig. 19), NtN2c (Fig. 24) and FS (Fig. 25), visible necrosis is observable before similar symptoms appear in control plants. While NIMIN proteins share many important functional domains and their general structure it remains to be elucidated how the observed differences in protein accumulation are caused.

4.4.1. Domain architecture of NIMIN1

While both N1 and N1b are able to suppress the SA mediated activity of the *PR1a* promoter, these proteins differ considerably in their accumulation and cell death promoting activity. It is therefore of great interest to observe differences between the amino acid sequences of N1 and N1b to gain a deeper understanding of the underlying mechanisms responsible for differential activity. Sequence alignment of N1 and N1b using Clustal Omega [Goujon *et al.*, 2010; Sievers *et al.*, 2011] shows the overall high similarity between both proteins and an almost identical domain structure (Fig. 59A). Noticeable are two regions of low overall similarity, the C-terminal acidic Poly (E/D) domain from N1b which is absent in N1, and the N-terminal 15 amino acids from N1 which are missing in N1b. Coinciding with these observations, hydrophobicity plots of both proteins using the Kyte-Doolittle scale on ProtScale [Kyte & Doolittle, 1982; Gasteiger *et al.*, 2005], besides showing regions of high hydrophobicity corresponding to known protein-protein interaction domains (the DXFFK motif, the EDF motif, and the EAR motif), revealed another prominent region of higher hydrophobicity in the N-terminal region of N1 corresponding to the first 15 amino acids (Fig. 59B). Hereinafter this region will be called the N1 N-terminal domain (N1nT).

A

```

NIMIN1  MYPKQFSLYNYSLETMSKDENVESKETIRVDKRVREDEEEEEEEKIDTFFKLIKHYQEAR 60
NIMIN1b -----MNQE--EETENKRINEIDEDDEEELENKKMDMFNLIKNYQDAK 43
          *:::  *..*. *:::  ..:*** *:*** * *:***:***:
          *:::  *..*. *:::  ..:*** *:*** * *:***:***:

NIMIN1  KRRREELAENSGVVRKSNNGERSGIVVPAFQPEDFSQCRTG-LKPPLMFVSDHKENTK 119
NIMIN1b KRRRQYLTDQSGDVASMPTKR-SDYSIVPVFRAEDFSHCMDLNLKPSNIIISTKNQEEEE 102
          ****: *:::** * . . :***: ****:* *** :*: **: *

NIMIN1  VEQEEDQ--TE-----ERNEDKALDLNLAL 142
NIMIN1b QEEEEEDDEEEEDDDEGEEVEKVMRKDNGLDLNLAL 140
          *:***: * .:***:*****

```

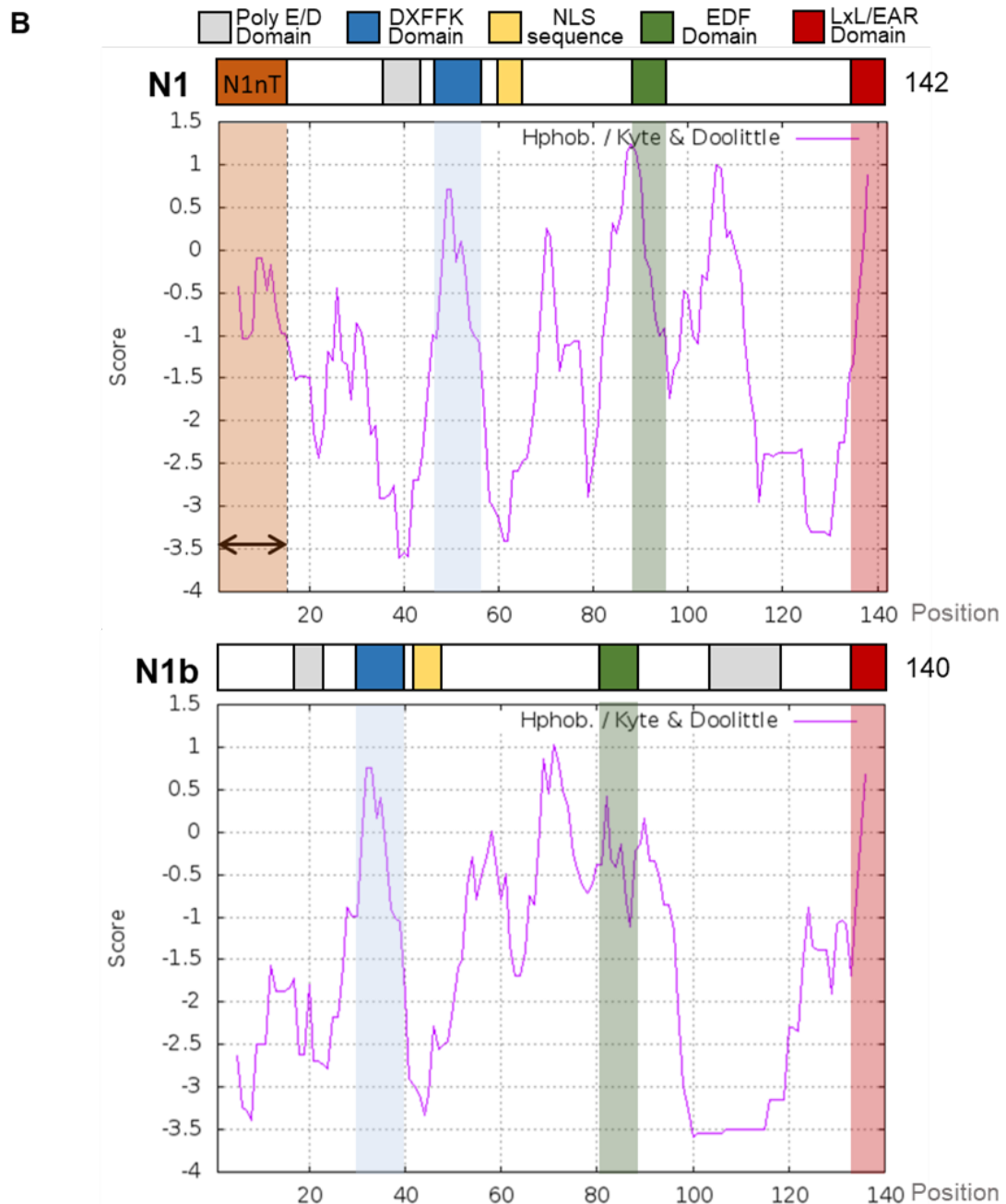


Fig. 59 Analysis of the amino acids sequence and hydrophobic properties of NIMIN1 and NIMIN1b. (A) Sequence alignment of N1 and N1b using Clustal Omega at EMBL-EBI. A star (*) indicates perfect alignment, while a colon (:) indicates strong and a period (.) indicates weak similarity. The N-terminal domain of N1 (N1nT) is marked in orange. The second Poly E/D domain from N1b is marked in grey. (B) Hydropathicity diagrams of N1 and N1b using the Kyte-Doolittle scale generated utilizing the ExPASy proteomics server. The N1nT domain is marked in orange. Protein-protein interaction domains are color coded as follows: DXFFK domain– blue, EDF domain – green, LxL/EAR domain – red.

4. Results

An alignment of several known or predicted NIMIN1 homologs from different plant species, including alpine rock cress (*Arabidopsis thaliana*), rapeseed (*Brassica napus*), wild cabbage (*Brassica oleracea* var. *oleracea*), field mustard (*Brassica rapa* subsp. *oleifera*), camelina (*Camelina sativa*), pink sheperd's-purse (*Capsella rubella*), radish (*Raphanus sativus*) and the extremophyte *Eutrema salsaugineum*, revealed high conservation of the N1nT region with 32 % identity and 68 % similarity (Fig. 60). The highest conservation lies in the initial four amino acids (MYPK), a leucine residue at position 9 within an area of several polar amino acids and a threonine residue at position 15. This high conservation suggests an important role for the function of NIMIN1.

<i>Arabidopsis thaliana</i>	MYPKQ-FSLYNYS---LET
<i>Arabidopsis alpina</i>	MYPKQ-LNLHNYP--LLKT
<i>Brassica napus</i>	MYPKL-FNLHDNPYSVLKT
<i>Brassica oleracea</i>	MYPKL-FNLHDNPYSVLKT
<i>Brassica rapa</i>	MYPKL-FNLHDNPYSVLKT
<i>Camelina sativa</i>	MYPKQQVKLYNYS---LET
<i>Capsella rubella</i>	MYPKQ-LELYKYA---LDT
<i>Eutrema salsaugineum</i>	MYPKQ-FNLHDYPSNAIKT
<i>Raphanus sativus</i>	MYPKQ-LNLHDCPSSALKT
	**** . . * : . . : . *

Fig. 60 Conservation of the N-terminus of NIMIN1-like proteins. Sequence alignment of the N-terminal domain of N1 proteins from different plant species using Clustal Omega at EMBL-EBI: *Arabidopsis thaliana* (NP_563653.2), *Arabidopsis alpina* (LT669788.1), *Brassica napus* (XP_013695558.1), *Brassica oleracea* var. *oleracea* (XP_013584896.1), *Brassica rapa* subsp. *oleifera* (XP_009119632.1), *Camelina sativa* (XP_010457224.1), *Capsella rubella* (XP_006305772.2), *Eutrema salsaugineum* (XP_006418339.1) and *Raphanus sativus* (XP_018489127.1). A star (*) indicates perfect alignment, while a colon (:) indicates strong and a period (.) indicates weak similarity. Color code: red (Small + hydrophobic, includes aromatic amino acids without tyrosine), blue (Acidic), magenta (Basic, without histidine), green (hydroxyl + sulfhydryl + amine, including glycine).

A *N1* mutant harboring a deletion of the N1nT region starting the transcription at the second methionine at position 16 of the *N1* ORF was already available as a *Venus* fusion under control of the *35S* promoter. This *Pro35S:N1 16/142-Venus* construct (Fig. 61A) was shown to not induce accelerated cell death during transient overexpression in *N. benthamiana* (U. M. Pfitzner, personal communication). To verify these results and to observe accumulation of the N1 16/142-Venus fusion protein, agrobacteria strains harboring *N1-V* or *N1 16/142-V* were infiltrated into *N. benthamiana* leaf tissue. Indeed, *N1 16/142-V* does not promote accelerated emergence of necrotic tissue even 8 days post infiltration (Fig. 61B). Immunodetection using the α -GFP (FL) antiserum, however, revealed no accumulation of the full-length N1 16/142-V protein at 44 kDa (Fig. 61C). Interestingly, the two lower 35kDa and 27kDa bands can still be detected with the 27 kDa band corresponding to Venus exhibiting a stronger signal than for N1-V. Moreover, N1 16/142-V is unable to suppress the SA mediated activity of the *PR1a* promoter (Fig. 61D).

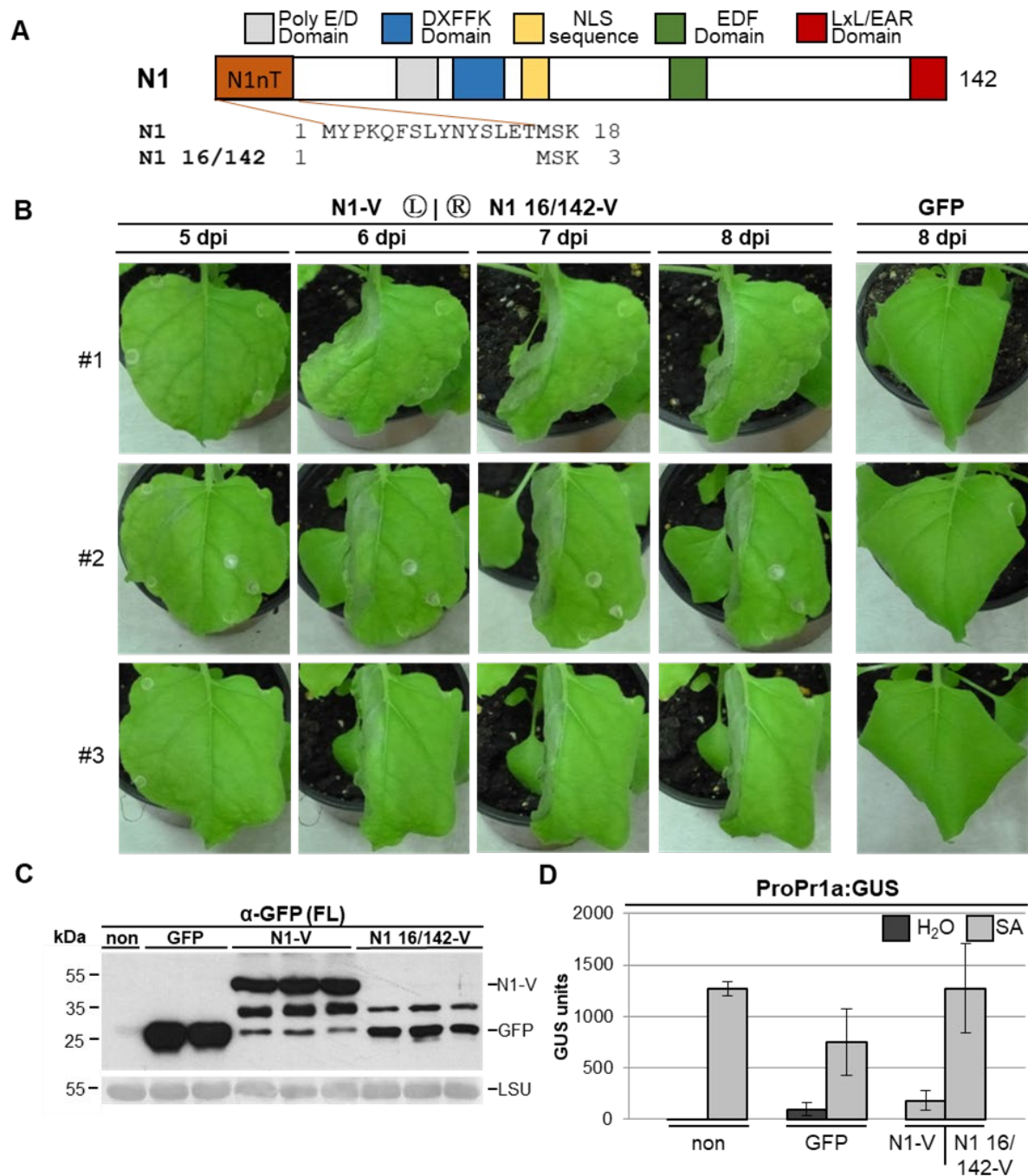


Fig. 61 Transient overexpression of *NIMIN1-Venus* and *NIMIN1 16/142-Venus* in *N. benthamiana Pro-1533PR-1a:GUS* plants. (A) Schematic representation of *NIMIN1* indicating deleted amino acids in the mutant. (B) Phenotype of infiltrated *N. benthamiana* leaves. Left leaf half: *Pro35S:N1-V*; Right leaf half: *Pro35S:N1 16/142-V*. Symptom development was documented from three independent plants at 5, 6, 7 and 8 dpi. Plants infiltrated with *Pro35S:GFP* were used as a control. (C) Immunodetection of Venus fusion proteins from protein extracts prepared 4 dpi from three independent plants, using the α -GFP (FL) antiserum. Ponceau S staining of the RuBisCO large subunit (LSU) was used as loading control. (D) GUS reporter gene activity measured from leaf disc extracts. Four days post infiltration two leaf discs each were stamped out from the top infiltrated leaves from three independent plants and incubated for 2 days on H₂O on 1mM SA.

Together these results show that N1 carries a conserved domain at its N-terminus which is not present in N1b. Loss of this N1nT domain prevents the accumulation of the full-length protein and thereby not only abolishes the cell death promoting activity of N1 but also its function as a repressor of NPR1 mediated gene induction.

4.4.2. Analysis of NIMIN hybrid proteins comprising the N1 N-terminal domain

Since the removal of the N1nT domain drastically reduces N1-V protein accumulation and the associated cell death and repression of the *PRIa* promoter observed during transient overexpression, the next logical step was to create hybrid proteins with the N1nT domain fused to the N-terminus of NIMIN proteins displaying low protein accumulation. In the context of these studies, hybrid *N1nT-N1b* and *N1nT-N2* genes were created (see Appendix V) and used to analyze their biochemical properties and phenotypic effects of the resulting proteins during transient overexpression.

4.4.2.1. Analysis of hybrid N1nT-N1b proteins

The hybrid protein expressed from the *N1nT-N1b* gene construct consists of 157 amino acids and with a mass of 18.5 kDa it is slightly larger than the known NIMIN proteins. The hydrophobicity profiles of N1 and N1nT-N1b are almost identical, showing only slight shifts corresponding to the actual position of functional domains (Fig. 62A).

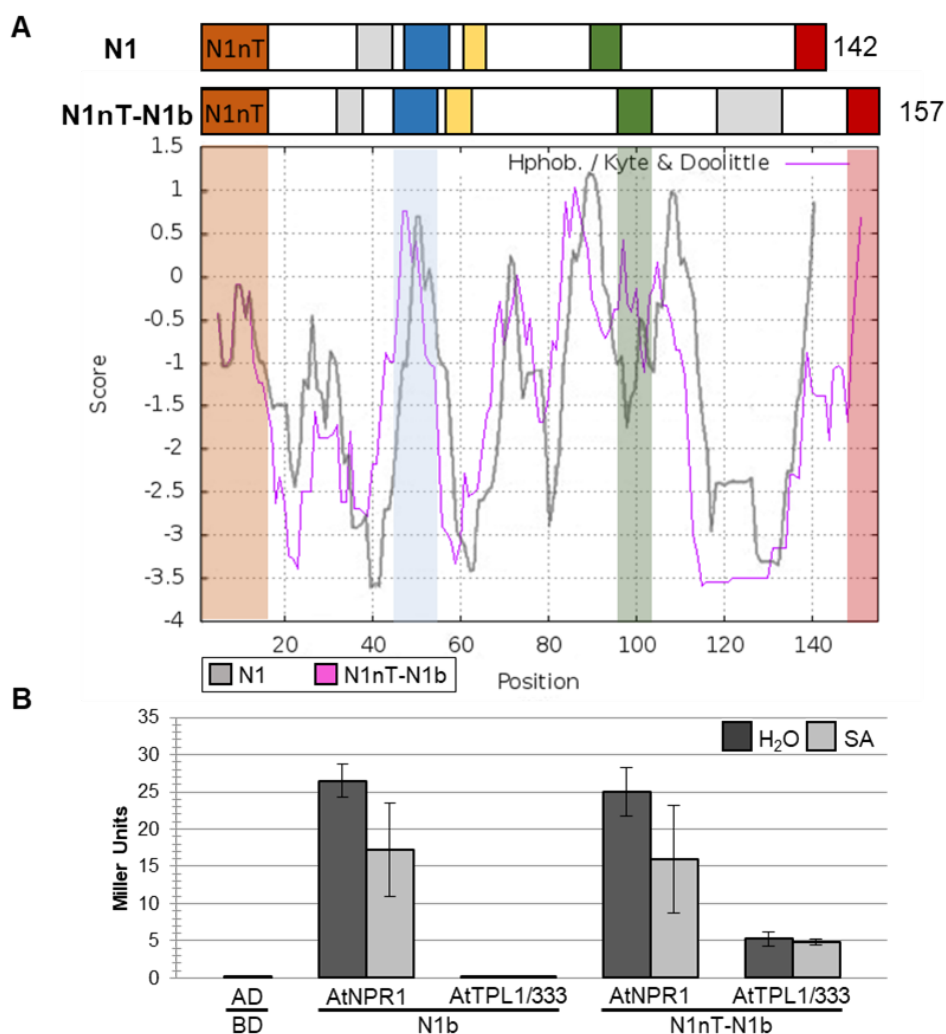


Fig. 62 Hydrophobic properties and interaction of N1nT-NIMIN1b with AtNPR1 and AtTPL1/333. (A) Overlay of hydrophobicity diagrams of N1 (grey) and N1nT-N1b (magenta) created using the Kyte-Doolittle scale generated utilizing the ExPASy proteomics server. The N1nT domain is marked in orange. Protein-protein interaction domains are color coded as follows: DXFFK domain– blue, EDF domain – green, LxL/EAR domain – red. (B) Quantitative Y2H assay for interaction of GAL4BD fusion proteins of N1b and N1nT-N1b with GAL4AD fusions of AtNPR1 and AtTPL 1/333. The assays were performed under standard conditions using three independent colonies with two replicates for each colony.

To ensure that the N-terminal fusion of the N1nT domain does not change the binding properties of N1nT-N1b a quantitative yeast two-hybrid assay was used (Fig. 62B). A Gal4BD fusion of the hybrid N1nT-N1b protein shows an equally strong interaction with a GAL4AD fusion of AtNPR1 as observed for N1b showing that N-terminal fusion of this peptide does not affect this property of N1b. It was a great surprise to see, that while N1b is unable to interact with the TPL1/333 fragment, N1nT-N1b shows a notable interaction significantly above background activity, comparable to the interaction strength observed between TPL1/333 and N1 and N3 (Fig. 46).

To determine whether there are differences in other properties of the N1nT-N1b protein compared to N1b, *Pro35S:N1nT-N1b-V* was transiently overexpressed in *N. benthamiana* leaf tissue. Agrobacteria strains overexpressing *N1-V* and *N1b-V* were infiltrated as controls (Fig. 63A). Confirming previous results, leaf tissue infiltrated with agrobacteria harboring *Pro35S:N1b-V* displays no accelerated cell death and only develops small necrotic patches at 11 days post infiltration, the same as in control plants overexpressing *GFP*. Meanwhile leaf halves overexpressing *N1nT-N1b-V* show comparable cell death promotion as observed for *N1-V*. Using the α -GFP (FL) antiserum it could be observed that, unlike *N1b-V*, which shows no visible accumulation, the protein band detected for the hybrid *N1nT-N1b-V* protein shows similar signal strength and banding pattern as observed for *N1-V* (Fig. 63B). This protein band is visible at 46 kDa slightly above the 44 kDa band of *N1-V* corresponding to the larger size of the protein. These results clearly show that N-terminal fusion of the N1nT peptide to N1b not only affects the accumulation of the resulting *N1nT-N1b-V* fusion protein, but also enables its interaction with the TPL1/333 fragment and the cell death promoting activity associated with N1.

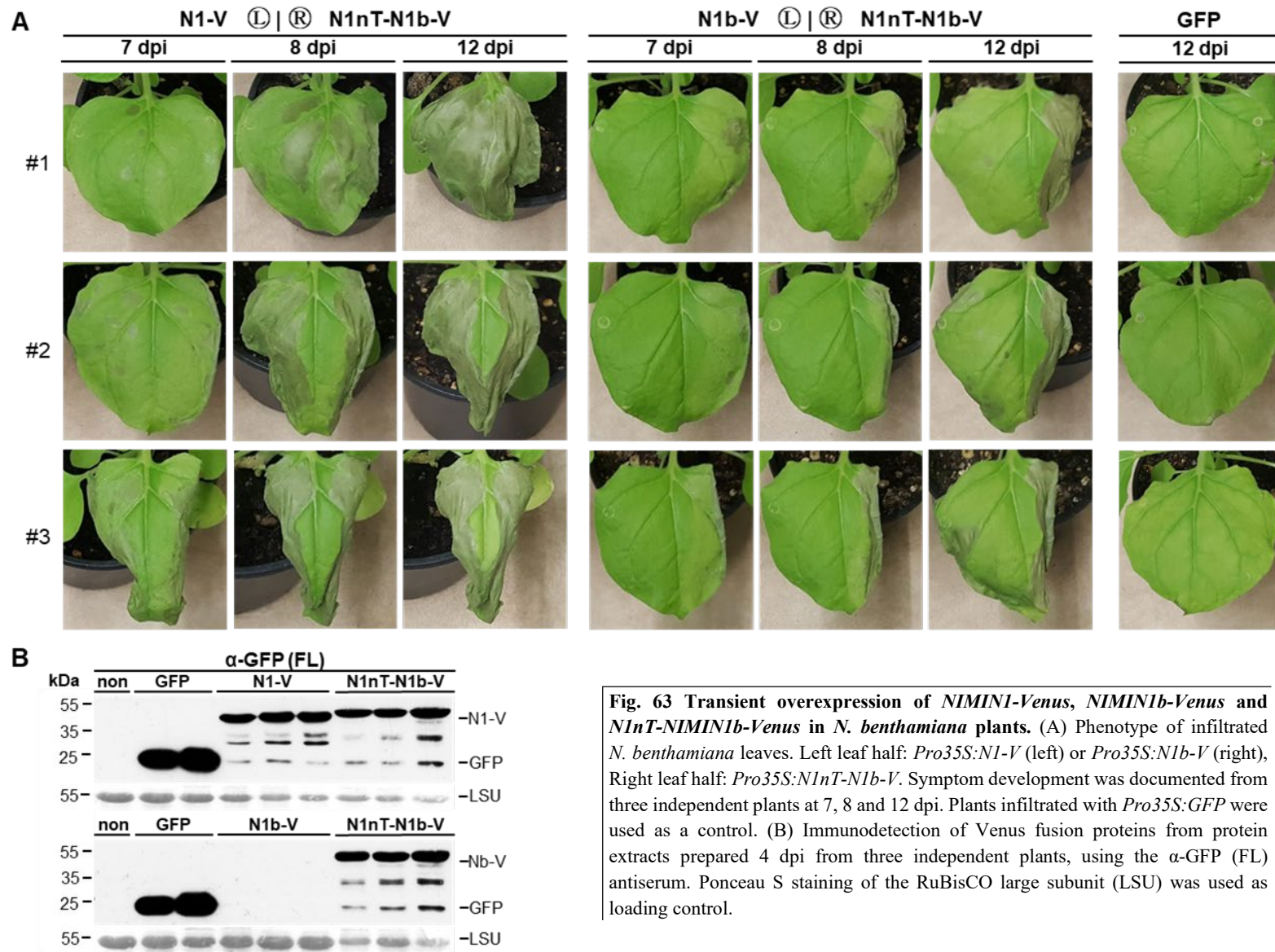


Fig. 63 Transient overexpression of *NIMIN1-Venus*, *NIMIN1b-Venus* and *N1nT-NIMIN1b-Venus* in *N. benthamiana* plants. (A) Phenotype of infiltrated *N. benthamiana* leaves. Left leaf half: *Pro35S:N1-V* (left) or *Pro35S:N1b-V* (right), Right leaf half: *Pro35S:N1nT-N1b-V*. Symptom development was documented from three independent plants at 7, 8 and 12 dpi. Plants infiltrated with *Pro35S:GFP* were used as a control. (B) Immunodetection of Venus fusion proteins from protein extracts prepared 4 dpi from three independent plants, using the α-GFP (FL) antiserum. Ponceau S staining of the RuBisCO large subunit (LSU) was used as loading control.

For N1-V, mutation or deletion of the EAR motif strongly slows down its cell death promoting activity without significantly affecting the accumulation of the mutant proteins (see 4.3.2.). To determine whether an equivalent mutant of N1nT-N1b-V would act similarly a *N1nT-N1bΔEAR* gene construct was created in which the six C-terminal amino acids, including three leucine residues belonging to the EAR motif, are deleted (Fig. 64A; see Appendix V). In a quantitative yeast-two-hybrid assay N1nT-N1bΔEAR shows similar binding affinity for AtNPR1 as observed with N1b and N1nT-N1b (Fig. 64B). However, no interaction with TPL1/333 could be observed after deletion of the EAR motif. Accumulation of GAL4BD fusion proteins of N1nT-N1b, as for N1b, can be detected at 40 kDa using the α -Gal4BD antiserum. N1nT-N1bΔEAR accumulates slightly below this displaying similar signal strength. In terms of protein interaction, N1nT-N1bΔEAR therefore behaves according to the corresponding N1-V mutants.

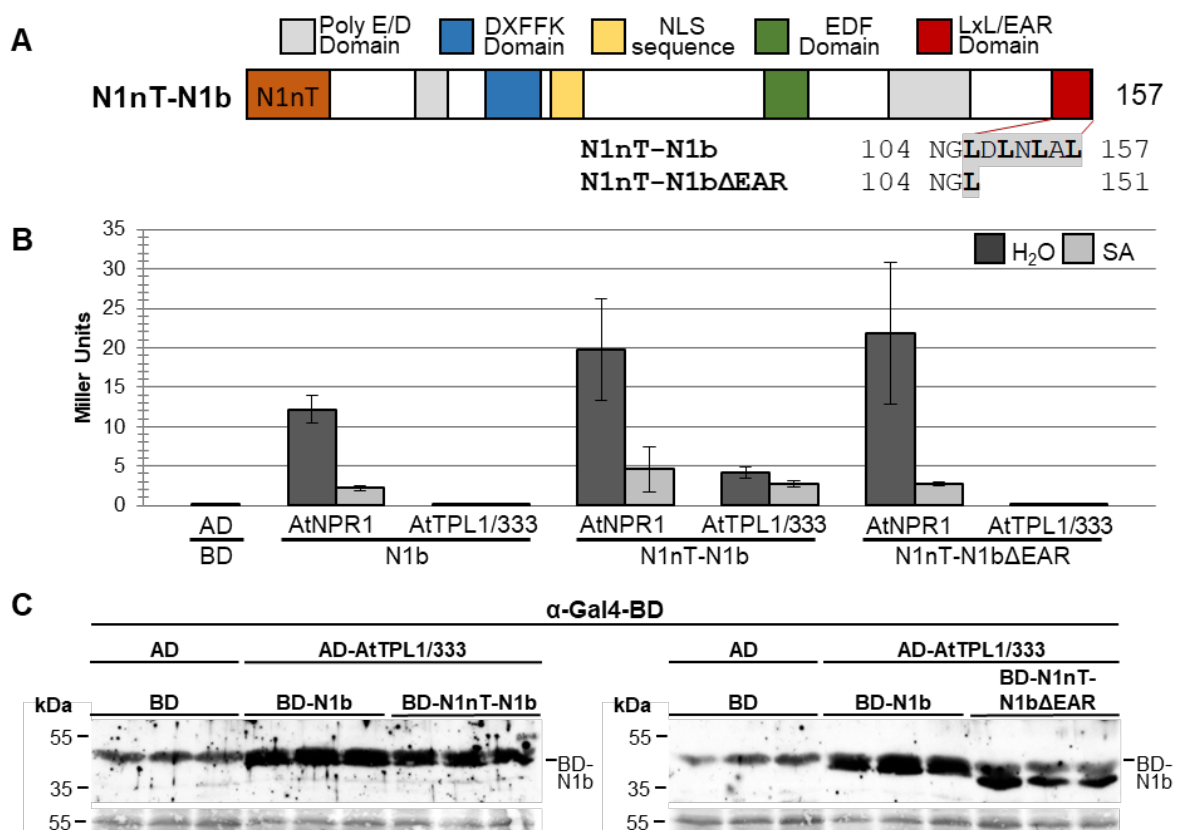


Fig. 64 Interaction of NIMIN1b, N1nT-NIMIN1b and N1nT-NIMIN1bΔEAR with AtNPR1 and AtTPL1/333 in yeast. (A) Schematic representation N1nT-N1b indicating the site of amino acid changes. (B) Quantitative Y2H assay for interaction of GAL4BD fusion proteins of N1b, N1nT-N1b and N1nT-N1bΔEAR with GAL4AD fusions AtNPR1 and AtTPL 1/333. The assays were performed under standard conditions using three independent colonies with two replicates for each colony. (C) Immunodetection of GAL4BD fusion proteins from protein extracts prepared from three independent yeast liquid cultures, using the α -Gal4BD antiserum. Ponceau S staining was used as loading control.

4. Results

During transient overexpression of agrobacteria harboring *Pro35S:N1nT-N1bΔEAR-V* cell death promotion is strongly decelerated when compared to *Pro35S:N1nT-N1b-V* (Fig. 65A). Immunodetection using the α -GFP (MC) antiserum shows that the N1nT-N1b Δ EAR-V protein accumulates just as strong as its counterpart harboring an intact EAR motif (Fig. 65B). The decreased emergence of cell death without visible reduction in protein accumulation shows that deletion of the EAR motif in the chimeric N1nT-N1b-V fusion protein has the same effects as for other cell death promoting NIMIN proteins.

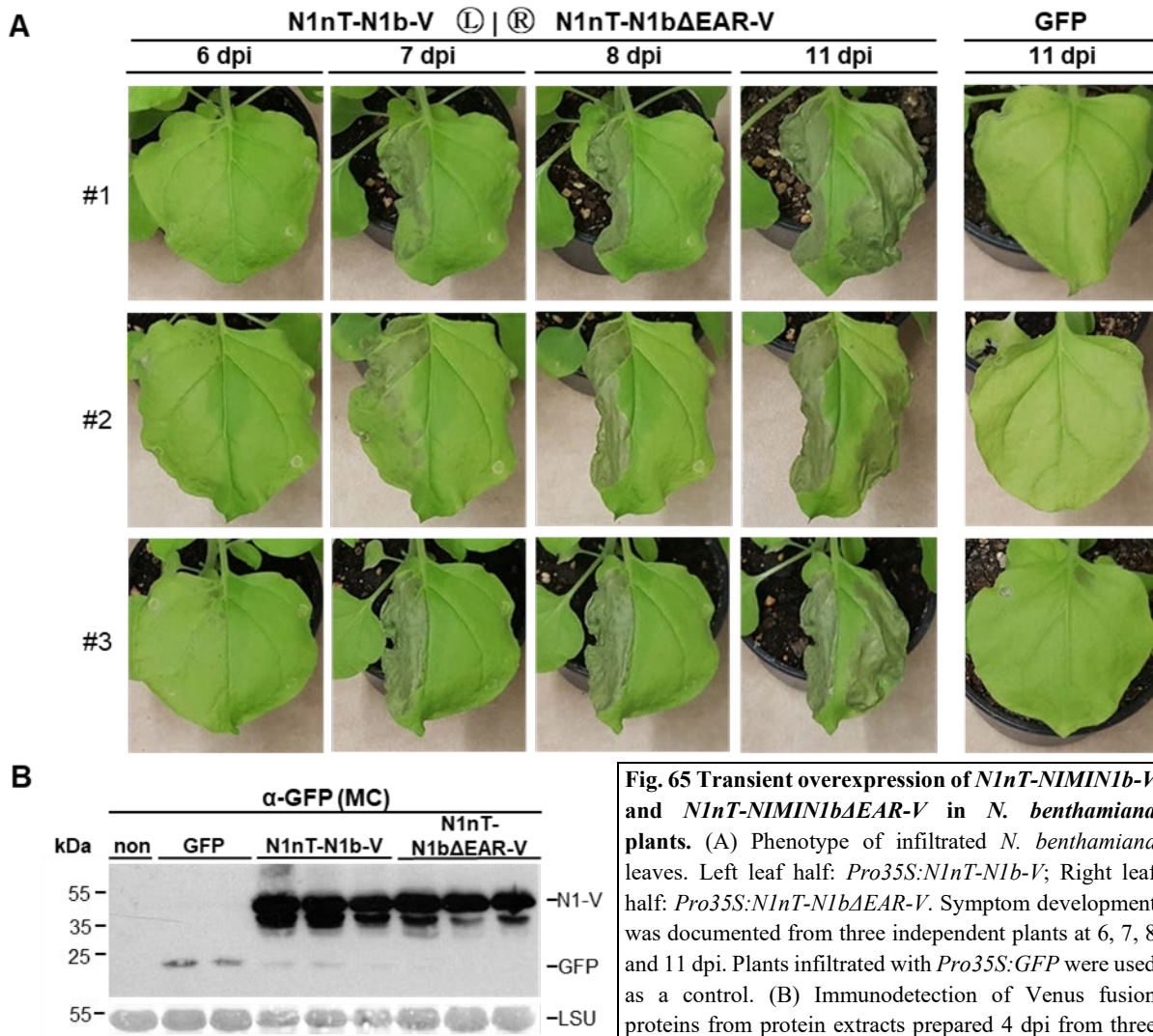


Fig. 65 Transient overexpression of *N1nT-NIMIN1b-V* and *N1nT-NIMIN1b Δ EAR-V* in *N. benthamiana* plants. (A) Phenotype of infiltrated *N. benthamiana* leaves. Left leaf half: *Pro35S:N1nT-N1b-V*; Right leaf half: *Pro35S:N1nT-N1b Δ EAR-V*. Symptom development was documented from three independent plants at 6, 7, 8 and 11 dpi. Plants infiltrated with *Pro35S:GFP* were used as a control. (B) Immunodetection of Venus fusion proteins from protein extracts prepared 4 dpi from three independent plants, using the α -GFP (MC) antiserum. Ponceau S staining of the RuBisCO large subunit (LSU) was used as loading control.

The observations from yeast and transient overexpression in *N. benthamiana* show that N-terminal fusion of the N1nT region to N1b significantly enhances the accumulation of the hybrid N1nT-N1b protein and enables the interaction with the TPL1/333 fragment. This is accompanied by gain of the ability to promote the emergence of cell death during transient overexpression which can be restricted by removal of the EAR motif.

4.4.2.2. Analysis of hybrid N1nT-NIMIN2-Venus

N2 is the only other NIMIN protein from Arabidopsis besides N1b, which shows low protein accumulation and no cell death promoting activity. While N2 lacks an EDF motif, the other known functional domains are present. To determine whether the presence of the N1nT domain has similar effects on other members of the same protein family as observed for N1nT-N1b, a chimeric *Pro35S:N1nT-N2-V* gene construct (Fig. 66) was overexpressed in *N. benthamiana* leaf tissue. Similar to N1b, the N2 protein has a low hydrophobicity score in its N-terminal region. N-terminal fusion of N1nT increases this score to similar levels as observed for N1 (Fig. 59B) and N1nT-N1b (Fig. 62A).

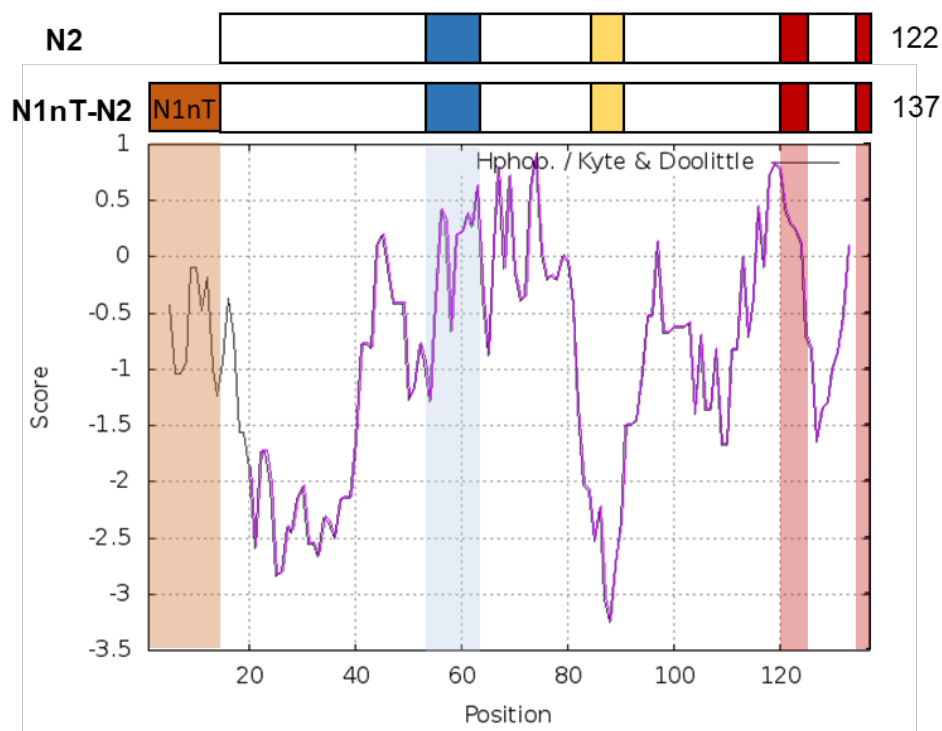
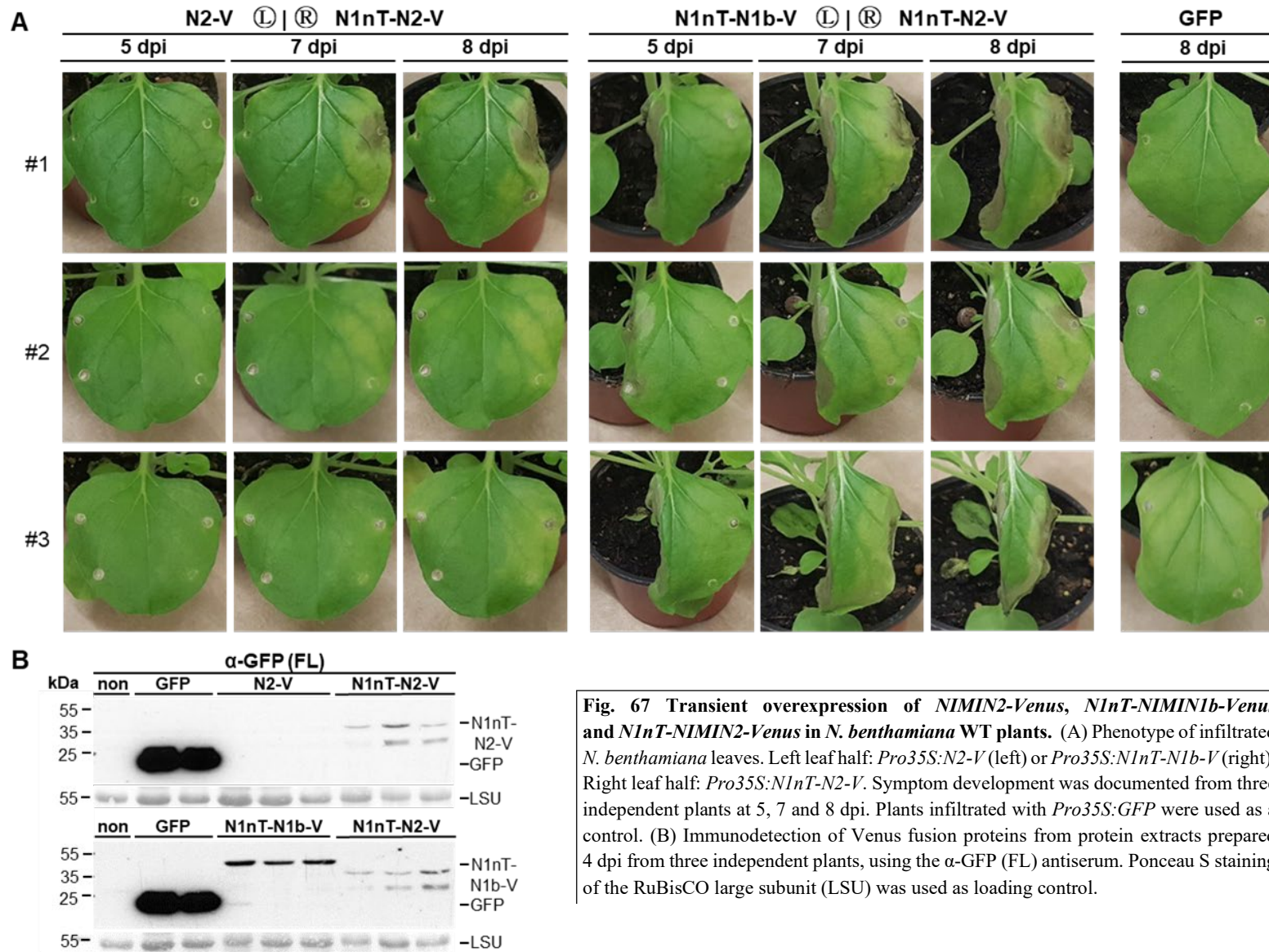


Fig. 66 Hydrophobic properties of N1nT-NIMIN2. Overlay of hydrophobicity diagrams of N2 (magenta) and N1nT-N2 (grey) created using the Kyte-Doolittle scale generated utilizing the ExPASy proteomics server. The N1nT domain is marked in orange. Protein-protein interaction domains are color coded as follows: DXFFK domain– blue, LxL/EAR domain – red.

While *N1nT-N1b-V* infiltrated leaf tissue exhibits strong necrosis after only five days post infiltration, cell death develops much slower for *N1nT-N2-V* (Fig. 67A). Small amounts of dead leaf tissue become visible seven days post infiltration accompanied with observable chlorosis in the surrounding infiltrated tissue. These necrotic patches increase in size after another day. When detecting protein accumulation using the α -GFP (FL) antiserum the N1nT-N2-V protein accumulates at the estimated size of 42 kDa while N2-V could not be detected (Fig. 67B). When compared directly to N1nT-N1b-V it becomes apparent that accumulation of N1nT-N2-V shows a discernable lower accumulation. These results show that while the N1nT region is able to enhance accumulation for both N1nT-N1b-V and N1nT-N2-V, which in both cases is accompanied by a gain of cell death promoting activity, this effect is much less pronounced for N1nT-N2-V.



4.4.2.3. Analysis of Venus proteins comprising the N1 N-terminal domain

N-terminal fusion of the N1nT region to two independent members of the NIMIN protein family from *Arabidopsis* has shown a significant enhancing effect on protein accumulation which is less pronounced for N1nT-N2-V than for N1nT-N1b-V. The next step was to determine if N-terminal fusion of this N1nT peptide to a completely unrelated protein can produce similar effects. While almost identical to GFP previous experiments have shown the differential detection of GFP and Venus proteins using the polyclonal α -GFP (FL) or the monoclonal α -GFP (MC) antiserum (see Appendix I), with the former detecting a much weaker signal for Venus than for GFP and the latter detecting signals of similar intensity. Therefore, Venus was chosen to generate another hybrid protein to be analyzed during transient overexpression (see Appendix V). The resulting N1nT-Venus protein has the advantage, that it can readily be detected using any of the two α -GFP antibodies without requiring any additional tags. To determine whether this hybrid protein has any phenotypical effects during transient overexpression, agrobacteria carrying *Pro35S:N1nT-V* were infiltrated into *N. benthamiana* leaf tissue (Fig. 68). Unlike *NI-V* overexpression of N1nT-V does not elicit accelerated emergence of cell death even 10 days post infiltration.

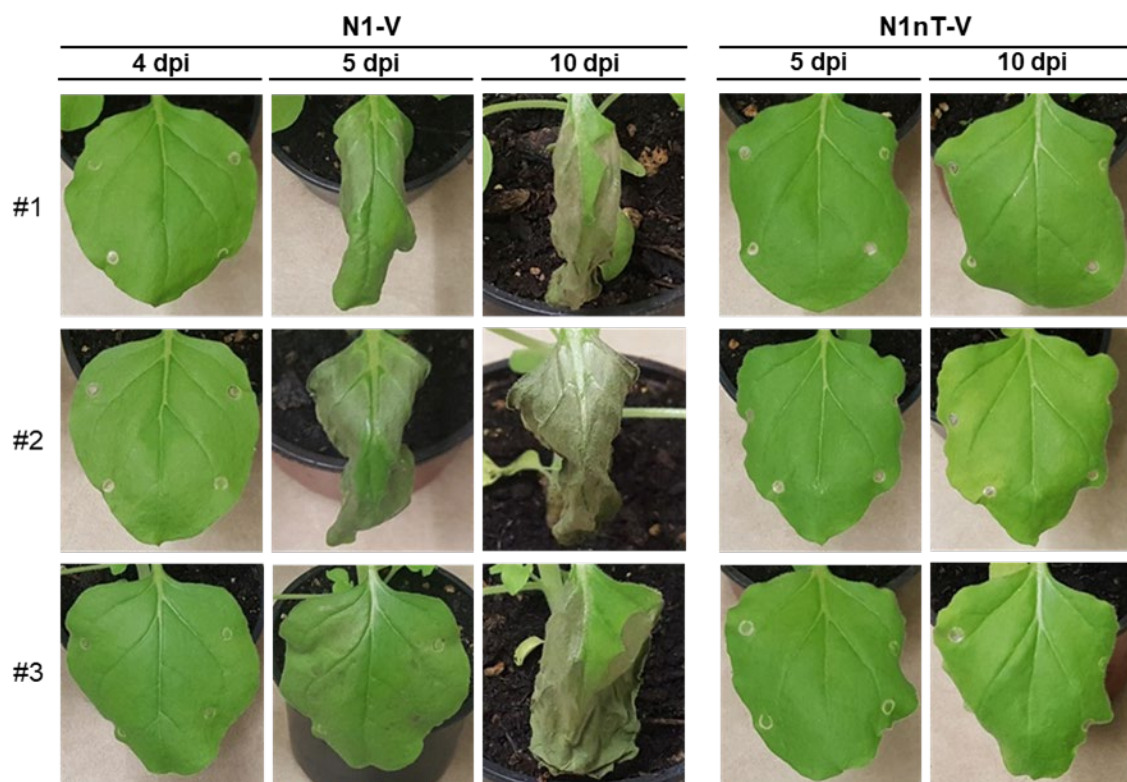


Fig. 68 Transient overexpression of *NIMIN1-Venus* and *N1nT-Venus* in *N. benthamiana* plants. Phenotype of infiltrated *N. benthamiana* leaves expressing either *Pro35S:NI-V* or *Pro35S:N1nT-V*. Symptom development was documented from three independent plants at 4, 5, and 10 dpi.

To compare N1nT-V protein accumulation to GFP and Venus, agrobacteria harboring *Pro35S:GFP*, *Pro35S:Venus* and *Pro35S:N1nT-Venus* were infiltrated into *N. benthamiana* leaf tissue. When infiltrated leaves were observed under UV light, GFP is strongly visible as a green-fluorescent area corresponding to the infiltrated leaf tissue (Fig. 69A). Meanwhile the *Venus* infiltrated area is only barely

4. Results

discernible. Interestingly, while still weaker than for overexpression of *GFP*, leaf tissue infiltrated with agrobacteria harboring *Pro35S:N1nT-V* shows clearly stronger fluorescence than tissues infiltrated with agrobacteria harboring *Pro35S:Venus*. To discern whether this increase in fluorescence is caused by increased protein accumulation, protein extracts from those plants were analyzed using the α -GFP (FL) antiserum. Immunodetection revealed that the N1nT-V protein accumulates much stronger at 27 kDa exhibiting a similar signal strength to GFP (Fig. 69B).

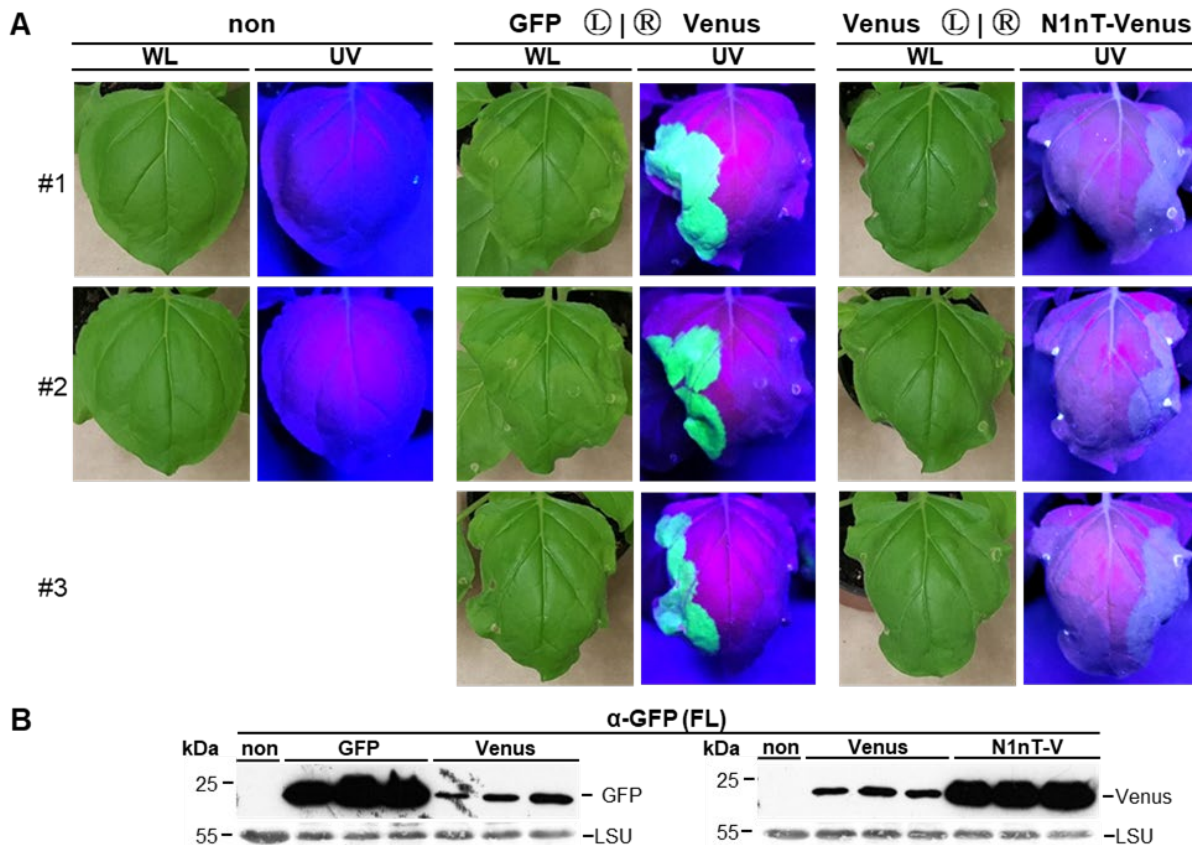


Fig. 69 Fluorescence and protein accumulation of N1nT-Venus in *N. benthamiana* plants. (A) Fluorescence of infiltrated *N. benthamiana* leaves. Left leaf half: *Pro35S:GFP* (middle) or *Pro35S:Venus* (right), right leaf half: *Pro35S:Venus* (middle) or *Pro35S:N1nT-V* (right). Pictures were taken from three independent plants under white light (WL) or ultraviolet (UV) light at 6 dpi. Noninfiltrated plants were used as controls. (B) Immunodetection of fluorescent proteins from protein extracts prepared 4 dpi from three independent plants, using the α -GFP (FL) antiserum.

The accumulation of proteins is often regulated by their degradation. To determine whether GFP, Venus or N1nT-Venus are a target of protease mediated degradation it was tested whether the activity of proteases affects the detectable amount of the fluorescent proteins. Therefore, protein extracts from infiltrated plant tissue overexpressing *GFP*, *Venus* and *N1nT-V* were incubated with specific proteases for using untreated protein extracts as controls (Fig. 70). The proteases chosen for this experiment were the serine proteases Proteinase K from *Engyodontium album* and Trypsin, as well as Papain, a plant-based cysteine protease from papaya. Application of the ExpASY Peptide Cutter tool [Gasteiger *et al.*, 2005] predicts 112 potential cleavage sites for Proteinase K in the GFP protein, 116 in the Venus protein and 124 in N1nT-V. For Trypsin 26 cleavage sites are predicted for both GFP and Venus, while N1nT-V contains an additional site within the N1nT region. Papain cleaves preferentially after an

arginine or lysine, following a hydrophobic residue with the restriction that no valine is on the other side of the cleavage site. Each of the proteins of interest harbors nine potential cleavage sites for Papain. After determining the concentration of protein extracts, 20 μg protein were adjusted to the same volume and the specific reaction buffers and proteases were added. The reactions using Proteinase K and Trypsin were incubated at 37 °C in a heating cabinet for 4 or 24 hours and analyzed using the α -GFP (FL) antiserum (Fig. 70A). On the other hand, the reactions with activated papain enzyme were incubated for 24, 48 and 72 hours at 55 °C in a thermocycler and analyzed using the α -GFP (MC) antiserum (Fig. 70B). To achieve similar signal strength to Venus while using the monoclonal α -GFP (MC) Antiserum, protein extracts from plants overexpressing *Pro35S:N1nT-V* were diluted 1:10 with a protein extract from noninfiltrated *N. benthamiana* leaves. For both experiments Ponceau S staining was used to determine the effect of proteases on background protein levels.

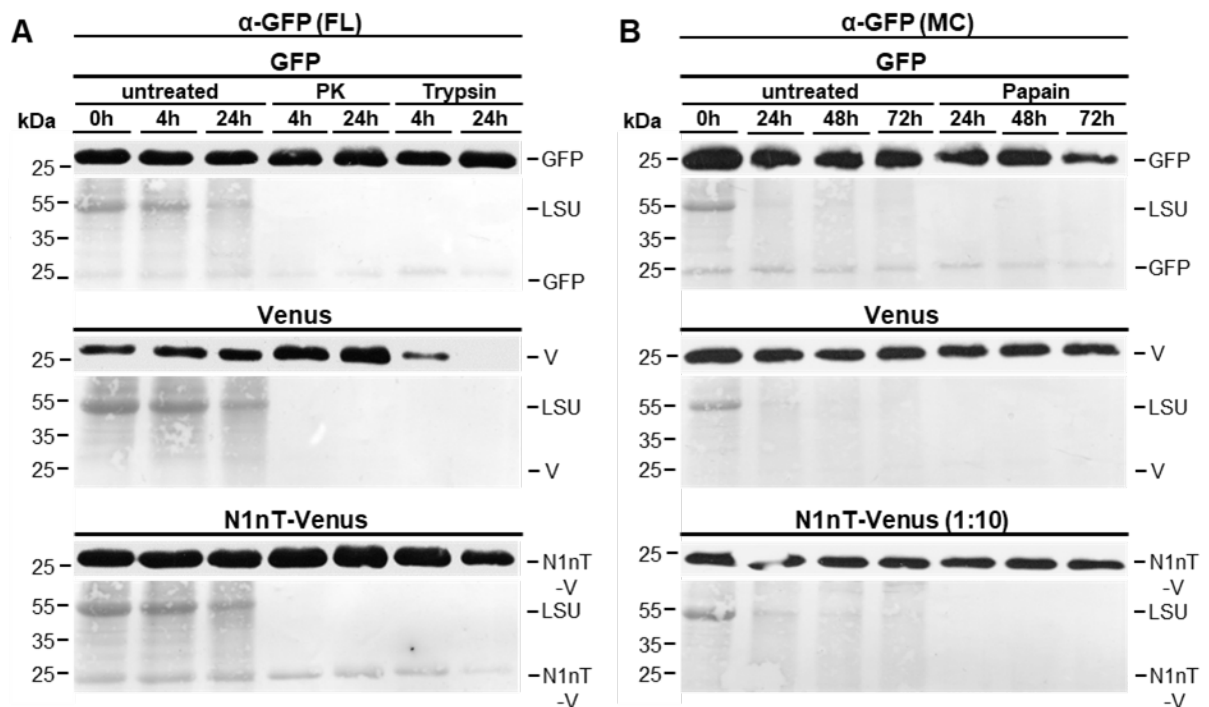


Fig. 70 Proteolytic degradation of the fluorescent proteins GFP, Venus and N1nT-Venus under influence of Proteinase K, Trypsin and Papain. Proteolytic degradation in protein extracts produced from *N. benthamiana* plants transiently overexpressing *Pro35S:GFP*, *Pro35S:Venus* or *Pro35S:N1nT-V*. Untreated extracts were incubated as controls. Ponceau S staining was used as a control for overall protein degradation. (A) Degradation of fluorescent proteins during incubation with Proteinase K or Trypsin. Aliquots of 20 μg protein were adjusted to the same volume and incubated for 4 and 24 h at 37 °C in a heat cabinet after application of Proteinase K (PK) or Trypsin. Untreated extracts were incubated as controls. Immunodetection was conducted using the α -GFP (FL) antiserum. The X-ray film for Venus was exposed for 10 min before developing, for GFP and N1nT-Venus the films were exposed for 20 seconds. (B) Degradation in protein extracts during incubation with Papain. Aliquots of 20 μg protein were adjusted to the same volume and incubated for 24, 48 and 72h at 55 °C in a thermocycler after application of Papain. Immunodetection was conducted using the α -GFP (MC) antiserum. A 1:10 dilution of the N1nT-V protein extract using an extract from noninfiltrated *N. benthamiana* plants was used to compensate the enhanced signal strength for N1nT-V detected by the α -GFP (MC) antiserum.

Ponceau S staining revealed an overall decrease in protein levels in untreated extracts after 24 h of incubation at 37 °C which is visible through the 55 kDa band corresponding to the RuBisCO LSU (Fig. 70A). By comparison 24h of incubation at 55 °C reduces the background levels of intrinsic innate plant proteins strongly even in absence of additional proteases with longer incubation times showing a complete disappearance of the RuBisCO LSU (Fig. 70B). Interestingly, immunodetection of GFP, Venus and N1nT-V shows no discernible decrease in signal strength for all three observed proteins (Fig. 70A,B), indicating a higher overall stability. Ponceau S staining showed that after incubation of protein extracts with any of the used proteases that background protein levels including the RuBisCO large subunit have completely vanished when compared to the untreated controls. This effect is already visible after 4 hours of incubation (Fig. 70A). At 27 kDa protein bands corresponding to GFP and N1nT-V are clearly visible in samples incubated with or without protease with no equivalent band visible for Venus or the 1:10 dilution of N1nT-V, confirming the much lower accumulation of Venus compared to GFP and N1nT-V (Fig. 70A,B). Immunodetection using the α -GFP antibodies revealed none of the proteins of interest is affected by Proteinase K (Fig. 70A) activity. Though, while GFP is unaffected by presence of Trypsin, the amount of Venus protein is visibly reduced after only 4 h of incubation with the signal completely gone after 24 h. This effect is much weaker for N1nT-Venus with only slight visible reduction in the amount of protein after 24 h of incubation. In contrast to Trypsin, which appears to have a greater effect on Venus and N1nT-V, immunodetection on protein extracts treated with Papain revealed no significant degradation of Venus and N1nT-Venus but limited reduction of GFP protein levels (Fig. 70B).

These results show that GFP, Venus and N1nT-Venus proteins are stable under proteolytic conditions mediated by Proteinase K but differ in their sensitivity towards Trypsin and Papain mediated degradation. In presence of Trypsin, Venus is visibly degraded while N1nT-V levels are only slightly reduced. This suggests that under specific conditions the N1nT-V proteins are more stable than their counterparts without N-terminal fusion of the N1nT domain.

As shown in the previous experiments, fusion of the N1nT region from N1 to the N-terminus of the weakly accumulating NIMIN proteins N1b and N2 (Fig. 63, 67), as well as to the fluorescent Venus protein (Fig. 69), enhances the accumulation of each of them. To determine if this effect is dependent on the position of the peptide in the amino acid chain, two different fusion constructs were generated. The first construct, N1b-N1nT-V has the N1nT domain fused to the C-terminus of N1b on the one side and to the N-terminus of Venus on the other side, while the second, V-N1nT, has N1nT fused to the C-terminus of Venus (see Appendix V). Infiltration of *N. benthamiana* leaf tissue with agrobacteria harboring *Pro35S:N1b-N1nT-V* for transient overexpression does not, unlike *Pro35S:N1nT-N1b-V*, promote the emergence of cell death (Fig. 71A). To determine if only the central position of the N1nT domain affects the accumulation of N1b-N1nT-V as well, protein extracts from the same plants were used for immunodetection. Using the α -GFP (FL) antiserum revealed a visible protein band at the expected 45 kDa for N1nT-N1b-V. However, for N1b-N1nT-V no detectable protein accumulation was visible on the X-ray film. (Fig. 71B).

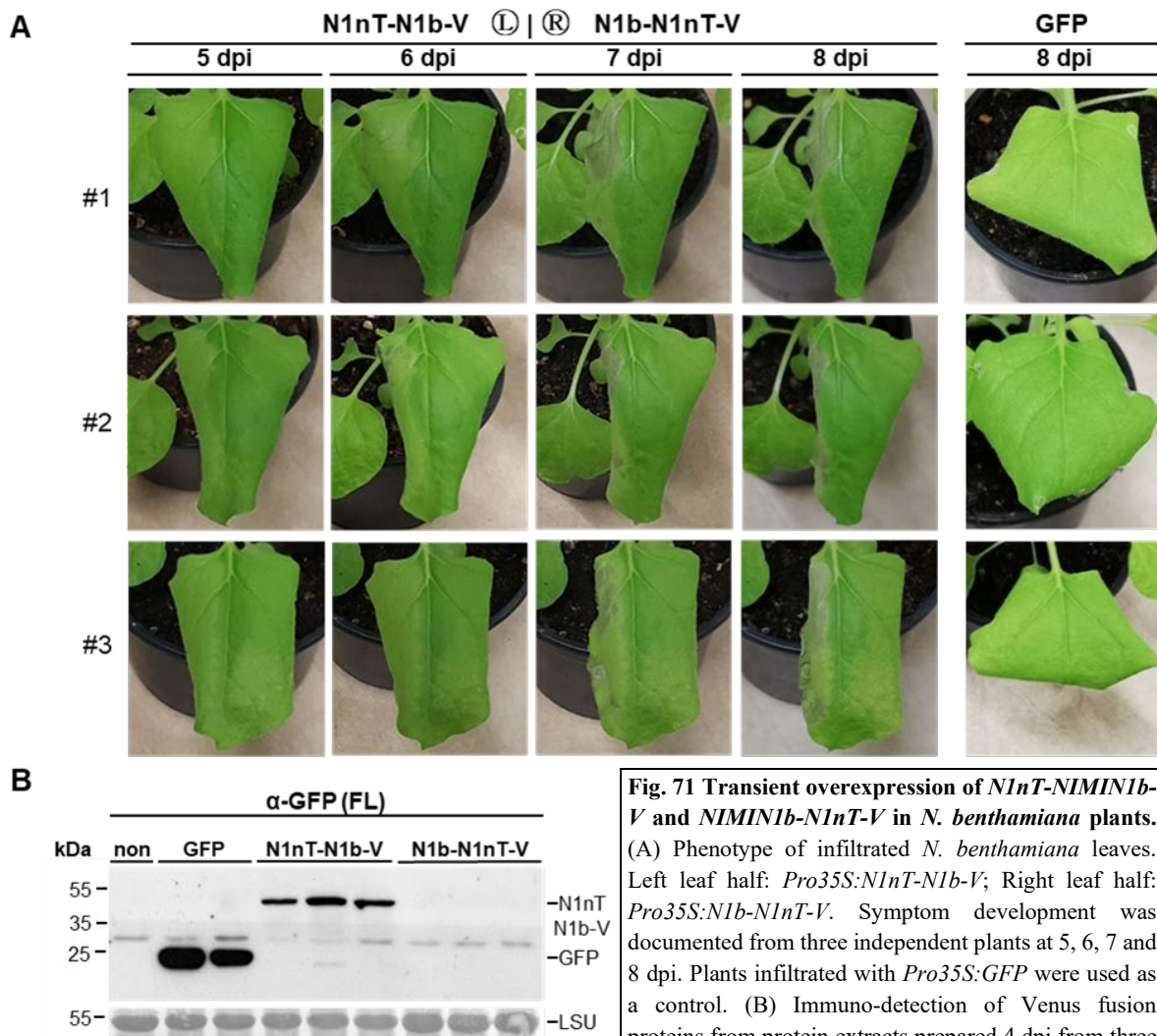


Fig. 71 Transient overexpression of *N1nT-NIMIN1b-V* and *NIMIN1b-N1nT-V* in *N. benthamiana* plants. (A) Phenotype of infiltrated *N. benthamiana* leaves. Left leaf half: *Pro35S:N1nT-N1b-V*; Right leaf half: *Pro35S:N1b-N1nT-V*. Symptom development was documented from three independent plants at 5, 6, 7 and 8 dpi. Plants infiltrated with *Pro35S:GFP* were used as a control. (B) Immuno-detection of Venus fusion proteins from protein extracts prepared 4 dpi from three independent plants, using the α -GFP (FL) antiserum. Ponceau S staining of the RuBisCO large subunit (LSU) was used as loading control.

4. Results

Similar to the absence of cell death during *N1b-N1nT-V* overexpression, during transient overexpression of *Pro35S:V-N1nT* there is less visible fluorescence as observed for *Pro35S:N1nT-V* (Fig. 72A). Surprisingly, no accumulation of V-N1nT could be detected (Fig. 72B), indicating that C-terminal fusion of the N1nT peptide to Venus might interfere with the binding of the α -GFP (FL) antiserum. Together with the observations from *N1b-N1nT-V*, these results show that placement of N1nT between N1b and Venus or at the C-terminus of Venus does not convey the same effects as N-terminal fusion.

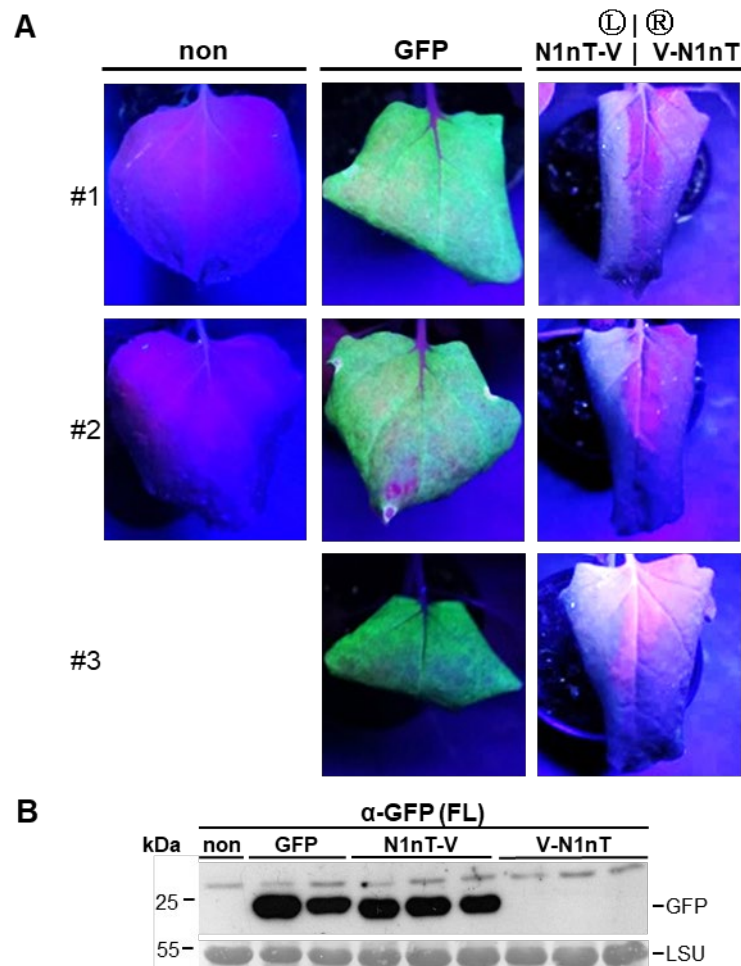


Fig. 72 Fluorescence and protein accumulation of N1nT-Venus and Venus-N1nT in *N. benthamiana* plants. (A) Fluorescence of infiltrated *N. benthamiana* leaves. Left leaf half: *Pro35S:N1nT-V*, Right leaf half: *Pro35S:V-N1nT*. Pictures were taken from three independent plants under UV light at 6 dpi. Noninfiltrated plants and plants infiltrated with *Pro35S:GFP* were used as a control. (B) Immunodetection of fluorescent proteins from protein extracts prepared 4 dpi from three independent plants, using the α -GFP (FL) antiserum. Ponceau S staining of the RuBisCO large subunit (LSU) was used as loading control.

4.4.2.4. Analysis of mutants in the N1 N-terminal domain

As shown in the previous section, the N-terminal position of the N1nT domain is important for its protein accumulation enhancing properties. Because the amino acid sequence is conserved among different plant species (Fig. 60), the question arose, which part of the N1nT sequence mediates the observed effects. In the context of these investigations several mutants harboring deletions or amino acid exchanges were generated (see Appendix V). The first likely targets for this analysis were the highly conserved triad of tyrosine, proline and lysine located at the N-terminus directly behind the starting

methionine, as well as the leucine residue at position eight. *N1nT-N1b-V* and the two mutants *N1nTΔ2-4-N1b-V* and *N1nT L8G-N1b-V* (Fig. 73A) were transiently overexpressed in leaf tissue of separate *N. benthamiana* plants to compare both, their cell death promoting activity, and accumulation. Like *N1nT-N1b-V*, both mutants display strong emergence of cell death after only 5 days post infiltration affecting the whole infiltrated leaf area after one more day (Fig. 73B). During immunodetection using the α -GFP (FL) antiserum *N1nTΔ2-4-N1b-V* and *N1nT L8G-N1b-V* can be detected as strong signals at 45 kDa with no visible decrease or banding pattern change compared to *N1nT-N1b-V* (Fig. 73C).

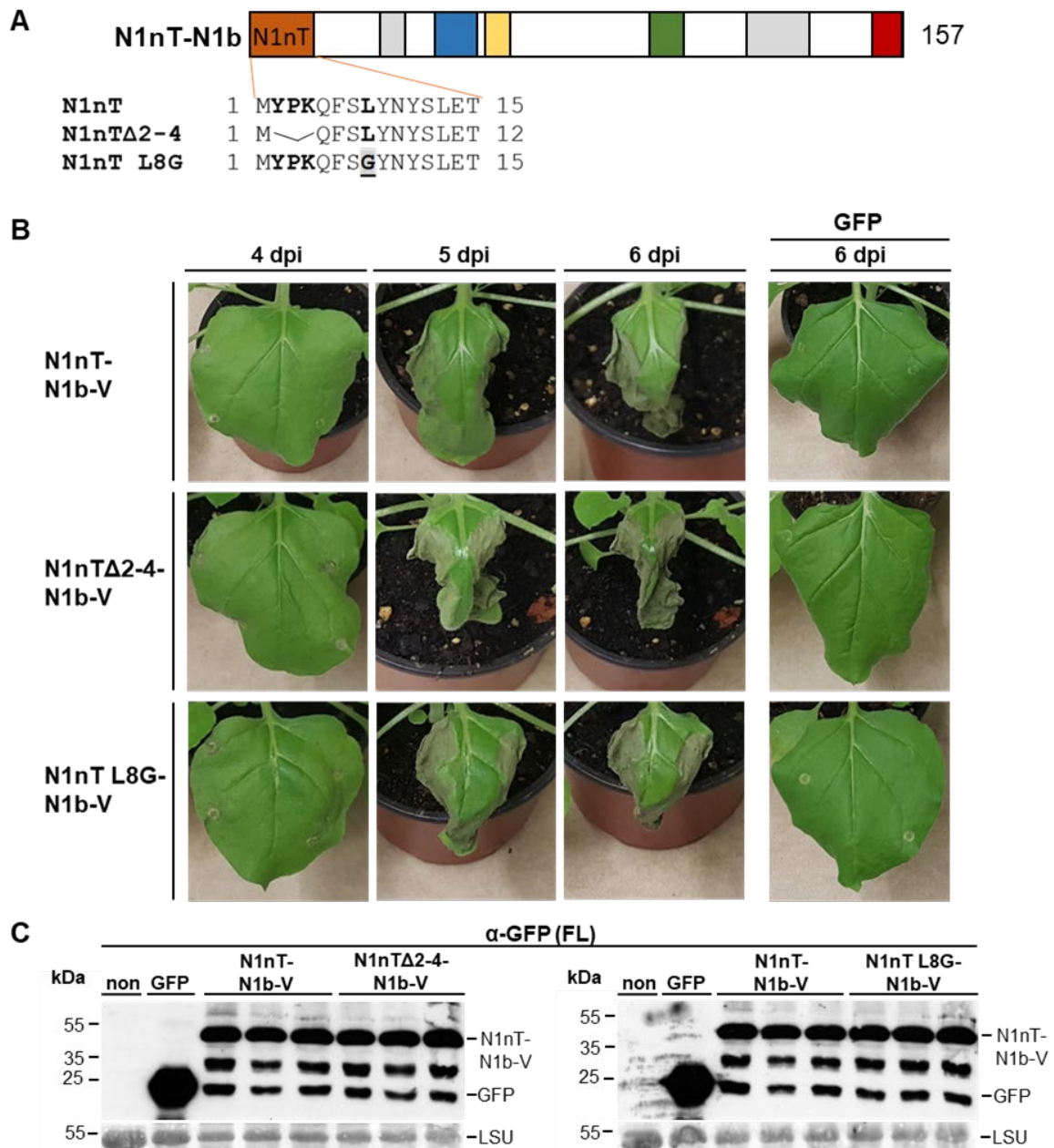


Fig. 73 Transient overexpression of *N1nT-NIMIN1b-Venus*, *N1nTΔ2-4-NIMIN1b-Venus* and *N1nT L8G-NIMIN1b-V* in *N. benthamiana* plants. (A) Schematic representation of N1nT-N1b indicating amino acid changes and deletions in the mutants. (B) Phenotype of infiltrated *N. benthamiana* leaves overexpressing *Pro35S:N1nT-N1b-V*, *Pro35S:N1nTΔ2-4-N1b-V* or *Pro35S:N1nT L8G-N1b-V* in both leaf halves. Symptom development was documented at 4, 5 and 6 dpi. A representative plant was chosen from three independent infiltrated plants. Plants infiltrated with *Pro35S:GFP* were used as a control. (C) Immunodetection of Venus fusion proteins from protein extracts prepared 4 dpi from three independent plants, using the α -GFP (FL) antiserum. Ponceau S staining of the RuBisCO large subunit (LSU) was used as loading control.

4. Results

As changes in the highly conserved amino acids produced no discernible effect, a mutant was generated in which the N1nT gene sections encoding the amino acids at positions two to nine were deleted. During transient overexpression, *Pro35S:N1nTΔ2-9-N1b-V* (Fig. 74A), like the previously observed mutants, does still promote the accelerated emergence of cell death (Fig. 74B). Likewise, the accumulation of the N1nTΔ2-9-N1b-V protein is not visibly reduced even without the removed eight amino acids (Fig. 74C).

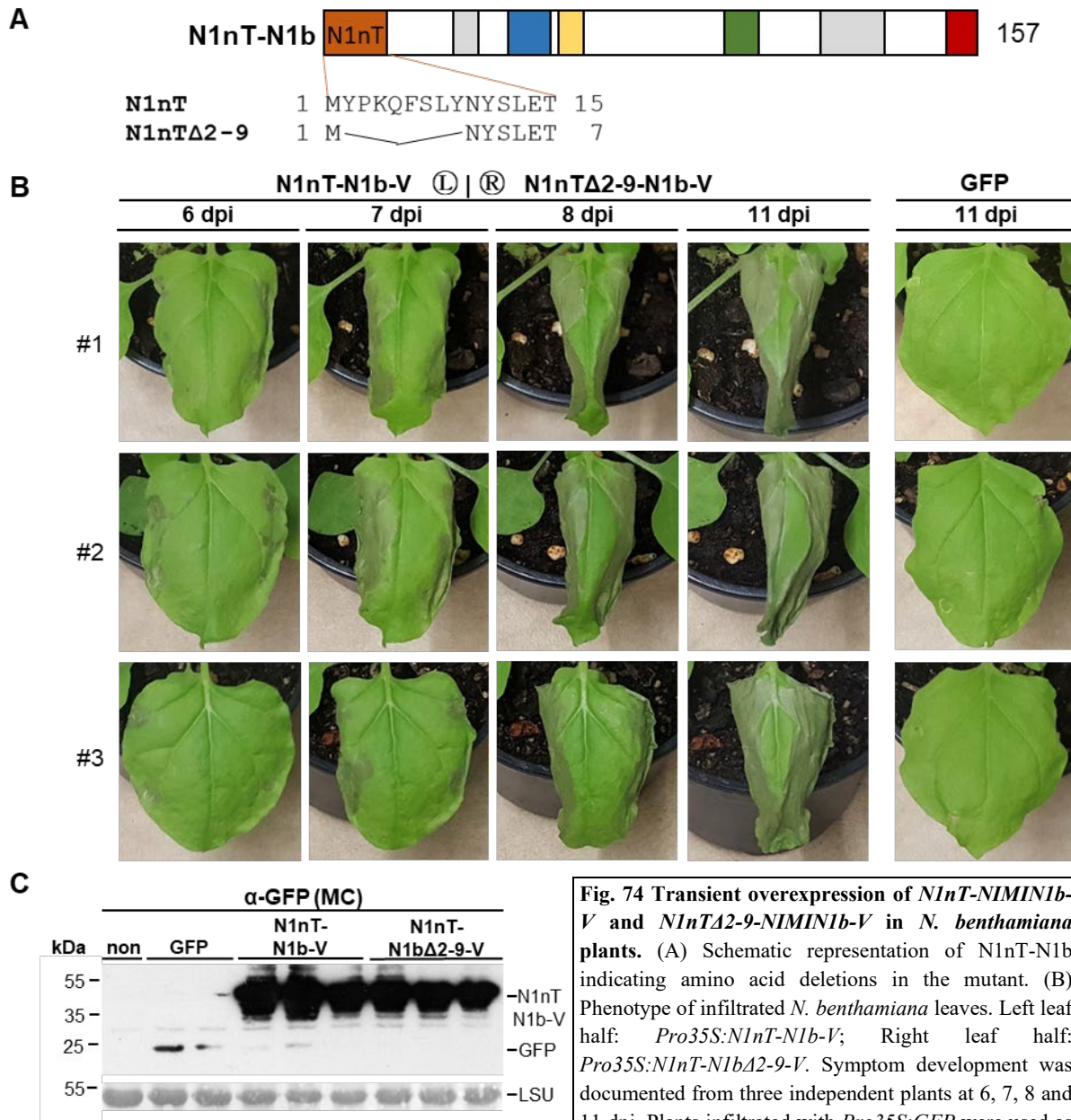


Fig. 74 Transient overexpression of *N1nT-N1b-V* and *N1nTΔ2-9-N1b-V* in *N. benthamiana* plants. (A) Schematic representation of N1nT-N1b indicating amino acid deletions in the mutant. (B) Phenotype of infiltrated *N. benthamiana* leaves. Left leaf half: *Pro35S:N1nT-N1b-V*; Right leaf half: *Pro35S:N1nT-N1bΔ2-9-V*. Symptom development was documented from three independent plants at 6, 7, 8 and 11 dpi. Plants infiltrated with *Pro35S:GFP* were used as a control. (C) Immunodetection of Venus fusion proteins from protein extracts prepared 4 dpi from three independent plants, using the α-GFP (MC) antiserum. Ponceau S staining of the RuBisCO large subunit (LSU) was used as

The N1nT sequence also contains several polar amino acid residues in its C-terminal moiety. A mutant harboring amino acid exchanges of two serine residues at positions 7 and 12 and two tyrosine residues at positions 9 and 11, all replaced with alanine residues, was used to determine if the polar properties of those amino acids are important for the function of the N1nT domain. Overexpression of *Pro35S:N1nT S7A Y9A Y11A S12A-N1b-V* (*N1nT SY-N1b-V*, Fig. 75A) revealed a strong delay in cell death emergence with necrotic tissue becoming visible at 11 days post infiltration, five days later than for *Pro35S:N1nT-N1b-V* (Fig. 75B). Interestingly, the N1nT SY-N1b-V fusion protein accumulates to similar levels as N1nT-N1b-V when detected using the α -GFP (MC) antiserum (Fig. 75C).

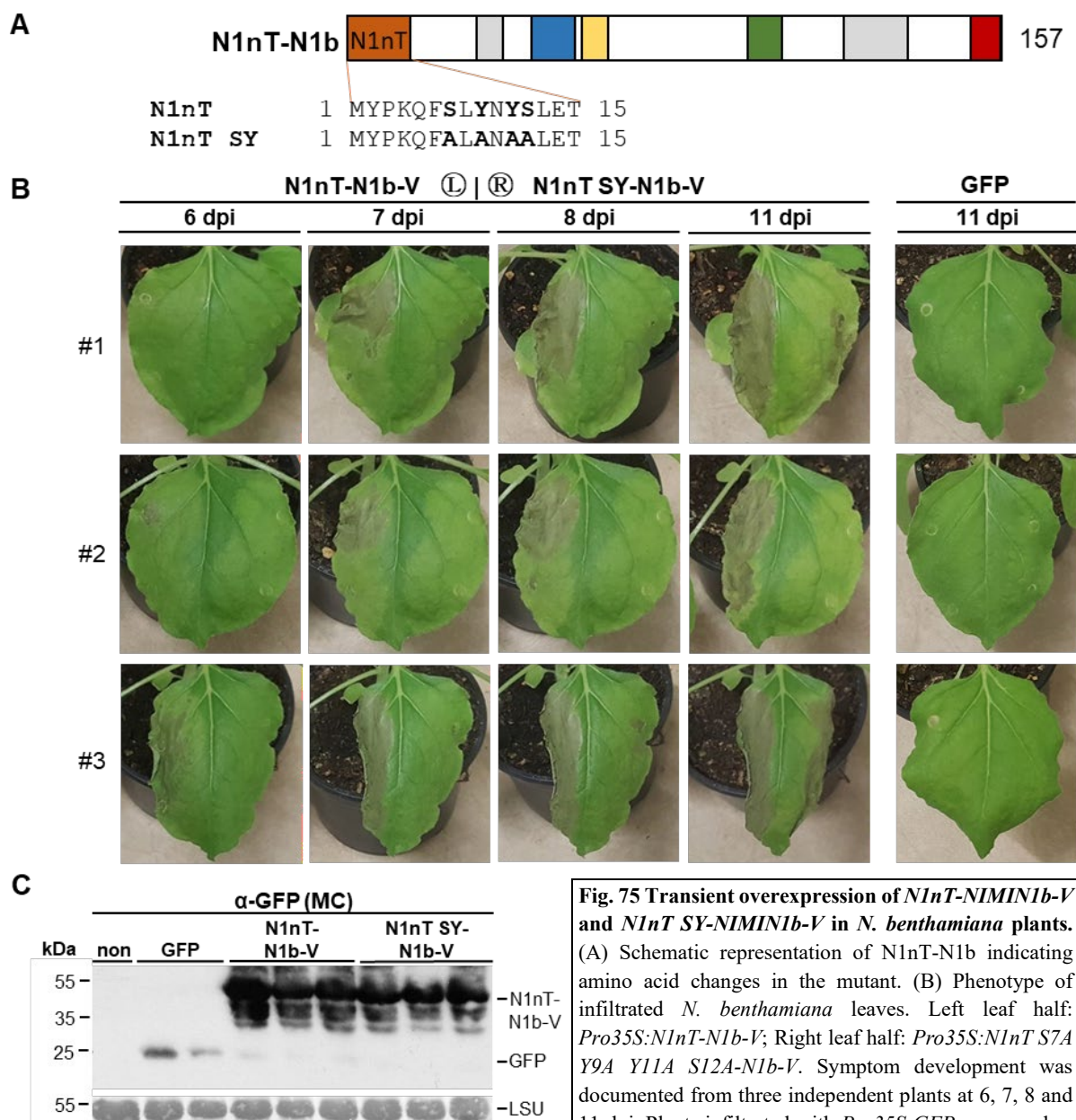


Fig. 75 Transient overexpression of *N1nT-N1b-V* and *N1nT SY-N1b-V* in *N. benthamiana* plants. (A) Schematic representation of N1nT-N1b indicating amino acid changes in the mutant. (B) Phenotype of infiltrated *N. benthamiana* leaves. Left leaf half: *Pro35S:N1nT-N1b-V*; Right leaf half: *Pro35S:N1nT S7A Y9A Y11A S12A-N1b-V*. Symptom development was documented from three independent plants at 6, 7, 8 and 11 dpi. Plants infiltrated with *Pro35S:GFP* were used as a control. (C) Immunodetection of Venus fusion proteins from protein extracts prepared 4 dpi from three independent plants, using the α -GFP (MC) antiserum. Ponceau S staining of the RuBisCO large subunit (LSU) was used as loading control.

4. Results

None of the previously observed mutations has significant effects on the accumulation of the chimeric N1nT-N1b-Venus proteins. To observe if translation of the N1nT peptide is actually required, a mutant in which the ATG for translation initiation is replaced by CTG was created. In this *Pro35S:N1nT MIL-N1b-V* mutant translation should be initiated at the natural ATG codon found in the *N1b* ORF and lead to the synthesis of a N1b-Venus protein (Fig. 76A). Contrary to the expectations, *Agrobacterium* mediated transient overexpression of *N1nT MIL-N1b-V* does not reduce the cell death promoting activity compared to *N1nT-N1b-V* (Fig. 76B) and the resulting protein accumulates to similar levels, showing strong signals at 45 kDa (Fig. 76C).

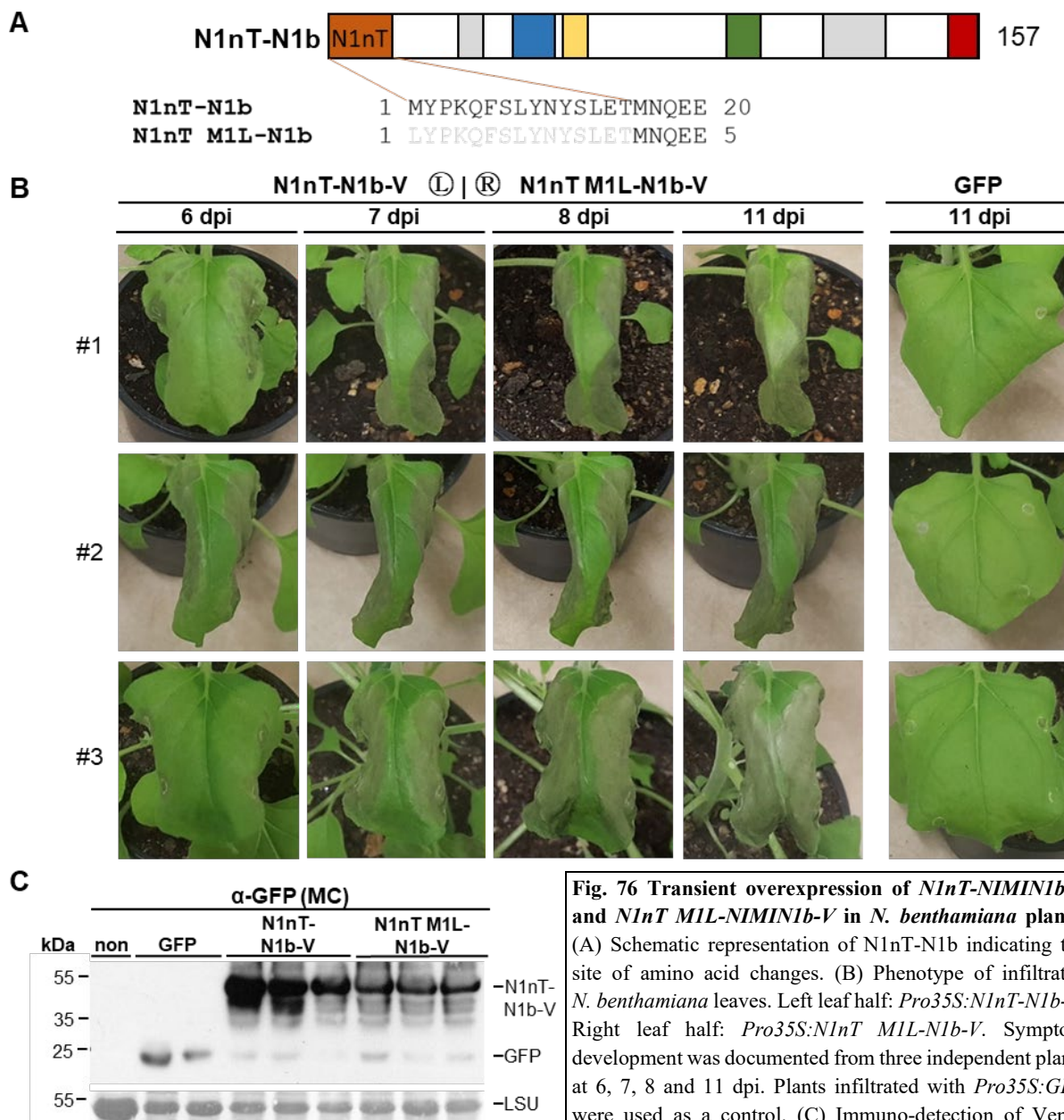


Fig. 76 Transient overexpression of *N1nT-N1b-V* and *N1nT M1L-N1b-V* in *N. benthamiana* plants. (A) Schematic representation of N1nT-N1b indicating the site of amino acid changes. (B) Phenotype of infiltrated *N. benthamiana* leaves. Left leaf half: *Pro35S:N1nT-N1b-V*; Right leaf half: *Pro35S:N1nT M1L-N1b-V*. Symptom development was documented from three independent plants at 6, 7, 8 and 11 dpi. Plants infiltrated with *Pro35S:GFP* were used as a control. (C) Immuno-detection of Venus fusion proteins from protein extracts prepared 4 dpi from three independent plants, using the α-GFP (MC) antiserum. Ponceau S staining of the RuBisCO large subunit (LSU) was used as loading control.

To confirm the increased accumulation even in presence of a mutant start codon of the N1nT domain, an equivalent *N1nT MIL-Venus* mutant was generated (Fig. 77A). As an additional control a *N1nTΔ2-9-Venus* mutant was used as deletion of the amino acids 2-9 was shown to have no effect on the emergence of cell death and accumulation of the hybrid protein. Both *N1nTΔ2-9-V* and *N1nT MIL-V* show similar levels of fluorescence as observed for *N1nT-V* (Fig. 77B). Likewise, protein accumulation of both proteins is unaffected by the introduction of those mutations (Fig. 77C) confirming the observations made for *N1nT-N1b-V*.

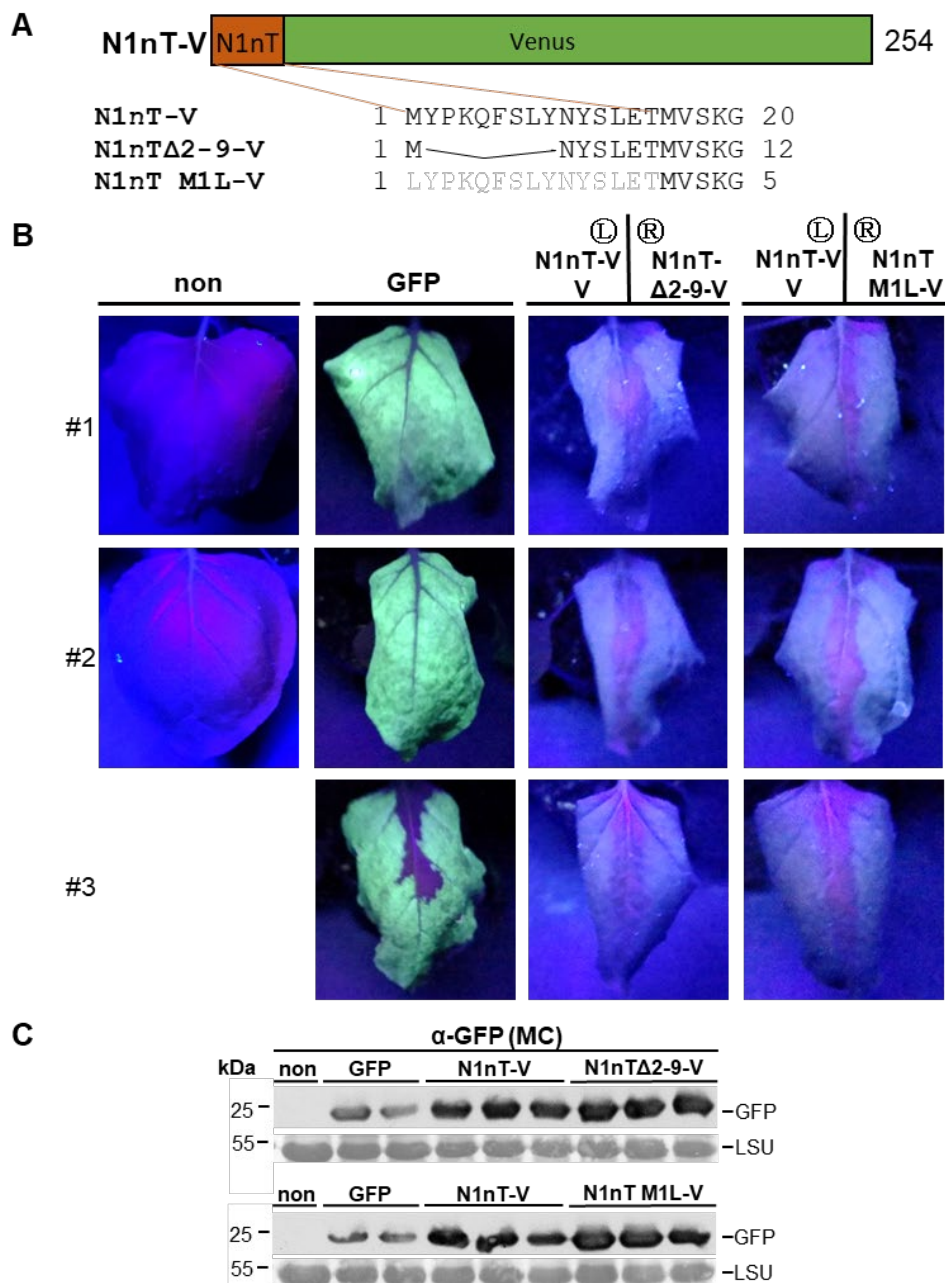


Fig. 77 Fluorescence and protein accumulation of N1nT-Venus, N1nTΔ2-9-Venus and N1nT MIL-Venus in *N. benthamiana* WT plants. (A) Schematic representation of N1nT-V indicating amino acid deletions in the mutant. (B) Fluorescence of infiltrated *N. benthamiana* leaves. Left leaf half: *Pro35S:N1nT-V*, Right leaf half: *Pro35S:N1nTΔ2-9-V* or *Pro35S:N1nT MIL-V*. Pictures were taken from three independent plants under UV light at 6 dpi. Noninfiltrated plants and plants infiltrated with *Pro35S:GFP* were used as a control. (C) Immunodetection of fluorescent proteins from protein extracts prepared 4 dpi from three independent plants, using the α-GFP (MC) antiserum. Ponceau S staining of the RuBisCO large subunit (LSU) was used as loading control.

4. Results

To ensure the correct introduction of the M1L mutant, binary vector plasmid DNA from both *E. coli* DH5 α and *A. tumefaciens* LBA4404 strains harboring the relevant gene constructs was isolated and analyzed using PCR and restriction digestion. Amplification of the introduced gene constructs using the primer combination 35S/Venus-2 produced amplicons of the expected sizes of about 500 bp for *N1nT-V* and *N1nT MIL-V*, and 950 bp for *N1nT-N1b-V* and *N1nT MIL-N1b-V*, respectively (Fig. 78A). The introduction of the M1L mutant removes a *NdeI* restriction site, which encompasses the start codon. The pBin19 vector also contains a single *NdeI* restriction site about 2.5 kb behind the NOS terminator. Vector DNA containing *N1nT-V* or *N1nT-N1b-V* is cut at both sites and produces two fragments at 10 kb and 3.5 kb for *N1nT-V* or 4 kb for *N1nT-N1b-V*, respectively (Fig. 78B). Meanwhile vector DNA containing *N1nT MIL-V* or *N1nT MIL-N1b-V* is only cut once and linearized to a fragment size of around 14 kDa. These results together with sequence data confirm the correct introduction of the M1L mutation into the N1nT domain of both *N1nT MIL-V* and *N1nT MIL-N1b-V* and show that the effect of the N1nT domain is not dependent on a functional start codon.

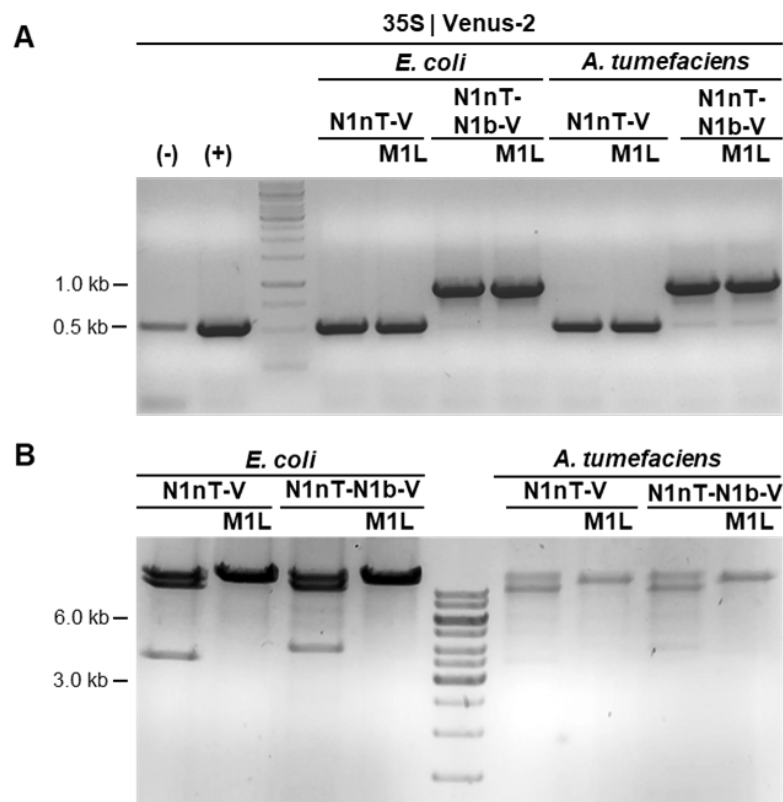


Fig. 78 Amplification and analytic restriction of chimeric N1nT and N1nT M1L gene constructs. (A) PCR amplification of *Pro35S:N1nT-V* and *Pro35S:N1nT-N1b-V* and their respective M1L mutants using the primers combination 35S/Venus-2. pBin19 plasmid DNA extracted from *E. coli* or *A. tumefaciens* was used as template. H₂O was used as negative control (-). Plasmid DNA harboring *Pro35S:NI-V* was used as positive control (+). Plasmid DNA was diluted 1:1000. The size of the amplicons is around 500 bp for *N1nT-V* and *N1nT MIL-V* and 950 kb for *N1nT-N1b-V* and *N1nT MIL-N1b-V*. (B) *NdeI* restriction digestion of pBin19 plasmid DNA containing *Pro35S:N1nT-V* and *Pro35S:N1nT-N1b-V* and their respective M1L mutants.

5. Discussion

Due to their sessile nature plants are unable to completely evade detrimental abiotic and biotic environmental influences. Therefore, they had to develop a variety of passive and active defense mechanisms, allowing them to react to threats in a stimulus-specific manner. The defense responses are often orchestrated by different phytohormones depending on the nature of the respective pathogen. In case of infestation by biotrophic pathogens plants establish a long-lasting broad-spectrum resistance against a variety of different pathogens like bacteria, fungi, and viruses. This immune response, called systemic acquired resistance (SAR), is typically associated with an increase of endogenous levels of salicylic acid and the accumulation of PR-Proteins. Due to the strong correlation between SAR establishment and *PR* gene expression, *PR1* is typically recognized as a molecular marker for SAR response. Experiments by independent working groups have identified NPR1 (also NIM1/SAI1) as the central regulator of SAR (see 1.2.2.). While NPR1 was recently shown to act as the receptor for SA by undergoing intramolecular rearrangements, the exact mechanisms behind regulation of *PR1* gene expression must still be clarified. As NPR1 does not contain known DNA-binding domains, it exerts its functions through interaction with other proteins. NPR1 is known to interact with members of two protein families associated with gene regulation: TGA transcription factors and NIMIN proteins. The TGA factors are members of the bZIP-transcription factors and were shown to mediate DNA binding to *as-1* and *as-1*-like elements, as they can also be found in *PR1* promoters. The NIMIN protein family was discovered during a screening of an *Arabidopsis thaliana* cDNA library using NPR1 as bait and consists of four known members – NIMIN1, NIMIN1b, NIMIN2, and NIMIN3 [Weigel *et al.*, 2001]. NIMIN proteins have also been documented in other higher plants like tobacco, which harbors six members of the NIMIN family [Zwicker *et al.*, 2007, Masroor, 2013, U. M. Pfitzner personal communication], and rice, containing four NIMIN proteins [Chern *et al.*, 2005b]. During SAR establishment NIMIN genes are expressed differentially and NIMIN proteins, together with NPR1 and TGA transcription factors, can assemble into ternary complexes on the *as-1*-like element of the *PR1* promoter. The ability of some NIMIN proteins to suppress the SA-mediated induction of this promoter suggests an important role of NIMIN proteins as regulators of the SAR response [Hermann *et al.*, 2013]. Transient overexpression experiments revealed that certain NIMIN proteins can promote cell death in affected tissues [Masroor, 2013].

The aim of this work was to gain further insight into gene expression patterns of different *NIMIN* genes, with special attention being given to the elusive *NIMIN1b*. Additionally, the properties of different NIMIN proteins from *Arabidopsis* and tobacco were compared and analyzed to determine differences in their regulatory and cell-death promoting activity, and to decipher the underlying mechanisms by which they mediate these functions. In the context of these experiments close attention was given to the examination of different functional domains and protein accumulation.

5.1. The *NIMIN1* and *NIMIN2* promoters are regulated similarly to *PR1a*

The *NIMIN* genes from *Arabidopsis* are expressed differentially during SAR establishment. As *NIMIN3* was shown to be expressed constitutively at low levels and is not responsive to plant defense signals like SA or JA it is assumed that *N3* suppresses the activation of NPR1-dependent genes in unchallenged plants and may be relieved from NPR1 by rising levels of SA emerging during SAR establishment [Glocova *et al.*, 2005; Hermann *et al.*, 2013]. In contrast to *N3*, the promoters of *NIMIN1* and *NIMIN2*, like the promoter of *PR1a*, are induced by SA and functional analogs, but show repressing influence of JA signaling during simultaneous treatment with JA and SA [Hermann, 2009]. However, comparative analysis also revealed differences in temporal expression kinetics, tissue specificity, as well as sensitivity to other signal substances. During SAR establishment, *N1*, *N2*, and *PR1a* are induced in a clear chronological sequence. The *N2* gene was categorized as an immediate early SA responsive gene as its expression begins within 30 min after SA treatment and reaches its maximum after only 1 h, which is maintained for 24 hours. *N1* gene expression on the other hand is even more transient with transcripts accumulating about 2 h after application of SA. This expression is already shut down around 10 h after the treatment at the same time as *PR1* transcripts begin to arise. Induction of *N1/N2* gene expression, unlike *PR1a*, which is predominantly active in leaf tissue, was also shown in root tissue [Hermann *et al.*, 2013] and relies only on SA but not on HR-associated cell death signals [Glocova *et al.*, 2005].

In this study, to further elucidate the similarities and differences in the activity of *N1* and *N2* promoters, reporter gene expression was compared after application of known inducers, including SA and the functional analog BTH, and other defense signaling molecules including 3,5-dichloroanthranilic acid and pipecolic acid (Fig. 6). Confirming the results by Glocova *et al.* [2005], the *N1* and *N2* promoters, like *PR1a*, can be induced by both SA and BTH, but not the structural but non-functional analog 4-hydroxybenzoic acid, which carries the hydroxy group in para position rather than ortho position when compared to SA (Fig. 7B). Neither 3,5-dichloroanthranilic acid, which is associated with the immune response against the oomycete pathogen *Hyaloperonospora parasitica*, as well as *Pseudomonas syringae*, nor its structural analog anthranilic acid [Knoth *et al.*, 2009] are able to significantly induce one of the examined promoters (Fig. 7C,D). This highlights the high specificity of *N1* and *N2* promoters toward SA. Interestingly, while the *PR1a* promoter can be induced by pipecolic acid, which, together with its derivate N-hydroxypipecolic acid, has been shown to be the systemic signals required for long-distance signalling during SAR [Návarová *et al.*, 2012; Ding *et al.*, 2016; Hartmann *et al.*, 2017], neither *NIMIN* promoter is affected by Pip (Fig. 7D).

The similar induction profiles after chemical induction of *PR1a*, *N1*, and *N2* promoters correlate with their sequential induction during SAR establishment (Fig. 7). However, when comparing the overall total strength of promoter induction, the *N2* promoter shows a much weaker induction than the *PR1a* or *N1* promoters. This coincides with earlier observations showing that *N2* gene expression, unlike *N1* and *PR1a*, is clearly detectable in plants carrying *npr1* mutants. Also, while *NIMIN1* is only expressed after

induction, the *NIMIN2* gene is occasionally found active without previous chemical treatment [Hermann *et al.*, 2013]. This could imply that SA-mediated induction of *N2* is not sufficient to achieve equal levels of gene expression and that other pathways might be involved. This is further supported by the observation that transient overexpression of *N1-Venus*, but not *N2-Venus*, negatively affects the reporter gene expression from the *N1* promoter (Fig. 20B), mimicking the effects observed for the *PR1a* promoter (Fig. 16B, 17C), while the effect on the *N2* promoter is much less pronounced (Fig. 20C, D). These observations support the hypothesis by Hermann *et al.* [2013], which suggests separate pathways to be involved in the induction of *N1* and *N2* promoters and that *NIMIN2* expression may only be partially dependent upon NPR1. As all three promoters carry *as-1* like sequences containing TGACG motifs, which were shown to interact with TGA transcription factors in yeast [Hermann, 2009.] and expression from the *PR1a* promoter is regulated by the SA-sensitive interaction between NPR1 and NIMIN proteins [Zwicker *et al.*, 2007; Hermann *et al.*, 2013], this also hints at the existence of some form of autoregulatory negative feedback loop during the regulation of *NIMIN* gene expression.

Autoregulatory feedback loops are common elements in the regulation of gene expression of transcription factors or other transcriptional regulators, and examples can be found in all living organisms including pro- and eukaryotes. For example, the human transcriptional regulator NF- κ B (nuclear factor binding near the κ light-chain gene in B cells), which has been shown to be involved in gene induction during a variety of cellular responses including inflammation during the immune response, is inhibited in unstimulated cells through its interaction with proteins of the I κ B (Inhibitor of κ B) family [Ghosh & Hayden, 2012; Zhang *et al.*, 2017b]. After cytokine stimulation I κ B α and I κ B β are phosphorylated and undergo selective proteolysis, allowing NF- κ B translocate into the nucleus to induce the transcription of target genes including one of its own inhibitors – I κ B α [Han *et al.*, 1999]. Interestingly, NPR1 and I κ B share substantial homology in their amino acid sequences especially in regions containing ankyrin repeats [Ryals *et al.*, 1997], which could be indicative of similar underlying control mechanisms. In plants, activation of the basic helix-loop-helix (bHLH) transcription factor MYC2, the master regulator of JA responses regarding mechanical wounding or infestation with necrotrophic pathogens, is inactivated by a repression complex consisting of Jasmonate-ZIM domain (JAZ) proteins and the transcriptional co-repressor TOPLESS, preventing the induction of JA responsive genes [Chini *et al.*, 2007; Pauwels *et al.*, 2010; Fernández-Calvo *et al.*, 2011]. The presence of jasmonoyl-isoleucine (JA-Ile) triggers degradation of JAZ proteins allowing MYC2 to induce transcriptional activation of target genes by interaction with the MED25 subunit of the plant Mediator complex [Cevik *et al.*, 2012; Liu *et al.*, 2019]. MYC2 is involved in the activation of the JA-inducible Myc2-targeted bHLH (MTB) proteins MTB1, MTB2 and MTB3 which in turn negatively regulate JA regulated transcriptional responses by interfering with the formation of the MYC2-MED25 complex [Liu *et al.*, 2019]. It has also been recently shown in *Arabidopsis* that NPR1 can promote its own expression in a SA-dependent manner by recruiting the Cyclin-dependent Kinase 8 (CDK8) and the WRKY18 transcription factor [Chen *et al.*, 2019].

While the results indicate similar regulation of *NI* and *N2* promoters when compared to the *PR1a* promoter, there are still open questions regarding the differences between their expression profiles. Examination of gene expression from the *N2* promoter might help to identify other factors involved in its regulation, which cause the NPR1 independent expression of *N2*. Also, closer investigation of the partial induction of the *PR1a* promoter by exogenous application of Pip could help to identify a Pip responsive element within the *PR1a* promoter.

5.2. The activity of the *NIMIN1b* promoter remains ambiguous

The *NIMIN1b* gene was identified during comparison of the NIMIN proteins to DNA sequence databases by using a BLAST search [Altschul *et al.*, 1990]. The N1b protein is highly similar to N1 (38 % identity, 67 % similarity) and shows a comparably strong interaction with AtNPR1 in yeast [Weigel *et al.*, 2001]. Like the promoters of *NI* and *N2*, the *N1b* promoter also contains a TCACG motif, which is however, in contrast to the previously mentioned, close to the 5' end of the promoter region between positions -1033 and -1038 and consists of only a single TGACG sequence. Previous reports on the expression from the *N1b* promoter were unable to verify promoter activity during development or after chemical induction in Arabidopsis or transgenic tobacco plants. The research by Meike Hermann could not detect the presence of *N1b* transcripts in Arabidopsis seedlings or plants, even when observing different types of tissues including cotyledons, the shoot axis, or roots. Chemical induction by SA was also unable to induce detectable accumulation of *N1b* mRNA in all studied tissues. Similarly, neither the functional analog BTH nor the SAR antagonist jasmonic acid showed any involvement in the activation of the *N1b* promoter. A reporter gene based approach using a *ProN1b:GUS* construct transformed into transgenic tobacco plants was also unable to detect gene expression from the *N1b* promoter during examination of leaf tissue or during histochemical analysis of seedlings, independent of SA application. This led to the assumption that *N1b* might be an inoperative pseudo-gene, which does not show transcriptional activity [Hermann, 2009].

To determine if the promoter of *N1b* could be active only during specific phases of development and to determine the respective tissues, the pro-apoptotic human *Bax* gene was used as a more visible marker for gene expression. While *Bax* expression from the *NI* promoter in transgenic tobacco seeds was inducible by presence of SA in the medium, which completely prevented the germination of seeds containing the reporter construct (Fig. 9,10,11), the *ProN1b:Bax* construct did not produce similar symptoms in presence or absence of SA. Likewise, chemical treatment of grown tobacco plants using SA or BTH was able to induce *Bax* expression from the *NI* promoter, resulting in strong development of cell death, but not from the *N1b* promoter (Fig. 12). These results indicate that *N1b* is unlikely to be involved in the same SA mediated induction process that mediates the expression of *NI*, *N2* and *PR1* genes. As no spontaneous emergence of cell death or other noticeable phenotypes could be observed during the development of untreated *ProNI:Bax* and *ProN1b:Bax* plants during their whole life cycle,

it can be assumed that both promoters are inactive in absence of exogenous induction. Together this confirms the observations made by Meike Hermann [Hermann, 2009].

Interestingly, during transient overexpression in *Nicotiana benthamiana* leaves, tissues infiltrated with agrobacteria harboring *ProNI:Bax* and *ProN1b:Bax* showed strong development of cell death. This development was considerably slower if the *Bax* gene was expressed from the *N1b* promoter (Fig. 8). This is also supported by previous observations using the *N1* and *N1b* promoters for regulation of transient expression of the *GUS* reporter gene (U.M. Pfitzner, personal communication). While the 1135 bp upstream promoter region *N1b* is functional during expression of two independent reporter genes the extent of its activity during the natural development of the plant must remain open for further investigation. As of now, the *N1b* promoter is only active under the specific circumstances as prevalent during *Agrobacterium* mediated transient overexpression. To gain further insight it will be required to identify factors differing between classical SAR establishment and other defense reactions emerging during agrobacteria infestation.

5.3. Some NIMIN proteins promote cell death during transient overexpression in *N. benthamiana* and in transgenic tobacco plants

Since their discovery in 2001 [Weigel *et al.*, 2001], different NIMIN proteins from Arabidopsis, as well as from tobacco and rice, have been studied regarding their biochemical properties in quite some detail. However, most of these studies focused primarily on their regulatory functions during the induction of defense related genes like *PR1a*, which play an important role during SAR establishment. Ashir Masroor first described his observations of the emergence of cell death of some NIMIN proteins during transient overexpression in *N. benthamiana* leaf tissue [Masroor, 2013]. These observations could be confirmed in this study (Fig. 13).

For more thorough analysis of this phenomenon NIMIN-Venus fusion proteins were used. The utilization of the fluorescent protein Venus as a tag not only allowed easy detection of NIMIN protein accumulation during transient overexpression (e.g. Fig. 4B) and in transgenic plants (e.g. Fig. 28C), but also allowed to confirm the cellular co-localization of N1-V and similarly constructed NPR1-V and NPR3-V fusion proteins (Fig. 5). The Venus tag does not interfere with the interaction between N1 and NPR1 in yeast (Fig. 14) or with the cell death promoting activity displayed during transient overexpression in *N. benthamiana* leaf tissue (Fig. 15), making utilization of Venus-tagged fusion proteins a highly effective tool when directly comparing different NIMIN proteins. Interestingly, N1-V promotes cell death even stronger than N1 (Fig. 16A). As Venus, like GFP, is a very stable protein under different environmental conditions, the stronger induction of this phenotype suggests that Venus might stabilize the N1 protein to some extent.

Side by side comparison of transient overexpression of N1-V and other NIMIN-Venus fusion proteins from both Arabidopsis and tobacco revealed differential ability to promote cell death. For Arabidopsis,

both *NI-V* (Fig. 15, 16A) and *N3-V* (Fig. 19A) induce development of necrotic tissue while *N1b-V* (Fig. 17A) and *N2-V* (Fig. 18A) do not. For tobacco *NIMIN* genes, the accelerated emergence of cell death could be observed for *NtN2c-V* (Fig. 24A) and *FS-V* (Fig. 25A), but not for *BP-V* or *FG-V* (Fig. 23A). These results confirm the observations of Ashir Masroor [2013] and Jaqueline Jung [2019], who reported cell death induction mediated by overexpression of Arabidopsis *NI* and *N3*, and tobacco *NtN2a* and *NtN2c*. Somewhat surprisingly, the *NIMIN* proteins reported to induce cell death like symptoms belong to different groups. In tobacco only N2-like proteins trigger this reaction while in Arabidopsis only N1 and N3 proteins are involved. Furthermore, observation of protein accumulation of the utilized *NIMIN*-Venus fusion proteins revealed a strong correlation between detectable protein levels and enhanced emergence of cell death, as seen for N1-V, N3-V (Fig. 19B), NtN2c-V (Fig. 26A), and FS-V (Fig. 26B). Together, differential accumulation and cell death promoting activity of different groups of *NIMIN* proteins strongly suggest that, while similar, these groups of *NIMIN* proteins may have different functions among both species. This idea is further corroborated by the absence of a N3 equivalent in tobacco. While the tobacco N1-like proteins BP and FG could theoretically compensate this, as they also carry a EDF motif, Arabidopsis N3 was shown to be unable to bind NtNPR1 [Maier *et al.*, 2011] indicating distinct adaptations in the biochemical mechanism of NPR1 mediated gene induction in Arabidopsis and tobacco, respectively.

Another striking observation was the occurrence of cell death symptoms during the reproductive stage of self-pollinated transgenic tobacco plants overexpressing *NI-V*. In the T1 generation about 60 % of the observed plants developed deformed leaves and necrosis at the base of petioles, pedicels or on the stem which often led to early shedding of leaves, floral organs, or seed capsules (Fig. 30, Table 1). Besides cell division and growth, programmed cell death (PCD) plays an important role during vegetative and reproductive development in plants, including the formation of different organs [Rogers, 2006; Daneva *et al.*, 2016]. The promotion of cell death in tissues which would naturally undergo cell death, although in much weaker quantities, correlates with the accelerated development of cell death observed during transient overexpression. Interestingly, in the T2 and T3 generations, there is a noticeable reduction in visibly necrotic tissues which goes hand in hand with an increase in leaf deformations (Fig. 31, 32A,B) as well as stunted growth (Fig. 32C). Transgenic tobacco plants overexpressing the cell death inducing tobacco *NIMIN* proteins NtN2c-V and FS-V show similar symptoms during their T1 generation (Fig. 39), indicating a similar mode of action of Arabidopsis and tobacco *NIMIN* proteins regarding this phenomenon. The leaf phenotypes are particularly intriguing as they not only comprise asymmetrical blades and forked midribs but also show an extension of the blades reaching down the petioles up to the stem. These phenotypes share some similarities with the blade-on-petiole phenotype observed in loss-of-function mutants of NPR5 and NPR6 (also BOP1 and BOP2) from Arabidopsis [Ha *et al.*, 2003; Hepworth *et al.*, 2005]. The tobacco genome also contains a gene for *NPR5* which encodes a BOP protein with high homology to those found in Arabidopsis [Hepworth *et al.*, 2005; Wu *et al.*, 2012b]. Unlike NPR1, which is primarily involved in the SA

dependent pathways involved in SAR associated defense regulation, BOP proteins have important functions during all stages of plant development [Khan *et al.*, 2014]. These functions comprise, besides the already mentioned, involvement in leaf patterning, flower development [Hepworth *et al.*, 2005], inflorescence architecture [Khan *et al.*, 2012], and abscission control during detachment of floral organs and leaves [McKim *et al.*, 2008; Wu *et al.*, 2012b]. This aligns surprisingly well with the phenotypes observed during overexpression of Arabidopsis and tobacco NIMIN proteins in transgenic tobacco plants (Fig. 30, 31, 32 & 39). Independent reports have shown that BOP proteins, similar to NPR1, can translocate to the nucleus as well as interact with TGA transcription factors like TGA1, TGA4 and PERIANTHIA [Hepworth *et al.*, 2005; Wang *et al.*, 2019c]. Through these interactions, BOP proteins promote the activation of other key regulators involved in floral meristem fate and differentiation of the corolla abscission zone [Xu *et al.*, 2010, Wu *et al.*, 2012b]. While this could hint at a function of NIMIN proteins in BOP mediated gene regulation, BOP proteins from Arabidopsis do not contain the conserved N1/N2 binding domain associated with regulation of NPR1 through interaction with NIMIN proteins [Hepworth *et al.*, 2005; Maier *et al.*, 2011]. However, it could be possible that NIMIN proteins mediate this function through association with another, yet unknown, protein.

In addition to the morphological phenotypes, transgenic plants overexpressing NIMIN proteins produced relatively few seeds. Even though only plants with detectable accumulation of the respective NIMIN protein were chosen for seed generation and those plants were self-pollinated to produce stable lines, a substantial portion of plants of the T2 generation, descending from *NI-V* overexpressing plants, show no or strongly reduced accumulation of the full-length N1-V protein (Fig. 36A). Lines transformed with *Pro35S:NtN2c-V* or *Pro35S:FS-V* exhibited only low transformation rates in the T0 generation and while showing the emergence of the described phenotypes, the proteins could not be detected in T1 plants. The low seed count and passing of gene expression to the next generation, together with the reduced cell death symptoms in the T2 and T3 generation of *NI-V* overexpression lines suggest a strong selection against the presence of the transgenic construct in the genome. It cannot be ruled out that the low number of seeds may be caused by development of cell death during the formation of homozygous seeds.

5.4. Cell death promoting activity is strongly connected to the EAR motif

NIMIN proteins harbor several conserved domains which are associated with the mediation of their function as transcriptional repressors of defense gene activation during SAR establishment. The most studied among these domains are the two different NPR1 binding domains, the DXFFK and the EDF motif. Additionally, all known NIMIN proteins from Arabidopsis and tobacco carry an EAR motif in close proximity to their C-terminus, which is associated with the mediation of transcriptional repression. To gain a deeper understanding of the mechanism behind cell death promoting activity of NIMIN proteins, analysis of mutants in these domains was used to narrow to down their importance in the establishment of the observed phenotypes.

The DXFFK domain is important for the interaction of Arabidopsis and tobacco NIMIN proteins with the N1/N2 binding domain located in the C-terminal moiety of NPR1 [Weigel *et al.*, 2005], with exception of Arabidopsis N3, which is suggested to interact with the N-terminus through its EDF motif [Chern *et al.*, 2005b; Masroor, 2013]. While N1 type NIMIN proteins, Arabidopsis N1 and N1b, as well as tobacco BP and FG also contain the EDF motif, no change in interaction strength could be detected in an EDF mutant of N1 (Fig. 27), in which the conserved Glu and Asp residues are exchanged with Ala and Val. This indicates, that these proteins use the DXFFK motif as their primary interaction site with NPR1. Mutagenesis of the DXFFK motif in both Arabidopsis N1 and tobacco FS, replacing the two consecutive Phe residues of the motif with serine, completely abolishes their interaction with NPR1 (Fig. 27, Fig. 52C). However, neither NPR1 binding mutant is sufficient to significantly reduce the emergence of cell death during transient overexpression (Fig. 41B, 42B), which is only slightly delayed for N1 F49/50S and the double mutant N1 F49/50S E94A D95V, containing both mutations (Fig. 44A). Interestingly, observation of transgenic tobacco plants overexpressing *N1 F49/50S* show similar symptoms to *N1-V* overexpressors during the flowering stage of the T1 generation (Fig. 30). The cell death associated phenotypes were even more pronounced for N1 F49/50S (Table 1) showing that the inability to interact with NPR1 has no significant influence on the development of cell death.

Examination of different EAR motif mutants revealed a strong reduction in cell death promoting activity. Both mutation of conserved leucine residues in the LxLxL type EAR motif of Arabidopsis N1 (Fig. 47), as well as deletion of said motif (Fig.49) strongly decelerate the emergence of necrotic tissue during transient overexpression. Similar observations were made for deletion of the DLNxxP type EAR motif found in tobacco NtN2c (Fig. 55A) and FS (Fig. 53A), hinting that, despite their differences, both types of EAR motifs are involved in the promotion of cell death. EAR motifs are known transcriptional repression motifs shared by a variety of active repressors of transcription [Ohta *et al.*, 2001, Kagale *et al.*, 2010]. Among those, TOPLESS, a member of the Gro/Tup1 corepressors which is involved in multiple plant developmental pathways, has already been suggested to play a role in the SAR pathway through interaction with NIMIN proteins [Arabidopsis Interactome Mapping Consortium, 2011]. In yeast, both cell death promoting NIMIN proteins from Arabidopsis, N1 and N3, are able to interact with N-terminal fragments of TPL which include the CTLH domain (Fig. 46A,C). This confirms earlier observations showing this domain to be the site of interaction between TPL and LxLxL type EAR motifs [Späth, 2012; Wang *et al.*, 2013; Martin-Arevallio *et al.*, 2017]. In this study, the interaction between N3 and full-length TPL could not be proven (Fig. 46A), suggesting that the binding site might not be accessible during normal development. In accordance with the development of cell death, EAR motif mutants of N3 are unable to interact with TPL1/333 in yeast. These mutants do not affect the interaction between N3 and NPR1 (Fig. 46B), matching the observations that despite reduced cell death EAR motif mutants of N1 show similar levels of reduction in *PR1a* promoter activity as proteins with an intact EAR motif (Fig. 48B, 49C). Unlike the LxLxL type EAR motif from Arabidopsis NIMIN proteins, the DLNxxP type motif found in tobacco does not convey the ability to interact with the N-terminus of TPL

(Fig. 52B). Recent studies of Ramosa Enhancer Locus2 (REL2), a member of the TPL family in *Zea mays*, showed that DLNxxP type EAR motifs are able to interact with the C-terminal WD40 domain of REL2 rather than its N-terminus [Liu *et al.*, 2019b]. As NtN2c and FS show similar reduction in their cell death promoting activity after deletion of the EAR motif as observed for Arabidopsis N1 and N3, it can be assumed that tobacco NIMIN proteins also interact with the WD40 domain of TPL. This interaction, however, has yet to be established for Arabidopsis and tobacco. Interestingly, the N1 F49/50S E94A D95V double mutant, while having an intact EAR motif also shows reduced interaction with TPL1/333 (Fig. 43). This could suggest that mutation of NPR1 binding motifs could lead to structural changes making the EAR motif more difficult to access. Together the results suggest the EAR motif to be the primary domain to be involved in NIMIN mediated cell death promotion.

The interaction between NIMIN proteins and TPL is interesting from different points of view. TPL is involved in many different signaling pathways regulated by phytohormones. This includes not only auxin signaling, but also in signaling processes mediated by jasmonic acid, strigolactone and gibberellic acid [Plant *et al.*, 2021]. In auxin signaling, the Auxin/Indole-3-acetic acid (AUX/IAA) transcriptional repressors suppress the activity of auxin response factors (ARFs) through their simultaneous interaction with TPL as a co-repressor. The interaction between TPL and AUX/IAA, like the one between TPL and N1, is mediated through interaction with a LxLxL type EAR motif [Tiwari *et al.*, 2004; Szenemyei *et al.*, 2008]. This correlation is especially fascinating when regarding the involvement of auxin signaling in many developmental processes associated with programmed cell death, including leaf formation [Mattsson *et al.*, 2003], floral organ development [Tabata *et al.*, 2010], and abscission control [Meir *et al.*, 2015]. This coincides with the observation that transient overexpression of the N-terminal TPL fragment TPL1/333 is sufficient to promote cell death in a similar intensity as observed during overexpression of N1 (Fig. 56). Co-expression of N1, N2 and N3 with TPL1/333 revealed a delaying effect on cell death emergence for N1 and N3 when compared to tissue only overexpressing TPL1/333 (Fig. 57). As N2 is unable to bind TPL1/333 and does not affect the promotion of cell death it can be concluded that cell death emergence during transient overexpression is caused by an imbalance between TPL1/333 and interacting NIMIN proteins.

Together with the mutation analysis of NPR1 binding and EAR mutants it is implied that the cell death promoting activity works independent from the regulation of NPR1 mediated SAR establishment. This is further supported by the results from transgenic plants, as N1 F49/50S like N1-V promotes the emergence of cell death related phenotypes (Fig. 30). These observations correlate with earlier reports in which coexpression of *NPR1* has no significant influence on the development of cell death [Jung, 2019]. NIMIN proteins could fulfill different functions via their distinct functional domains. These functions must not be limited to processes dependent on salicylic acid but, through interaction with TPL, could affect different hormonal pathways in the plant. Considering the phenotypical effects observed in transgenic plants (Fig. 30, 31, 32 & 39), involvement with BOP proteins or the auxin pathway seems plausible. As both the phytohormone auxin and BOP proteins share similar downstream

factors and repress the expression of the Knotted-like homeobox (KNOX) transcription factor [Satterlee & Scanlon, 2019]. It will therefore be interesting to determine if NIMIN proteins do actually have functions in other pathways or if the associated phenotypes seen during transient overexpression and in transgenic tobacco plants are caused by competitive binding of TPL and related proteins.

5.5. Repression of *PR1a* promoter activity is often interlinked with cell death

Repression of the *PR1a* promoter has been accepted as the key regulatory function of NIMIN proteins during SAR establishment and was shown in different organisms including Arabidopsis [Weigel *et al.*, 2005], tobacco [Zwicker *et al.*, 2007], and rice [Chern *et al.*, 2008]. However, this ability of certain NIMIN proteins to suppress expression from the *PR1a* promoter does not correlate completely with the ability to interact with NPR1. For example, while all Arabidopsis NIMIN proteins interact with NPR1, during transient overexpression, N2 does not mediate transcriptional repression (Fig. 18C). There is, however, a strong correlation between the cell death promoting activity of NIMIN proteins from Arabidopsis and tobacco, and their ability to downregulate chemically induced reporter gene expression from the *PR1a* promoter. Arabidopsis N1 (Fig. 16B), as well as tobacco NtN2c (Fig. 24B) and FS (Fig. 25B) all strongly reduce the expression from the *PR1a* promoter. In contrast, most NIMIN proteins, which do not promote cell death, like Arabidopsis N2 (Fig. 18C), as well as tobacco BP and FG (Fig. 23B) do not show a similar suppression. N1b constitutes the obvious exception here, as despite the apparent lack in cell death emergence, there is a visible moderate reduction in *PR1a* promoter activity.

It was initially surprising to observe that cell death promoting NPR1 binding mutants, including N1 F49/50S (Fig. 41D), the double mutant N1 F49/50S E94A D95V (Fig. 44C), as well as FS F48/49S (Fig. 53B), despite their inability to interact with NPR1 in yeast (Fig. 27, 43B and 52C respectively), were still able to prevent expression from the *PR1a* promoter. In complete contrast, mutants with amino acid exchanges or deletions in the EAR motif show strong reduction in cell death promoting activity but are still able to interact with NPR1 (Fig. 46C, 52C) and all, N1 L138/140A (Fig. 48B), N1 Δ EAR (Fig. 49C), and FS Δ EAR (Fig. 53), suppress the *PR1a* promoter. Observation of transient overexpression of the independent cell death inducer Bax, however, also revealed reduced induction of the *PR1a* promoter in a dilution dependent manner (Fig. 58). Higher dilutions of agrobacteria harboring a *Bax* overexpressing *ProN1b:Bax* construct with agrobacteria without a binary vector for transient overexpression only partially inhibited *PR1a* promoter activity, while also causing slower emergence of cell death than lower dilutions which completely abolishes the expression from the *PR1a* promoter.

This strongly suggests that cells programmed for cell death show reduced reporter activity even before emergence of visible necrosis and results regarding the repression of the *PR1a* promoter by NIMIN proteins able to induce cell death are most likely distorted. However, measurement of *PR1a* promoter activity is still viable for constructs not showing a similar pronounced acceleration of cell death. When compared, the triple mutant N1 F49/50S E94A D95V Δ EAR, which contains mutations in both NPR1 binding domains, the DXFFK and the EDF motif, as well as the EAR motif, shows strongly reduced

repression of the *PR1a* promoter (Fig. 51C) when compared to the N1 Δ EAR mutant (Fig. 49C). This confirms that interaction between N1 and NPR1 is required for the negative regulatory activity exerted by NIMIN proteins. The reduced cell death promotion in EAR motif mutants therefore allows the assessment of regulatory activity of otherwise cell death promoting NIMIN proteins. From the observations made during this study Arabidopsis N1 and N1b, as well as tobacco FS were shown to suppress the *PR1a* promoter even without a functional EAR motif. This once again underlines the differing functions of different groups of NIMIN proteins from different species. The creation of equivalent mutants for other NIMIN proteins sharing cell death promoting activity could therefore help to gain further insight into the differences between members of the NIMIN family.

The overexpression of NIMIN proteins in transgenic tobacco plants remains largely unaffected by the interference of cell death as cell death associated phenotypes at large only emerge at the end of the vegetative stage during flower formation and seed production. However, while showing a trend towards a reduction in PR1 protein accumulation in presence of N1-V after chemical induction in some experiments (Fig. 34), overall, the results were rather inconclusive. There were several plants showing strong PR1 accumulation in presence of strong N1-V accumulation (Fig. 34B; 36A,C line 493-19/4), as well as plants with no detectable accumulation of N1-V but strong reduction in detectable PR1 proteins (Fig. 35A). Therefore, a direct correlation between N1-V accumulation and *PR1a* repression could not be shown in transgenic tobacco plants.

5.6. Accumulation of N1 is mediated by its N-terminal domain

The investigation of cell death promotion mediated by NIMIN proteins revealed a strong divergence in protein accumulation with some members of the protein family accumulating strongly, while others are only barely detectable even after fusion of the Venus tag. Differential promoter activity can be ruled out as the cause for this difference in accumulation, as all *NIMIN-Venus* fusion genes were expressed from the 35S promoter from CaMV. To determine what factors are important for NIMIN protein accumulation N1 and N1b were compared. While highly similar and sharing the ability to repress the *PR1a* promoter (Fig. 17C), N1b unlike N1 shows almost no detectable protein accumulation (Fig. 17B) and does not promote cell death (Fig. 17A). The main difference between the N1 and N1b amino acid sequences lies in the fifteen N-terminal amino acids of N1, forming a region of high overall hydrophobicity which is strongly conserved among N1 homologs from different species (Fig. 59, Fig. 60). Results from deletion of this domain showed that its removal from N1 not only prevents accumulation of the full-length protein but the emergence of cell death and repression of the *PR1a* promoter (Fig. 61).

Analysis of hybrid proteins comprising the N1-N-terminal (N1nT) domain, having it fused to their N-terminus, revealed a significant increase in protein accumulation for both N1b and N2. This effect is more pronounced for N1nT-N1b-V (Fig. 63B) than for N1nT-N2-V (Fig. 67B) and is accompanied by an equally enhanced ability to promote cell death (Fig. 63A and 67A, respectively). Additionally, it could be shown that N1nT-N1b acquires the ability to interact with TPL1/333, which could not be shown

for N1b (Fig. 62B). This could indicate structural rearrangements in presence of the N1nT domain allowing N1nT-N1b to exert functions similar to N1. Deletion of the EAR motif prevents interaction with TPL1/333 (Fig. 64B) and reduces the cell death promoting activity without affecting protein stability (Fig. 65).

Rather surprisingly, a similar increase in protein accumulation could be observed for a hybrid N1nT-Venus protein where N-terminal fusion of N1nT elicits an increase in detectable protein fluorescence (Fig. 69). The effect of this domain, however, appears position dependent. A hybrid N1b-N1nT-V protein harboring the N1nT domain in-between N1b and Venus (Fig. 71) as well as a V-N1nT protein with N1nT fused to the C-terminus (Fig. 72) showed no increase in protein accumulation. Together with an enhanced ability of N1nT-V to resist certain proteases when compared to Venus (Fig. 70A), these results suggest that the N1nT domain might help to protect proteins against N-terminal proteolytic degradation. Analysis of several mutants in the N1nT domain also suggest another possible mode of action. Deletions of large segments of the N1nT-domain did not affect its ability to bestow enhanced protein accumulation upon N1nT-N1b-V (Fig. 74) and N1nT-V (Fig. 77, N1nT Δ 2-9-V), and neither did amino acid exchanges of highly conserved amino acids, as for N1nT L8G-N1b-V (Fig. 73), or exchange of hydrophobic groups, as for N1nT SY-N1b-V (Fig. 75). This indicates that length and composition of the N1nT domain may play only a minor role for its function. Indeed, a MIL mutant, exchanging the N-terminal methionine of the N1nT domain for leucine by replacing the ATG codon with CTG still shows enhanced protein accumulation for both N1nT MIL-N1b-V (Fig. 76) and N1nT MIL-V (Fig. 77) without loss of accompanying properties like cell death promotion or fluorescence, respectively.

While these results show strong enhancement of protein accumulation by N-terminal fusion of N1nT to other NIMIN proteins as well as the unrelated Venus protein, the exact mechanism is still not entirely uncovered. The results from N1nT-N1b-V and N1nT-N1b Δ EAR-V suggest changes in protein structure mediated by N1nT and could, together with the difficulties to induce expression from the N1b promoter region, hint that the *N1b* gene might be a duplicate of *N1* which lost its activity by sequence alterations during evolution. Further investigations of N1nT-N2-V and creation of similar hybrid proteins for other NIMIN proteins featuring low protein accumulation could help to understand how the function of different NIMIN proteins might be influenced by their protein structure. Another factor which could bear some importance for the accumulation of NIMIN proteins is the resistance against protease activity observed for N1nT-V. To prevent cell death to from affecting the protein levels of different NIMIN constructs, it would be advisable to use EAR motif mutants in conjunction with N-terminal fusion of N1nT to determine if similar effects can be observed for this protein family. There also remains the question to what extend the sequence of the N1nT domain is important as several deletion and substitution mutants did not significantly affect the ability of this domain to mediate increased protein accumulation. For example, it has been shown that N-terminal His₆ tags can affect to the stability of proteins against external influences like temperature [Parshin *et al.*, 2020]. The MIL mutant raises further questions. As the resulting proteins still accumulate like those carrying an intact methionine at

the start of the N1nT sequence, the fusion of different gene sequences might induce regulation of protein accumulation on the mRNA level. Untranslated regions (UTRs) can regulate different properties of the respective mRNA including stability and translation efficiency. This allows additional control over gene expression in addition to transcriptional controls. The biological activity mediated by regulatory motifs of mRNA relies not only on their primary, but also on their secondary structure. A large fraction of mRNAs contain hairpin like structures, also called stem-loops, which can not only increase the stability of mRNAs by protecting them from degradation, but also regulate translation [Nowakovski & Tinoco, 1997; Mignone *et al.*, 2002; Svoboda & Di Cara, 2006]. The mRNA transcribed from the chloroplast gene *psbA* from tobacco, which encodes Photosystem II protein D1, contains a hairpin loop and base alterations or deletions in this region often leads to reduced mRNA levels and translation efficiency [Zou *et al.*, 2003]. It may therefore be possible that the nucleotide sequence of *N1nT* contained in the mRNA might be sufficient to increase its stability. To get an insight into the potential presence of similar structures in the mRNAs of constructs used in this thesis secondary mRNA structures were predicted using RNAfold using minimum free energy prediction visualized by forna (Fig. 79) [Mathews *et al.*, 2004; Gruber *et al.*, 2008; Lorenz *et al.*, 2011; Kerpedjiev *et al.*, 2015]. The mRNA sequences used for calculation consist of the coding sequences of *N1nT-N1b-V* and *N1nT-Venus* constructs followed by the 3' NOS terminator. The poly(A) tail length was presumed to be 50 nucleotides, the average length in *Arabidopsis* (Fig. 79A) [Subtelny *et al.*, 2014]. The overall secondary structures predicted for *N1nT-N1b-V* and *N1nT-Venus* mRNAs remain largely unaffected by addition of the *N1nT* sequence when compared to *N1b-V* and *Venus* (Fig. 79B). However, presence of *N1nT* leads to the formation of stem-loops close to the 5' end (red boxes), which could mediate the enhanced protein accumulation. When comparing the 5' end of different *N1nT* mutants (Fig. 79C) the stem-loops remain intact or are only slightly altered in the deletion mutant $\Delta 2-4$ and the substitution mutants L8G, SY (S7A Y9A Y11A S12A), and M1L. The deletion mutant N1nT $\Delta 2-9$, however, remains an exception and is not predicted to form a stem-loop even though both N1nT $\Delta 2-9$ -N1b-V and N1nT $\Delta 2-9$ -Venus, accumulate strongly during transient overexpression (Fig. 74C, 77C). To determine if these structures actually play a role would require to obtain crystal structures of the observed mRNA molecules. A much easier first step to determine if N1nT influences mRNA stability could be achieved by comparing transcript levels from different *NIMIN* and hybrid *N1nT-NIMIN* gene constructs expressed from the same promoter. The observations showing that N1nT M1L-N1b-V and N1nT M1L-Venus accumulate at the same size as N1nT-N1b-V and N1nT-Venus (Fig. 76C, 77C) could also imply that the *N1nT M1L* sequence is translated despite its lack of an ATG codon. While CTG is not typically used as a translation initiation codon on prokaryotes (0,13 %) [Bachvarov *et al.*, 2008], it cannot be completely ruled out that the sequence is still translated and experiments with the M1L mutant should be repeated using different amino acid substitutions.

It seems unlikely that a single one of those factors is solely responsible for mediating enhanced protein accumulation. Rather, enhanced accumulation of proteins carrying the N1nT domain might be a

combined result from translational regulation, structural rearrangement, and enhancement of resistance against N-terminal degradation. The specific importance of these processes in the accumulation of NIMIN proteins still has to be clarified in future research. Nonetheless, the N1nT domain could be an effective tool in allowing to study otherwise poorly accumulating proteins.

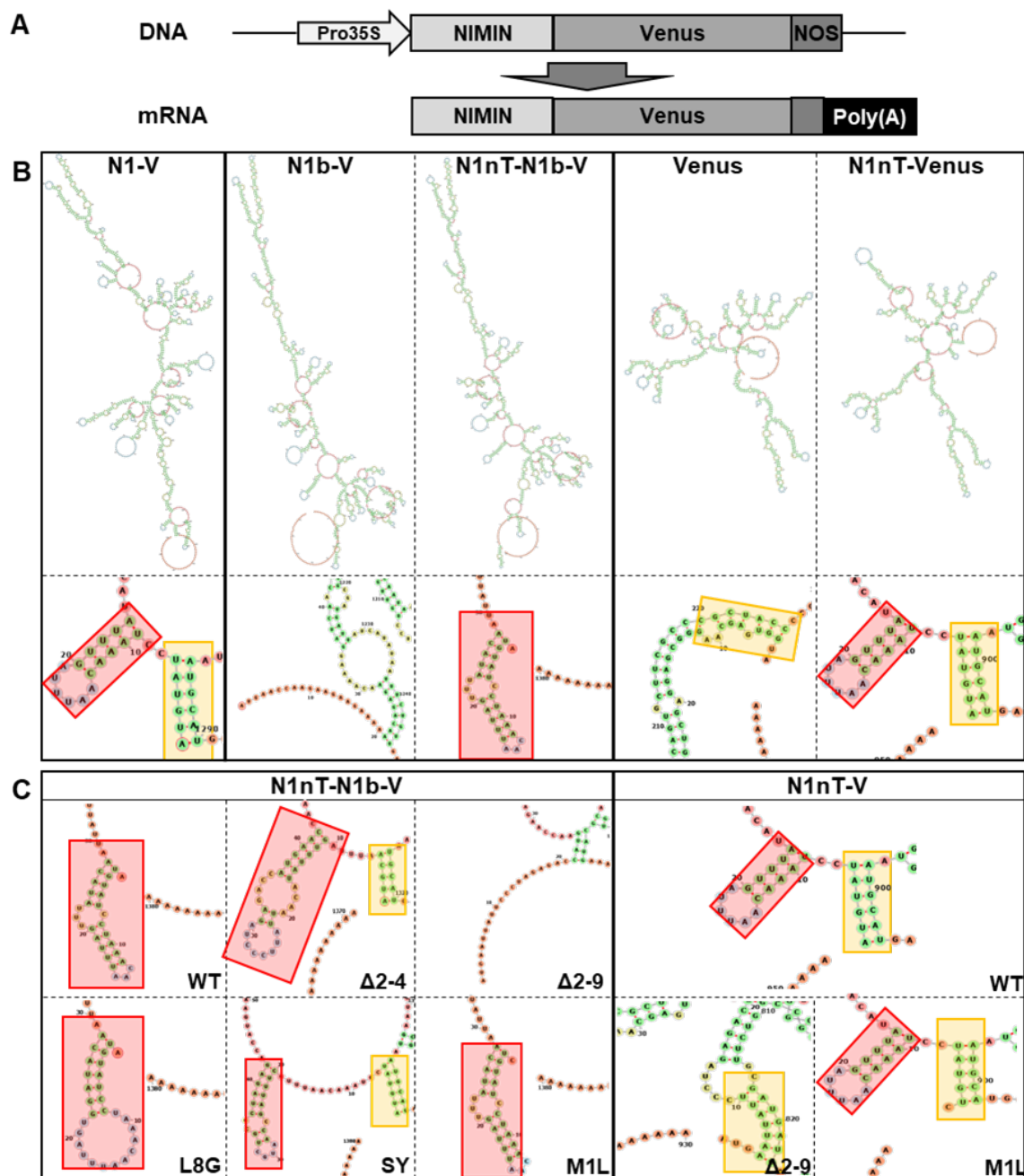


Fig. 79 Predicted secondary mRNA Structure for hybrid *N1nT-NIMIN1b-Venus* and *N1nT-Venus* genes. (A) Schematic representation of transcription of gene constructs from the binary vector pBin19 using the 35S promoter from CaMV and the NOS terminator from *Agrobacterium tumefaciens*. (B-C) Predicted secondary structure of mRNAs of hybrid N1nT-N1b-V and N1nT-Venus and mutants created using RNAfold. Color code of nucleotides: green – stems (canonical helices), red – multiloops, yellow – interior loops, blue – hairpin loops, orange – 5' and 3' unpaired region. Yellow boxes show paired nucleotides and red boxes show hairpin structures close 5' end of the mRNA. (B) Predicted secondary mRNA structures of N1nT-N1b-V and N1nT-V. N1-V, N1b-V and Venus were used as controls. Pictures show the predicted structures of the overall mRNA and of the 5'-end. The poly(A) tail length was presumed to be about 50 nucleotides. (C) Predicted secondary structure of the 5'-end of mRNA in mutants of the N1nT domain. For N1nT-N1b-V the mutants Δ2-4, Δ2-9, L8G, S7A Y9A Y11A S12A (SY), and M1L were used. For N1nT-Venus the mutants Δ2-9 and M1L were used.

The results from this study show not only the importance of different domains for different functions of NIMIN proteins, like protein accumulation, cell death promotion and transcriptional repression, but also hint at potential involvement in different signal pathways. The understanding that imminent cell death influences reporter gene activity will allow future studies to more effectively characterize NIMIN mediated transcriptional repression by using EAR motif mutants with limited development of cell death and could therefore help to compare the mechanisms by which NIMIN proteins mediate this function in other organisms. The knowledge that NIMIN proteins, through their interaction with TOPLESS, can affect multiple signal pathways contributes an important piece for expanding the current understanding of the interplay between those pathways and it will therefore be interesting to uncover this network of regulatory processes.

Literature

Adachi, H., Kamoun, S., & Maqbool, A. (2019). A resistosome-activated ‘death switch’. *Nature Plants*, 5(5), 457-458.

Albagli, O., Dhordain, P., Deweindt, C., Lecocq, G., & Leprince, D. (1995). The BTB/POZ domain: a new protein-protein interaction motif common to DNA- and actin-binding proteins. *Cell Growth & Differentiation: the molecular biology journal of the American Association for Cancer Research*, 6(9), 1193-1198.

Alhoraibi, H., Bigeard, J., Rayapuram, N., Colcombet, J., & Hirt, H. (2019). Plant Immunity: The MTI-ETI Model and Beyond. *Current Issues in Molecular Biology*, 30, 39-58.

Ali, S., Mir, Z. A., Tyagi, A., Mehari, H., Meena, R. P., Bhat, J. A., Yadav, P., Papalou, P., Rawat, S. & Grover, A. (2017). Overexpression of NPR1 in Brassica juncea confers broad spectrum resistance to fungal pathogens. *Frontiers in Plant Science*, 8, 1693.

Altschul, S. F., Gish, W., Miller, W., Myers, E. W., & Lipman, D. J. (1990). Basic local alignment search tool. *Journal of molecular biology*, 215(3), 403-410.

Alves, M. S., Dadalto, S. P., Gonçalves, A. B., De Souza, G. B., Barros, V. A., & Fietto, L. G. (2013). Plant bZIP transcription factors responsive to pathogens: a review. *International Journal of Molecular Sciences*, 14(4), 7815-7828.

Anderson, P. K., Cunningham, A. A., Patel, N. G., Morales, F. J., Epstein, P. R., & Daszak, P. (2004). Emerging infectious diseases of plants: pathogen pollution, climate change and agrotechnology drivers. *Trends in Ecology & Evolution*, 19(10), 535-544.

Annis, S. L., & Goodwin, P. H. (1997). Recent advances in the molecular genetics of plant cell wall-degrading enzymes produced by plant pathogenic fungi. *European Journal of Plant Pathology*, 103(1), 1-14.

Antoniw, J. F., & Pierpoint, W. S. (1978). The purification and properties of one of the ‘b’ proteins from virus-infected tobacco plants. *Journal of General Virology*, 39(2), 343-350.

Anulika, N. P., Ignatius, E. O., Raymond, E. S., Osasere, O. I., & Abiola, A. H. (2016). The chemistry of natural product: Plant secondary metabolites. *International Journal of Technology Enhancements and Emerging Engineering Research*, 4(8), 1-9.

Arabidopsis Interactome Mapping Consortium (2011). Evidence for network evolution in an Arabidopsis interactome map. *Science*, 333(6042), 601-607.

Aravind, L., & Koonin, E. V. (1999). Fold prediction and evolutionary analysis of the POZ domain: structural and evolutionary relationship with the potassium channel tetramerization domain. *Journal of Molecular Biology*, 285(4), 1353-1361.

Ausubel, F. M. (2005). Are innate immune signaling pathways in plants and animals conserved? *Nature Immunology*, 6(10), 973-979.

Bachvarov, B., Kirilov, K., & Ivanov, I. (2008). Codon usage in prokaryotes. *Biotechnology & Biotechnological Equipment*, 22(2), 669-682.

Baker, B., Zambryski, P., Staskawicz, B., & Dinesh-Kumar, S. P. (1997). Signaling in plant-microbe interactions. *Science*, 276(5313), 726-733.

Bardwell, V. J., & Treisman, R. (1994). The POZ domain: a conserved protein-protein interaction motif. *Genes & Development*, 8(14), 1664-1677.

Barrett, L. G., Thrall, P. H., Dodds, P. N., Van der Merwe, M., Linde, C. C., Lawrence, G. J., & Burdon, J. J. (2009). Diversity and evolution of effector loci in natural populations of the plant pathogen *Melampsora lini*. *Molecular Biology and Evolution*, 26(11), 2499-2513.

- Barsoum, M., Sabelleck, B., D. Spanu, P., & Panstruga, R. (2019).** Rumble in the effector jungle: Candidate effector proteins in interactions of plants with powdery mildew and rust fungi. *Critical Reviews in Plant Sciences*, 38(4), 255-279.
- Bartel, P.L., Chien, C.-T., Sternglanz, R., and Fields, S. (1993).** Using the two-hybrid system to detect protein-protein interactions. In *Cellular interactions in Development: A Practical Approach*, ed. Hartley, D.A. (Oxford University Press, Oxford), 153-179.
- Beckers, G. J., Jaskiewicz, M., Liu, Y., Underwood, W. R., He, S. Y., Zhang, S., & Conrath, U. (2009).** Mitogen-activated protein kinases 3 and 6 are required for full priming of stress responses in *Arabidopsis thaliana*. *The Plant Cell*, 21(3), 944-953.
- Bej, A. K., Mahbubani, M. H., & Atlas, R. M. (1991).** Amplification of nucleic acids by polymerase chain reaction (PCR) and other methods and their applications. *Critical reviews in Biochemistry and Molecular Biology*, 26(3-4), 301-334.
- Bektas, Y., & Eulgem, T. (2015).** Synthetic plant defense elicitors. *Frontiers in Plant Science*, 5, 804.
- Bernsdorff, F., Döring, A. C., Gruner, K., Schuck, S., Bräutigam, A., & Zeier, J. (2016).** Pipecolic acid orchestrates plant systemic acquired resistance and defense priming via salicylic acid-dependent and-independent pathways. *The Plant Cell*, 28(1), 102-129.
- Bevan, M. (1984).** Binary *Agrobacterium* vectors for plant transformation. *Nucleic Acids Research*, 12(22), 8711-8721.
- Block, A., Li, G., Fu, Z. Q., & Alfano, J. R. (2008).** Phytopathogen type III effector weaponry and their plant targets. *Current Opinion in Plant Biology*, 11(4), 396-403.
- Boller, T., & Felix, G. (2009).** A renaissance of elicitors: perception of microbe-associated molecular patterns and danger signals by pattern-recognition receptors. *Annual Review of Plant Biology*, 60, 379-406.
- Bonardi, V., & Dangl, J. L. (2012).** How complex are intracellular immune receptor signaling complexes? *Frontiers in Plant Science*, 3, 237.
- Bork, P. (1993).** Hundreds of ankyrin-like repeats in functionally diverse proteins: mobile modules that cross phyla horizontally? *Proteins: Structure, Function, and Bioinformatics*, 17(4), 363-374.
- Boudsocq, M., Willmann, M. R., McCormack, M., Lee, H., Shan, L., He, P., Bush, J., Cheng, S. & Sheen, J. (2010).** Differential innate immune signalling via Ca²⁺ sensor protein kinases. *Nature*, 464(7287), 418-422.
- Boutrot, F., & Zipfel, C. (2017).** Function, discovery, and exploitation of plant pattern recognition receptors for broad-spectrum disease resistance. *Annual Review of Phytopathology*, 55, 257-286.
- Bowling, S. A., Clarke, J. D., Liu, Y., Klessig, D. F., & Dong, X. (1997).** The *cpr5* mutant of *Arabidopsis* expresses both NPR1-dependent and NPR1-independent resistance. *The Plant Cell*, 9(9), 1573-1584.
- Bradford, M. M. (1976).** A rapid and sensitive method for the quantitation of microgram quantities of protein utilizing the principle of protein-dye binding. *Analytical Biochemistry*, 72(1-2), 248-254.
- Breen, S., Williams, S. J., Outram, M., Kobe, B., & Solomon, P. S. (2017).** Emerging insights into the functions of pathogenesis-related protein 1. *Trends in Plant Science*, 22(10), 871-879.
- Buell, C. R., Joardar, V., Lindeberg, M., Selengut, J., Paulsen, I. T., Gwinn, M. L., Dodson, R. J., Deboy, R. T., Durkin, A. S., Kolonay, J. F., Madupu, R., Daugherty, S., Brinkac, L., Beanan, M. J., Haft, D. H., Nelson, W. C., Davidsen, T., Zafar, N., Zhou, L., Liu, J., Yuan, Q., Khouri, H., Fedorova, N., Tran, B., Russel, D. Berry, K., Utterback, T., Van Aken, S. E., Feldblyum, T. V., D'Ascenzo, M., Deng, W., Ramos, A. R., Alfano, J. R., Cartinhour, S., Chatterjee, A. K., Delaney, T. P., Lazarowitz, S. G., Martin, G. B., Schneider, D. J., Tang, X., Bender, C. L., White, O., Fraser, C. M. & Collmer, A. (2003).** The complete genome sequence of the *Arabidopsis* and tomato pathogen *Pseudomonas syringae* pv. tomato DC3000. *Proceedings of the National Academy of Sciences*, 100(18), 10181-10186.

- Canet, J. V., Dobón, A., Roig, A., & Tornero, P. (2010).** Structure-function analysis of npr1 alleles in Arabidopsis reveals a role for its paralogs in the perception of salicylic acid. *Plant, Cell & Environment*, 33(11), 1911-1922.
- Cao, H., Bowling, S. A., Gordon, A. S., & Dong, X. (1994).** Characterization of an Arabidopsis mutant that is nonresponsive to inducers of systemic acquired resistance. *The Plant Cell*, 6(11), 1583-1592.
- Cao, H., Glazebrook, J., Clarke, J. D., Volko, S., & Dong, X. (1997).** The Arabidopsis NPR1 gene that controls systemic acquired resistance encodes a novel protein containing ankyrin repeats. *Cell*, 88(1), 57-63.
- Cao, H., Li, X., & Dong, X. (1998).** Generation of broad-spectrum disease resistance by overexpression of an essential regulatory gene in systemic acquired resistance. *Proceedings of the National Academy of Sciences*, 95(11), 6531-6536.
- Carr, J. P., & Klessig, D. F. (1989).** The pathogenesis-related proteins of plants. In *Genetic Engineering* (pp. 65-109). Springer, Boston, MA.
- Catanzariti, A. M., Dodds, P. N., Lawrence, G. J., Ayliffe, M. A., & Ellis, J. G. (2006).** Haustorially expressed secreted proteins from flax rust are highly enriched for avirulence elicitors. *The Plant Cell*, 18(1), 243-256.
- Catanzariti, A. M., Dodds, P. N., Ve, T., Kobe, B., Ellis, J. G., & Staskawicz, B. J. (2010).** The AvrM effector from flax rust has a structured C-terminal domain and interacts directly with the M resistance protein. *Molecular Plant-Microbe Interactions*, 23(1), 49-57.
- Césari, S., Kanzaki, H., Fujiwara, T., Bernoux, M., Chalvon, V., Kawano, Y., Shimamoto, K., Dodds, P. Terauchi, R. & Kroj, T. (2014).** The NB-LRR proteins RGA 4 and RGA 5 interact functionally and physically to confer disease resistance. *The EMBO Journal*, 33(17), 1941-1959.
- Çevik, V., Kidd, B. N., Zhang, P., Hill, C., Kiddle, S., Denby, K. J., Holub, E. B., Cahill, D. M., Manners, J. M., Schenk, P. M.; Beynon, J. & Kazan, K. (2012).** MEDIATOR25 acts as an integrative hub for the regulation of jasmonate-responsive gene expression in Arabidopsis. *Plant Physiology*, 160(1), 541-555.
- Chanda, B., Xia, Y., Mandal, M. K., Yu, K., Sekine, K. T., Gao, Q. M., Selote, D., Hu, Y., Stromberg, A., Navarre, D., Kachroo, A. & Kachroo, P. (2011).** Glycerol-3-phosphate is a critical mobile inducer of systemic immunity in plants. *Nature Genetics*, 43(5), 421-427.
- Chaturvedi, R., Venables, B., Petros, R. A., Nalam, V., Li, M., Wang, X., Takemoto, L. J. & Shah, J. (2012).** An abietane diterpenoid is a potent activator of systemic acquired resistance. *The Plant Journal*, 71(1), 161-172.
- Cheeseman, J. (2016).** Food security in the face of salinity, drought, climate change, and population growth. In *Halophytes for food security in dry lands* (pp. 111-123). Academic Press.
- Chen, X., Ding, X., & Song, W. Y. (2003).** Isolation of Plasmid DNA rescued from single colonies of *Agrobacterium tumefaciens* by means of rolling circle amplification. *Plant Molecular Biology Reporter*, 21(4), 411-415.
- Chen, Z., Zheng, Z., Huang, J., Lai, Z., & Fan, B. (2009).** Biosynthesis of salicylic acid in plants. *Plant Signaling & Behavior*, 4(6), 493-496.
- Chen, Y. L., Lee, C. Y., Cheng, K. T., Chang, W. H., Huang, R. N., Nam, H. G., & Chen, Y. R. (2014).** Quantitative peptidomics study reveals that a wound-induced peptide from PR-1 regulates immune signaling in tomato. *The Plant Cell*, 26(10), 4135-4148.
- Chen, Y. C., Holmes, E. C., Rajniak, J., Kim, J. G., Tang, S., Fischer, C. R., Mudgett, M. B. & Sattely, E. S. (2018).** N-hydroxy-pipecolic acid is a mobile metabolite that induces systemic disease resistance in Arabidopsis. *Proceedings of the National Academy of Sciences*, 115(21), E4920-E4929.

- Chen, J., Mohan, R., Zhang, Y., Li, M., Chen, H., Palmer, I. A., Chang, M., Qi, G., Spoel, S. H., Mengiste, T., Wang, D., Liu, F. & Fu, Z. Q. (2019). NPR1 promotes its own and target gene expression in plant defense by recruiting CDK8. *Plant Physiology*, 181(1), 289-304.
- Chern, M., Fitzgerald, H. A., Canlas, P. E., Navarre, D. A., & Ronald, P. C. (2005a). Overexpression of a rice NPR1 homolog leads to constitutive activation of defense response and hypersensitivity to light. *Molecular Plant-Microbe Interactions*, 18(6), 511-520.
- Chern, M., Canlas, P. E., Fitzgerald, H. A., & Ronald, P. C. (2005b). Rice NRR, a negative regulator of disease resistance, interacts with Arabidopsis NPR1 and rice NH1. *The Plant Journal*, 43(5), 623-635.
- Chern, M., Canlas, P. E., & Ronald, P. C. (2008). Strong Suppression of Systemic Acquired Resistance in Arabidopsis by NRR is Dependent on its Ability to Interact with NPR1 and its Putative Repression Domain. *Molecular Plant*, 1(3), 552-559.
- Chern, M., Bai, W., Sze-To, W. H., Canlas, P. E., Bartley, L. E., & Ronald, P. C. (2012). A rice transient assay system identifies a novel domain in NRR required for interaction with NH1/OsNPR1 and inhibition of NH1-mediated transcriptional activation. *Plant Methods*, 8(1), 6.
- Chester, K. S. (1933). The problem of acquired physiological immunity in plants. *The Quarterly Review of Biology*, 8(3), 275-324.
- Chien, P. S., Nam, H. G., & Chen, Y. R. (2015). A salt-regulated peptide derived from the CAP superfamily protein negatively regulates salt-stress tolerance in Arabidopsis. *Journal of Experimental Botany*, 66(17), 5301-5313.
- Chinchilla, D., Bauer, Z., Regenass, M., Boller, T., & Felix, G. (2006). The Arabidopsis receptor kinase FLS2 binds flg22 and determines the specificity of flagellin perception. *The Plant Cell*, 18(2), 465-476.
- Chinchilla, D., Zipfel, C., Robatzek, S., Kemmerling, B., Nürnberger, T., Jones, J. D. G., Felix, G. & Boller, T. (2007). A flagellin-induced complex of the receptor FLS2 and BAK1 initiates plant defence. *Nature*, 448(7152), 497-500.
- Chini, A., Fonseca, S. G. D. C., Fernandez, G., Adie, B., Chico, J. M., Lorenzo, O., García-Casado, G., López-Vidriero, I., Lozano, F. M., Ponce, M. R., Micol, J. L. & Solano, R. (2007). The JAZ family of repressors is the missing link in jasmonate signalling. *Nature*, 448(7154), 666-671.
- Choi, J., Huh, S. U., Kojima, M., Sakakibara, H., Paek, K. H., & Hwang, I. (2010). The cytokinin-activated transcription factor ARR2 promotes plant immunity via TGA3/NPR1-dependent salicylic acid signaling in Arabidopsis. *Developmental Cell*, 19(2), 284-295.
- Choi, H. W., & Klessig, D. F. (2016). DAMPs, MAMPs, and NAMPs in plant innate immunity. *BMC Plant Biology*, 16(1), 232.
- Choi, H. W., Manohar, M., Manosalva, P., Tian, M., Moreau, M., & Klessig, D. F. (2016). Activation of plant innate immunity by extracellular high mobility group box 3 and its inhibition by salicylic acid. *PLOS Pathogens*, 12(3), e1005518.
- Chuang, C. F., Running, M. P., Williams, R. W., & Meyerowitz, E. M. (1999). The PERIANTHIA gene encodes a bZIP protein involved in the determination of floral organ number in Arabidopsis thaliana. *Genes & Development*, 13(3), 334-344.
- Clarke, J. D., Liu, Y., Klessig, D. F., & Dong, X. (1998). Uncoupling PR gene expression from NPR1 and bacterial resistance: characterization of the dominant Arabidopsis cpr6-1 mutant. *The Plant Cell*, 10(4), 557-569.
- Coll, N. S., Epple, P., & Dangl, J. L. (2011). Programmed cell death in the plant immune system. *Cell Death & Differentiation*, 18(8), 1247-1256.
- Cornelissen, B. J., Horowitz, J., van Kan, J. A., Goldberg, R. B., & Bol, J. F. (1987). Structure of tobacco genes encoding pathogenesis-related proteins from the PR-1 group. *Nucleic Acids Research*, 15(17), 6799-6811.

- Daneva, A., Gao, Z., Van Durme, M., & Nowack, M. K. (2016).** Functions and regulation of programmed cell death in plant development. *Annual Review of Cell and Developmental Biology*, 32, 441-468.
- Dangl, J. L., & Jones, J. D. (2001).** Plant pathogens and integrated defence responses to infection. *Nature*, 411(6839), 826-833.
- Darvill, A. G., & Albersheim, P. (1984).** Phytoalexins and their elicitors—a defense against microbial infection in plants. *Annual Review of Plant Physiology*, 35(1), 243-275.
- Delaney, T. P., Uknes, S., Vernooij, B., Friedrich, L., Weymann, K., Negrotto, D., Gaffney, T., Gut-Rella, M., Kessmann, H., Ward, E. & Ryals, J. (1994).** A central role of salicylic acid in plant disease resistance. *Science*, 266(5188), 1247-1250.
- Delaney, T. P., Friedrich, L., & Ryals, J. A. (1995).** Arabidopsis signal transduction mutant defective in chemically and biologically induced disease resistance. *Proceedings of the National Academy of Sciences*, 92(14), 6602-6606.
- Dempsey, D. M. A., & Klessig, D. F. (2012).** SOS—too many signals for systemic acquired resistance? *Trends in Plant Science*, 17(9), 538-545.
- Denbigh, G. L., Dauphinee, A. N., Fraser, M. S., Lacroix, C. R., & Gunawardena, A. H. (2020).** The role of auxin in developmentally regulated programmed cell death in lace plant. *American Journal of Botany*, 107(4), 577-586.
- Denoux, C., Galletti, R., Mammarella, N., Gopalan, S., Werck, D., De Lorenzo, G., Ferrari, S., Ausubel, F. M. & Dewdney, J. (2008).** Activation of defense response pathways by OGs and Flg22 elicitors in Arabidopsis seedlings. *Molecular Plant*, 1(3), 423-445.
- Després, C., DeLong, C., Glaze, S., Liu, E., & Fobert, P. R. (2000).** The Arabidopsis NPR1/NIM1 protein enhances the DNA binding activity of a subgroup of the TGA family of bZIP transcription factors. *The Plant Cell*, 12(2), 279-290.
- Després, C., Chubak, C., Rochon, A., Clark, R., Bethune, T., Desveaux, D., & Fobert, P. R. (2003).** The Arabidopsis NPR1 disease resistance protein is a novel cofactor that confers redox regulation of DNA binding activity to the basic domain/leucine zipper transcription factor TGA1. *The Plant Cell*, 15(9), 2181-2191.
- Dietrich, R. A., Delaney, T. P., Uknes, S. J., Ward, E. R., Ryals, J. A., & Dangl, J. L. (1994).** Arabidopsis mutants simulating disease resistance response. *Cell*, 77(4), 565-577.
- Ding, P., Rekhter, D., Ding, Y., Feussner, K., Busta, L., Haroth, S., Xu, S., Li, X., Jetter, R., Feussner, I. & Zhang, Y. (2016).** Characterization of a pipelicolic acid biosynthesis pathway required for systemic acquired resistance. *The Plant Cell*, 28(10), 2603-2615.
- Ding, Y., Sun, T., Ao, K., Peng, Y., Zhang, Y., Li, X., & Zhang, Y. (2018).** Opposite roles of salicylic acid receptors NPR1 and NPR3/NPR4 in transcriptional regulation of plant immunity. *Cell*, 173(6), 1454-1467.
- Dodds, P. N., Lawrence, G. J., Catanzariti, A. M., Ayliffe, M. A., & Ellis, J. G. (2004).** The *Melampsora lini* AvrL567 avirulence genes are expressed in haustoria and their products are recognized inside plant cells. *The Plant Cell*, 16(3), 755-768.
- Dodds, P. N., Lawrence, G. J., Catanzariti, A. M., Teh, T., Wang, C. I. A., Ayliffe, M. A., Kobe, B. & Ellis, J. G. (2006).** Direct protein interaction underlies gene-for-gene specificity and coevolution of the flax resistance genes and flax rust avirulence genes. *Proceedings of the National Academy of Sciences*, 103(23), 8888-8893.
- Dong, X., Mindrinos, M., Davis, K. R., & Ausubel, F. M. (1991).** Induction of Arabidopsis defense genes by virulent and avirulent *Pseudomonas syringae* strains and by a cloned avirulence gene. *The Plant Cell*, 3(1), 61-72.
- Dong, X. (2004).** NPR1, all things considered. *Current Opinion in Plant Biology*, 7(5), 547-552.

- Dubiella, U., Seybold, H., Durian, G., Komander, E., Lassig, R., Witte, C. P., Schulze, W. X. & Romeis, T. (2013).** Calcium-dependent protein kinase/NADPH oxidase activation circuit is required for rapid defense signal propagation. *Proceedings of the National Academy of Sciences*, 110(21), 8744-8749.
- Durrant, W. E., & Dong, X. (2004).** Systemic acquired resistance. *Annual Review of Phytopathology*, 42, 185-209.
- Ecker, J. R., & Davis, R. W. (1987).** Plant defense genes are regulated by ethylene. *Proceedings of the National Academy of Sciences*, 84(15), 5202-5206.
- Eggl, U., and Nyffeler, R. (2009).** Living under temporarily arid conditions - succulence as an adaptive strategy. *Bradleya*, 27: 13-36.
- Ellenberger, T. E., Brandl, C. J., Struhl, K., & Harrison, S. C. (1992).** The GCN4 basic region leucine zipper binds DNA as a dimer of uninterrupted α helices: crystal structure of the protein-DNA complex. *Cell*, 71(7), 1223-1237.
- Erhardt, M., Namba, K., & Hughes, K. T. (2010).** Bacterial nanomachines: the flagellum and type III injectisome. *Cold Spring Harbor Perspectives in Biology*, 2(11), a000299.
- Eulgem, T., & Somssich, I. E. (2007).** Networks of WRKY transcription factors in defense signaling. *Current Opinion in Plant Biology*, 10(4), 366-371.
- Faize, L., & Faize, M. (2018).** Functional analogues of salicylic acid and their use in crop protection. *Agronomy*, 8(1), 5.
- Fernández-Calvo, P., Chini, A., Fernández-Barbero, G., Chico, J. M., Gimenez-Ibanez, S., Geerinck, J., Eeckhout, D., Schweizer, F.; Godoy, M.; Franco-Zorilla, J. M., Pauwels, L., Witters, E., Puga, M. I., Paz-Ares, J., Goossens, A. Reymond, P., Jaeger, G. D. & Solano, R. (2011).** The Arabidopsis bHLH transcription factors MYC3 and MYC4 are targets of JAZ repressors and act additively with MYC2 in the activation of jasmonate responses. *The Plant Cell*, 23(2), 701-715.
- Fields, S., & Song, O. K. (1989).** A novel genetic system to detect protein-protein interactions. *Nature*, 340(6230), 245-246.
- Figurski, D. H., & Helinski, D. R. (1979).** Replication of an origin-containing derivative of plasmid RK2 dependent on a plasmid function provided in trans. *Proceedings of the National Academy of Sciences*, 76(4), 1648-1652.
- Flor, H. H. (1942).** Inheritance of pathogenicity in *Melampsora lini*. *Phytopathology*, 32, 653-669.
- Flor, H. H. (1971).** Current status of the gene-for-gene concept. *Annual Review of Phytopathology*, 9(1), 275-296.
- Foley, R. C., & Singh, K. B. (2004).** TGA5 acts as a positive and TGA4 acts as a negative regulator of ocs element activity in Arabidopsis roots in response to defence signals. *FEBS Letters*, 563(1-3), 141-145.
- Fonseca, J. P., Menossi, M., Thibaud-Nissen, F., & Town, C. D. (2010).** Functional analysis of a TGA factor-binding site located in the promoter region controlling salicylic acid-induced NIMIN-1 expression in Arabidopsis. *Genetics and Molecular Research*, 9(1), 167-175.
- Foster, R., Izawa, T., & Chua, N. H. (1994).** Plant bZIP proteins gather at ACGT elements. *The FASEB Journal*, 8(2), 192-200.
- Friedrich, L., Vernooij, B., Gaffney, T., Morse, A., & Ryals, J. (1995).** Characterization of tobacco plants expressing a bacterial salicylate hydroxylase gene. *Plant Molecular Biology*, 29(5), 959-968.
- Friedrich, L., Lawton, K., Ruess, W., Masner, P., Specker, N., Rella, M. G., Meier, B., Dincher, S., Staub, T., Uknes, S., Métraux, J.P., Kessmann, H. & Ryals, J. (1996).** A benzothiadiazole derivative induces systemic acquired resistance in tobacco. *The Plant Journal*, 10(1), 61-70.

- Fromm, H., Katagiri, F., & Chua, N. H. (1991).** The tobacco transcription activator TGA1a binds to a sequence in the 5' upstream region of a gene encoding a TGA1a-related protein. *Molecular and General Genetics MGG*, 229(2), 181-188.
- Fu, Z. Q., Yan, S., Saleh, A., Wang, W., Ruble, J., Oka, N., Mohan, R., Spoel, S. H., Tada, Y., Zheng, N. & Dong, X. (2012).** NPR3 and NPR4 are receptors for the immune signal salicylic acid in plants. *Nature*, 486(7402), 228-232.
- Fu, Z. Q., & Dong, X. (2013).** Systemic acquired resistance: turning local infection into global defense. *Annual Review of Plant Biology*, 64, 839-863.
- Fulton, T. M., Chunwongse, J., & Tanksley, S. D. (1995).** Microprep protocol for extraction of DNA from tomato and other herbaceous plants. *Plant Molecular Biology Reporter*, 13(3), 207-209.
- Gaffney, T., Friedrich, L., Vernooij, B., Negrotto, D., Nye, G., Uknes, S., Ward., E., Kessmann, H. & Ryals, J. (1993).** Requirement of salicylic acid for the induction of systemic acquired resistance. *Science*, 261(5122), 754-756.
- Gamir, J., Darwiche, R., van't Hof, P., Choudhary, V., Stumpe, M., Schneider, R., & Mauch, F. (2017).** The sterol-binding activity of PATHOGENESIS-RELATED PROTEIN 1 reveals the mode of action of an antimicrobial protein. *The Plant Journal*, 89(3), 502-509.
- Gao, X., Chen, X., Lin, W., Chen, S., Lu, D., Niu, Y., Li, L., Cheng, C., McCormack, M., Sheen, J., Shan, L., & He, P. (2013).** Bifurcation of Arabidopsis NLR immune signaling via Ca²⁺-dependent protein kinases. *PLOS Pathogens*, 9(1), e1003127.
- Garcion, C., Lohmann, A., Lamodièrre, E., Catinot, J., Buchala, A., Doermann, P., & Métraux, J. P. (2008).** Characterization and biological function of the ISOCHORISMATE SYNTHASE2 gene of Arabidopsis. *Plant Physiology*, 147(3), 1279-1287.
- Gasteiger, E., Hoogland, C., Gattiker, A., Duvaud, S., Wilkins, M.R., Appel, R.D., Bairoch, A. (2005).** Protein Identification and Analysis Tools on the ExPASy Server; (In) John M. Walker (ed): *The Proteomics Protocols Handbook*, Humana Press, pp. 571-607
- Gatz, C. (2013).** From pioneers to team players: TGA transcription factors provide a molecular link between different stress pathways. *Molecular Plant-Microbe Interactions*, 26(2), 151-159.
- Ghosh, S., & Hayden, M. (2012).** Celebrating 25 years of NF-κB research. *Immunological Reviews*, 246(1), 5-13.
- Gibbs, G. M., Roelants, K., & O'bryan, M. K. (2008).** The CAP superfamily: cysteine-rich secretory proteins, antigen 5, and pathogenesis-related 1 proteins—roles in reproduction, cancer, and immune defense. *Endocrine Reviews*, 29(7), 865-897.
- Gilbert, G. S., Mejía-Chang, M., & Rojas, E. (2002).** Fungal diversity and plant disease in mangrove forests: salt excretion as a possible defense mechanism. *Oecologia*, 132(2), 278-285.
- Giuliano, G., Pichersky, E., Malik, V. S., Timko, M. P., Scolnik, P. A., & Cashmore, A. R. (1988).** An evolutionarily conserved protein binding sequence upstream of a plant light-regulated gene. *Proceedings of the National Academy of Sciences*, 85(19), 7089-7093.
- Glazebrook, J., & Ausubel, F. M. (1994).** Isolation of phytoalexin-deficient mutants of Arabidopsis thaliana and characterization of their interactions with bacterial pathogens. *Proceedings of the National Academy of Sciences*, 91(19), 8955-8959.
- Glazebrook, J., Rogers, E. E., & Ausubel, F. M. (1996).** Isolation of Arabidopsis mutants with enhanced disease susceptibility by direct screening. *Genetics*, 143(2), 973-982.
- Glazebrook J. (2005).** Contrasting mechanisms of defense against biotrophic and necrotrophic pathogens. *Annual Review of Phytopathology*, 43, 205-227.

- Glocova, I., Thor, K., Roth, B., Babbick, M., Pfitzner, A. J., & Pfitzner, U. M. (2005).** Salicylic acid (SA)-dependent gene activation can be uncoupled from cell death-mediated gene activation: the SA-inducible NIMIN-1 and NIMIN-2 promoters, unlike the PR-1a promoter, do not respond to cell death signals in tobacco. *Molecular Plant Pathology*, 6(3), 299-314.
- Gómez-Gómez, L., & Boller, T. (2000).** FLS2: an LRR receptor-like kinase involved in the perception of the bacterial elicitor flagellin in Arabidopsis. *Molecular Cell*, 5(6), 1003-1011.
- Görlach, J., Volrath, S., Knauf-Beiter, G., Hengy, G., Beckhove, U., Kogel, K. H., Oostendorp, M., Staub, T., Ward, E. Kessmann, H. & Ryals, J. (1996).** Benzothiadiazole, a novel class of inducers of systemic acquired resistance, activates gene expression and disease resistance in wheat. *The Plant Cell*, 8(4), 629-643.
- Goujon, M., McWilliam, H., Li, W., Valentin, F., Squizzato, S., Paern, J., & Lopez, R. (2010).** A new bioinformatics analysis tools framework at EMBL–EBI. *Nucleic Acids Research*, 38(suppl_2), W695-W699.
- Greenberg, J. T., & Ausubel, F. M. (1993).** Arabidopsis mutants compromised for the control of cellular damage during pathogenesis and aging. *The Plant Journal*, 4(2), 327-341.
- Gruber, A. R., Lorenz, R., Bernhart, S. H., Neuböck, R., & Hofacker, I. L. (2008).** The Vienna RNA websuite. *Nucleic Acids Research*, 36(Web Server issue), W70–W74.
- Grüner, R., & Pfitzner, U. M. (1994).** The upstream region of the gene for the pathogenesis-related protein 1a from tobacco responds to environmental as well as to developmental signals in transgenic plants. *European Journal of Biochemistry*, 220(1), 247-255.
- Gruner, K., Griebel, T., Návarová, H., Attaran, E., & Zeier, J. (2013).** Reprogramming of plants during systemic acquired resistance. *Frontiers in Plant Science*, 4, 252.
- Gurr, S., Samalova, M., & Fisher, M. (2011).** The rise and rise of emerging infectious fungi challenges food security and ecosystem health. *Fungal Biology Reviews*, 25(4), 181-188.
- Gust, A. A., Biswas, R., Lenz, H. D., Rauhut, T., Ranf, S., Kemmerling, B., Götz, F., Glawischnig, E., Lee, J., Felix, G. & Nürnberger, T. (2007).** Bacteria-derived peptidoglycans constitute pathogen-associated molecular patterns triggering innate immunity in Arabidopsis. *Journal of Biological Chemistry*, 282(44), 32338-32348.
- Ha, C. M., Kim, G. T., Kim, B. C., Jun, J. H., Soh, M. S., Ueno, Y., Machida, Y., Tsukaya, H. & Nam, H. G. (2003).** The BLADE-ON-PETIOLE 1 gene controls leaf pattern formation through the modulation of meristematic activity in Arabidopsis. *Development*, 130(1), 161-172.
- Hamann, T. (2012).** Plant cell wall integrity maintenance as an essential component of biotic stress response mechanisms. *Frontiers in Plant Science*, 3, 77.
- Hammond-Kosack, K. E., & Jones, J. D. (1997).** Plant disease resistance genes. *Annual Review of Plant Biology*, 48(1), 575-607.
- Han, Y., Meng, T., Murray, N. R., Fields, A. P., & Brasier, A. R. (1999).** Interleukin-1-induced nuclear factor- κ B-I κ B α autoregulatory feedback loop in hepatocytes: a role for protein kinase C α in post-transcriptional regulation of I κ B α resynthesis. *Journal of Biological Chemistry*, 274(2), 939-947.
- Hanahan, D. (1983).** Studies on transformation of Escherichia coli with plasmids. *Journal of Molecular Biology*, 166(4), 557-580.
- Hartmann, M., Kim, D., Bernsdorff, F., Ajami-Rashidi, Z., Scholten, N., Schreiber, S., Zeier, T., Schuck, S., Reichel-Deland, V. & Zeier, J. (2017).** Biochemical principles and functional aspects of piperolic acid biosynthesis in plant immunity. *Plant Physiology*, 174(1), 124-153.
- Hartmann, M., Zeier, T., Bernsdorff, F., Reichel-Deland, V., Kim, D., Hohmann, M., Scholten, N., Schuck, S., Bräutigam, A., Hölzel, T., Ganter, C. & Zeier, J. (2018).** Flavin monooxygenase-generated N-hydroxypiperolic acid is a critical element of plant systemic immunity. *Cell*, 173(2), 456-469.
- Hartmann, M., & Zeier, J. (2019).** N-Hydroxypiperolic acid and salicylic acid: A metabolic duo for systemic acquired resistance. *Current Opinion in Plant Biology*, 50, 44-57.

- Heath, M. C. (2000).** Nonhost resistance and nonspecific plant defenses. *Current Opinion in Plant Biology*, 3(4), 315-319.
- Heese, A., Hann, D. R., Gimenez-Ibanez, S., Jones, A. M. E., He, K., Li, J., Schroeder, J. I., Peck, S. C. & Rathjen, J. P. (2007).** The receptor-like kinase SERK3/BAK1 is a central regulator of innate immunity in plants. *Proceedings of the National Academy of Sciences*, 104(29), 12217-12222.
- Hepworth, S. R., Zhang, Y., McKim, S., Li, X., & Haughn, G. W. (2005).** BLADE-ON-PETIOLE-dependent signaling controls leaf and floral patterning in Arabidopsis. *The Plant Cell*, 17(5), 1434-1448.
- Hermann, M. (2009).** Regulation von NIMIN- und PRI-Genen aus *Arabidopsis thaliana* (L.) Heynh. und *Nicotiana tabacum* (L.) in der Salicylat-abhängigen Pathogenabwehr. Dissertation. University of Hohenheim
- Hermann, M., Maier, F., Masroor, A., Hirth, S., Pfitzner, A. J., & Pfitzner, U. M. (2013).** The Arabidopsis NIMIN proteins affect NPR1 differentially. *Frontiers in Plant Science*, 4, 88.
- Ho, S. N., Hunt, H. D., Horton, R. M., Pullen, J. K., & Pease, L. R. (1989).** Site-directed mutagenesis by overlap extension using the polymerase chain reaction. *Gene*, 77(1), 51-59.
- Hoekema, A., Hirsch, P. R., Hooykaas, P. J., & Schilperoort, R. A. (1983).** A binary plant vector strategy based on separation of vir-and T-region of the *Agrobacterium tumefaciens* Ti-plasmid. *Nature*, 303(5913), 179-180.
- Hogenhout, S. A., Van der Hoorn, R. A., Terauchi, R., & Kamoun, S. (2009).** Emerging concepts in effector biology of plant-associated organisms. *Molecular Plant-Microbe Interactions*, 22(2), 115-122.
- Holsters, M., Silva, B., Van Vliet, F., Genetello, C., De Block, M., Dhaese, P., Depicker, A., Inzé, D., Engler, G., Villarreal, R., Shell, J. & Van Montagu, M. (1980).** The functional organization of the nopaline *A. tumefaciens* plasmid pTiC58. *Plasmid*, 3(2), 212-230.
- Horsch, R. B., Rogers, S. G., & Fraley, R. T. (1985).** Transgenic plants. *Cold Spring Harbor Symposia on Quantitative Biology*, 50, 433-437.
- Horvath, D. M., Huang, D. J., & Chua, N. H. (1998).** Four classes of salicylate-induced tobacco genes. *Molecular Plant-Microbe Interactions*, 11(9), 895-905.
- Inoue, H., Nojima, H., & Okayama, H. (1990).** High efficiency transformation of *Escherichia coli* with plasmids. *Gene*, 96(1), 23-28.
- Jakoby, M., Weisshaar, B., Dröge-Laser, W., Vicente-Carbajosa, J., Tiedemann, J., Kroj, T., & Parcy, F. (2002).** bZIP transcription factors in Arabidopsis. *Trends in Plant Science*, 7(3), 106-111.
- Jefferson, R. A. (1987).** Assaying chimeric genes in plants: the GUS gene fusion system. *Plant Molecular Biology Reporter*, 5(4), 387-405.
- Jeworutzki, E., Roelfsema, M. R. G., Anshütz, U., Krol, E., Elzenga, J. T. M., Felix, G., Boller, T., Hedrich, R. & Becker, D. (2010).** Early signaling through the Arabidopsis pattern recognition receptors FLS2 and EFR involves Ca²⁺-associated opening of plasma membrane anion channels. *The Plant Journal*, 62(3), 367-378.
- Johnson, C., Boden, E., & Arias, J. (2003).** Salicylic acid and NPR1 induce the recruitment of trans-activating TGA factors to a defense gene promoter in Arabidopsis. *The Plant Cell*, 15(8), 1846-1858.
- Jones, J. D., & Dangl, J. L. (2006).** The plant immune system. *Nature*, 444(7117), 323-329.
- Jung, H. W., Tschaplinski, T. J., Wang, L., Glazebrook, J., & Greenberg, J. T. (2009).** Priming in systemic plant immunity. *Science*, 324(5923), 89-91.
- Jung, J. (2019).** Untersuchungen zum Einfluss von NIMIN-Proteinen auf NPR-Proteine. Master Thesis. University of Hohenheim.

- Kadota, Y., Sklenar, J., Derbyshire, P., Stransfeld, L., Asai, S., Ntoukakis, V., Jones, J. D. G., Shirasu, K., Menke, F., Jones, A. & Zipfel, C. (2014).** Direct regulation of the NADPH oxidase RBOHD by the PRR-associated kinase BIK1 during plant immunity. *Molecular Cell*, 54(1), 43-55.
- Kagale, S., Links, M. G., & Rozwadowski, K. (2010).** Genome-wide analysis of ethylene-responsive element binding factor-associated amphiphilic repression motif-containing transcriptional regulators in Arabidopsis. *Plant Physiology*, 152(3), 1109-1134.
- Katagiri, F., Lam, E., & Chua, N. H. (1989).** Two tobacco DNA-binding proteins with homology to the nuclear factor CREB. *Nature*, 340(6236), 727-730.
- Katagiri, F., & Tsuda, K. (2010).** Understanding the plant immune system. *Molecular Plant-Microbe Interactions*, 23(12), 1531-1536.
- Kauffmann, S., Legrand, M., Geoffroy, P., & Fritig, B. (1987).** Biological function of 'pathogenesis-related' proteins: four PR proteins of tobacco have 1, 3- β -glucanase activity. *The EMBO Journal*, 6(11), 3209-3212.
- Kawata, T., Imada, T., Shiraishi, H., Okada, K., Shimura, Y., & Iwabuchi, M. (1992).** A cDNA clone encoding HBP-1b homologue in Arabidopsis thaliana. *Nucleic Acids Research*, 20(5), 1141.
- Kerpedjiev, P., Hammer, S., & Hofacker, I. L. (2015).** Forna (force-directed RNA): Simple and effective online RNA secondary structure diagrams. *Bioinformatics (Oxford, England)*, 31(20), 3377-3379
- Khan, M., Xu, M., Murmu, J., Tabb, P., Liu, Y., Storey, K., McKim, S. M., Douglas, C. J. & Hepworth, S. R. (2012).** Antagonistic interaction of BLADE-ON-PETIOLE1 and 2 with BREVIPEDICELLUS and PENNYWISE regulates Arabidopsis inflorescence architecture. *Plant Physiology*, 158(2), 946-960.
- Khan, M., Xu, H., & Hepworth, S. R. (2014).** BLADE-ON-PETIOLE genes: setting boundaries in development and defense. *Plant Science*, 215, 157-171.
- Kim, H. S., & Delaney, T. P. (2002).** Over-expression of TGA5, which encodes a bZIP transcription factor that interacts with NIM1/NPR1, confers SAR-independent resistance in Arabidopsis thaliana to Peronospora parasitica. *The Plant Journal*, 32(2), 151-163.
- Kinkema, M., Fan, W., & Dong, X. (2000).** Nuclear localization of NPR1 is required for activation of PR gene expression. *The Plant Cell*, 12(12), 2339-2350.
- Klessig, D. F., Choi, H. W., & Dempsey, D. M. A. (2018).** Systemic acquired resistance and salicylic acid: past, present, and future. *Molecular Plant-Microbe Interactions*, 31(9), 871-888.
- Knoth, C., Salus, M. S., Girke, T., & Eulgem, T. (2009).** The synthetic elicitor 3, 5-dichloroanthranilic acid induces NPR1-dependent and NPR1-independent mechanisms of disease resistance in Arabidopsis. *Plant Physiology*, 150(1), 333-347.
- Kobayashi, I., Kobayashi, Y., Yamaoka, N., & Kunoh, H. (1992).** Recognition of a pathogen and a nonpathogen by barley coleoptile cells. III. Responses of microtubules and actin filaments in barley coleoptile cells to penetration attempts. *Canadian Journal of Botany*, 70(9), 1815-1823.
- Kobayashi, Y., Yamada, M., Kobayashi, I., & Kunoh, H. (1997).** Actin microfilaments are required for the expression of nonhost resistance in higher plants. *Plant and Cell Physiology*, 38(6), 725-733.
- Konopka, E. (2018).** Funktionelle Bedeutung unterschiedlicher NPR-Proteine für die Salicylsäure-abhängige Genexpression im Rahmen der systemisch aktivierten Resistenz in *Arabidopsis thaliana* und *Nicotiana tabacum*. Dissertation. University of Hohenheim
- Koornneef, A., & Pieterse, C. M. (2008).** Cross talk in defense signaling. *Plant Physiology*, 146(3), 839-844.
- Kopp, E. B., & Medzhitov, R. (1999).** The Toll-receptor family and control of innate immunity. *Current Opinion in Immunology*, 11(1), 13-18.

Kroemer, G. (1997). The proto-oncogene Bcl-2 and its role in regulating apoptosis. *Nature Medicine*, 3(6), 614-620.

Kuč, J. (1982). Induced immunity to plant disease. *Bioscience*, 32(11), 854-860.

Kuhlemeier, C., Green, P. J., & Chua, N. H. (1987). Regulation of gene expression in higher plants. *Annual Review of Plant Physiology*, 38(1), 221-257.

Kuhlen, L., Abrusci, P., Johnson, S., Gault, J., Deme, J., Caesar, J., Dietsche, T., Mebrhatu, M. T., Ganief, T., Macek, B., Wagner, S., Robinson, C. V. & Lea, S. M. (2018). Structure of the core of the type III secretion system export apparatus. *Nature Structural & Molecular Biology*, 25(7), 583-590.

Kyte, J., & Doolittle, R. F. (1982). A simple method for displaying the hydropathic character of a protein. *Journal of Molecular Biology*, 157(1), 105-132.

Lacombe, S., Rougon-Cardoso, A., Sherwood, E., Peeters, N., Dahlbeck, D., Van Esse, H. P., Smoker, M., Rallapalli, G., Thomma, B. P. H. J., Staskawicz, B., Jones, J. D. G. & Zipfel, C. (2010). Interfamily transfer of a plant pattern-recognition receptor confers broad-spectrum bacterial resistance. *Nature Biotechnology*, 28(4), 365-369.

Lacomme, C., & Santa Cruz, S. (1999). Bax-induced cell death in tobacco is similar to the hypersensitive response. *Proceedings of the National Academy of Sciences*, 96(14), 7956-7961.

Laemmli, U. K. (1970). Cleavage of structural proteins during the assembly of the head of bacteriophage T4. *Nature*, 227(5259), 680-685.

Lam, E., Benfey, P. N., Gilmartin, P. M., Fang, R. X., & Chua, N. H. (1989). Site-specific mutations alter in vitro factor binding and change promoter expression pattern in transgenic plants. *Proceedings of the National Academy of Sciences*, 86(20), 7890-7894.

Landschulz, W. H., Johnson, P. F., & McKnight, S. L. (1988). The leucine zipper: a hypothetical structure common to a new class of DNA binding proteins. *Science*, 240(4860), 1759-1764.

Lascombe, M. B., Bakan, B., Buhot, N., Marion, D., Blein, J. P., Larue, V., Lamb, C. & Prangé, T. (2008). The structure of “defective in induced resistance” protein of *Arabidopsis thaliana*, DIR1, reveals a new type of lipid transfer protein. *Protein Science*, 17(9), 1522-1530.

Lassowskat, I., Böttcher, C., Eschen-Lippold, L., Scheel, D., & Lee, J. (2014). Sustained mitogen-activated protein kinase activation reprograms defense metabolism and phosphoprotein profile in *Arabidopsis thaliana*. *Frontiers in Plant Science*, 5, 554.

Lawton, K. A., Friedrich, L., Hunt, M., Weymann, K., Delaney, T., Kessmann, H., Staub, T. & Ryals, J. (1996). Benzothiadiazole induces disease resistance in *Arabidopsis* by activation of the systemic acquired resistance signal transduction pathway. *The Plant Journal*, 10(1), 71-82.

Lebel, E., Heifetz, P., Thorne, L., Uknes, S., Ryals, J., & Ward, E. (1998). Functional analysis of regulatory sequences controlling PR-1 gene expression in *Arabidopsis*. *The Plant Journal*, 16(2), 223-233.

Lee, H. J., Park, Y. J., Seo, P. J., Kim, J. H., Sim, H. J., Kim, S. G., & Park, C. M. (2015). Systemic immunity requires SnRK2.8-mediated nuclear import of NPR1 in *Arabidopsis*. *The Plant Cell*, 27(12), 3425-3438.

Lefevre, H., Bauters, L., & Gheysen, G. (2020). Salicylic acid biosynthesis in plants. *Frontiers in Plant Science*, 11, 338.

Legrand, M., Kauffmann, S., Geoffroy, P., & Fritig, B. (1987). Biological function of pathogenesis-related proteins: four tobacco pathogenesis-related proteins are chitinases. *Proceedings of the National Academy of Sciences*, 84(19), 6750-6754.

Lehmann, L. (2014). Functional analysis of NIMIN proteins in *Nicotiana benthamiana*. Bachelor Thesis. University of Hohenheim

- Leon, J., Shulaev, V., Yalpani, N., Lawton, M. A., & Raskin, I. (1995).** Benzoic acid 2-hydroxylase, a soluble oxygenase from tobacco, catalyzes salicylic acid biosynthesis. *Proceedings of the National Academy of Sciences*, 92(22), 10413-10417.
- Li, M., Chen, H., Chen, J., Chang, M., Palmer, I. A., Gassmann, W., Liu, F. & Fu, Z. Q. (2018).** TCP transcription factors interact with NPR1 and contribute redundantly to systemic acquired resistance. *Frontiers in Plant Science*, 9, 1153.
- Liu, Y., Schiff, M., Marathe, R., & Dinesh-Kumar, S. P. (2002).** Tobacco Rar1, EDS1 and NPR1/NIM1 like genes are required for N-mediated resistance to tobacco mosaic virus. *The Plant Journal*, 30(4), 415-429.
- Liu, Y., Du, M., Deng, L., Shen, J., Fang, M., Chen, Q., Lu, Y., Wang, Q., Li, C. & Zhai, Q. (2019).** MYC2 regulates the termination of jasmonate signaling via an autoregulatory negative feedback loop. *The Plant Cell*, 31(1), 106-127.
- Liu, X., Galli, M., Camehl, I., & Gallavotti, A. (2019b).** RAMOSA1 ENHANCER LOCUS2-mediated transcriptional repression regulates vegetative and reproductive architecture. *Plant physiology*, 179(1), 348-363.
- Lorenz, R., Bernhart, S. H., Höner Zu Siederdisen, C., Tafer, H., Flamm, C., Stadler, P. F., & Hofacker, I. L. (2011).** ViennaRNA Package 2.0. *Algorithms for Molecular Biology : AMB*, 6, 26.
- Lotze, M. T., & Tracey, K. J. (2005).** High-mobility group box 1 protein (HMGB1): nuclear weapon in the immune arsenal. *Nature Reviews Immunology*, 5(4), 331-342.
- Lotze, M. T., Zeh, H. J., Rubartelli, A., Sparvero, L. J., Amoscato, A. A., Washburn, N. R., DeVera, M. E., Liang, X., Tör, M. & Billiar, T. (2007).** The grateful dead: damage-associated molecular pattern molecules and reduction/oxidation regulate immunity. *Immunological Reviews*, 220(1), 60-81.
- Lucas, J. A. (1999).** Plant immunisation: from myth to SAR. *Pesticide Science*, 55(2), 193-196.
- Maeda, H., Yoo, H., & Dudareva, N. (2011).** Prephenate aminotransferase directs plant phenylalanine biosynthesis via arogenate. *Nature Chemical Biology*, 7(1), 19-21.
- Maier, F., Zwicker, S., Hueckelhoven, A., Meissner, M., Funk, J., Pfitzner, A. J., & Pfitzner, U. M. (2011).** NONEXPRESSOR OF PATHOGENESIS-RELATED PROTEINS1 (NPR1) and some NPR1-related proteins are sensitive to salicylic acid. *Molecular Plant Pathology*, 12(1), 73-91.
- Malamy, J., Carr, J. P., Klessig, D. F., & Raskin, I. (1990).** Salicylic acid: a likely endogenous signal in the resistance response of tobacco to viral infection. *Science*, 250(4983), 1002-1004.
- Maldonado, A. M., Doerner, P., Dixon, R. A., Lamb, C. J., & Cameron, R. K. (2002).** A putative lipid transfer protein involved in systemic resistance signalling in Arabidopsis. *Nature*, 419(6905), 399-403.
- Manohar, M., Tian, M., Moreau, M., Park, S. W., Choi, H. W., Fei, Z., Friso, G., Asif, M., Manosalva, P., von Dahl, C. C., Shi, K., Ma, S., Dinesh-Kumar, S. P., O'Doherty, I., Schroeder, F. S., van Wijk, K. J. & Klessig, D. F. (2015).** Identification of multiple salicylic acid-binding proteins using two high throughput screens. *Frontiers in Plant Science*, 5, 777.
- Martin-Arevalillo, R., Nanao, M. H., Larriau, A., Vinos-Poyo, T., Mast, D., Galvan-Ampudia, C., Brunoud, G., Vernoux, T., Dumas, R. & Parcy, F. (2017).** Structure of the Arabidopsis TOPLESS corepressor provides insight into the evolution of transcriptional repression. *Proceedings of the National Academy of Sciences*, 114(30), 8107-8112.
- Masroor, A. (2013).** Effects of overexpression of *NIMIN* genes on Salicylic acid-mediated *PR-1* gene activation and phenotype in *Nicotiana benthamiana* (Domin). Dissertation. University of Hohenheim
- Mathews, D. H., Disney, M. D., Childs, J. L., Schroeder, S. J., Zuker, M., & Turner, D. H. (2004).** Incorporating chemical modification constraints into a dynamic programming algorithm for prediction of RNA secondary structure. *Proceedings of the National Academy of Sciences*, 101(19), 7287-7292.

- Mattsson, J., Ckurshumova, W., & Berleth, T. (2003).** Auxin signaling in Arabidopsis leaf vascular development. *Plant Physiology*, *131*(3), 1327-1339.
- McKim, S. M., Stenvik, G. E., Butenko, M. A., Kristiansen, W., Cho, S. K., Hepworth, S. R., Aalen, R. B. & Haughn, G. W. (2008).** The BLADE-ON-PETIOLE genes are essential for abscission zone formation in Arabidopsis. *Development*, *135*(8), 1537-1546.
- Meir, S., Sundaresan, S., Riov, J., Agarwal, I., & Philosoph-Hadas, S. (2015).** Role of auxin depletion in abscission control. *Stewart Postharvest Review*, *11*(2), 1-15.
- Melotto, M., Underwood, W., & He, S. Y. (2008).** Role of stomata in plant innate immunity and foliar bacterial diseases. *Annual Review of Phytopathology*, *46*, 101–122.
- Mendgen, K., Hahn, M., & Deising, H. (1996).** Morphogenesis and mechanisms of penetration by plant pathogenic fungi. *Annual Review of Phytopathology*, *34*(1), 367-386.
- Métraux, J. P., Signer, H., Ryals, J., Ward, E., Wyss-Benz, M., Gaudin, J., Raschdorf, K., Schmid, E., Blum, W. & Inverardi, B. (1990).** Increase in salicylic acid at the onset of systemic acquired resistance in cucumber. *Science*, *250*(4983), 1004-1006.
- Miao, Z. H., Liu, X., & Lam, E. (1994).** TGA3 is a distinct member of the TGA family of bZIP transcription factors in Arabidopsis thaliana. *Plant Molecular Biology*, *25*(1), 1-11.
- Mignone, F., Gissi, C., Liuni, S., & Pesole, G. (2002).** Untranslated regions of mRNAs. *Genome Biology*, *3*(3), 1-10.
- Misas-Villamil, J. C., & Van der Hoorn, R. A. (2008).** Enzyme–inhibitor interactions at the plant–pathogen interface. *Current Opinion in Plant Biology*, *11*(4), 380-388.
- Mishina, T. E., & Zeier, J. (2006).** The Arabidopsis flavin-dependent monooxygenase FMO1 is an essential component of biologically induced systemic acquired resistance. *Plant Physiology*, *141*(4), 1666-1675.
- Mosavi, L. K., Cammett, T. J., Desrosiers, D. C., & Peng, Z. Y. (2004).** The ankyrin repeat as molecular architecture for protein recognition. *Protein Science*, *13*(6), 1435-1448.
- Mou, Z., Fan, W., & Dong, X. (2003).** Inducers of plant systemic acquired resistance regulate NPR1 function through redox changes. *Cell*, *113*(7), 935-944.
- Murmu, J., Bush, M. J., DeLong, C., Li, S., Xu, M., Khan, M., Malcolmson, C., Fobert, P. R., Zachgo, S. & Hepworth, S. R. (2010).** Arabidopsis basic leucine-zipper transcription factors TGA9 and TGA10 interact with floral glutaredoxins ROXY1 and ROXY2 and are redundantly required for anther development. *Plant Physiology*, *154*(3), 1492-1504.
- Mysore, K. S., & Ryu, C. M. (2004).** Nonhost resistance: how much do we know?. *Trends in Plant Science*, *9*(2), 97-104.
- Návarová, H., Bernsdorff, F., Döring, A. C., & Zeier, J. (2012).** Pipecolic acid, an endogenous mediator of defense amplification and priming, is a critical regulator of inducible plant immunity. *The Plant Cell*, *24*(12), 5123-5141.
- Nawrath, C., & Métraux, J. P. (1999).** Salicylic acid induction–deficient mutants of Arabidopsis express PR-2 and PR-5 and accumulate high levels of camalexin after pathogen inoculation. *The Plant Cell*, *11*(8), 1393-1404.
- Neeley, D., Konopka, E., Straub, A., Maier, F., Pfitzner, A. J., & Pfitzner, U. M. (2019).** Salicylic acid-driven association of LENRV and NIMIN1/NIMIN2 binding domain regions in the C-terminus of tobacco NPR1 transduces SAR signal. *bioRxiv*, 543645.
- Niderman, T., Genetet, I., Bruyere, T., Gees, R., Stintzi, A., Legrand, M., Fritig, B. & Mosinger, E. (1995).** Pathogenesis-related PR-1 proteins are antifungal (isolation and characterization of three 14-kilodalton proteins of tomato and of a basic PR-1 of tobacco with inhibitory activity against *Phytophthora infestans*). *Plant Physiology*, *108*(1), 17-27.

- Niggeweg, R., Thurow, C., Kegler, C., & Gatz, C. (2000a).** Tobacco transcription factor TGA2. 2 is the main component of as-1-binding factor ASF-1 and is involved in salicylic acid-and auxin-inducible expression of as-1-containing target promoters. *Journal of Biological Chemistry*, 275(26), 19897-19905.
- Niggeweg, R., Thurow, C., Weigel, R., Pfitzner, U., & Gatz, C. (2000b).** Tobacco TGA factors differ with respect to interaction with NPR1, activation potential and DNA-binding properties. *Plant Molecular Biology*, 42(5), 775-788.
- Noman, A., Liu, Z., Aqeel, M., Zainab, M., Khan, M. I., Hussain, A., Ashraf, M. F., Li, X., Weng, Y. & He, S. (2017).** Basic leucine zipper domain transcription factors: the vanguards in plant immunity. *Biotechnology Letters*, 39(12), 1779-1791.
- Nowakowski, J., & Tinoco Jr, I. (1997).** RNA structure and stability. *Seminars in Virology*, 8(3), 153-165.
- Ohta, M., Matsui, K., Hiratsu, K., Shinshi, H., & Ohme-Takagi, M. (2001).** Repression domains of class II ERF transcriptional repressors share an essential motif for active repression. *The Plant Cell*, 13(8), 1959-1968.
- Park, S. W., Kaimoyo, E., Kumar, D., Mosher, S., & Klessig, D. F. (2007).** Methyl salicylate is a critical mobile signal for plant systemic acquired resistance. *Science*, 318(5847), 113-116.
- Parshin, P. D., Pometun, A. A., Martysuk, U. A., Kleymenov, S. Y., Atroshenko, D. L., Pometun, E. V., Savin, S. S. & Tishkov, V. I. (2020).** Effect of His 6-tag Position on the Expression and Properties of Phenylacetone Monooxygenase from *Thermobifida fusca*. *Biochemistry (Moscow)*, 85, 575-582.
- Pauwels, L., Barbero, G. F., Geerinck, J., Tilleman, S., Grunewald, W., Pérez, A. C., Chico, J. M., Bossche, R. V., Sewell, J., Gil, E., García-Casado, G., Witters, E., Inzé, D., Long, J. A., Jaeger, G. D., Solano R. & Goossens, A. (2010).** NINJA connects the co-repressor TOPLESS to jasmonate signalling. *Nature*, 464(7289), 788-791.
- Petersen, M., Brodersen, P., Næsted, H., Andreasson, E., Lindhart, U., Johansen, B., Nielsen, H. B., Austin, M. J., Parker, J. E., Sharma, S. B., Klessig, D. F., Martienssen, R., Mattsson, O., Jensen, A. B. & Mundy, J. B. (2000).** Arabidopsis MAP kinase 4 negatively regulates systemic acquired resistance. *Cell*, 103(7), 1111-1120.
- Pfitzner, U. M., & Goodman, H. M. (1987).** Isolation and characterization of cDNA clones encoding pathogenesis-related proteins from tobacco mosaic virus infected tobacco plants. *Nucleic Acids Research*, 15(11), 4449-4465.
- Pieterse, C. M., Leon-Reyes, A., Van der Ent, S., & Van Wees, S. C. (2009).** Networking by small-molecule hormones in plant immunity. *Nature Chemical Biology*, 5(5), 308-316.
- Pieterse, C. M., Van der Does, D., Zamioudis, C., Leon-Reyes, A., & Van Wees, S. C. (2012).** Hormonal modulation of plant immunity. *Annual review of Cell and Developmental Biology*, 28, 489-521
- Plant, A. R., Larrieu, A., & Causier, B. (2021).** Repressor for hire! The vital roles of TOPLESS-mediated transcriptional repression in plants. *New Phytologist*, 10.1111/nph.17428. Advance online publication.
- Qi, D., & Innes, R. W. (2013).** Recent advances in plant NLR structure, function, localization, and signaling. *Frontiers in Immunology*, 4, 348.
- Qin, X. F., Holuigue, L., Horvath, D. M., & Chua, N. H. (1994).** Immediate early transcription activation by salicylic acid via the cauliflower mosaic virus as-1 element. *The Plant Cell*, 6(6), 863-874.
- Rafiqi, M., Gan, P. H. P., Ravensdale, M., Lawrence, G. J., Ellis, J. G., Jones, D. A., Hardham, A. R. & Dodds, P. N. (2010).** Internalization of flax rust avirulence proteins into flax and tobacco cells can occur in the absence of the pathogen. *The Plant Cell*, 22(6), 2017-2032.
- Raikhel, N. (1992).** Nuclear targeting in plants. *Plant Physiology*, 100(4), 1627-1632.
- Ramirez-Prado, J. S., Abulfaraj, A. A., Rayapuram, N., Benhamed, M., & Hirt, H. (2018).** Plant immunity: from signaling to epigenetic control of defense. *Trends in Plant Science*, 23(9), 833-844.

Ranf, S., Eschen-Lippold, L., Pecher, P., Lee, J., & Scheel, D. (2011). Interplay between calcium signalling and early signalling elements during defence responses to microbe-or damage-associated molecular patterns. *The Plant Journal*, *68*(1), 100-113.

Raskin, I. (1992). Role of salicylic acid in plants. *Annual Review of Plant Biology*, *43*(1), 439-463.

Ravensdale, M., Bernoux, M., Ve, T., Kobe, B., Thrall, P. H., Ellis, J. G., & Dodds, P. N. (2012). Intramolecular interaction influences binding of the Flax L5 and L6 resistance proteins to their AvrL567 ligands. *PLOS Pathogens*, *8*(11), e1003004.

Rekas, A., Alattia, J. R., Nagai, T., Miyawaki, A., & Ikura, M. (2002). Crystal structure of venus, a yellow fluorescent protein with improved maturation and reduced environmental sensitivity. *Journal of Biological Chemistry*, *277*(52), 50573-50578.

Rekhter, D., Lüdke, D., Ding, Y., Feussner, K., Zienkiewicz, K., Lipka, V., Wiermer, M., Zhang, Y. & Feussner, I. (2019). Isochorismate-derived biosynthesis of the plant stress hormone salicylic acid. *Science*, *365*(6452), 498-502.

Richmond, T. A., & Bleecker, A. B. (1999). A defect in β -oxidation causes abnormal inflorescence development in Arabidopsis. *The Plant Cell*, *11*(10), 1911-1923.

Robert-Seilaniantz, A., Grant, M., & Jones, J. D. (2011). Hormone crosstalk in plant disease and defense: more than just jasmonate-salicylate antagonism. *Annual Review of Phytopathology*, *49*, 317-343.

Rochon, A., Boyle, P., Wignes, T., Fobert, P. R., & Després, C. (2006). The coactivator function of Arabidopsis NPR1 requires the core of its BTB/POZ domain and the oxidation of C-terminal cysteines. *The Plant Cell*, *18*(12), 3670-3685.

Rogers, H. J. (2006). Programmed cell death in floral organs: how and why do flowers die?. *Annals of Botany*, *97*(3), 309-315.

Rose, J. K., Ham, K. S., Darvill, A. G., & Albersheim, P. (2002). Molecular cloning and characterization of glucanase inhibitor proteins: coevolution of a counterdefense mechanism by plant pathogens. *The Plant Cell*, *14*(6), 1329-1345.

Ross, A. F. (1961). Systemic acquired resistance induced by localized virus infections in plants. *Virology*, *14*(3), 340-358.

Ross A. F., (1966). Systemic effects of local lesion formation In: A. B. R. Beemster & J. Dijkstra (Eds), *Viruses of plants*. 127-150. North-Holland Publ. Comp., Amsterdam.

Roux, M., Schwessinger, B., Albrecht, C., Chinchilla, D., Jones, A., Holton, N., Malinovsky, F. G., Tör, M., de Vries, S. & Zipfel, C. (2011). The Arabidopsis leucine-rich repeat receptor-like kinases BAK1/SERK3 and BKK1/SERK4 are required for innate immunity to hemibiotrophic and biotrophic pathogens. *The Plant Cell*, *23*(6), 2440-2455.

Running, M. P., & Meyerowitz, E. M. (1996). Mutations in the PERIANTHIA gene of Arabidopsis specifically alter floral organ number and initiation pattern. *Development*, *122*(4), 1261-1269.

Ryals, J., Weymann, K., Lawton, K., Friedrich, L., Ellis, D., Steiner, H. Y., Johnson, J., Delaney, T. P., Jesse, T. Vos, P. & Uknes, S. (1997). The Arabidopsis NIM1 protein shows homology to the mammalian transcription factor inhibitor I kappa B. *The Plant Cell*, *9*(3), 425-439.

Saijo, Y., Loo, E. P. I., & Yasuda, S. (2018). Pattern recognition receptors and signaling in plant-microbe interactions. *The Plant Journal*, *93*(4), 592-613.

Saiki, R. K., Gelfand, D. H., Stoffel, S., Scharf, S. J., Higuchi, R., Horn, G. T., Mullis, K. B. & Erlich, H. A. (1988). Primer-directed enzymatic amplification of DNA with a thermostable DNA polymerase. *Science*, *239*(4839), 487-491.

- Saleh, A., Withers, J., Mohan, R., Marqués, J., Gu, Y., Yan, S., Zavaliev, R., Nomoto, M., Tada, Y. & Dong, X. (2015). Posttranslational modifications of the master transcriptional regulator NPR1 enable dynamic but tight control of plant immune responses. *Cell Host & Microbe*, 18(2), 169-182.
- Sambrook, J., Fritsch, E.F., and Maniatis, T. (1989). *Molecular cloning: A laboratory manual*. Cold Spring Harbour Laboratory Press, Cold Spring Harbour, NY.
- Sanger, F., Nicklen, S., & Coulson, A. R. (1977). DNA sequencing with chain-terminating inhibitors. *Proceedings of the National Academy of Sciences*, 74(12), 5463-5467.
- Satterlee, J. W., & Scanlon, M. J. (2019). Coordination of leaf development across developmental axes. *Plants*, 8(10), 433.
- Savary, S., Willocquet, L., Pethybridge, S. J., Esker, P., McRoberts, N., & Nelson, A. (2019). The global burden of pathogens and pests on major food crops. *Nature Ecology & Evolution*, 3(3), 430-439.
- Schiermeyer, A., Thurow, C., & Gatz, C. (2003). Tobacco bZIP factor TGA10 is a novel member of the TGA family of transcription factors. *Plant Molecular Biology*, 51(6), 817-829.
- Schindler, U., Beckmann, H., & Cashmore, A. R. (1992). TGA1 and G-box binding factors: two distinct classes of Arabidopsis leucine zipper proteins compete for the G-box-like element TGACGTGG. *The Plant Cell*, 4(10), 1309-1319.
- Schurter, R., Kunz, W., and Nyfelder, R. (1987). EU Patent 0313-512, US Patent 4-931-581.
- Schurter, R., Kunz, W., and Nyfeler, R. (1993). Process and a composition for immunizing plants against diseases. USPatent, US5190928A
- Sevilla, F., Camejo, D., Ortiz-Espín, A., Calderón, A., Lázaro, J. J., & Jiménez, A. (2015). The thioredoxin/peroxiredoxin/sulfiredoxin system: current overview on its redox function in plants and regulation by reactive oxygen and nitrogen species. *Journal of Experimental Botany*, 66(10), 2945-2955.
- Shah, J., Tsui, F., & Klessig, D. F. (1997). Characterization of a salicylic acid-insensitive mutant (sai1) of Arabidopsis thaliana, identified in a selective screen utilizing the SA-inducible expression of the tms2 gene. *Molecular Plant-Microbe Interactions*, 10(1), 69-78.
- Shah, J., Chaturvedi, R., Chowdhury, Z., Venables, B., & Petros, R. A. (2014). Signaling by small metabolites in systemic acquired resistance. *The Plant Journal*, 79(4), 645-658.
- Shan, L., He, P., Li, J., Heese, A., Peck, S. C., Nürnberger, T., Martin, G. B. & Sheen, J. (2008). Bacterial effectors target the common signaling partner BAK1 to disrupt multiple MAMP receptor-signaling complexes and impede plant immunity. *Cell Host & Microbe*, 4(1), 17-27.
- Shen, L., Liu, Z., Yang, S., Yang, T., Liang, J., Wen, J., Liu, Y., Li, J., Shi, L., Tang, Q., Shi, W., Hu, J., Liu, C., Zhang, Y., Lin, W., Wang, R., Yu, H., Mou, S., Hussain, A., Cheng, W., Cai, H., He, L. Guan, D., Wu, Y. & He, S. (2016). Pepper CabZIP63 acts as a positive regulator during Ralstonia solanacearum or high temperature-high humidity challenge in a positive feedback loop with CaWRKY40. *Journal of Experimental Botany*, 67(8), 2439-2451.
- Shi, Z., Maximova, S., Liu, Y., Verica, J., & Guiltinan, M. J. (2013). The salicylic acid receptor NPR3 is a negative regulator of the transcriptional defense response during early flower development in Arabidopsis. *Molecular Plant*, 6(3), 802-816.
- Shi, X., Dong, S., & Liu, W. (2019). Structures of plant resistosome reveal how NLR immune receptors are activated. *aBIOTECH*, 1, 147-150
- Shine, M. B., Yang, J. W., El-Habbak, M., Nagyabhyru, P., Fu, D. Q., Navarre, D., Ghabrial, S.; Kachroo, P. & Kachroo, A. (2016). Cooperative functioning between phenylalanine ammonia lyase and isochorismate synthase activities contributes to salicylic acid biosynthesis in soybean. *New Phytologist*, 212(3), 627-636.

Sievers, F., Wilm, A., Dineen, D., Gibson, T. J., Karplus, K., Li, W., Lopez, R., McWilliam, H., Remmert, M., Söding, J., Thompson, J. D. & Higgins, D. G. (2011). Fast, scalable generation of high-quality protein multiple sequence alignments using Clustal Omega. *Molecular Systems Biology*, 7(1), 539.

Singh, K. B., Foley, R. C., & Oñate-Sánchez, L. (2002). Transcription factors in plant defense and stress responses. *Current Opinion in Plant Biology*, 5(5), 430-436.

Späth, M. (2012). Vergleichende Analyse der Interaction von NIMIN-Proteinen mit NPR1 und TOPLESS. Bachelor Thesis. University of Hohenheim.

Spoel, S. H., Johnson, J. S., & Dong, X. (2007). Regulation of tradeoffs between plant defenses against pathogens with different lifestyles. *Proceedings of the National Academy of Sciences*, 104(47), 18842-18847.

Spoel, S. H., Mou, Z., Tada, Y., Spivey, N. W., Genschik, P., & Dong, X. (2009). Proteasome-mediated turnover of the transcription coactivator NPR1 plays dual roles in regulating plant immunity. *Cell*, 137(5), 860-872.

Staal, J., & Dixelius, C. (2007). Tracing the ancient origins of plant innate immunity. *Trends in Plant Science*, 12(8), 334-342.

Stos-Zweifel, V., Neeley, D., Konopka, E., Meissner, M., Hermann, M., Maier, F., Häfner, V., Pfitzner, A. J. P. & Pfitzner, U. M. (2018). Tobacco TGA7 mediates gene expression dependent and independent of salicylic acid. *bioRxiv*, 341834.

Strawn, M. A., Marr, S. K., Inoue, K., Inada, N., Zubieta, C., & Wildermuth, M. C. (2007). Arabidopsis isochorismate synthase functional in pathogen-induced salicylate biosynthesis exhibits properties consistent with a role in diverse stress responses. *Journal of Biological Chemistry*, 282(8), 5919-5933.

Strid, Å., Chow, W. S., & Anderson, J. M. (1994). UV-B damage and protection at the molecular level in plants. *Photosynthesis Research*, 39(3), 475-489.

Strompen, G., Grüner, R., & Pfitzner, U. M. (1998). An as-1-like motif controls the level of expression of the gene for the pathogenesis-related protein 1a from tobacco. *Plant Molecular Biology*, 37(5), 871-883.

Subramaniam, R., Desveaux, D., Spickler, C., Michnick, S. W., & Brisson, N. (2001). Direct visualization of protein interactions in plant cells. *Nature biotechnology*, 19(8), 769-772.

Subtelny, A. O., Eichhorn, S. W., Chen, G. R., Sive, H., & Bartel, D. P. (2014). Poly(A)-tail profiling reveals an embryonic switch in translational control. *Nature*, 508(7494), 66-71.

Sun, Y., Li, L., Macho, A. P., Han, Z., Hu, Z., Zipfel, C., Zhou, J. M. & Chai, J. (2013). Structural basis for flg22-induced activation of the Arabidopsis FLS2-BAK1 immune complex. *Science*, 342(6158), 624-628.

Svoboda, P., & Di Cara, A. (2006). Hairpin RNA: a secondary structure of primary importance. *Cellular and Molecular Life Sciences : CMLS*, 63(7-8), 901-908.

Szemenyei, H., Hannon, M., & Long, J. A. (2008). TOPLESS mediates auxin-dependent transcriptional repression during Arabidopsis embryogenesis. *Science*, 319(5868), 1384-1386.

Szurek, B., Rossier, O., Hause, G., & Bonas, U. (2002). Type III-dependent translocation of the Xanthomonas AvrBs3 protein into the plant cell. *Molecular Microbiology*, 46(1), 13-23.

Tabata, R., Ikezaki, M., Fujibe, T., Aida, M., Tian, C. E., Ueno, Y., Yamamoto, K. T., Machida, Y., Makamura, K. & Ishiguro, S. (2010). Arabidopsis auxin response factor6 and 8 regulate jasmonic acid biosynthesis and floral organ development via repression of class I KNOX genes. *Plant and Cell Physiology*, 51(1), 164-175.

Tada, Y., Spoel, S. H., Pajerowska-Mukhtar, K., Mou, Z., Song, J., Wang, C., Zou, J. & Dong, X. (2008). Plant immunity requires conformational changes of NPR1 via S-nitrosylation and thioredoxins. *Science*, 321(5891), 952-956.

- Tameling, W. I., Elzinga, S. D., Darmin, P. S., Vossen, J. H., Takken, F. L., Haring, M. A., & Cornelissen, B. J. (2002).** The tomato R gene products I-2 and MI-1 are functional ATP binding proteins with ATPase activity. *The Plant Cell*, *14*(11), 2929-2939.
- Tameling, W. I. L., Vossen, J. H., Albrecht, M., Lengauer, T., Berden, J. A., Haring, M. A., Cornelissen, B. J. C. & Takken, F. L. (2006).** Mutations in the NB-ARC domain of I-2 that impair ATP hydrolysis cause autoactivation. *Plant Physiology*, *140*(4), 1233-1245.
- Tao, Y., Xie, Z., Chen, W., Glazebrook, J., Chang, H. S., Han, B., Zhu, T., Zou, G. & Katagiri, F. (2003).** Quantitative nature of Arabidopsis responses during compatible and incompatible interactions with the bacterial pathogen *Pseudomonas syringae*. *The Plant Cell*, *15*(2), 317-330.
- Thomma, B. P., Eggermont, K., Penninckx, I. A., Mauch-Mani, B., Vogelsang, R., Cammue, B. P., & Broekaert, W. F. (1998).** Separate jasmonate-dependent and salicylate-dependent defense-response pathways in Arabidopsis are essential for resistance to distinct microbial pathogens. *Proceedings of the National Academy of Sciences*, *95*(25), 15107-15111.
- Thurow, C., Schiermeyer, A., Krawczyk, S., Butterbrodt, T., Nickolov, K., & Gatz, C. (2005).** Tobacco bZIP transcription factor TGA2. 2 and related factor TGA2. 1 have distinct roles in plant defense responses and plant development. *The Plant Journal*, *44*(1), 100-113.
- Tiwari, S. B., Hagen, G., & Guilfoyle, T. J. (2004).** Aux/IAA proteins contain a potent transcriptional repression domain. *The Plant Cell*, *16*(2), 533-543.
- Torrens-Spence, M. P., Bobokalonova, A., Carballo, V., Glinkerman, C. M., Pluskal, T., Shen, A., & Weng, J. K. (2019).** PBS3 and EPS1 complete salicylic acid biosynthesis from isochorismate in Arabidopsis. *Molecular Plant*, *12*(12), 1577-1586.
- Tripathi, A. D., Mishra, R., Maurya, K. K., Singh, R. B., & Wilson, D. W. (2019).** Estimates for world population and global food availability for global health. In *The role of functional food security in global health* (pp. 3-24). Academic Press.
- Tsuda, K., Sato, M., Glazebrook, J., Cohen, J. D., & Katagiri, F. (2008a).** Interplay between MAMP-triggered and SA-mediated defense responses. *The Plant Journal*, *53*(5), 763-775.
- Tsuda, K., Glazebrook, J., & Katagiri, F. (2008b).** The interplay between MAMP and SA signaling. *Plant Signaling & Behavior*, *3*(6), 359-361.
- Tsuda, K., & Katagiri, F. (2010).** Comparing signaling mechanisms engaged in pattern-triggered and effector-triggered immunity. *Current Opinion in Plant Biology*, *13*(4), 459-465.
- Uknes, S., Mauch-Mani, B., Moyer, M., Potter, S., Williams, S., Dincher, S., Chandler, D., Slusarenko, A., Ward, E. & Ryals, J. (1992).** Acquired resistance in Arabidopsis. *The Plant Cell*, *4*(6), 645-656.
- Uknes, S., Winter, A. M., Delaney, T., Vernooij, B., Morse, A., Friedrich, L., Nye, G., Potter, S., Ward, E. & Ryals, J. (1993).** Biological induction of systemic acquired resistance in Arabidopsis. *Molecular Plant-Microbe Interactions*, *6*(6), 692-698.
- Van Der Biezen, E. A., & Jones, J. D. (1998).** Plant disease-resistance proteins and the gene-for-gene concept. *Trends in Biochemical Sciences*, *23*(12), 454-456.
- van der Hoorn, R. A., & Kamoun, S. (2008).** From guard to decoy: a new model for perception of plant pathogen effectors. *The Plant Cell*, *20*(8), 2009-2017.
- Van Etten, H. D., Mansfield, J. W., Bailey, J. A., & Farmer, E. E. (1994).** Two classes of plant antibiotics: phytoalexins versus "phytoanticipins". *The Plant Cell*, *6*(9), 1191.
- Van Huijsduijnen, R. H., Alblas, S. W., De Rijk, R. H., & Bol, J. F. (1986).** Induction by salicylic acid of pathogenesis-related proteins and resistance to alfalfa mosaic virus infection in various plant species. *Journal of General Virology*, *67*(10), 2135-2143.

- Van Loon, L. C., & Van Kammen, A. (1970).** Polyacrylamide disc electrophoresis of the soluble leaf proteins from *Nicotiana tabacum* var. 'Samsun' and 'Samsun NN': II. Changes in protein constitution after infection with tobacco mosaic virus. *Virology*, *40*(2), 199-211.
- Van Loon, L. C. (1983).** The induction of pathogenesis-related proteins by pathogens and specific chemicals. *Netherlands Journal of Plant Pathology*, *89*(6), 265-273.
- Van Loon, L. C. (1997).** Induced resistance in plants and the role of pathogenesis-related proteins. *European Journal of Plant Pathology*, *103*(9), 753-765.
- Van Loon, L. C., & Van Strien, E. A. (1999).** The families of pathogenesis-related proteins, their activities, and comparative analysis of PR-1 type proteins. *Physiological and Molecular Plant Pathology*, *55*, 85-97.
- Van Loon L.C., & Glick B.R. (2004)** Increased Plant Fitness by Rhizobacteria. In: Sandermann H. (eds) *Molecular Ecotoxicology of Plants*. Ecological Studies (Analysis and Synthesis), vol 170. Springer, Berlin, Heidelberg.
- Van Loon, L. C., Rep, M., & Pieterse, C. M. (2006).** Significance of inducible defense-related proteins in infected plants. *Annual Review of Phytopathology*, *44*, 135-162.
- Vernooij, B., Friedrich, L., Morse, A., Reist, R., Kolditz-Jawhar, R., Ward, E., Uknes, S., Kessmann, H. & Ryals, J. (1994).** Salicylic acid is not the translocated signal responsible for inducing systemic acquired resistance but is required in signal transduction. *The Plant Cell*, *6*(7), 959-965.
- Vernooij, B., Friedrich, L., Goy, P.A., Staub, T., Kessmann, H., & Ryals, J. (1995).** 2,6-Dichloroisonicotinic acid-induced resistance to pathogens without the accumulation of salicylic acid. *Molecular Plant-Microbe Interactions*, *8*(2): 228-234.
- Vinson, C. R., Sigler, P. B., & McKnight, S. L. (1989).** Scissors-grip model for DNA recognition by a family of leucine zipper proteins. *Science*, *246*(4932), 911-916.
- Vleeshouwers, V. G., & Oliver, R. P. (2014).** Effectors as tools in disease resistance breeding against biotrophic, hemibiotrophic, and necrotrophic plant pathogens. *Molecular Plant-Microbe Interactions*, *27*(3), 196-206.
- Wagner, K. (2016).** Untersuchungen zum Einfluss von NIMIN-Proteinen auf NPR1 und Zelltodinduktion in *Nicotiana benthamiana*. Master Thesis. University of Hohenheim.
- Wang, L., Kim, J., & Somers, D. E. (2013).** Transcriptional corepressor TOPLESS complexes with pseudoresponse regulator proteins and histone deacetylases to regulate circadian transcription. *Proceedings of the National Academy of Sciences*, *110*(2), 761-766.
- Wang, G., Roux, B., Feng, F., Guy, E., Li, L., Li, N., Zhang, X., Lautier, M., Jardinaud, M. F., Chabannes, M., Arlat, M., Chen, S., He, C., Noël, L. D. & Zhou, J. M. (2015).** The decoy substrate of a pathogen effector and a pseudokinase specify pathogen-induced modified-self recognition and immunity in plants. *Cell Host & Microbe*, *18*(3), 285-295.
- Wang, J., Hu, M., Wang, J., Qi, J., Han, Z., Wang, G., Qi, Y., Wang, H. W., Zhou, J. M. & Chai, J. (2019a).** Reconstitution and structure of a plant NLR resistosome conferring immunity. *Science*, *364*(6435).
- Wang, J., Wang, J., Hu, M., Wu, S., Qi, J., Wang, G., Han, Z., Qi, Y., Gao, N., Wang, H. W., Zhou, J. M. & Chai, J. (2019b).** Ligand-triggered allosteric ADP release primes a plant NLR complex. *Science*, *364*(6435), eaav5870.
- Wang, Y., Salasini, B. C., Khan, M., Devi, B., Bush, M., Subramaniam, R., & Hepworth, S. R. (2019c).** Clade I TGACG-motif binding basic leucine zipper transcription factors mediate BLADE-ON-PETIOLE-dependent regulation of development. *Plant Physiology*, *180*(2), 937-951.
- Wang, W., Withers, J., Li, H., Zwack, P. J., Rusnac, D. V., Shi, H., Liu, L., Yan, S., Hinds, T. R., Guttman, M., Dong, X., & Zheng, N. (2020).** Structural basis of salicylic acid perception by Arabidopsis NPR proteins. *Nature*, *586*(7828), 311-316

- Ward, E. R., Uknes, S. J., Williams, S. C., Dincher, S. S., Wiederhold, D. L., Alexander, D. C., Ahl-Goy, P., Metraux, J. P. & Ryals, J. A. (1991). Coordinate gene activity in response to agents that induce systemic acquired resistance. *The Plant Cell*, 3(10), 1085-1094.
- Wasternack, C., & Parthier, B. (1997). Jasmonate-signalled plant gene expression. *Trends in Plant Science*, 2(8), 302-307.
- Wei, K., Chen, J., Wang, Y., Chen, Y., Chen, S., Lin, Y., Pan, S., Zhong, X. & Xie, D. (2012). Genome-wide analysis of bZIP-encoding genes in maize. *DNA Research*, 19(6), 463-476.
- Weigel, R. R. (2000). Identifizierung und Charakterisierung von NIMIN-1, NIMIN-2 und NIMIN-3, Mitgliedern einer neuen Familie von Proteinen aus *Arabidopsis thaliana* (L.) Heynh., die mit NPR1/NIMI, einem Schlüsselprotein in der systemisch aktivierten Resistenz, interagieren. Dissertation. University of Hohenheim
- Weigel, R. R., Bäuscher, C., Pfitzner, A. J., & Pfitzner, U. M. (2001). NIMIN-1, NIMIN-2 and NIMIN-3, members of a novel family of proteins from *Arabidopsis* that interact with NPR1/NIM1, a key regulator of systemic acquired resistance in plants. *Plant Molecular Biology*, 46(2), 143-160.
- Weigel, R. R., Pfitzner, U. M., & Gatz, C. (2005). Interaction of NIMIN1 with NPR1 modulates PR gene expression in *Arabidopsis*. *The Plant Cell*, 17(4), 1279-1291.
- White, R. F. (1979). Acetylsalicylic acid (aspirin) induces resistance to tobacco mosaic virus in tobacco. *Virology*, 99(2), 410-412.
- Wildermuth, M. C., Dewdney, J., Wu, G., & Ausubel, F. M. (2001). Isochorismate synthase is required to synthesize salicylic acid for plant defence. *Nature*, 414(6863), 562-565.
- Wink, M. (1988). Plant breeding: importance of plant secondary metabolites for protection against pathogens and herbivores. *Theoretical and Applied Genetics*, 75(2), 225-233.
- Wöhrle, N. (2014). Untersuchungen zur funktionellen Bedeutung von NIMIN-Proteinen bei der Induktion von Zelltod und der Interaktion von NPR1 und TOPLESS. Master Thesis. University of Hohenheim.
- Wu, Y., Zhang, D., Chu, J. Y., Boyle, P., Wang, Y., Brindle, I. D., De Luca, V. & Després, C. (2012). The *Arabidopsis* NPR1 protein is a receptor for the plant defense hormone salicylic acid. *Cell Reports*, 1(6), 639-647.
- Wu, X. M., Yu, Y., Han, L. B., Li, C. L., Wang, H. Y., Zhong, N. Q., Yao, Y. & Xia, G. X. (2012b). The tobacco BLADE-ON-PETIOLE2 gene mediates differentiation of the corolla abscission zone by controlling longitudinal cell expansion. *Plant Physiology*, 159(2), 835-850.
- Xiang, C., Miao, Z., & Lam, E. (1997). DNA-binding properties, genomic organization and expression pattern of TGA6, a new member of the TGA family of bZIP transcription factors in *Arabidopsis thaliana*. *Plant Molecular Biology*, 34(3), 403-415.
- Xie, Z., Fan, B., & Chen, Z. (1998). Induction of PR-1 proteins and potentiation of pathogen signals by salicylic acid exhibit the same dose response and structural specificity in plant cell cultures. *Molecular Plant-Microbe Interactions*, 11(6), 568-571
- Xu, M., Hu, T., McKim, S. M., Murmu, J., Haughn, G. W., & Hepworth, S. R. (2010). *Arabidopsis* BLADE-ON-PETIOLE1 and 2 promote floral meristem fate and determinacy in a previously undefined pathway targeting APETALA1 and AGAMOUS-LIKE24. *The Plant Journal*, 63(6), 974-989.
- Yamamoto, S., Katagiri, M., Maeno, H., & Hayaishi, O. (1965). Salicylate hydroxylase, a monooxygenase requiring flavin adenine dinucleotide I. Purification and general properties. *Journal of Biological Chemistry*, 240(8), 3408-3413.
- Yan, Z., Reddy, M. S., Ryu, C. M., McInroy, J. A., Wilson, M., & Kloepper, J. W. (2002). Induced systemic protection against tomato late blight elicited by plant growth-promoting rhizobacteria. *Phytopathology*, 92(12), 1329-1333.

- Yanisch-Perron, C., Vieira, J., & Messing, J. (1985).** Improved M13 phage cloning vectors and host strains: nucleotide sequences of the M13mpl8 and pUC19 vectors. *Gene*, 33(1), 103-119.
- Yeats, T. H., & Rose, J. K. (2013).** The formation and function of plant cuticles. *Plant Physiology*, 163(1), 5-20.
- Yi, S. Y., Shirasu, K., Moon, J. S., Lee, S. G., & Kwon, S. Y. (2014).** The activated SA and JA signaling pathways have an influence on flg22-triggered oxidative burst and callose deposition. *PLOS ONE*, 9(2), e88951.
- Yu, K., Soares, J. M., Mandal, M. K., Wang, C., Chanda, B., Gifford, A. N., Fowler, J. S., Navarre, D., Kachroo, A. & Kachroo, P. (2013).** A feedback regulatory loop between G3P and lipid transfer proteins DIR1 and AZI1 mediates azelaic-acid-induced systemic immunity. *Cell Reports*, 3(4), 1266-1278.
- Yuan, Y., Zhong, S., Li, Q., Zhu, Z., Lou, Y., Wang, L., Wang, J., Wang, M., li, Q., Yang, D. & He, Z. (2007).** Functional analysis of rice NPR1-like genes reveals that OsNPR1/NH1 is the rice orthologue conferring disease resistance with enhanced herbivore susceptibility. *Plant Biotechnology Journal*, 5(2), 313-324.
- Zavaliev, R., Mohan, R., Chen, T., & Dong, X. (2020).** Formation of NPR1 condensates promotes cell survival during the plant immune response. *Cell*, 182(5), 1093-1108.
- Zhang, B., Foley, R. C., & Singh, K. B. (1993).** Isolation and characterization of two related Arabidopsis ocselement bZIP binding proteins. *The Plant Journal*, 4(4), 711-716.
- Zhang, Y., Fan, W., Kinkema, M., Li, X., & Dong, X. (1999).** Interaction of NPR1 with basic leucine zipper protein transcription factors that bind sequences required for salicylic acid induction of the PR-1 gene. *Proceedings of the National Academy of Sciences*, 96(11), 6523-6528.
- Zhang, Y., Tessaro, M. J., Lassner, M., & Li, X. (2003).** Knockout analysis of Arabidopsis transcription factors TGA2, TGA5, and TGA6 reveals their redundant and essential roles in systemic acquired resistance. *The Plant Cell*, 15(11), 2647-2653.
- Zhang, Y., Cheng, Y. T., Qu, N., Zhao, Q., Bi, D., & Li, X. (2006).** Negative regulation of defense responses in Arabidopsis by two NPR1 paralogs. *The Plant Journal*, 48(5), 647-656.
- Zhang, J., Shao, F., Li, Y., Cui, H., Chen, L., Li, H., Zou, Y., Long, C. Lan, L., Chai, J., Chen, S., Tang, X. & Zhou, J. M. (2007).** A *Pseudomonas syringae* effector inactivates MAPKs to suppress PAMP-induced immunity in plants. *Cell Host & Microbe*, 1(3), 175-185.
- Zhang, X., Valdés-López, O., Arellano, C., Stacey, G., & Balint-Kurti, P. (2017a).** Genetic dissection of the maize (*Zea mays* L.) MAMP response. *Theoretical and Applied Genetics*, 130(6), 1155-1168.
- Zhang, Q., Lenardo, M. J., & Baltimore, D. (2017b).** 30 years of NF- κ B: a blossoming of relevance to human pathobiology. *Cell*, 168(1-2), 37-57.
- Zhou, J. M., Trifa, Y., Silva, H., Pontier, D., Lam, E., Shah, J., & Klessig, D. F. (2000).** NPR1 differentially interacts with members of the TGA/OBF family of transcription factors that bind an element of the PR-1 gene required for induction by salicylic acid. *Molecular Plant-Microbe Interactions*, 13(2), 191-202.
- Zipfel, C., Robatzek, S., Navarro, L., Oakeley, E. J., Jones, J. D., Felix, G., & Boller, T. (2004).** Bacterial disease resistance in Arabidopsis through flagellin perception. *Nature*, 428(6984), 764-767.
- Zipfel, C., & Felix, G. (2005).** Plants and animals: a different taste for microbes?. *Current Opinion in Plant Biology*, 8(4), 353-360.
- Zipfel, C., Kunze, G., Chinchilla, D., Caniard, A., Jones, J. D., Boller, T., & Felix, G. (2006).** Perception of the bacterial PAMP EF-Tu by the receptor EFR restricts Agrobacterium-mediated transformation. *Cell*, 125(4), 749-760.
- Zou, Z., Eibl, C., & Koop, H. U. (2003).** The stem-loop region of the tobacco psbA 5'UTR is an important determinant of mRNA stability and translation efficiency. *Molecular Genetics and Genomics : MGG*, 269(3), 340-349.

Zwicker, S. (2002) Untersuchungen zu Wechselwirkungen von NIMIN-Proteinen mit NPR1/NIM1 in Hefe und in transgenen Tabakpflanzen. Diploma Thesis. University of Hohenheim.

Zwicker, S., Mast, S., Stos, V., Pfitzner, A. J., & Pfitzner, U. M. (2007). Tobacco NIMIN2 proteins control PR gene induction through transient repression early in systemic acquired resistance. *Molecular Plant Pathology*, 8(4), 385-400.

Appendix

This Appendix of this work includes the following parts:

- I. Differences between α -GFP antisera

- II. Mean values and standard deviations of the mean values for all yeast two-hybrid assays

- III. Mean values and standard deviations of the mean values for β -glucuronidase enzyme assays

- IV. Accession numbers for genes used in this work

- V. Cloning strategies for generation of various gene constructs used in this work

I. Differences between GFP antisera

During this study, two different α -GFP antisera were used: the polyclonal α -GFP (FL) antiserum (see 2.6.1.) and the monoclonal α -GFP (MC) (see 2.6.2.) antiserum. These antisera differ in their composition and therefore their ability to detect different fluorescent proteins including GFP, Venus and the hybrid N1nT-Venus created during this study.

The α -GFP (FL) antiserum consists of polyclonal IgG from rabbit and was raised against the full length GFP protein from *Aequorea victoria* as the targeted epitope. This antiserum, produced by Santa Cruz Biotechnology (GFP (FL) polyclonal IgG, # sc-8334), has been discontinued and is no longer available for purchase.

The α -GFP (MC) antiserum consists of monoclonal IgG from rabbit and was raised against the full length GFP protein from *Aequorea victoria* as the targeted epitope. Unlike typical monoclonal antibodies, this recombinant monoclonal antiserum is produced animal origin-free and derives only from DNA, decreasing variability while increasing specificity. This antiserum was produced by Thermo Fischer Scientific (GFP Recombinant Rabbit Monoclonal Antibody, # G10362). The exact binding site on the GFP protein, however, is unknown (J. Petri, PhD; Thermo Fischer Scientific, Tech Support, personal communication).

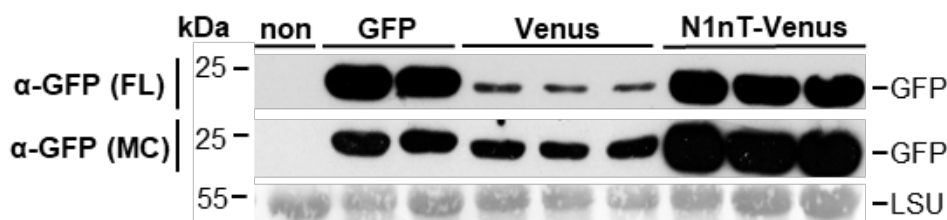


Fig. A1 Differential detection of the fluorescent proteins GFP, Venus and N1nT-Venus by the α -GFP (FL) and α -GFP (MC) antisera. Immunodetection of fluorescent proteins using the polyclonal α -GFP (FL) or the monoclonal α -GFP (MC) antiserum. Protein extracts were prepared 4 dpi from three independent plants infiltrated with agrobacteria harboring *Pro35S:GFP*, *Pro35S:Venus* or *Pro35S:N1nT-V*.

The α -GFP (FL) antiserum produces very strong signals for both GFP and N1nT Venus while Venus, a yellow fluorescent variant of GFP carrying several mutations to enhance both protein maturation and stability, shows a much weaker detection (Fig. A1). In comparison, the α -GFP (MC) antiserum produces protein bands of approximately the same intensity for both GFP and Venus while only producing a very strong signal for N1nT-V. This differential detection of fluorescent proteins suggests that the antibodies contained in the polyclonal α -GFP (FL) antiserum bind, among others, to binding sites that are not present in the Venus protein due to the mutations, which distinguish it from GFP.

II. Mean values and standard deviations in yeast two-hybrid assays

MV – mean value; SD – standard deviation; SA – salicylic acid

Fig. 14A

GAL4BD // GAL4AD	MV	SD
pGBT9 // pGAD424	0,11	0,02
N1 // AtNPR1	35,55	5,69
+0,3 mM SA	14,66	6,01
N1-Venus // AtNPR1	32,52	9,44
+0,3 mM SA	8,17	0,34
Venus // AtNPR1	0,15	0,06
+0,3 mM SA	0,14	0,03

Fig. 22A

GAL4BD // GAL4AD	MV	SD
pGBT9 // pGAD424	0,07	0,01
NtN2a // NgNPR1	22,19	2,34
+ 0,3 mM SA	0,24	0,04
NtN2c // NgNPR1	22,48	4,81
+ 0,3 mM SA	0,15	0,05
BP// NgNPR1	21,76	3,15
+ 0,3 mM SA	0,55	0,11
FG // NgNPR1	13,71	0,81
+ 0,3 mM SA	0,36	0,07
FS // NgNPR1	22,06	1,49
+ 0,3 mM SA	0,29	0,05

Fig. 22B

GAL4BD // GAL4AD	MV	SD
pGBT9 // pGAD424	0,16	0,02
NtN2a // NgNPR1	54,16	17,33
+ 0,3 mM SA	0,51	0,04
NtN2a // NtNIM1-like1	4,37	1,00
+ 0,3 mM SA	0,09	0,00
NtN2c // NtNIM1-like1	4,37	0,59
+ 0,3 mM SA	0,10	0,01
BP // NtNIM1-like1	7,08	2,62
+ 0,3 mM SA	0,46	0,10
FG // NtNIM1-like1	3,66	1,50
+ 0,3 mM SA	0,20	0,09
FS // NtNIM1-like1	4,83	0,68
+ 0,3 mM SA	0,11	0,02

Fig. 27

GAL4BD // GAL4AD	MV	SD
pGBT9 // pGAD424	0,21	0,07
N1 // AtNPR1	38,53	7,58
+0,3 mM SA	7,80	0,73
N1 F49/50S // AtNPR1	0,11	0,01
+0,3 mM SA	0,08	0,00
N1 E94A D95V // AtNPR1	26,36	2,47
+0,3 mM SA	3,71	0,83
N1 // NgNPR1	42,30	2,00
+0,3 mM SA	0,36	0,08
N1 F49/50S // NgNPR1	0,09	0,01
+0,3 mM SA	0,07	0,01
N1 E94A D95V // NgNPR1	47,84	6,37
+0,3 mM SA	1,26	0,25

Fig. 43 B,C

GAL4BD // GAL4AD	MV	SD
pGBT9 // pGAD424	0,09	0,02
N1 // AtNPR1	13,03	3,08
+ 0,3 mM SA	2,36	0,20
N1 // AtTPL1/333	0,93	0,21
+ 0,3 mM SA	0,57	0,09
N1 F49/50S E94A D95V // AtNPR1	0,09	0,01
+ 0,3 mM SA	0,08	0,01
N1 F49/50S E94A D95V // AtTPL1/333	0,30	0,09
+ 0,3 mM SA	0,20	0,02

Fig. 46A

GAL4BD // GAL4AD	MV	SD
pGBT9 // pGAD424	0,07	0,01
- // AtTPL	0,09	0,02
N3 // AtTPL	0,09	0,01
+0,3 mM SA	0,08	0,01
N3 // AtTPL1/333	4,12	1,09
+0,3 mM SA	1,52	0,30
N3 // AtTPL1/196	7,52	1,36
+0,3 mM SA	3,40	2,11

Fig. 46B

GAL4BD // GAL4AD	MV	SD
pGBT9 // pGAD424	0,05	0,01
N3 // AtNPR1	4,36	0,65
N3 // AtTPL1/333	4,06	0,52
N3 ΔEAR // AtNPR1	2,01	0,55
N3 ΔEAR // AtTPL1/333	0,09	0,04
N3 L108/110A // AtNPR1	3,30	0,22
N3 L108/110A // AtTPL1/333	0,05	0,02

Fig. 46C

GAL4BD // GAL4AD	MV	SD
pGBT9 // pGAD424	0,11	0,02
N1 // TPL1/333	2,60	0,10
+0,3 mM SA	3,63	1,23
N1-Venus // TPL1/333	0,65	0,14
+0,3 mM SA	0,54	0,12
Venus // TPL1/333	0,13	0,02
+0,3 mM SA	0,13	0,04

Fig. 50B

GAL4BD // GAL4AD	MV	SD
pGBT9 // pGAD424	0,14	0,04
N1 // AtNPR1#44	38,83	2,75
N1 F49/50S E94A D95V Δ EAR // AtNPR1	0,10	0,01
N1 F49/50S E94A D95V Δ EAR // AtTPL1/333	0,10	0,01

Fig. 52B

GAL4BD // GAL4AD	MV	SD
pGBT9 // pGAD424	0,18	0,01
N3 // AtTPL1/333	13,55	3,80
+0,3 mM SA	7,90	1,31
NtN2c // AtTPL1/333	0,09	0,00
+0,3 mM SA	0,08	0,01
NtN2c ΔEAR // AtTPL1/333	0,11	0,03
+0,3 mM SA	0,08	0,00
BP // AtTPL1/333	0,10	0,01
+0,3 mM SA	0,07	0,01
FG // AtTPL1/333	0,07	0,01
+0,3 mM SA	0,07	0,02
FS // AtTPL1/333	0,12	0,02
+0,3 mM SA	0,10	0,01

Fig. 52C

GAL4BD // GAL4AD	MV	SD
pGBT9 // pGAD424	0,13	0,01
NtFS // NgNPR1	33,17	6,68
+0,3 mM SA	0,29	0,08
NtFS ΔEAR // NgNPR1	25,27	7,69
+0,3 mM SA	0,23	0,06
NtFS F48/49S // NgNPR1	0,25	0,25
+0,3 mM SA	0,09	0,03

Fig. 62B

GAL4BD // GAL4AD	MV	SD
pGBT9 // pGAD424	0,19	0,02
N1b // AtNPR1	26,49	2,22
+0,3 mM SA	17,19	6,27
NIMIN1b // AtTPL 1/333	0,23	0,02
+0,3 mM SA	0,19	0,02
N1nT-N1b // AtNPR1	24,98	3,23
+0,3 mM SA	15,97	7,26
N1nT-N1b // AtTPL 1/333	5,29	0,96
+0,3 mM SA	4,80	0,42

Fig. 64B

GAL4BD // GAL4AD	MV	SD
pGBT9 // pGAD424	0,20	0,03
N1b // AtNPR1	12,20	1,77
+0,3 mM SA	2,18	0,33
N1b // AtTPL1/333	0,20	0,03
+0,3 mM SA	0,15	0,04
N1nT-N1b // AtNPR1	19,75	6,51
+0,3 mM SA	4,59	2,84
N1nT-N1b // AtTPL1/333	4,16	0,77
+0,3 mM SA	2,69	0,44
N1nT-N1b Δ EAR // AtNPR1	21,85	8,95
+0,3 mM SA	2,69	0,24
N1nT-N1b Δ EAR // AtTPL1/333	0,18	0,02
+0,3 mM SA	0,15	0,01

III. Mean values and standard deviations in β -glucuronidase enzyme assays

MV – mean value; SD – standard deviation; SA – salicylic acid; 4-OH BA – 4-hydroxybenzoic acid;

BTH – S-methyl 1,2,3-benzothiadiazole-7-carbothiate; AA – anthranilic acid;

3,5-DCA – 3,5-dichloroanthranilic acid; Pip – pipercolic acid

Unless stated otherwise the indicated proteins were expressed from the 35S promoter from CaMV.

Fig. 7B

ProPR1a:GUS	MV	SD
H ₂ O	8,33	4,55
1 mM SA	797,41	336,40
1 mM 4-OH BA	36,39	14,74
0,3 mM BTH	1098,47	208,81

Fig. 7C

ProPR1a:GUS	MV	SD
0,1 % DMSO	5,11	7,51
1 mM SA	38,14	5,74
0,1 mM AA	1,17	0,18
0,1 mM 3,5-DCA in 0,1 % DMSO	1,79	0,42

ProN1:GUS

ProN1:GUS	MV	SD
H ₂ O	9,73	3,60
1 mM SA	376,03	184,22
1 mM 4-OH BA	32,80	10,89
0,3 mM BTH	393,81	99,67

ProN1:GUS

ProN1:GUS	MV	SD
0,1 % DMSO	8,69	3,87
1 mM SA	128,36	87,25
0,1 mM AA	10,30	7,08
0,1 mM 3,5-DCA in 0,1 % DMSO	17,78	6,90

ProN2:GUS

ProN2:GUS	MV	SD
H ₂ O	3,17	1,81
1 mM SA	31,99	3,42
1 mM 4-OH BA	11,58	2,55
+0,3 mM BTH	31,09	10,01

ProN2:GUS

ProN2:GUS	MV	SD
0,1 % DMSO	5,88	2,55
1 mM SA	20,45	5,92
0,1 mM AA	4,05	0,86
0,1 mM 3,5-DCA in 0,1 % DMSO	5,84	2,24

Fig. 7D

ProPR1a:GUS	MV	SD
0,1 % DMSO	1,18	1,24
1 mM SA	264,46	86,49
1 mM Pip	60,73	15,01
0,1 mM 3,5-DCA in 0,1 % DMSO	8,54	2,77

ProN1:GUS

ProN1:GUS	MV	SD
0,1 % DMSO	5,77	3,80
1 mM SA	265,10	111,49
1 mM Pip	16,92	6,98
0,1 mM 3,5-DCA in 0,1 % DMSO	19,77	11,64

ProN2:GUS

ProN2:GUS	MV	SD
0,1 % DMSO	1,89	0,35
1 mM SA	39,28	5,54
1 mM Pip	9,91	4,36
0,1 mM 3,5-DCA in 0,1 % DMSO	6,16	0,45

Fig. 16B

ProPR1a:GUS	MV	SD
non + H ₂ O	-0,06	0,74
non + 1 mM SA	320,00	15,91
GFP + H ₂ O	92,08	17,60
GFP + 1 mM SA	244,77	030,90
N1 + 1 mM SA	-0,92	0,67
N1-V + 1 mM SA	10,77	1,64

Fig. 17C

ProPR1a:GUS	MV	SD
non + H ₂ O	-3,67	1,15
non + 1 mM SA	416,54	41,11
GFP + H ₂ O	1426,34	186,45
GFP + 1 mM SA	2749,74	457,94
N1-V + 1 mM SA	1542,72	381,24
N1b-V + 1 mM SA	2041,30	212,39

Fig. 18C

ProPR1a:GUS	MV	SD
non + H ₂ O	1,06	0,34
non + 1 mM SA	460,08	158,21
GFP + H ₂ O	1106,26	207,36
GFP + 1 mM SA	1935,46	420,45
N1-V + 1 mM SA	567,46	368,04
N2-V + 1 mM SA	2364,89	406,05

Fig. 20B

ProN1:GUS (475-2/3)	MV	SD
non + H ₂ O	4,03	0,39
non + 1 mM SA	1173,50	122,33
GFP + H ₂ O	716,18	332,56
GFP + 1 mM SA	2113,99	268,07
N1-V + H ₂ O	746,94	525,93
N1-V + 1 mM SA	735,41	67,61
N2-V + H ₂ O	981,95	168,72
N2-V + 1 mM SA	2600,21	563,04

Fig. 20C

ProN2:GUS (476-2/2)	MV	SD
non + H ₂ O	-0,02	1,79
non + 1 mM SA	93,54	34,46
GFP + H ₂ O	47,38	4,51
GFP + 1 mM SA	137,65	13,64
N1-V + H ₂ O	75,35	23,00
N1-V + 1 mM SA	92,87	21,00
N2-V + H ₂ O	105,52	37,91
N2-V + 1 mM SA	152,88	28,46

Fig. 20D

ProN2:GUS (476-5/5)	MV	SD
non + H ₂ O	-3,82	0,97
non + 1 mM SA	71,90	2,81
GFP + H ₂ O	120,80	30,92
GFP + 1 mM SA	281,62	47,91
N1-V + H ₂ O	159,73	22,36
N1-V + 1 mM SA	198,17	27,35
N2-V + H ₂ O	248,88	102,69
N2-V + 1 mM SA	267,34	50,92

Fig. 23B

ProPR1a:GUS	MV	SD
non + H ₂ O	679,09	22,05
non + 1 mM SA	1375,13	172,17
GFP + H ₂ O	1082,20	219,28
GFP + 1 mM SA	1663,26	312,31
N1-V + 1 mM SA	566,95	178,30
BP-V + 1 mM SA	1147,48	51,84
N1-V + 1 mM SA	760,41	189,37
FG-V + 1 mM SA	1547,69	318,33

Fig. 24B

ProPR1a:GUS	MV	SD
non + H ₂ O	22,28	1,76
non + 1 mM SA	443,02	4,97
GFP + H ₂ O	262,45	83,25
GFP + 1 mM SA	1340,96	378,97
N1-V + 1 mM SA	42,42	9,93
NtN2c-V + 1 mM SA	255,84	22,99

Fig. 25B

ProPR1a:GUS	MV	SD
non + H ₂ O	149,75	20,63
non + 1 mM SA	1377,65	228,61
GFP + H ₂ O	159,19	29,61
GFP + 1 mM SA	686,66	81,15
N1-V + 1 mM SA	184,15	49,28
FS-V + 1 mM SA	339,53	115,72

Fig. 41D

ProPR1a:GUS	MV	SD
non + H ₂ O	42,68	29,19
non + 1 mM SA	379,66	102,41
GFP + H ₂ O	596,20	379,04
GFP + 1 mM SA	1707,38	487,54
N1-V + 1 mM SA	662,37	192,97
N1 F49/50S-V + 1 mM SA	682,56	104,31

Fig. 42D

ProPR1a:GUS	MV	SD
non + H ₂ O	-4,13	1,19
non + 1 mM SA	846,11	505,75
GFP + H ₂ O	270,01	201,03
GFP + 1 mM SA	880,49	51,92
N1-V + 1 mM SA	368,40	214,08
N1 E94A D95V-V + 1 mM SA	238,74	80,00

Fig. 44C

ProPR1a:GUS	MV	SD
non + H ₂ O	-6,93	2,96
non + 1 mM SA	1550,95	518,63
GFP + H ₂ O	168,07	80,77
GFP + 1 mM SA	3087,10	495,71
N1-V + 1 mM SA	711,21	42,58
N1 F49/50S E94A D95V-V + 1 mM SA	843,11	311,72

Fig. 48B

ProPR1a:GUS	MV	SD
non + H ₂ O	-1,17	0,17
non + 1 mM SA	2215,89	448,42
GFP + H ₂ O	239,04	107,37
GFP + 1 mM SA	1345,04	480,63
N1 + 1 mM SA	270,86	190,08
N1 L138/140A + 1 mM SA	402,72	218,51
N1-V + 1 mM SA	130,97	114,51
N1 L138/140A-V + 1 mM SA	638,03	368,07

Fig. 49C

ProPR1a:GUS	MV	SD
non + H ₂ O	-2,38	0,83
non + 1 mM SA	323,35	13,66
GFP + H ₂ O	171,75	37,38
GFP + 1 mM SA	1332,07	276,91
N1 + 1 mM SA	154,96	61,58
N1ΔEAR + 1 mM SA	305,41	172,55

Fig. 51C

ProPR1a:GUS	MV	SD
non + H ₂ O	22,28	1,76
non + 1 mM SA	443,02	4,97
GFP + H ₂ O	262,45	83,25
GFP + 1 mM SA	1340,96	378,97
N1-V + 1 mM SA	75,48	9,93
N1 F49/50S E94A D95V ΔEAR-V + 1 mM SA	927,66	22,99

Fig. 53B

ProPR1a:GUS	MV	SD
non + H ₂ O	2,09	2,06
non + 1 mM SA	410,07	99,15
GFP + H ₂ O	2293,07	718,61
GFP + 1 mM SA	3068,16	612,29
FS-V + 1 mM SA	147,33	31,21
FS F48/49S-V + 1 mM SA	532,50	88,95
FS-V + 1 mM SA	94,92	54,87
FSΔEAR-V + 1 mM SA	668,66	524,89

Fig. 58B

ProPR1a:GUS	MV	SD
non + H ₂ O	-2,63	0,76
non + 1 mM SA	382,89	73,35
Pro35S:GFP + H ₂ O	108,23	68,28
Pro35S:GFP + 1 mM SA	852,70	285,00
Pro35S:N1-V + 1 mM SA	69,65	106,29
ProN1b:Bax (1:2) + 1 mM SA	81,62	123,07
Pro35S:N1-V + 1 mM SA	12,29	11,86
ProN1b:Bax (1:4) + 1 mM SA	297,08	193,82

Fig. 61D

ProPR1a:GUS	MV	SD
non + H ₂ O	-1,98	0,40
non + 1 mM SA	1270,33	66,76
GFP + H ₂ O	98,71	67,94
GFP + 1 mM SA	749,57	320,44
N1-V + 1 mM SA	182,08	92,21
N1 16/142-V + 1 mM SA	1272,19	436,08

IV. Accession numbers

Table A.1 Accession numbers of utilized sequences

Species	Gene	Accession number
<i>A. thaliana</i>	NIMIN1	AJ250184.1
	NIMIN1b	AJ252204.1
	NIMIN2	AJ250185.1
	NIMIN3	AJ250186.1
	AtNPR1	At1g64280
	AtNPR3	At5g45110
	AtTPL	At1g15750
<i>N. tabacum</i>	NtN2a (G8-1)	AF057379.1
	NtN2b	DQ859891.1
	NtN2c	EF015598.1
	N1-like 1 (BP)	BP531936.1
	N1-like 2 (FG)	FG635992.1
	N2-like (FS)	FS401103.1
	NgNPR1	AF480488
	NtNIM1-like1	AY640382

V. Cloning strategies

1. *Arabidopsis thaliana*

1.1. Cloning of NIMIN genes for transient overexpression and Yeast Two Hybrid Assays

1.1.1. pGBT9/Venus and pGBT9/AtNIMIN1-Venus

The *Venus* ORF was PCR amplified from pBin19/35S:Venus [Neeley *et al.*, 2019] with the primers Venus-5 and Venus-6, introducing a *Bam*HI restriction site at the N-terminus and a *Sal*I restriction site at the C-terminus, to allow in-frame fusion to the C-terminus of the GAL4 activation and DNA binding domains in yeast vectors as well as NIMIN proteins. The amplicon was subcloned into the T-vector and verified by sequencing. The verified sequence was transferred into the pGBT9 vector using a restriction digestion with *Bam*HI and *Sal*I. The *AtNIMIN1* sequence was isolated from pGBT9/AtNIMIN1 [Weigel *et al.*, 2001] using restriction digestion with *Bam*HI and ligated into equally digested pGBT9/Venus to allow C-terminal fusion to the GAL4 DNA binding domain and N-terminal fusion to the Venus reporter protein.

1.1.2. pGBT9/AtNIMIN1 F49/50S E94A D95V and pBin19/35S:AtNIMIN1 F49/50S E94A D95V-Venus

Sequences of *AtNIMIN1 F49/50S* and *AtNIMIN1 E94A D95V* were available as pUC19/NIMIN1-M1 [Weigel *et al.* 2005] and pGBT9/NIMIN1 E94A D95V [Hermann *et al.*, 2013] respectively. The *AtNIMIN1 E94A D95V* sequence was subcloned into pUC19 using restriction digestion with *Bam*HI. The orientation was verified using restriction digestion. The *AtNIMIN1* gene contains an internal *Hind*III restriction site directly 3' behind the DXFFK domain which together with the *Hind*III restriction site in the MCS of pUC19 allows isolation of a 5' fragment of the gene containing the domain. A fragment of *AtNIMIN1 F49/50S*, containing the mutant DXSSK domain was isolated from pUC19/NIMIN1-M1 using restriction digestion with *Hind*III and ligated into equally digested and purified pUC19/NIMIN1 E94A D95V. The resulting *AtNIMIN1 F49/50S E94A D95V* construct was verified through sequencing. The construct was isolated from pUC19/AtNIMIN1 F49/50S E94A D95V using restriction digestion with *Bam*HI and transferred into equally digested pBin19/35S:Venus and into pGBT9.

1.1.3. pGBT9/AtNIMIN1 F49/50S E94A D95V ΔEAR and pBin19/35S:AtNIMIN1 F49/50S E94A D95V ΔEAR-Venus

The pGBT9/AtNIMIN1 F49/50S E94A D95V construct (see 1.1.3.) was used as template for a PCR reaction to create a mutant lacking the EAR motif at the C-terminus. The primers N1fwd and N1-13 were used to truncate the sequence so that the resulting protein only extends to amino acid 136. The 0.4 kb amplicon was subcloned into the T-vector. The verified *AtNIMIN1 F49/50S E94A D95V ΔEAR* sequence was isolated from the T-vector using restriction digestion with *Bam*HI and ligated into equally digested pBin19/35S:Venus, and into pGBT9.

1.1.4. pBin19/35S:AtNIMIN1b-Venus

The *AtNIMIN1b* ORF was PCR amplified from pGBT9/AtNIMIN1b [Weigel et al. 2001] with the primers N1b-1 and N1b-2. The primers introduce *Bam*HI restriction sites and were designed in a way that allows in-frame fusion to the C-terminus of the GAL4 activation and DNA binding domains contained in yeast vectors, as well as to the N-terminus of the Venus reporter gene contained in pBin19/35S:Venus. The 0.4 kb amplicon was subcloned into the T-vector. The verified *AtNIMIN1b* sequence was isolated from the T-vector using restriction digestion with *Bam*HI and ligated into equally digested pBin19/35S:Venus.

1.1.5. pBin19/35S:AtNIMIN2-Venus

The *AtNIMIN2* sequence contained in pGBT9/AtNIMIN2 [Weigel et al., 2001] is flanked by two *Bam*HI restriction sites allowing in-frame fusion to the N-terminus of the Venus reporter gene contained in pBin19/35S:Venus. The sequence was isolated using restriction digestion with *Bam*HI and ligated into an equally digested pBin19/35S:Venus.

1.1.6. Hybrid *NIMIN* constructs in pGBT9 and pBin19/35S:Venus

Table A.2 Primer combinations for generation of chimeric *NIMIN* constructs

Construct	Template	Primer	
		Forward	Reverse
pGBT9/N1nT-NIMIN1b pBin19/35S:N1nT-NIMIN1b-Venus	pGBT9/NIMIN1b	N1b-4	N1b-2
pBin19/35S:N1nT Δ 2-4-NIMIN1b-Venus	pGBT9/N1nT-NIMIN1b	N1-14	N1b-2
pBin19/35S:N1nT Δ 2-9-NIMIN1b-Venus	pGBT9/N1nT-NIMIN1b	N1-16	N1b-2
pBin19/35S:N1nT L8G-NIMIN1b-Venus	pGBT9/N1nT-NIMIN1b	N1-15	N1b-2
pBin19/35S:N1nT M1L-NIMIN1b-Venus	pGBT9/N1nT-NIMIN1b	N1-17	N1b-2
pBin19/35S:N1nT S7A Y9A Y11A S12A-NIMIN1b-Venus	pGBT9/NIMIN1b	N1b-5	N1b-2
pGBT9/N1nT-NIMIN1b Δ EAR(1/134) pBin19/35S:N1nT-NIMIN1b Δ EAR(1/134)-Venus	pGBT9/N1nT-NIMIN1b	N1fwd	N1b-6
pBin19/35S:NIMIN1b-N1nT-Venus	pGBT9/NIMIN1b	N1b-1	N1b-7
pBin19/35S:N1nT-NIMIN2-Venus	pGBT9/NIMIN2	N2-5	N2-3

Chimeric *NIMIN* constructs with the N-terminal domain of AtNIMIN1 (M1-T15; N1nT) or mutants thereof fused to other *NIMIN* genes were created using PCR (see Table A.2). All primers introduce *Bam*HI restriction sites and were designed to allow in-frame fusion to the C-terminus of the GAL4 activation and DNA binding domains contained in yeast vectors, as well as to the N-terminus of the Venus reporter gene contained in pBin19/35S:Venus. PCR amplicates were subcloned into the T-vector and verified by sequencing. The verified sequences were isolated from the T-vector using restriction digestion with *Bam*HI and ligated equally digested into pBin19/35S:Venus and pGBT9.

1.1.7. Chimeric *Venus* constructs in pBin19/35S:NOS

Table A.3 Primer combinations for generation of chimeric *Venus* constructs

Construct	Template	Primer	
		Forward	Reverse
pBin19/35S:N1nT-Venus	pBin19/35S:Venus	Venus-7	Venus-4
pBin19/35S:N1nT Δ 2-9-Venus	pBSKS(+)/N1nT-Venus	N1-16	Venus-4
pBin19/35S:N1nT M1L-Venus	pBSKS(+)/N1nT-Venus	N1-17	Venus-4
pBin19/35S:Venus-N1nT	pBin19/35S:Venus	Venus-5	Venus-8

Chimeric Venus constructs with the N-terminal domain of AtNIMIN1 (M1-T15; N1nT) or mutants fused to the *Venus* reporter gene were created using PCR (Table A.3). All primer combinations introduce a *Bam*HI restriction site at the 5'-end and a *Sac*I restriction site at the 3'-end. PCR amplicates were subcloned into the T-vector and verified by sequencing. The verified sequences were isolated from the T-vector using restriction digestion with *Bam*HI and *Sac*I and ligated into *pBin19/35S:GUS* [Jefferson et al., 1987], digested using *Bam*HI and *Sac*I to remove the GUS sequence.

1.2. Cloning of NPR genes for transient overexpression

1.2.1. pBin19/35S:AtNPR1-Venus

The *AtNPR1* sequence contained in pUC19/AtNPR1 [Weigel *et al.*, 2001] is flanked by two *Bam*HI restriction sites, allowing in-frame fusion to the N-terminus of the Venus reporter gene contained in pBin19/35S:Venus. The sequence was isolated using restriction digestion with *Bam*HI and ligated into an equally digested pBin19/35S:Venus.

1.2.2. pBin19/35S:AtNPR3-Venus

The *AtNPR3* sequence contained in pGBT/AtNPR3 [U.M. Pfitzner, personal communication] is flanked by two *Bam*HI restriction sites, allowing in-frame fusion to the N-terminus of the Venus reporter gene contained in pBin19/35S:Venus. The sequence was isolated using restriction digestion with *Bam*HI and ligated into an equally digested pBin19/35S:Venus.

1.3. Cloning of TOPLESS (TPL) for yeast two-hybrid assays

1.3.1. pGAD424/AtTPL 1/196

An *AtTPL 1/196* fragment was isolated from the pUC19/AtTPL 1/333 [U. M. Pfitzner, personal communication] vector using restriction digestion with *Bam*HI and *Eco*RV and subcloned into the T-vector digested with *Bam*HI and *Sma*I. *AtTPL 1/196* was isolated from the T-vector using a restriction digestion with *Bgl*II and *Pst*I and ligated into pGAD424 digested with *Bam*HI and *Pst*I.

2. *Nicotiana tabacum*

2.1. Cloning of *NIMIN* genes for transient overexpression and yeast two-hybrid assays

2.1.1. pBin19/35S:NtBP-Venus

The *NtBP* sequence contained in pGBT9/NtBP [Masroor, 2013] is flanked by two *Bam*HI restriction sites allowing in-frame fusion to the N-terminus of the Venus reporter gene contained in pBin19/35S:Venus. The sequence was isolated using restriction digestion with *Bam*HI and ligated into an equally digested pBin19/35S:Venus.

2.1.2. pBin19/35S:NtFG-Venus

The *NtFG* sequence contained in pGBT9/NtFG [U.M. Pfitzner, personal communication] is flanked by two *Bam*HI restriction sites allowing in-frame fusion to the N-terminus of the Venus reporter gene contained in pBin19/35S:Venus. The sequence was isolated using restriction digestion with *Bam*HI and ligated into an equally digested pBin19/35S:Venus.

2.1.3. pBin19/35S:NtFS-Venus

The *NtFS* sequence contained in pGBT9/NtFS [Masroor, 2013] is flanked by two *Bam*HI restriction sites allowing in-frame fusion to the N-terminus of the Venus reporter gene contained in pBin19/35S:Venus. The sequence was isolated using restriction digestion with *Bam*HI and ligated into an equally digested pBin19/35S:Venus.

2.1.4. pGBT9/NtFS Δ EAR and pBin19/35S:NtFS Δ EAR-Venus

The *NtFS* ORF was amplified from pGBT9/NtFS [Masroor, 2013] with the primers FS-1 and FS-5. The primers add *Bam*HI restriction sites to allow in-frame fusion to the C-terminus of the GAL4 activation and DNA binding domains contained in yeast vectors, as well as to the N-terminus of the Venus reporter gene contained in pBin19/35S:Venus, and truncate the sequence, so that the resulting protein only extends to amino acid 101 with no functional EAR motif. The 0.3 kb amplicon was subcloned into the T-vector and was verified through sequencing. The verified *NtFS* Δ EAR sequence was isolated from the T-vector using restriction digestion with *Bam*HI and ligated into equally digested pBin19/35S:Venus, and into pGBT9.

2.1.5. pGBT9/NtFS F48/49S and pBin19/35S:NtFS F48/49S-Venus

In vitro mutagenesis of *NtFS* was done using overlap extension PCR [Ho *et al.*, 1989]. The *NtFS* ORF was amplified from pGBT9/NtFS [Masroor, 2013] with the primer combinations FS-1 and FS-4, as well as FS-3 and FS-2, to obtain overlapping partial 5' and 3' amplicons. The primers FS-1 and FS-2 introduce *BamHI* restriction sites at the 5'-end and the 3'-end respectively, allowing in-frame fusion to the C-terminus of the GAL4 activation and DNA binding domains contained in yeast vectors, as well as to the N-terminus of the Venus reporter gene contained in pBin19/35S:Venus. The primers FS-3 and FS-4 are complementary, introducing two mutations at positions 48 and 49, changing the phenylalanine residues to serine (TTC→TCC). The amplicons were used as template for a second PCR reaction using FS-1 and FS-2 as primers to amplify the full-length sequence containing the mutant. The 0.3 kb amplicon was subcloned into the T-vector and verified through sequencing. The verified *NtFS F48/48S* sequence was isolated from the T-vector using restriction digestion with *BamHI* and ligated into equally digested pBin19/35S:Venus, and into pGBT9.

2.1.6. pBin19/35S:NtN2c-Venus

The *NtN2c* sequence contained in pGBT9/NtN2c [Zwicker *et al.*, 2007] is flanked by two *BamHI* restriction sites allowing in-frame fusion to the N-terminus of the Venus reporter gene contained in pBin19/35S:Venus. The sequence was isolated using restriction digestion with *BamHI* and ligated into an equally digested pBin19/35S:Venus.

2.1.7. pGBT9/NtN2c ΔEAR and pBin19/35S:NtN2c ΔEAR-Venus

The *NtN2c* ORF was amplified from pGBT9/NtN2c [Zwicker *et al.*, 2007] with the primers AD10-2 and N2c-9 to truncate the sequence, so that the resulting protein only extends to amino acid 111 with no functional EAR motif. The 0.35 kb amplicon was subcloned into the T-vector and was verified through sequencing. The verified *NtN2c ΔEAR* sequence was isolated from the T-vector using restriction digestion with *BamHI* and ligated into pBin19/35S:Venus and into pGBT9.

Affidavit

Annex 3 of the University of Hohenheim's Doctoral Regulations

Declaration in lieu of an oath on independent work according to Sec. 18(3) sentence 5 of the University of Hohenheim's Doctoral Regulations for the Faculties of Agricultural Sciences, Natural Sciences, and Business, Economics and Social Sciences

1. The dissertation submitted on the topic "Expression and functional domains of Arabidopsis and tobacco *NIMI-INTERACTING (NIMIN)* genes" is work done independently by me.
2. I only used the sources and aids listed and did not make use of any impermissible assistance from third parties. In particular, I marked all content taken word-for-word or paraphrased from other works.
3. I did not use the assistance of a commercial doctoral placement or advising agency.
4. I am aware of the importance of the declaration in lieu of oath and the criminal consequences of false or incomplete declarations in lieu of oath.

I confirm that the declaration above is correct. I declare in lieu of oath that I have declared only the truth to the best of my knowledge and have not omitted anything.

Altbach, 22.7.2021



Signature (Mathias Saur)

Curriculum vitae

Personal Details

Name: Mathias Wolfgang Saur
Date of Birth/Place: 31.01.1990 / Göppingen, Baden, Württemberg, Germany
Nationality: German

Educational background

05/2015 - 07/2021 Thesis work for Doctorate, Institute of Biology, Department of General Virology, University of Hohenheim, Stuttgart, Germany
10/2012 - 03/2015 Master of Sciences / M.Sc. Biology, Major: Pathogen-Host-Interactions, University of Hohenheim, Stuttgart, Germany
10/2009 - 11/2012 Bachelor of Sciences / B.Sc. Biology, Specialization: Genetics, University of Hohenheim, Stuttgart, Germany
09/2000 - 06/2009 Gymnasium Plochingen, School-leaving qualification: Abitur

Work experience

01/2018 – 06/2020 Research Associate, (TV-L E13), Institute of Genetics, Department of General Virology, University of Hohenheim, Stuttgart, Germany
07/2017 - 12/2017 Research assistant, Institute of Genetics, Department of General Virology, University of Hohenheim, Stuttgart, Germany
04/2016 - 06/2017 Research Associate, (TV-L E13), Institute of Genetics, Department of General Virology, University of Hohenheim, Stuttgart, Germany
05/2015 - 03/2016 Research assistant, Institute of Genetics, Department of General Virology, University of Hohenheim, Stuttgart, Germany

Internships

03/2014 – 05/2014 MRC Protein Phosphorylation and Ubiquitylation Unit, Dundee, Scotland
Under supervision of Dr. Thimo Kurz
Generation of knock-out tissue culture cell lines using the CRISPR/Cas9 system
08/2011 - 09/2011 University hospital for blood group serology and transfusion medicine in Graz, Austria, Under supervision of Univ.-Prof. Dr. G. Lanzer
Genetic testing of patient samples for Faktor V Leiden

Altbach, 22.7.2021



Signature (Mathias Saur)

Scientific contributions

Publications

Konopka, E., Saur, M., Pfitzner, A. J. P., Pfitzner, U. M. Differential binding of salicylic acid (SA), SA derivatives and co-factors determines the roles of Arabidopsis NPR1 to NPR4 in plant immunity. In preparation.

Lindner, K., Stark, J., Saur, M., Schleicher, L., Gerber, S., Witte, S., Tyler, L. Pfitzner, U. M. and Pfitzner, A. J. P. Ubiquitin-mediated protein degradation and modulation is regulated by ATCV-1. In preparation.

Conference contributions

Saur, M., Pfitzner, U.M. (2019). The N-terminal domain of NIMIN1 is important for protein stability. 11th Regio Plant Science Meeting, University of Hohenheim, March 2019, poster presentation

Saur, M., Pfitzner, U.M. (2017). Overexpression of Arabidopsis *NIMIN1* promotes cell death induction. 9th Regio Plant Science Meeting, MPI Tübingen, April 2017, poster presentation

Acknowledgements

At this point, I would like to take the opportunity to express my sincere thanks to all people who, actively or passively, contributed to the success of this thesis. I am especially thankful for all the mental support, during this last year of COVID19 pandemic, which came with its own difficulties.

I want to thank Prof. Dr. Arthur Pfitzner and Dr. Ursula Pfitzner who provided me with an interesting research subject and allowed me to work and practice science in their labs.

I am particularly grateful to Dr. Ursula Pfitzner for giving her professional supervision and helpful feedback during practical lab work, as well as for the scientific discussions regarding not only the subject of my thesis, but also related topics. Her support and objective criticism at all stages of my research and writing processes considerably improved the final product.

I also want to thank Prof. Dr. Andreas Schaller for agreeing to be the second reviewer of my thesis, and Prof. Dr. Anke Steppuhn for her willingness to be part of the examination committee for my oral exam.

Another thanks goes to all members of the Department of General Virology for the pleasant working environment and collegial and friendly cooperation. I want to thank Ingrid and Christine for their support and advice and for handling the transformation of tobacco plants. I want to thank Evelyn for her good cooperation and relaxed conversations and discussions during private and work-related communication. I also want to thank Kamila for her input during the final stages of my doctorate and her critical eye during proofreading. Thanks also to Roxy, Thomas and Thorsten for cultivation and care for my plants in the greenhouse.

I want to thank my family for their constant support and their loving care during all this time. My family is my anchor which allowed me to go through with all of this and providing me a place I can call home. Great thanks toward my girlfriend Franziska who not only gave me her loving support but also motivated and encouraged me and endured even my grumpy days.

I want to thank my friends who gave me some distraction from the constant work and helped to clear my head, encouraging new ideas and challenging my creativity. Special thanks also go to Joachim, Steffen and Megan, who went over my English formatting and helped during proofreading.

I could not have done this without all of you.